

https://dspace.org/

Formulation of an instantly dissolvable solid eye drop device for topical ocular delivery

Moosa, Raeesa Mahomed

2014-02-19
http://hdl.handle.net10539/13879

Downloaded from a DSpace repository. https://dspace.org/

FORMULATION OF AN INSTANTLY DISSOLVABLE SOLID EYE DROP DEVICE FOR TOPICAL OCULAR DELIVERY

RAEESA MAHOMED MOOSA

A dissertation submitted to the Faculty of Health Sciences, University of the Witwatersrand, in fulfillment of the requirements for the degree of Master of Pharmacy

Supervisor:

Professor Viness Pillay

University of the Witwatersrand

Department of Pharmacy and Pharmacology

South Africa

Co-supervisors:

Professor Yahya E. Choonara University of the Witwatersrand,

Department of Pharmacy and Pharmacology, South Africa

Miss Lisa C. du Toit University of the Witwatersrand,

Department of Pharmacy and Pharmacology, South Africa

Johannesburg, 2013

I, Raeesa Mahomed Moosa declare that this dissertation is my own work. It has being submitted for the degree of Master of Pharmacy in the Faculty of Health Sciences in the University, Johannesburg. It has not submitted before for any degree or examination at this or any other University.

…….

This 29th day of March 2013

ABSTRACT

Ocular diseases of the anterior segment are ubiquitous, especially among elderly patients. The development of novel drug delivery systems on the journey for improved treatment is therefore imperative. Aside from anatomical and physiological barriers of the eye, the actual dosage form plays a crucial role. Although liquid eye drops are the first-choice dosage form, the shortcomings do not go unnoticed. In an attempt to circumvent these drawbacks, a novel instantly soluble eye drop device was developed. The system aimed to provide an easier administration form, comfort for the patient and improve drug bioavailability to anterior chamber. This was a steer toward attaining patient-convenience and compliance which are critically challenging factors. Preformulatory studies allowed for the screening and selection of candidate components and key processing conditions. Hydrophilic polymers and excipients were selected for attainment of small, rapid disintegrating yet robust matrices via lyophilization of solutions. Design of experiments generated formulations by means of a Face centred central composite design (FCCCD) that underwent thorough physicochemical and mechanical assessment. Overall, robust rapidly disintegrating solid eye drops were produced. Fastest disintegration time was noted to be 0.200s. Drug content ranged from 79-96%. An improved permeation of formulations compared to a pure drug dispersion was seen. Mathematical modeling was conducted for better insight into the behavior of the device on the eye surface. Statistical analysis through constraint optimization yielded a single optimal formulation. Thermal and molecular transition analysis showed congruent findings with no incompatibility between components. Combinatory surface morphology and porositometric studies confirmed the presence of interconnecting pores across the matrix surface. Drug release kinetic evaluation predicted that best model fit was first-order release. Ocular irritancy studies by means of the HET-CAM test indicated that both drug-loaded and drug-free eye drops had an irritation score of 0 with the inference of good tolerability. Ex vivo permeation across excised rabbit cornea showed an improved steady state drug flux ($0.00052 mg.cm^{-2}.min^{-1}$) and permeability co-efficient ($1.7x10^{-4} cm.min^{-1}$) for the optimized device compared to pure drug and a marketed eye drop preparation. In vivo analysis was conducted on the rabbit model with insertion of the device into the ocular cul-de-sac. Subsequently, ultra performance liquid chromatography (UPLC) analysis of the aspirated aqueous humour for model drug timolol maleate detection was conducted. The device demonstrated improved drug levels (Cmax = 3ug/mL) in comparison to commercial eye drops (Cmax = 1.97ug/mL) and was well tolerated. Level A point-to-point IVIVC plots indicated a R^2 value of 0.84. This served to imply that the in vitro dissolution data can be compared to and may serve as a surrogate to that of in vivo pK data. Histopathological assessment on the enucleated eye ball confirmed the lack of noxious effects of the device on ocular tissue. From this study, the solid eye drop device was concluded to be safe as a drug delivery system for the anterior eye. Looking toward innovative trends and modifications, a bi-layered solid eye drop system with enhanced permeability capabilities employing low molecular weight chitosan was further fabricated for preliminary investigation.

RESEARCH OUTPUTS

1. Review Paper

a. Topically Administered 'Matriserts' Developed for Drug Delivery to the Anterior Segment of the Eye. Viness Pillay, Raeesa M. Moosa, Valence M. K. Ndesendo, Yahya E. Choonara, Lisa C. du Toit, Pradeep Kumar, Lomas K. Tomar, Charu Tyagi and Trevor Carmichael (abstract Appendix A1). *Submitted to Journal of Pharmacy and Pharmacology.*

2. Research Papers

b. Characterization and Statistical Optimization of an Instantly Soluble Eye Drop Device (ISED) developed for drug delivery to the anterior segment of the eye. Raeesa M. Moosa, Yahya E. Choonara, Lisa C. du Toit, Pradeep Kumar, Valence M. K. Ndesendo, Lomas K. Tomar, Trevor Carmichael and Viness Pillay. *Submitted to Journal of Pharmaceutical Sciences.*

c. In depth elucidation of the properties of an optimized Instantly Soluble Eye Drop Device (ISED). Raeesa M. Moosa, Yahya E. Choonara, Lisa C. du Toit, Pradeep Kumar, Lomas K. Tomar, Trevor Carmichael and Viness Pillay. *To be submitted*

d. *In vivo* evaluation of an Instantly Soluble Eye Drop Device (ISED) in the rabbit model. Raeesa M. Moosa, Yahya E. Choonara, Lisa C. du Toit, Pradeep Kumar, Lomas K. Tomar, Trevor Carmichael and Viness Pillay. *To be submitted*

PRESENTATIONS

1. Podium

a. 4th Cross Faculty Graduate Symposium, 22 October 2012, Wits University, Johannesburg. Abstract Title: Characterization of an Instantly Soluble Eye Drop Device (ISED) developed for drug delivery to the anterior segment of the eye. Raeesa M. Moosa, Yahya E. Choonara, Lisa C. du Toit, Pradeep Kumar, Valence M. K. Ndesendo, Trevor Carmichael and Viness Pillay. (abstract Appendix B1)

b. 1st Asia Pacific Glaucoma Congress (APGC), 7-9 December 2012. Bali, Indonesia Abstract Title: Determination of ex vivo permeation and irritation potential of rapidly disintegrating topically administered solid eye drops. Raeesa M. Moosa, Yahya E. Choonara, Lisa C. du Toit, Pradeep Kumar, Valence M. K. Ndesendo, Trevor Carmichael and Viness Pillay. (abstract Appendix B2)

2. Posters

a. Royal Society of South Africa Spring Science Showcase, 9 September 2012. Delta environmental centre, Johannesburg. Poster Title: *In vitro* characterization of novel solid eye drops. Raeesa M. Moosa, Yahya E. Choonara, Lisa C. du Toit, Pradeep Kumar, Valence M. K. Ndesendo, Trevor Carmichael and Viness Pillay.

b. 33rd Annual Conference of the Academy of Pharmaceutical Sciences of South Africa, 12-15 September 2012, Rhodes University, Grahamstown. Poster Title: Design, Development and optimization of a novel instantly soluble ophthalmic device. Raeesa M. Moosa, Yahya E. Choonara, Lisa C. du Toit, Pradeep Kumar, Valence M. K. Ndesendo, Trevor Carmichael and Viness Pillay (abstract Appendix B3).

c. Opthalmological Society of South Africa congress 14-17 March 2013, Cape Town International Convention Centre, Cape Town. Poster title: *in vivo* evaluation of topically administered solid eye drops in the rabbit model. Raeesa M. Moosa, Yahya E. Choonara, Lisa C. du Toit, Pradeep Kumar, Valence M. K. Ndesendo, Trevor Carmichael and Viness Pillay. (abstract appendix B4).

ANIMAL ETHICS CLEARANCE

I hereby confirm that the study entitled: ‘In vivo assessment of a novel instantly soluble eye drop device in the rabbit model’, received approval from the animal ethics screening committee of the University of the Witwatersrand.

Ethics clearance number: 2012/12/05 (See Appendix C1)

PATENT APPLICATION

2012/06792 ~ Provisional ~ 54: OCULAR PHARMACEUTICAL DOSAGE FORM ~ 71:UNIVERSITY OF THE WITWATERSRAND,JOHANNESBURG 7 York Road Parktown Johannesburg ~ 72:CHOONARA YAHYA ESSOP KUMAR PRADEEP MOOSA RAEESA M DU TOIT LISA CLAIRE PILLAY VINESS JHETAM RAFEEQ

ACKNOWLEDGEMENTS

The author wishes to extend her gratitude to the following individuals who have contributed to the completion of this study:

My esteemed gratitude goes out to my supervisor Professor Viness Pillay for providing me with the platform to carry out this degree. Thank you for always pushing us to strive for excellence. I am honored to have been supervised by an exceptional pharmaceutical scientist. Many thanks to my co-supervisors Professor Yahya E. Choonara for his contribution and advice towards the completion and correction of this dissertation. Thank you for reminding me to look and think beyond the simple. I am most grateful to my co-supervisor Miss Lisa C. du toit for her pleasant nature, willingness to assist at all times and her vast knowledge on ocular aspects. Thank you for assuring me that it will be ok. I wish you all the success. Mr. Pradeep Kumar's brilliant ideas and constant guidance were a source of inspiration. You are an extremely intelligent yet humble individual who I sincerely respect. Appreciation goes to Dr. Lomas Tomar and Dr. Charu Tyagi for their efforts with corrections of papers. Many thanks to Prof S. Van Vuuren for allowing me the use of the microbiology lab during my studies. It is a pleasure to pay tribute to Professor Michael Dankwerts and Professor Robyn Van Zyl, our heads of department, for their support. My sincere thanks to Dr.Valence MK. Ndesendo for his encouragement and assistance not only during my masters but also in the completion of the undergraduate elective project. He is a dedicated individual who will surely prosper. Thank you to Professor Trevor Carmichael and Dr. Aubrey Magotloe for their tireless efforts with the ethics and *in vivo* component of this work. Your contribution in terms of clinical expertise are highly appreciated.

My deepest appreciation goes out to my family who have provided me with unconditional love, support and who have instilled in me qualities that helped me grow as a person. I would like to thank my parents Ayesha and M.E.E. Moosa for providing me with far more opportunities than they were ever offered in life and for working extremely hard to ensure that I have always had the best in life. My deepest gratitude to Zuneid and Halima Osman for supporting and assisting me to blossom as an individual and for believing in me. Your support, prayers and love helped steer me through this journey. I would like to extend my sincere and special thanks to Professor Ames Dhai and Dr. Faruk Mahomed for encouraging me to persue this degree. Thank you for reminding me that quitting is never an option. Your encouragement and care will never be forgotten. To my siblings (biological and unbiological, in order of age): Shabeer, Safia, Zain, Zaheer, Sabeeha, Zeenat, Tasneem, Muhammad and Zubair for playing a part in my life, understanding me, tolerating me and giving me the opportunity to have different experiences with each one of you at various times in my life. Thank you for being my pillars of strength. Love is sent to my granny Huri Mahomed for her prayers and best wishes for me.

To my fellow collegues and friends: Ameena, Derusha, Tasneem, Latavia, Mpho, Martina, Teboho, Felix, Angus, Lebo. Khadija, Noni, Zama, Ndidi, Jonathan, Femi, Ahmed, Stephanie and Unathi for their help and advice. A special thank you to Thiresen for his guidance through this difficult journey and for always believing in me. Kind words to Steven for going out of your way to ensure that I always did the right thing. You are brilliant and I am thankful to you more than you know. To my friends and office mates: Hrishi, Mershen and Tahir for tolerating my many moods and random disappearances ('temporary quitting'), making me smile, turning me into a rebel and maintaining my sanity. You have shown me how to take a break once in a while, appreciate life and never to let anyone bring me down. You have all become my family and have made campus bearable when progress seemed impossible. To Sunaina, Femida, Naeema, Fatema, Pavan, Mandla and Kusi thank you for becoming part of the team and I wish you all the best in your studies. I appreciate your contributions and friendship. Thank you to all team members for creating a vibrant environment.

My appreciation goes out to Mr. David Beyever for his advice and motivation when times were tough. Thank you for reminding me that I can do it. The wits staff: Ms Shirona Naidoo, Ms Neha Singh, Mrs. Deanne Hazel-Johnston are mentioned for their encouragement and smiles. Their moral support cannot be forgotten. To Mr. Bafana, Mr. Kleinbooi, Ms. Busi, Mr. Sello, Ms.Tebogo, Ms. Pride for their assistance and ensuring that our work environment was conducive to carry out the studies. My sincere attributes go out to the CAS staff for all their assistance with the animal studies. Thank you for granting me your time.

Thanks to Mrs. Pam Sharp for assistance with the confocal microscope and Dr. Clem Penny for his advice regarding operation of the fluorescence microscope. Gratitude goes out to to Dr. Amorel Van eyk for her guidance with obtaining tissue for *ex vivo* studies. A word of thanks to Mr. Rhameez S. Herbst from the department of applied mathematics for his help with the 'mind-boggling' mathematical modeling which takes my work to another level. Thank you to Ziyaad Bhobat for his advice on statistical analysis and interpretation.

The completion of this study would not have been possible without the sponsorship of the NRF, GDARD and TIA funding and I am grateful for the opportunity they have provided to optimally carry out the studies. Thank you to the University of the Witwatersrand for being my educational institution and to South Africa for the great development and opportunities.

Most importantly, I thank the ALMIGHTY for all the blessings, love, family and friends He has given me. Thank you for allowing me to come this far in life and for making me realize that I am here for a reason and showing me the light when I was in the depths of despair during these difficult years of my life. This degree, although challenging, has definitely moulded me into a better person as I have learnt to be independent, work hard, deal with disappointments, to know my priorities, to face my fears, dry my tears and never to give up in the face of adversity.

DEDICATION

This dissertation is dedicated to my mother Ayesha, who was never offered the opportunities she has given to me. She has dedicated her life to her children and her sacrifices are endless. You are beautiful, inside and out. Thank you for being my inspiration to push myself beyond my limits when quitting crossed my mind. Thank you for instilling in me values and teaching me that hard work and sacrifice lead to success. I hope I have made you proud.

TABLE OF CONTENTS

CHAPTER 1 **Page**

INTRODUCTION

1.1 Background ……..……..…....1

1.2 Statement of the problem……2

1.3 Common anterior ocular diseases and treatment……...3

1.4 Current marketed formulations for anterior eye drug delivery…….....3

1.5 Approach to the problem- Rationale for the development of an instantly soluble eye drop device for topical ocular drug delivery……...4

1.6 Advantages of a fast disintegrating system for ocular use……...6

1.7 Application of solid fast disintegrating systems for ophthalmic delivery…….....6

1.8 Novelty of study……...7

1.8 Aim of this study……...7

1.9 Objectives of this study…….7

1.10 Technology and equipment employed in this study…….8

1.11 Overview of dissertation…….11

CHAPTER 2

LITERATURE REVIEW : TOPICALLY ADMINISTERED 'MATRISERTS' DEVELOPED FOR DRUG DELIVERY TO THE ANTERIOR SEGMENT OF THE EYE

2.1 Introduction…….....14

2.2 Basic anatomical and physiological considerations of the eye……....16

2.3 Barriers to ocular drug delivery…….....16

2.3.1 Lachrymation, drainage and blood vessels…….16

2.3.2 Corneal-aqueous barrier…….……..…16

2.4 Fate of ocular drugs after administration: distribution and elimination…….....17

2.5 Possible routes of administration……..20

2.6 Anterior drug delivery…….....20

2.6.1 Topical ocular delivery…….20

2.6.2 Subconjunctival administration…….……..21

2.7 Steps to enhance ocular bioavailability…….……21

2.8 Rationale for development of mini-tablets as drug delivery systems…….……..22

2.9 Mini-tablets for topical ocular drug delivery……....23

2.10 Commonly employed polymers in ocular mini-tablets…….....24

2.10.1 Cellulose derivatives……....24

2.10.2 Acrylates……..25

2.10.3 Chitosan……25

2.10.4 Drum dried waxy maize starch (DDWMS)……....26

2.11 Mini-tablets developed for topical ocular drug delivery……..…….27

2.11.1 Timolol-containing mini-tablets……27

2.11.2 A Carbopol® and DDWMS mini-tablets……..28

2.12 Evaluation of physical properties and irritation potential of Carbopol® 974 P and DDWMS mini-tablets……29

2.12.1 Ciprofloxacin-loaded granules compressed into minitablets……....29

2.12.2 Amioca® and Cabopol® mini-tablets…….30

2.12.3 Gentamicin ocular mini-tablets…….....30

2.12.4 Mucoadhesive microdiscs formulated in a rapidly dissolving tablet…….....31

2.12.5 Pregelatinized starch and Carbopol® mini-tablets……..32

2.12.6 Ocular mini-tablets for the treatment of microbial keratitis…….....32

2.12.7 Ciprofloxacin loaded mini-tablets…….32

2.12.8 Sponge-like acyclovir mini-tablets……,,….....33

2.13 Examples of various additional solid devices developed for topical ocular delivery…….…34

2.14 Developments and future outlook……36

2.15 Concluding remarks……..…37

CHAPTER 3
PREREQUISITE THEORETICAL CONSIDERATIONS AND PREFORMULATION INVESTIGATIONS

3.1 Introduction……....38

3.1.1 Characteristics of topical ocular drug delivery systems…….....39

3.2 Preliminary investigations for appropriate component selection…….....39

3.3 Materials and methods…….41

3.3.1 Materials……...41

3.3.2 Preparation of polymeric solutions and synthesis of solid eye drops……....41

3.3.3 Weight uniformity…….45

3.5.1 Physical characteristics and weight uniformity……..46

3.4.3 Diameter and thickness…….46

3.4.4 Disintegration time…….46

3.4.5 Friability…….46

3.4.6 Effect of components on formulation properties…….47

3.5 Ideal processing conditions for the development of solid eye drops…….48

3.5.1 Duration required for complete dissolution of components…….48

3.5.2 Choice of moulds……...48

3.5.3 Type and concentration of constituents…….48

3.5.4 Determination of Limits for variables of formulations……..48

3.5.4.1 PF68 concentration…….49

3.5.4.2 MD concentration…….49

3.6 Concluding remarks…….49

CHAPTER 4

CHARACTERIZATION AND STATISTICAL OPTIMIZATION OF THE ISED THROUGH INSTITUTION OF AN EXPERIMENTAL DESIGN

4.1. Introduction……..……..50

4.2. Materials and Methods……..……..……..52

4.2.1 Materials……...52

4.2.2 Development of an experimental design…….52

4.2.3 Preparation of polymeric solutions and synthesis of solid eye drops according to the Face centred central composite design (FCCCD)…..……53

4.2.4 Determination of the physicomechanical properties of the solid eye drops by textural analysis……54

4.2.5 Disintegration Profiling……..……57

4.2.6 Determination of moisture content by Karl Fisher Titrimetry (KFT)……..…….59

4.2.7 Surface morphology by scanning electron microscopy (SEM)……..……..…..…….61

4.2.8 Visualization of dissolution process employing Stereomicroscopy……....61

4.2.9 Imaging of fluid ingression by Flourescence Microscopy……...……...……..…61

4.2.10 Construction of calibration curve…….……..61

4.2.11 Computation of Drug Entrapment Efficiency (DEE)…….……...62

4.2.12 *In vitro* drug release studies……...……..…..62

4.2.13 *Ex vivo* permeation studies……63

4.2.13.1 Tissue collection and storage…….……....63

4.2.13.2 Permeation test…….64

4.2.14 Statistical evaluation of responses based on constraint optimization……65

4.2.15 Mathematical modelling……..66

4.3. Results and Discussion……66

4.3.1 Physical properties of solid eye drops……..66

4.3.2 Textural profile analysis of solid eye drops……..66

4.3.3 Disintegration testing..……68

4.3.4 Moisture content studies……69

4.3.5 Morphological structure of the solid eye drops matrices……72

4.3.6 Stereomicroscopy of the solid eye drops matrices……....73

4.3.7 Flourescent microscopy of the solid eye drops……73

4.3.8 Drug entrapment efficiency……...76

4.3.9 Drug release studies……....76

4.3.10 *Ex vivo* permeation studies…….. ..78

4.3.11 Statistical analysis……80

4.3.11.1 Residual Plots……84

4.3.11.2 Basic statistical t-test and F-test for determination of variable effects on responses……....84

4.3.11.3 Response surface analysis……84

4.3.11.4 Main and interaction effects on responses……..88

4.3.11.5 Agreement between Experimental vs. Predicted values…….....89

4.3.11.6 Analysis of variance (ANOVA)……92

4.3.11.7 Response optimization procedure and identification of the optimum ISED formulation……95

4.3.11.8 Mathematical modeling……....96

4.4 Concluding remarks……98

CHAPTER 5

ELUCIDATION OF THE IN DEPTH PHARMACEUTICAL CHARACTERISTICS OF AN OPTIMIZED RAPIDLY DISINTEGRATING OPTHALMIC DRUG DELIVERY SYSTEM

5.1 Introduction……..……..99

5.2. Methods and Materials…..…….100

5.2.1 Materials……100

5.2.2 Preparation of polymeric solutions and synthesis of solid eye drops according to optimized constraints…….……101

5.2.3 Determination of the molecular vibrational transitions……..……...102

5.2.4 Determination of thermophysical and supplementary properties via temperature modulated differential scanning calorimetry (TMDSC) and Thermal Gravimetric analysis (TGA)……...102

5.2.5 Complementary surface morphology and porositometric analysis……..……102

5.2.6 Kinetic modelling of release data……...……104

5.2.7 Ocular tolerance testing employing modified Hen Egg Chorioallontoic (HET-CAM) test……106

5.2.7.1 Assay preparation and procedure……....106

5.2.8 Treatment of dissolution data by comparison of release profiles of the optimized ISED and a commercial product……...107

5.2.9 *Ex vivo* permeation studies of the optimized formulation in comparison to a commercial anti-glaucoma product……...108

5.3. Results and Discussion……....109

5.3.1 Molecular vibration transitions……..109

5.3.2 Thermal analysis…….113

5.3.3 Porositometric and surface imaging analysis comparison……119

5.4 Drug release kinetics……..123

5.5 Ocular toxicity evaluation……..……126

5.6 Comparison of dissolution data……..……...127

5.7 Determination of *ex vivo* permeation in comparison to a marketed product……..128

5.8. Concluding remarks……..130

CHAPTER 6

IRRADIATION STERILIZATION AND SUBSEQUENT CHRACATERIZATION OF THE OPTIMIZED ISED

6.1 Introduction……..…131

6.2 Materials and Methods……..…133

6.2.1 Materials……..133

6.2.2 Methods……...133

6.2.2.1 Gamma irradiation sterilization of the optimized ISED……..133

6.2.2.2 Determination of molecular vibrational transitions and complementary thermal analysis…….…..133

6.2.2.3 Determination of sterility efficacy through microbiological techniques……..133

6.2.2.4 Accelerated stability studies…….……135

6.3 Results and Discussion…….……..135

6.3.2 Sterility confirmation……..……,……..136

6.3.3 Stability studies……....137

6.4 Concluding remarks…….139

CHAPTER 7

DEVELOPMENT OF A NOVEL DRUG DETECTION METHOD AND *IN VIVO* ANALYSIS OF AN OPTIMIZED ISED IN THE RABBIT MODEL

7.1 Introduction……141

7.2 Materials and methods……142

7.2.1 Materials……142

7.2.2 Instrumentation……142

7.2.3 Chromatographic conditions……142

7.2.4 Sample preparation……143

7.2.5 Preparation……145

7.2.6 Sterilization……145

7.2.7 *In vivo* characterization in the rabbit model……145

7.2.7.1 Experimental procedures……147

7.2.7.2 Post-insertion assessment of the effect of the devive on the eye surface……149

7.2.7.3 Analysis of aqueous humour samples……150

7.2.8 Data analysis……151

7.2.9 *In vitro in vivo* correlation (IVIVC)……151

7.2.10 Histological evaluation of ISED ocular-compatibility……152

7.3 Results and discussion……152

7.3.1 Preparation of the device……152

7.3.2 Visual assessment of device effect on ocular tissue……153

7.3.3 Drug detection……153

7.3.4 *In vivo* results from the device in comparison to marketed eye drop preparation……154

7.3.5 In vitro on vivo correlation (IVIVC)……157

7.3.6 Histological assessment……159

7.4 Concluding remarks……160

CHAPTER 8

PRELIMINARY INVESTIGATION OF AN ISED WITH ENHANCED PERMEABILITY CAPABILITIES

8.1 Introduction……161

8.2 Materials and Methods……163

8.2.1 Materials……163

8.2.2 Preliminary screening and development of an experimental design……164

8.2.3 Preparation of the solid eye drop……165

8.2.4 Surface morphology……165

8.2.5 Matrix resilience……165

8.2.6 Disintegration time……165

8.2.7 Drug release……165

8.2.8 Corneal permeability……165

8.3 Results and Discussion……165

8.3.1 Physical features and surface appearance……165

8.3.2 Matrix resilience……166

8.3.3 Disintegration time……166

8.3.4 Drug release……167

8.3.5 Permeability……168

8.3.6 Response surface analysis……169

8.3 Preliminary insight into the design of a bi-layered ISED……170

8.3.1 Methodology for BLISED preparation……172

8.3.2 Results and discussion……172

8.4 Concluding remarks……173

CHAPTER 9

CONCLUSIONS AND RECOMMENDATIONS

9.1 Conclusions……174

9.2 Recommendations……175

9.3 Challenges observed……175

9.4 Future outlook……175

References……176

Appendices……202

LIST OF FIGURES

1.1 a) Schematic representing the proposed solid eye drop device and its operation once administered into the cul-de-sac of the eye. 5

1.2 Schematic of: a) phase diagram showing the triple point of water (Source: Baheti et al., 2010), b) State diagram of water (w)/solute (s) system (Source: Kasper and Fries, 2011) and c) the lyophilizer employed for freeze-drying of samples (adapted from Hunek et al., 2007). .. 9

1.3 Flow diagram illustrating rationale approach to the development of an instantly soluble eye drop device. . 13

2.1 Schematic of the corneal layer comprising different layers (adapted from Manerma et al., 2006). 17

2.2 Schematic showing the path of topically applied ophthalmic drug delivery systems. 19

2.3 Schematic of the disadvantages associated with various ocular drug delivery systems (adapted from Davis et al., 2004). 20

2.4 Diagram showing: a) difference in size between a one cent coin, mini-tablets (2mm) and mini-tablets (1mm) (Reproduced with permission from: Tissen et al., 2011) and b) 5 ml of a Brilliant Blue solution to simulate the required amount of hydrochlorothiazide (HCT) solution for a child weighing 5 kg (1 mg HCT/kg); right: five orally disintegrating mini-tablets (ODMT) with 1 mg HCT per mini-tablet (Reproduced with permission from: Stoltenberg and Breitkreutz, 2011). 23

2.5 Image representing the hydration of the mini-tablet once inserted into the eye: a) 0 hours b) 2 hours and c) 4.5 hours after insertion (Reproduced with permission from: Ceulemans et al., 2001). 28

2.6 Schematic of: a) ocular minitablet (6mg weight, diameter 2mm) prepared with

drum-dried waxy maize starch/Carbopol 974P/sodium stearylfumarate/ ciprofloxacin hydrochloride (90.5/5/1/3.5, w/w) and b) macroscopic examination of the gelling minitablet in the eye, 4 hours after application (Reproduced with permission from: Weyenberg et al., 2003). 29

2.7 Digital image depicting *in situ* gelling after insertion of two ocular mini-tablets (arrow) on the ventral bulbar conjunctiva of the right eye in a sedated pony (Reproduced with permission from: Gasthuys et al., 2007). 31

2.8 Scanning electron micrographs of microparticles prepared for ocular adhesion studies: a) PLG MS; b) PLG MD; c) PLG/PEG MS; d) PLG/PEG MD. (Scale bars 10 μm) (Reproduced with permission from: Choy et al. 2008). 31
MS-microspheres
MD-microdiscs

2.9 Digital images of: a) mini-tablet with a dimension of (4 × 2 mm) in comparison to a conventional oral tablet having a diameter of 12 mm (Reproduced with permission from: Refai and Tag, 2011). 3

2.10 Schematic of: a) NODS device; and b) Ocusert (adapted from Bourlais et al., 1998). 36

3.1 Schematic outlining important considerations in developing a novel ocular system (Information summarized from: Bawa, 1990; Ishikawa et al., 2001 and Conway, 2008). 39

3.2 Schematic of method employed for preformulation studies 44

3.3 Digital image of the top view of lyophilized drops of formulation 21 (diameter 11mm) 46 .

4.1 Schematic of FCCD. 51

4.2 Typical: a) force-time profile for matrix resilience calculation; b) force-distance profile for matrix tolerance computation, yield value and energy of absorption;

and c) force-distance profile for BHN determination. 56

4.3 a) Texture analyzer employed for disintegration testing, b) digital image of the disintegration rig with 20mm diameter probe showing channeled geometry to allow fluid to flow above tablet to contact upper surface during the test and c) typical distance-time graph for disintegration profiling. 58

4.4 Typical graph obtained for KFT. 60

4.5 Calibration curve of TM in SAH (pH7.4, 37°C) at 295nm (SD≤0.0543). 62

4.6 Digital images of: a) the enucleated eye ball, b) excision of the cornea, c) excised cornea and d) a single cell of Franz diffusion cell apparatus showing the set-up for permeation through corneal tissue. 65

4.7 Digital image depicting the typical solid eye drops of formulation 1 and 11 produced from the FCCCD. 66

4.8 3D bar graph of relationships observed for textural characteristics. 68

4.9 a) Horizontal bar graph depicting results from disintegration and moisture testing (error bars indicate standard deviation), b) chemical structure of PAANa, c) SAP network (adapted from www.m2polymer.com/html/superabsorbent_polymers.html) and d) process of charge repulsion resulting in polymer uncoiling and water interaction (adapted from *www.watercampws.uiuc.edu/waterclear/... /polymers _ teacher_guide.p.*) 71

4.10 a) SEM images depicting the porous matrix surface of formulation 1 (510x and 615x magnification) and b) stereomicroscopy images for visualization of the rapid dissolution process (light and darkfield field 10x magnification); and c) Fluorescent images depicting fluid ingression into the matrix (10x magnification). 74

4.11 Drug release profiles for the design formulations (error bars indicate

standard deviation). 77

4.12 Graphs depicting cumulative drug permeated (%) of: a) formulations 1-5, b) formulations 6-10, c) formulations 11-13 including TM dispersion and flux ($mg.cm^{-2}.min^{-1}$) calculated at 360 minutes for: d) formulations 1-13 including TM dispersion (error bars indicate standard deviation). 79

4.13 Residual plots for a) MR, b) DT and c) MDT_{50} 82

4.14 Response surface plots and corresponding contour plots for: a),b) MR vs PF68 and MD; c),d) DT vs MD, PF68; and e), f) MDT vs MD, PF68. and g) 3D scatter plot showing the relationship between MR and MD. 87

4.15 Typical: a) main effects plot for MR; b) interaction of the response values for MR; c) main effects plot for DT; d) interaction of the response values for DT; e) main effects plot for MDT; and f) interaction of the response values for MDT. 89

4.16 Agreement between experimental and predicted values for: a) MR; b) DT; and c) MDT. 92

4.17 Desirability plot depicting factor settings and desirability values for the variables and responses 95

4.18 Plots depicting: a) the mass increase of the ISED in the tear layer and b) concentration profile at several times. 97

5.1 Digital image of a batch of optimized ISED. 101

5.2 Digital images of: a) incubation process, b) eggs placed in an equatorial position after albumin removal, c) observation of embryo formation on day 3 and d) preparation of egg for sample testing. 103

5.3: Schematics of a) superimposed FTIR spectra of components, physical mixture

and final formulation, b) separated peaks of components, c) structure of TM, d) structure of PF68, and e) structure of MD, with respective observed groups highlighted. 110

5.4 DSC thermograms of a) pure drug timolol maleate, b) native PF68, c) native MD, d) physical mixture, e) DL final formulation f) ADSC graph of drug-loaded formulation, g) TGA graph of pure TM, h) DF formulation and i) DL formulation (N= 3 in all cases). 115

5.5: Porosity analysis plots and corresponding SEM images of drug-loaded optimized formulation: a) Linear isotherm, b) BET surface area, c) BJH adsorption cumulative pore volumes, d) BJH desorption cumulative dA/dD pore areas, e) typical t-plot. 120

5.6 Dissolution profiles compared to a) Zero order, b) first order and c) Hopfenberg models. 125

5.7 a) schematic of CAM (adapted from Vargas et al., 2007), b) CAM after exposure to optimized sample and c) after exposure to SDS. 127

5.8: Graph of drug release of ISED and commercial formulation. 128

5.9 Graphical representation of drug flux of the optimized formulation and TM drug dispersion (error bars indicate standard deviation). 129

6.1 Summary flow diagram of the gamma sterilization process. 132

6.2 Digital images depicting: a) the agar plates of different media, b) vortexing the solutions, c) preparing the pipette, d) transferring the solution to the plates, e) spreading the solution using the glass rod and f) candle jar. 134

6.3 FTIR graphs depicting: a) unsterilized ISED, b) sterilized ISED, DSC thermographs of: c) unsterilized ISED and d) sterilized ISED. 135

6.4 Digital images of a) a test sample and b) a negative control of sterile media after Incubation. 137

6.5 SEM images of: a) ISED at 0 months, b) ISED at 3months and c) typical resilience graph. 138

7.1 Schematic depicting the methodology of liquid-liquid extraction method *in vitro* UPLC analysis process. 144

7.2 Calibration curve obtained in blank aqueous humour samples. 145

7.3 Comparison of the rabbit and primate globes (adapted from Short, 2008). 146

7.4 Schematic of the procedure of experimental animal studies that will be conducted on rabbits. 148

7.5 Digital images outlining the step-wise *in vivo* studies: a) Left eye of New Zealand Albino Rabbit, b) cul-de-sac of the eye, c) insertion of ISED into the cul-de-sac, d) insertion of the needle for paracentesis, e) aqueous humour aspiration, f) sample collection into a plastic eppendorph, g) removal of surrounding tissue, h) enucleation of the eyeball, i) complete removal of the eye. 149

7.6 Schematic of process for drug extraction procedure. 150

7.7 Schematic of a one compartmental model. 151

7.8 Digital image of the ISED in comparison to a R5 coin. 152

7.9: 2D chromatograph of: a) TM and DS and corresponding 3D graph of b) TM and DS. 154

7.10 Graph depicting: a) *in vitro* ISED drug release results and b) *in vivo* ISED and Commercial eye drop drug concentrations 155

.**7.11** Graphs depicting: a) concentration vs time of ISED, b) residual plot of ISED. 157

7.12 Graphs depicting: a) residuals, b) *in vitro* release, c) *in vivo* absorption and d) level A point-to-point IVIVC plot 158

7.13 Digital images depicting corneal layer with a) DL ISED at 30 minutes and b) with DF ISED at 30 minutes, c) DL ISED at 240 minutes and d) DF ISED at 240 minutes 160

8.1 Schematic of classes of permeation enhancers. 162

8.2 SEM image of formulation 1 (magnification 615x). 166

8.3 Drug release curves for the 14 formulations. 167

8.4 Surface plots of a) MR vs. COS, HPMC, b) MDT vs. COS, HPMC and c) Kp vs. COS, HPMC. 169

8.5 Schematic of OROS technology (adapted from Plangio et al., 2002). 172

8.6 Images of: Schematic of bilayered ISED 173

LIST OF TABLES

2.1 The advantages of mini-tablets as drug delivery systems for topical ocular use (Extracted from Refai and Tag, 2011; Ceulemans et al.,2001; Weyenberg et al., 2003; Weyenberg et al., 2005). 23

2.1 The advantages of mini-tablets as drug delivery systems for topical ocular use (Extracted from Refai and Tag, 2011; Ceulemans et al.,2001; Weyenberg et al., 2003; Weyenberg et al., 2005). 26

2.3 Various additional solid ophthalmic devices 34

3.1 Polymers and excipients selected for preformulation 40

3.2 Components of the porous matrix and their concentrations ($\%^{w/}_{v}$) 40

3.3 Results obtained from preformulation studies (N=3). 41

3.4 Formulation variables identified and response objectives. 47

4.1 Thirteen formulations generated from the FCCCD. 53

4.2 Parameters employed for Textural analysis 55

4.3 Parameters employed for disintegration profiling 58

4.4 Constituents used to prepare simulated lachrymal fluid (SLF) (Gonjari et al., 2009) and simulated aqueous humour (SAH) (Gianniola et al., 2007) 58

4.5 Parameters employed for Karl Fisher Titration 60

4.6 Textural analysis results conducted on design formulations. 68

4.7 Moisture content of wafers under desiccated and ambient conditions 70

4.8 Mean dissolution times calculated for drug release characteristics 78

4.9 Correlation between experimental and predicted values. 91

4.10 Estimated p-values for MR, DT and MDT 93

4.11 ANOVA for dependant variables of the FCCCD 94

4.12 Constraints for the optimal formulation and experimental and predicted response values for the optimized formulation 96

5.1 Parameters employed for degassing phase of wafers 104

5.2 Scoring chart employed for the HET-CAM test (Velpandian et al., 2006) 107

5.3 Interpretation of vibrational bands obtained from FTIR analysis 112

5.4 Results obtained from porosity analysis 119

5.5 Release data obtained from various models 124

5.6 Results obtained for the HET-CAM test 127

5.7 Results obtained for permeability co-efficients 129

6.1 Methods of achieving sterilization of ophthalmic products (summarized from Weyenberg, 2004, Weiner 2010 and Kumar,2012) 131

6.2 Data obtained for accelerated stability studies at 0 and 3 months (37°C,75%RH). 139

7.1 Clinical evaluation scale of irritation (adapted from Mishra and Gilholtra, 2008) 150

7.2 Score for clinical assessment of ISED on ocular tissue 153

7.3 Pk parameters and diagnostic criteria for 'goodness of fit' of TM in the aqueous humour following topical application 156

8.1 14 formulations generated from the PB design 164

8.2 Data generated from analysis of the novel ISED 169

8.3 Summary of the characteristics of multi-layered tablets (Extracted from Kulkarni and Bhatia, 2009; Vaithiyalingam and Sayeed, 2010; Divya et al., 2011; Askok and Kumar 2012; Pujara et al., 2012). 171

LIST OF EQUATIONS

1.1 A thermodynamic representation of primary drying 10

3.1 Friability 46

4.1 Polynomial equation 53

4.2 Brinell Hardness Number 56

4.3 Drug entrapment efficiency 62

4.4 Mean dissolution time 63

4.5 Cumulative amount of drug 64

4.6 Drug flux 64

4.7 Karl Fisher reaction 70

4.8 Regression MR 94

4.9 Regression DT 94

4.10 Regression MDT 94

4.11 Full partial differential equation 96

4.12 Boundary conditions 97

5.1 First order release 104

5.2 Zero order release 105

5.3 a) Hopfenberg release 105

5.3 b) Modified Hopfenberg release 105

5.4 Irritation score 107

5.5 a) Difference factor 108

5.5 b) Similarity factor 108

5.6 a) Drug flux 109

5.6 b) Permeability 109

5.7 Model selection criteria 123

CHAPTER 1

INTRODUCTION

1.1 Background to the Study

The eye is a sophisticated yet essential feature of the human body. Ocular diseases are prevalent worldwide with an alarming increase generally encountered and expected in the elderly community. This is due to the natural aging processing which is unavoidable and inevitably impacts the health, immunity and functioning ability of people. Conditions such as cataracts, glaucoma and diabetic retinopathy are some examples of commonly occurring diseases which may be chronic in nature and require continual treatment. The mere fact that the diseases are chronic exacerbates the despondency of patients and fosters a poor outcome.

According to Pascolini and Marriot (2010), approximately 285 million people globally have a problem with eye sight, of which about 14% are completely blind. This is certainly a burden and majority of cases can be attributed to aging or preventable diseases. Currently, In the World Health Organization (WHO) African region, a total of 65.4 thousand people per million of the population have some sort of visual impairment, loss or complete blindness.

Taking the aging process as well as barriers of the eye itself (elaborated on in chapter 2) and finally, shortcomings of drug delivery systems into consideration, simpler yet effective means of treatment is of dire concern. This study aimed to synthesize a novel instantly dissolvable solid eye drop device which provides an easier administration form without significant disruption of activity. The proposed system aimed to dissolve within a time frame of seconds thus avoiding any irritation potential in the eye and allowing for time-effective administration. This could prove to be an effective system in overcoming the obstacle of difficulty of eye drop instillation by patients who cannot manipulate an eye drop bottle in the therapy of conditions of the anterior segment of the eye and ultimately enhance drug delivery and serve as tool to improve patient co-operation.

1.2 Statement of the Problem

Ocular conditions of the anterior segment of the eye require an effective, ‘easy’ topical drug delivery system that ensures effective therapeutic drug levels and patient compliance. Topical ocular drug delivery using a conventional system such as liquid eye drops is associated with several drawbacks. The following specific points are of paramount importance when considering

the use of such formulations: i) a very small volume of lachrymal fluid (7-9µL) is found on the eye surface while a dropper bottle dispenses more than this present volume of liquid. Majority of this is then flushed out upon instillation which consequently results in a loss of contained drug; ii) instillation of the liquid, due to foreign body sensation, may trigger a flow of tears which forces more of the liquid to be lost and iii) content of substances for preservation of the solution which may not be well tolerated with triggering of blinking and further loss of drug (Macdonald and Maurice, 1991; Davies, 2000; Noeker, 2001). Furthermore, these dosage forms are convenient and widely available, but have poor bioavailability due to dilution in the lachrimal fluid once the eye drop solution is administered and subsequent removal by the naso-lacrimal drainage system (Gonjari et al., 2009). Thus, continual instillation of eye drops is required in order to achieve therapeutic effects. This can result in poor patient compliance and in turn hinders the overall treatment process.

Hence, the following considerations are of paramount importance:

a) The use of conventional liquid eye drops displays the following problems:

- Most eye drops remain on the ocular surface for a small period of time and limited amount of drug is actually absorbed.
- Naso-lachrimal drainage and eye-lid reflex closure result in loss of liquid preparation from the eye surface once instilled.
- This results in low bioavailability of ophthalmic drugs when administered using these topical droppable dosage forms.

b) Patients often have difficulty instilling conventional eye drops due to the following reasons:

- It has to be administered many times during the course of the day and this can lead to non-compliance.
- Certain patients such as the elderly or those with conditions that impair hand movement have difficulty instilling the eye drops since a certain level of pressure has to be applied to the bottle to expel the eye drop. These patients are disadvantaged due to lack of control and synchronization of the dropper.
- If not correctly held, the eye drop bottle plastic tip may come into contact with the eye surface itself and lead to contamination of the bottle with several uses. This can also lead to injury of the cornea if not carefully used (Lux et al. 2011).

- Patients often present to health practitioners with a reduced intraocular pressure in conditions such as glaucoma as they instill the drops prior to the appointment, whereas the disease has progressed due to lack of willingness to adhere to therapy (Schwartz and Quigley, 2008).

1.3 Common Anterior Ocular Diseases and Treatment

A large number of individuals suffer from eye ailments. Ocular conditions are thus very common and if untreated, certain diseases can lead to impaired vision. Daily activities and productivity can be affected by ocular conditions which on initial inspection may seem trivial. Thus, correct treatment regimens must be selected to alleviate the suffering of the patient. Selected ocular conditions and their treatment include:

- *Conjunctivitis:* This is inflammation of the conjunctiva which can be caused by infection, allergens or pollutants. It is usually treated with topical antibiotics such as chloremphenicol or systemic antibiotics such as ceftrioxone, depending on the cause (Tarabishy and Jeng, 2008).
- *Keratitis:* It is an inflammatory condition of the cornea due to bacterial of viral infections. Keratitis is treated using a broad-spectrum antibiotic such as aminoglycoside in combination with vancomycin or alternatively a fluoroquinolone alone (Alan and Dart, 1995).
- *Uveitis:* Inflammation of the uveal tract (iris, ciliar body, and choroids). Treated with corticosteroids and immunosuppressants (Pato et al., 2011).
- *Glaucoma:* Increased intraocular pressure due to failure of aqueous humour drainage. This causes damage to the optic nerve with resultant blindness. It is commonly treated using non-selective beta blockers like timolol or parasympathomimetics such as pilocarpine (Grieshaber and Flammer, 2010).
- *Dry eye (keratoconjunctivitis sicca):* A decreased tear production which results in discomfort, visual disturbance and inflammation of the ocular surface (Gayton et al., 2009). Treatment involves the use of artificial tear substitutes.

1.4 Current Marketed Formulations for Anterior Eye Drug Delivery

Extensive progress in the field of ophthalmology and pharmaceutical drug delivery has been experienced but evidently, the simplest and early developed systems, namely eye drops, still dominate the market. For example, Voltaren® Optha (Novartis, Switzerland) eye drops contain the active diclofenac sodium and are indicated for inflammatory conditions. The solution

contains hydroxypropyl gamma cyclodextrin, an excipient of interest, which assists with corneal permeation of the drug (Pierre et al., 2012). Additionally gels and suspensions are also commonly prescribed for conditions such as dry eye, glaucoma and infections. The point to make is that although advancements are focused on, their success is absent.

1.5 Approach to the Problem- Rationale for the Development of an Instantly Soluble Eye Drop Device for Topical Ocular Drug Delivery

As mentioned previously, a topical route of administration for the eye is the most common and convenient route. A forward-thinking approach to achieve improved anterior eye drug delivery by the use of an instantly soluble eye drop device (ISED) is proposed. The novelty of this ISED lies in the formulation of a solid drug-loaded porous matrix that will instantly dissolve upon contact with the tear fluid of the eye surface. The device was directed to have the following features; 1) be light weight and porous, 2) small enough to enter the cul-de-sac of the eye, 3) avoid any irritation, 4) instantly dissolve once administered, 5) be stable since it will be in the form of a solid, 6) the ISED will be administered using an insertion probe which will avoid contamination of the device by the hand and allow for focused insertion.

The fabrication of this novel system could possibly be a steer in the direction in terms of improving topical ocular drug delivery. Figure 1.1 elicits the proposed ISED and its mechanism.

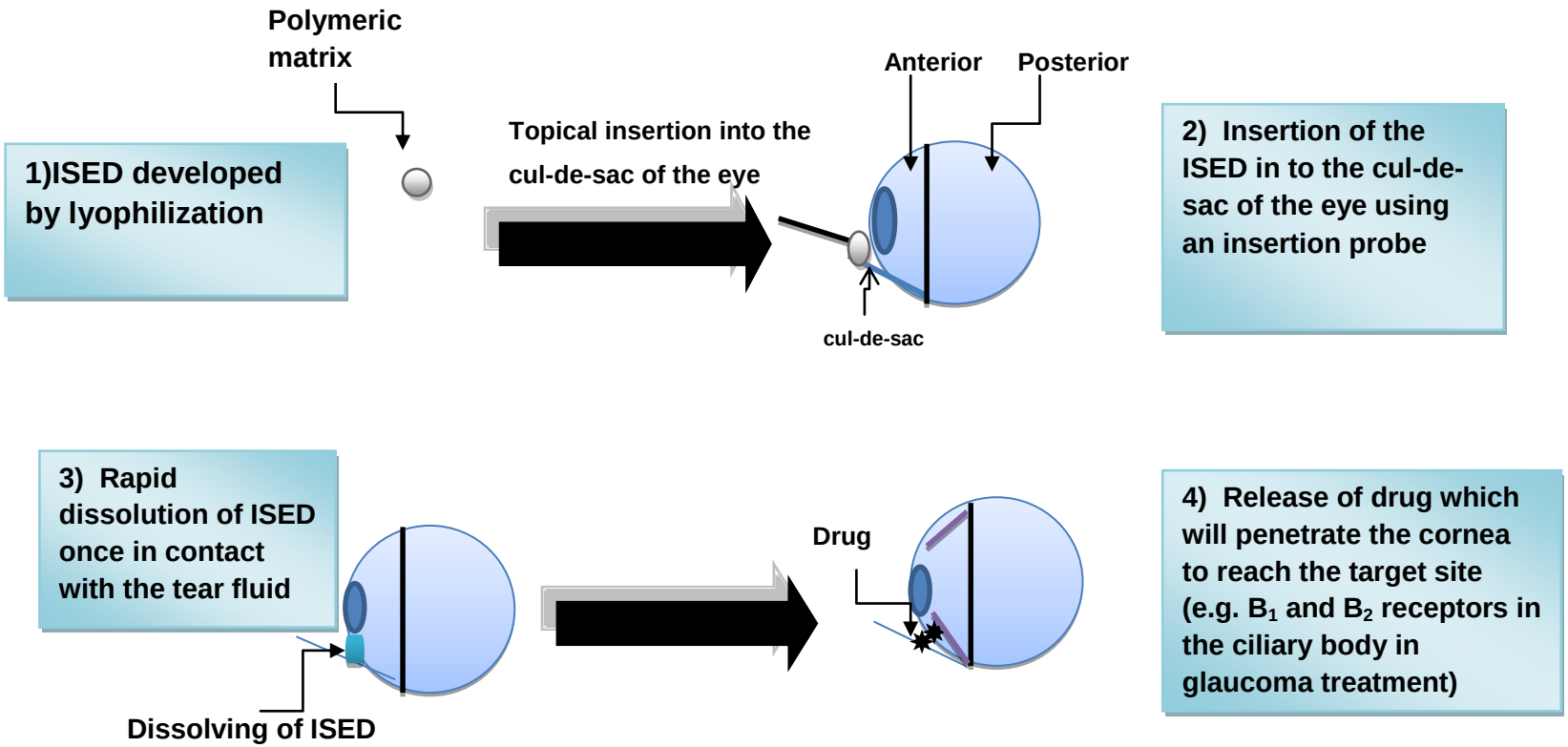


Figure 1.1: a) Schematic representing the proposed solid eye drop device and its operation once administered into the cul-de-sac of the eye

1.6 Advantages of a Fast Disintegrating System for Ocular use

Drug delivery systems research is making strides as investigators gain better insight to the factors that affect their mechanism of action. Fast disintegrating systems (also called '*fast-melt'* or *'fast-dissolving'*) as novel replacements for conventional solid tablets have been investigated. These systems are solid dosage forms which disintegrate rapidly, usually in the time frame of minutes or seconds. Most commonly applied for oral use, these systems quickly dissolve once exposed to salivary fluid and this minimizes the need for external water or fluid medium (Sastry et al., 2000; Mizumoto et al., 2005; Ciper et al., 2006). To help improve the administration, compliance and bioavailability of topically administered drugs the concept of fast disintegrating systems can be implemented to ocular drug delivery systems. In terms of solid fast disintegrating systems they offer the following advantages:

- Good feel of the product due to small and light structure.
- Reduction of force/pressure applied as in the case of tablets and thus minimized chances of damage and degradation (Tsinontides et al., 2004).
- Easier handling during transport and storage is noted (Carpenter et al., 1997).
- Aesthetically pleasing elegant cake-like appearance.
- Convenient form of administration and accurate dosing compared to liquid formulations (Virely and Yarwood, 1990).
- Rapid hydration of system due to porous structure thus reducing foreign body sensation in the eye.
- Preservatives are not required as in the case of conventional liquid formulations.

1.7 Application of Solid Fast Disintegrating Systems for Ophthalmic Delivery

The application of solid structures in the eye has gained some interest over the years (Ahmed and Aboul-Einien, 2007). A step ahead is the use of freeze-dried systems which have a quicker disintegration time compared to conventional tablets. This can be achieved by the lyophilization or freeze drying method which basically involves sublimation of water from a frozen sample from the solid to the gaseous phase (Tsinontides et al., 2004). The process involves selection of polymer-excipient concentrations and subjecting the solution to freezing followed by lyophilization of the sample. This results in the formation of the porous solid product which on exposure to fluid, it moves into the matrix with resultant dissolution and drug release.

Limited studies have been conducted on freeze-dried eye inserts. Among these, 'dry drops' made using the polymer hydroxypropylmethylcellulose (HPMC) showed lack of irritation in human eyes as observed in phase 1 studies (Diestelhorst et al., 1999). Lux and co-workers (2003), concluded that a HPMC lyophisilate displayed higher sodium florescein levels in the anterior eye of humans compared to liquid eye drops. In this study, improved bioavailability of sodium florescein was observed with a 1% hypromellose lyophisilate compared to eye drops (Abduljalil et al., 2008). A study by Refai and Tag 2011, investigated freeze-dried ocular chitosan mini-tablets for keratitis treatment. These mini-tablets reportedly displayed sustained release of the antiviral acyclovir ,bioadhesive properties and good permeation across the cornea in rabbits as well as resolving of herpal infection in the eyes of pigeons within 2 days. Thus, favourable results with fast dissolving ocular inserts can be seen.

1.8 Novelty of Study

- Rapidly soluble immediate release drug-loaded matrices have not been extensively studied for topical ocular use and are not available on the market.
- Screening of various polymers and excipients lead to the selection of a novel combination of components for the formation of the rapidly disintegrating yet robust structure.
- The use of an insertion probe to the eye drop eliminates the possibility of contamination upon insertion and allows for easier insertion procedure.

1.8 Aim of this Study

To synthesize a novel solid-like topical ocular drug delivery system which rapidly dissolves when exposed to lachrymal fluid for instant drug release and subsequent corneal penetration. The device will serve as an alternative to conventional liquid eye drops and allow for simpler administration in the hope of increasing patient acceptability.

1.9 Objectives of this Study

In order to achieve the aforementioned aim, the following objectives are outlined:

1. To investigate and elaborate on theoretical considerations in terms of development of an ocular pharmaceutical drug delivery system prior to practical evaluation.

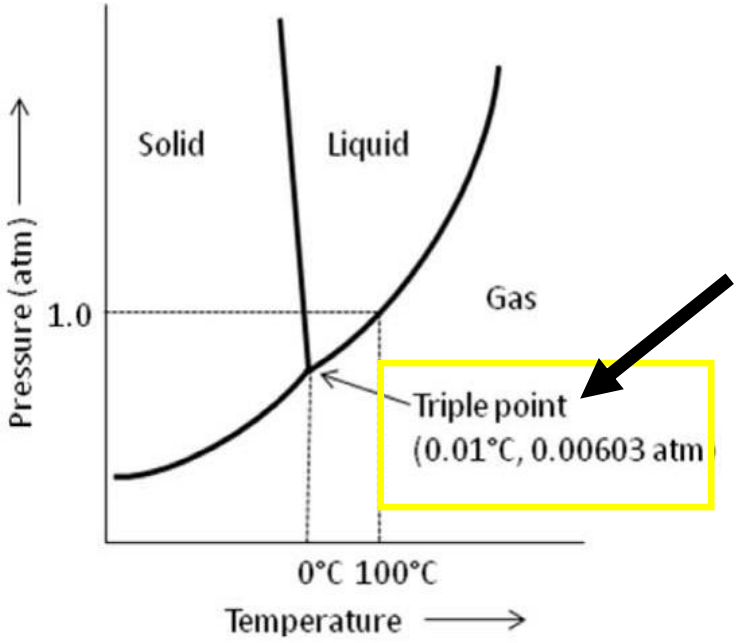
2. To select appropriate candidate polymer and excipient combinations for an instantly soluble system during preformulatory studies. Fabrication of an instantly dissolvable polymeric matrix by freezing and lyophilization of the polymeric solution.
3. To conduct initial tests on products to determine upper and lower limits of the formulation based on variables that are influential to the formulation properties.
4. To synthesize variants of the preferred formulation employing a Face Centred Central Composite Design (FCCCD) based on preliminary results. Subsequent characterization of the formulations generated by means of: textural analysis, disintegration testing, scanning electron microscopy (SEM), moisture content, *in vitro* drug release, *ex vivo* permeation by use of Franz diffusion cells and mathematical modeling.
5. To determine optimum parameters for synthesis of a single optimized formulation through constraint optimization.
6. To elucidate the in depth physicomechanical characteristics of the optimal formulation studies using the following tests: Fourier transmission infrared spectroscopy (FTIR), Differential Scanning Calorimetry (DSC), Thermal gravimetric analysis (TGA), porosity analysis, ocular tolerance testing and drug release kinetic modeling.
7. To subject the optimal formulation to gamma-irradiation sterilization and gauge the effects of this process on the properties of the formulation.
8. To carry out *in vivo* studies on the rabbit model to determine the safety and efficacy of the device in the eye. Ultra performance liquid chromatography (UPLC) for drug release and histological evaluation will be done.
9. To conduct a mini preliminary study for development of a bi-layered ISED with enhanced permeation capabilities.

1.10 Technology and Equipment Employed

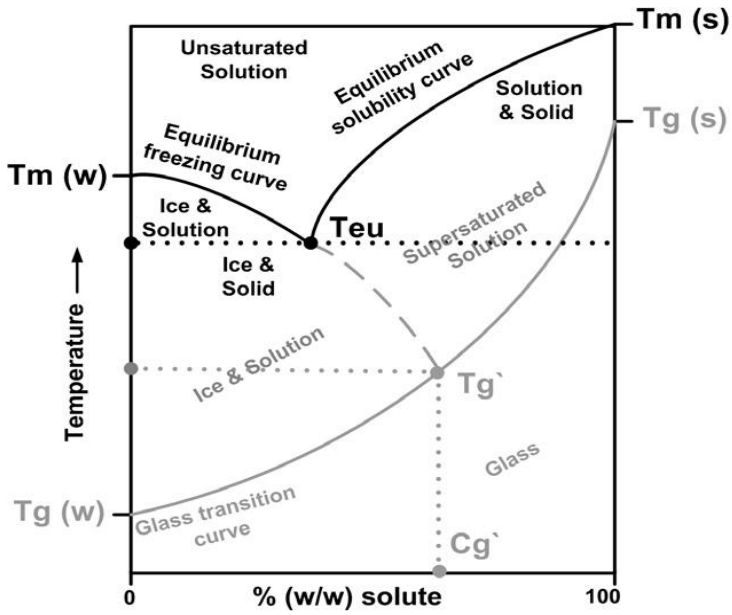
The lyophilization or freeze-drying method was employed for the formation of the ISED. As explained by Tsinontides and co-workers (2004), this process involves removing a solvent via sublimation which is the conversion of a solid directly into a vapour. This is achieved by having a pressure and temperature that is below that of the *triple point* of water (Figure 1.2 a and b). This is where all three phases of matter (solid, liquid, gas) exist at the same time (0.0075°C at 0.61 kPa 0r 610 Nm^{-2}, 0.01°C at 0.00603 atm). The water is removed from the sample by means of a vacuum and remains in a condenser in the form of a solid (ice). The resultant product is a porous solid. On exposure to a liquid, fluid is ingressed into the matrix at a rate depending on the properties of the components with resultant dissolution and drug release. The

lyophilizer, machinery employed for the process, comprises of shelves for sample placement which are connected to heating units, a freezing coil and a vacuum pump. Figure 1.2 c illustrates the basic structure of the machinery.

a)



b)

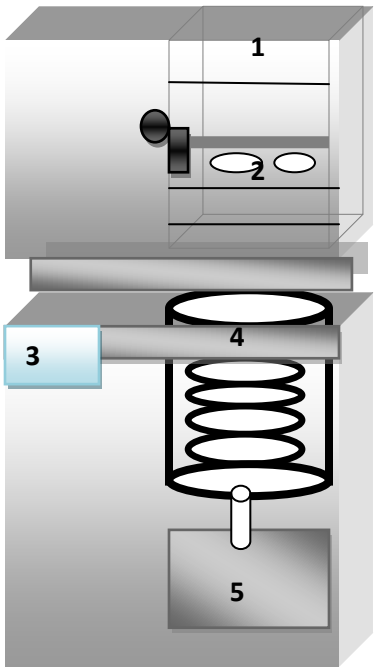


Teu - eutectic temperature is the lowest temperature at which the solute remains a liquid

Tg (w) and Tg (s) - glass transition temperature of water and solute

Tg - glass transition temperature of the maximally freeze-concentrated solution

c)



1.shelves
2.samples
3.control panel
4.collector chamber
5.vacuum chamber

Figure 1.2: Schematic of: a) phase diagram showing the triple point of water (Source: Baheti et al., 2010), b) State diagram of water (w)/solute (s) system (Source: Kasper and Fries, 2011) and c) the lyophilizer employed for freeze-drying of samples (adapted from Hunek et al., 2007).

There are 3 key steps in the lyophilization process:

1. **Freezing:** This involves freezing the product al low temperatures (-50 and -80°C). As elaborated by Kasper and Friess 2011, once the formulation is cooled, ice nucleation followed by ice growth occurs.
2. **Primary drying:** In this phase pressure is reduced (40-400 Torr) and heat allows sublimation to occur. A thermodynamic representation of this is expressed in equations by Pikal (1993):

$$\Delta H_s \times \frac{dm}{dt} = \frac{dQ}{dt} \qquad \textit{Equation 1.1}$$

Where:

ΔH_s is the heat of sublimation,
$\frac{dm}{dt}$ is the sublimation rate and
$\frac{dQ}{dt}$ is the rate of heat input

3. **Secondary drying:** This phase strives for the removal the water molecules that are not frozen. Finally, the product that remains is a solid porous structure.

1.11 Overview of Dissertation

The dissertation was constructed as follows in order to attain the previously outlined objectives: Figure 1.3 provides a summary of the rational approach to the development of such a system.

Chapter one provides an introduction to the study outlining the problem and rationale behind the development of the ISED. The limitations posed with current topical ocular drug delivery systems are described and the importance of novel systems that will ultimately improve compliance in patients.

Chapter two is a literature review of previously formulated topical ocular solid devices. This chapter describes various mini-tablets and their characterization in chronological order. Improvements to topical ocular systems are also mentioned

Chapter three is an initial summary of the significant theoretical considerations that are of paramount importance when considering the development of an ocular dosage form. These include pharmaceutical and patient factors. The preliminary investigations through polymer screening and tests for ideal formulation selection are explained. A candidate formulation with instant solubility, sufficient strength and simple reproducible manufacture was selected.

Chapter four follows on to design of experiments employing the face centered central composite design for the elucidation of optimal levels of constituents. Testing of responses such as textural profiling, drug release and disintegration time of the generated formulations was carried out for characterization. SEM, fluorescence microscopy and *ex vivo* permeation across excised corneas were also undertaken. Mathematical modeling was instituted for better understanding of the operation of the system.

Chapter five is the pinnacle of this research and discusses the optimization of the formulation through statistical analysis and characterization of this formulation based on thermal analysis, molecular transitions, porosity studies, kinetic analysis and ocular toxicity testing.

Chapter six provides a comparison between unsterilized and sterilized optimized products by gamma-irradiation as well as accelerated stability studies. Ocular systems need to be sterilized to avoid contamination of the eye and the effects of this on the product are tested. Accelerated stability studies were undertaken for further insight into the device stability upon storage.

Chapter seven involves *in vivo* studies conducted on the rabbit model. *In vivo* studies are essential to correlate the *in vitro* data and determine the feasibility of the system in the eye.

Aqueous humour samples were analyzed by UPLC and results interpreted. Histological evaluation of tissue was carried out to determine any untoward reactions of the system on the eye surface.

Chapter eight is a preliminary investigation of an eye drop system with enhanced permeability capabilities via institution of a Placket Burman design. A bi-layered system is also looked into and its potential ocular application.

Chapter nine, the final chapter concludes the study and provides recommendations for future applications of the system.

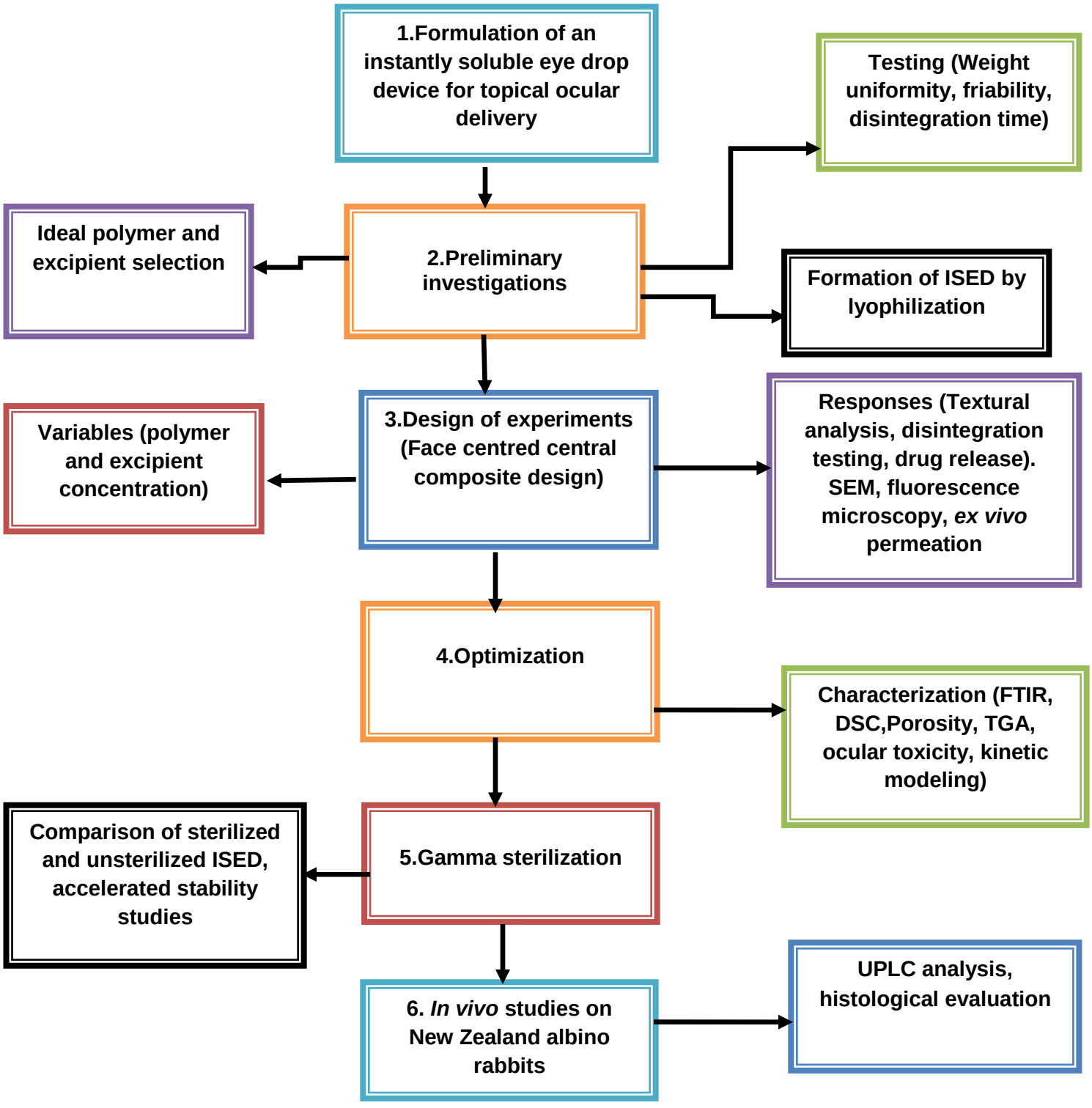


Figure 1.3: Flow diagram illustrating rationale approach to the development of an instantly soluble eye drop device.

CHAPTER 2
LITERATURE REVIEW : TOPICALLY ADMINISTERED 'MATRISERTS' DEVELOPED FOR DRUG DELIVERY TO THE ANTERIOR SEGMENT OF THE EYE

2.1 Introduction

Eyesight is a precious sense that most people may take for granted. It plays a vital role in our daily lives and enables us to function optimally. Thus, its significance must not be overlooked and full effort in ensuring preservation of this essential feature must be undertaken from a scientific perspective. On inspection, the human eye is divided into the anterior and posterior portions. Although anatomically separated; these areas function together and must be looked at in conjunction with respect to drug delivery. The anterior section consists of the cornea, iris, lens, ciliary body and aqueous humour. Liquid eye drop preparations are the most widely used dosage for topical ocular drug administration. However, topical ocular drug bioavailability to the anterior eye using eye drops is approximately 5% (Robinson,1993). This low level of drug results in reduced therapeutic effects since a minimal amount of drug reaches the actual target site. This is attributed to several hindrances to drug entry to the anterior chamber of the eye which include: nasolacrimal drainage, epithelial barriers of the cornea, clearance from the blood vessels in the conjunctiva, and reflex closure of the eye once the preparation is instilled (Ding et al., 1998; Anamolu et al., 2009; Kompella, 2010).

With respect to drug delivery in the eye there are mainly three important factors to consider: contact time, target area and patient acceptability (Weiner and Gilger, 2010). Firstly, the duration can vary from a few minutes for eye drops, up to months and years in the case of implant systems. Secondly, depending on whether the target is the anterior or posterior segment of the eye, different drug delivery systems are used. Topical systems are generally used for the anterior segment and implants or injections for the posterior segment (Weiner, 2010). Finally, in terms of patient acceptability, the system has to be easy to use, comfortable and convenient for the patient. This will assist in ensuring that the likelihood of the patient being compliant is increased as the use of complicated techniques will be avoided.

Over the years, various approaches have been attempted to have been made to optimize the bioavailibility of ocular topically administered drugs. Some of these approaches include; viscous vehicles and hydrogels (Rajas et al., 2010), facilitated transport via pro-drugs (Järvinen and

Järvinen, 1996), nanoparticles (Zimmer and Kreuter, 1995; Diebold and Calonge, 2010), contact lens delivery systems (Ali et al., 2007) and penetration enhancers (Kikuchi et al., 2005). These systems have been developed for and used to increase corneal contact time and allow for improved corneal drug penetration.

The ultimate goal of improving drug delivery systems is to ensure compliance so that the disease is effectively treated. Ocular diseases are common and often lead to blindness if left untreated. One such disease is glaucoma, which is characterized by an increase in pressure and this lead to damage to the optic nerve. In the United States of America (USA) alone, this disease is the 2nd cause of permanent blindness and is definitely a major concern worldwide (Reddy and Bodor, 1994; Quigley 1995; Mediero et al., 2009). Thus, this cannot be taken lightly and attention has to be given to this due to its prevalence and obviously devastating consequences.

Apart from improving bioavailability of topically administered ocular drugs, an improved administration form is required to ensure patient compliance and that drug reaches the target site. As mentioned above, eye drops may be difficult to instill and are easily flushed out thus resulting in poor bioavailability especially in elderly patients (Lang, 1995). Thus, innovative thinking has been steered towards the idea of novel drug delivery systems for ocular use. Solid vehicles have been investigated as probable delivery systems to overcome the challenges associated with the use of conventional eye drops (Gaudana et al., 2009). Previous reviews have delved into the structure, anatomy and physiology of the eye, and advances in devices developed for ophthalmic drug delivery. However, no significant focus has been given to ocular mini-tablet drug delivery systems. The purpose of this research therefore is to discuss the barriers to ocular drug delivery, limitations of conventional systems and summarize previously developed devices for topical administration to the eye and the advantages and limitations associated with these systems. The goal of the review is to discuss mini-tablets developed for ocular delivery in a chronological manner from early developments to present formulations. Recommendations for future considerations in the area of topical ocular delivery are also elaborated on.

2.2 Basic Anatomical and Physiological Considerations of the Eye

In order to gain an understanding of drug delivery to the eye, the first step is to inspect the basic structure of the eye. This is of interest since the effects of the system depends on where the actual target site is. The eye is a spherical structure that is made up of the sclera, choroid and retina. The outer sclera protects the inner layers, the choroid consists of blood vessels and is located inside the sclera (Kumaran et al., 2010). The retina is situated at the rear end of the eye and functions to detect light (Cunha-Vaz, 2004). The cornea is a protective barrier to the interior of the eye, has a small surface area and is comprises many layers. It consists of five layers namely: epithelium, Bowman's layer, stroma, Descemet's membrane and endothelium (Rathore and Nema, 2009). Two fluid media exist in the eye. The ciliary body located in the anterior segment, secretes the aqueous humour. It functions to balance the pressure and as a means of nutrient and metabolite exchange for this portion of the eye (Chang, 2010). The vitreous humour, found in the posterior section, is a gives the eye shape and support. These factors provide a basis for understanding the operation of this organ of which the anterior will be focused on.

2.3 Barriers to Ocular Drug Delivery

The eye remains impervious to foreign substances based on the anatomical and physiological defense mechanisms. It is thus protected from and prevents the entry of exogenous substances due to the barriers described hereunder.

2.3.1 Lachrymation, drainage and blood vessels

When drug is administered topically to the eye, reflex closure of the eye lid occurs due to a foreign-body sensation (Presl and Myatt, 2010; Bourlais et al., 1998). This results in the liquid preparations being forced out or even prevents entry into the anterior eye altogether. Furthermore, the lacrimal fluid flushes out instilled substances from the surface of the eye and fluid is then drained by the nasolacrimal duct (Saettone et al., 1994). Systemic drug absorption may also take place through vessels of the conjunctiva or from the nasal cavity after drainage (Urtti et al., 2006). Thus, drug is prevented from reaching the anterior part of the eye and this results in low bioavailability.

2.3.2 Corneal-aqueous barrier

The cornea serves as a protective layer of the eye and comprises of several layers (Figure 2.1) The epithelium is the initial layer (0.1mm) Patel et al., 2004; Barar et al., 2009). The multicellular

epithelium consists of 56 layers of cells and these tight junctions and hydrophobic regions pose a barrier to drug penetration (Mannerma et al., 2006). Therefore, evidently the cornea reduces drug absorption to the anterior eye. The residence time of drug on the eye surface as well as the permeability of drug across the cornea are two important factors that influence the drug absorption. Due to the corneal layer being lipophilic, poorly water soluble drugs have improved permeability then water-soluble drugs (Edwards and Prausnitz, 2009). The corneal route remains the main mechanism of drug entrance to the aqueous humour, despite the challenges encountered. The lachrymal and corneal barrier as explained, are the 2 most important challenges when looking at the drug delivery to the aqueous chamber. These mechanisms are inherent and cannot be changed so alternatives around them have to be given thought to.

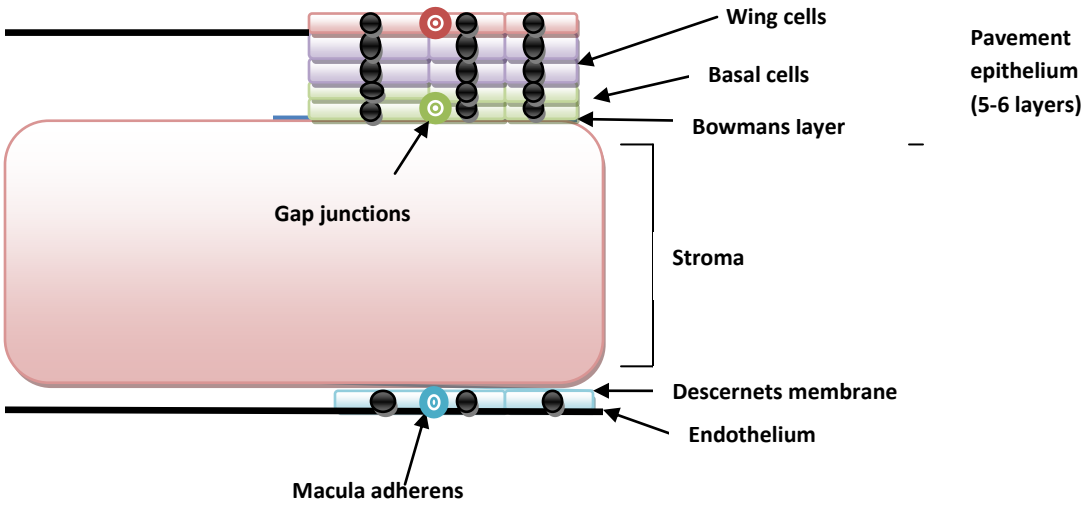


Figure 2.1: Schematic of the corneal layer comprising different layers (adapted from Mannerma et al., 2006).

2.4 Fate of Ocular Drugs after Administration: Distribution and Elimination

When drugs are applied topically to the eye, they permeate the cornea, followed by entrance to the aqueous humour and are then subsequently move to the ocular tissues (iris-ciliary body, lens, vitreous and retina). Although conventional eye drops are a common and convenient drug delivery system, they fail to have effective drug levels in the posterior segment of the eye (lens, vitreous, retina). This is due to the fact that eye drops result in a higher drug concentration in the anterior segment (cornea, conjunctiva, sclera, aqueous humor, iris-ciliary body) (Andres-Guerrero and Herrero-Vanrell, 2008). In terms of elimination, drugs are removed from both the anterior and posterior segments. For the anterior segment, drugs are removed by mainly 2

ways: aqueous humour turnover and anterior blood flow of the uvea (Hornof et al., 2005). In the case of the vitreous humour, elimination occurs via the anterior chamber or the posteriorly across the blood-retina barrier (Geroski and Edelhauser, 2000). Figure 2.2 illustrates the fate of topically administered ophthalmic systems.

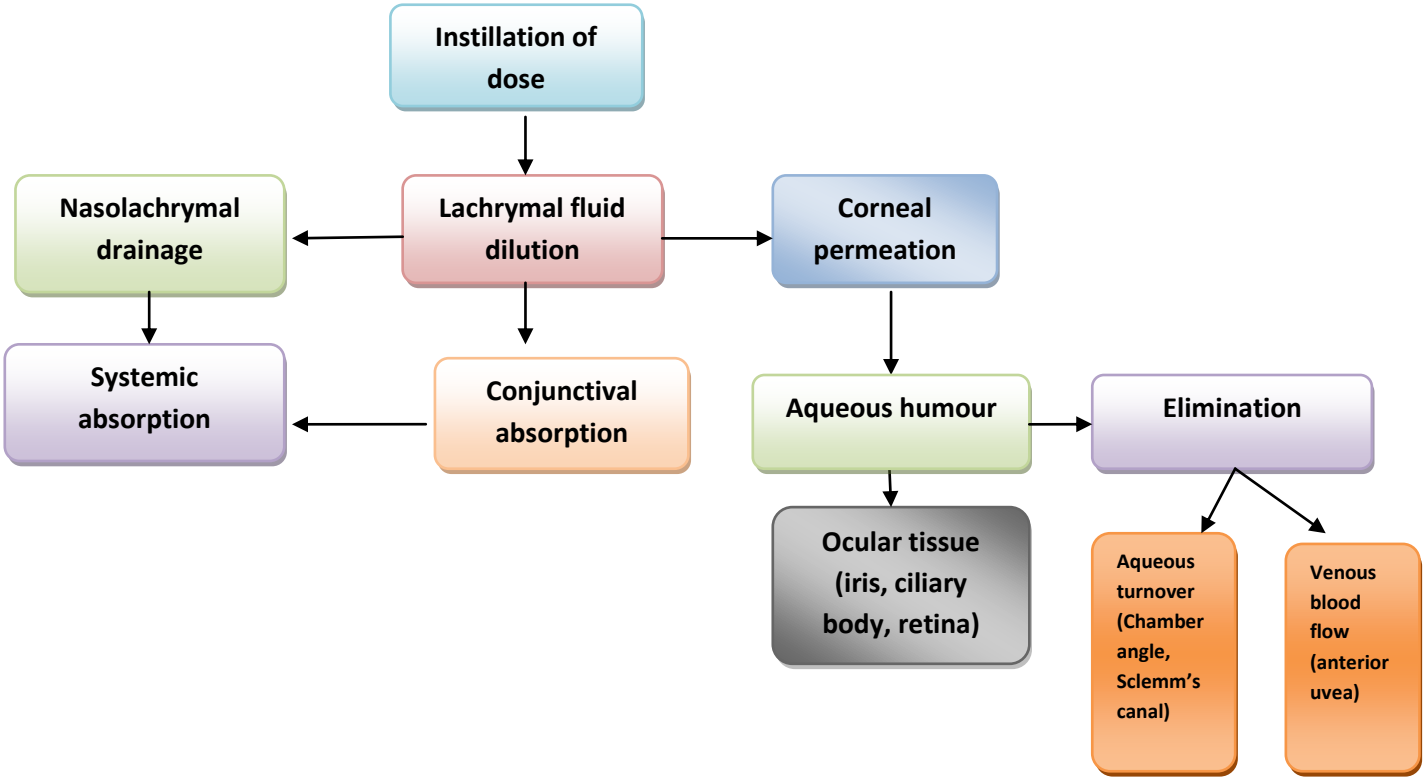


Figure 2.2: Schematic showing the path of topically applied ophthalmic drug delivery systems.

2.5 Possible Routes of Administration

A few routes of drug delivery into the ocular tissues exists and this depends on the intended target site. Topical and subconjunctival routes are mainly used for targeting the anterior segment of the eye. Intravitreal injections, periocular routes (retrobulbar, peribulbar, subtenon and subconjunctival routes) and implants are used for the posterior segment (Ahmed, 2003; Thrimawithana, 2010). Topical routes remain the most convenient since injections and implants are often invasive; and are associated with discomfort and pose the risk of retinal detachment and cataracts (Raghava et al., 2004). Each route of administration is associated with limitations as depicted in Figure 2.3.

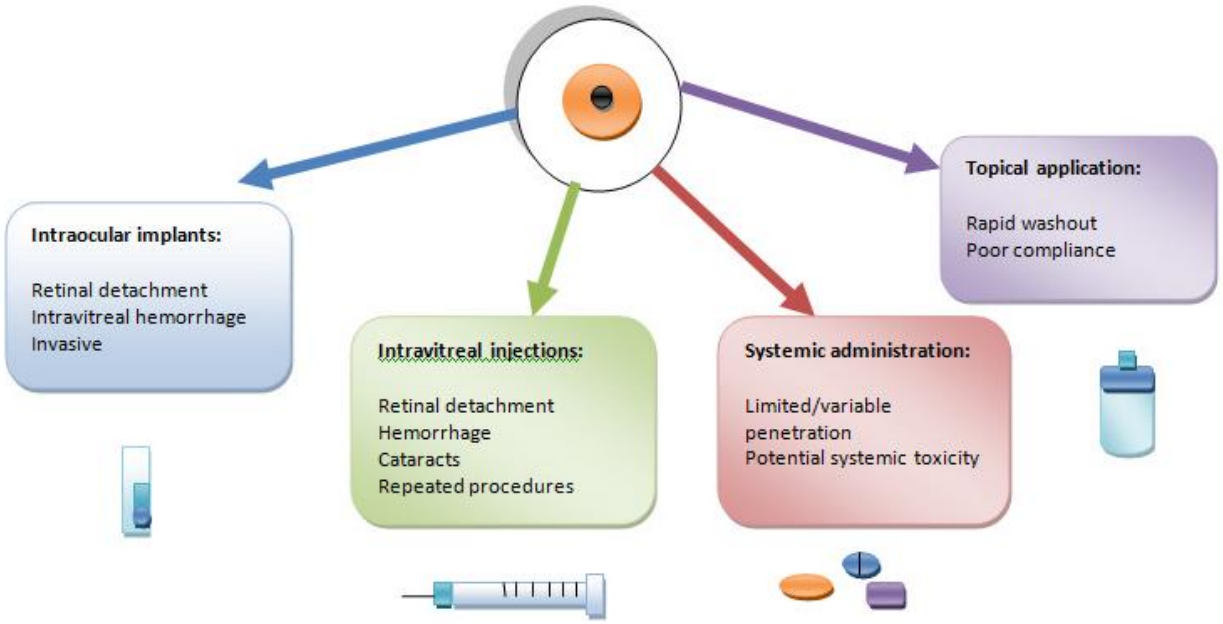


Figure 2.3: Schematic of the disadvantages associated with various ocular drug delivery systems (adapted from Davis et al., 2004).

2.6 Anterior Drug Delivery

2.6.1 Topical ocular delivery

Although eye drops are the most common system used for drug delivery to the anterior segment, they are disadvantaged due to limited ocular-surface contact time. This has been improved by the use of viscous vehicles such as gels. Lipophilic drugs permeate to the anterior chamber by residing on the epithelial layer followed by movement into the stroma (Kumaran et

al., 2010). Peak concentrations of drug in the anterior chamber are normally attained after approximately 30 minutes (Urrti et al., 1990, Wilson, 2004). Thereafter, the drug moves to the iris and ciliary body, where drug-melanin binding may occur resulting in gradual drug release and improved drug effect (Short, 2008). With regards to drug elimination from the aqueous humour, two main methods exist. Firstly, aqueous humour passage through the chamber angle and canal of Schlemm and secondly via the blood vessels of the uvea (Chowhan et al., 2002). Topically administered hydrophilic drugs may also be absorbed via another route *viz.* the conjunctiva to the posterior segment but this is not efficient enough and depends on the drug properties.

2.6.2 Subconjunctival administration

Subconjunctival administration is another method of topical drug delivery. Injections administered via this route results in drug permeation across the scleral route. Advantages of this route include: i) improved permeability of the sclera compared to the cornea (Hosoya et al., 2005), ii) large molecules (e.g. proteins) are able to pass through and iii) the lipophilic property of the drug does not affect scleral penetration (Janoria et al., 2007). However, these injections increase drug levels at the target area but cannot have entirely effective therapeutic levels in the case of certain drugs.

2.7 Steps to Enhance Ocular Bioavailability

Over the years, various approaches have been investigated to augment the bioavailability of topically administered ocular drugs. This goes beyond the use of simple 'traditional' suspensions or solutions to versatile agents. Some of these systems include but are not limited to the following selected examples:

1) **Controlled release ocular drug delivery systems.** These can be either erodible or non-erodible inserts. Erodible inserts dissolve once in contact with the ocular surface and examples include implants and ocuserts. However, they may cause discomfort for patience, require insertion or removal and this results in poor patient compliance (Short, 2008).
2) **Liposomes.** They are vesicular/ colloidal systems that are easy to synthesize. They have the disadvantage of instability and rapid clearance from the eye surface (Torchilin, 2005).
3) **Viscous vehicles and *in situ* forming hydrogels.** Viscous vehicles have been mentioned as a means of increasing corneal contact time of the formulation. However, their use is associated with a few disadvantages. For example, gels and ointments can blur vision and cause reflex blinking. Therefore, phase transition gels have been investigated. They are

initially in a liquid form upon instillation and convert to a gel once in the eye. The phase change can be due to temperature, pH or electrolytes (Kumar et al., 1994). Examples of polymers that display these properties include: carbomers, celluloses, poloxamers, and xyglucans (Najawande et al., 2007).

It can be noted that although various attempts have been made to circumvent ocular barriers, these systems are not free from disadvantages. Thus, newer systems are constantly being investigated in order to improve drug delivery to difficult sites such as the eye. This remains a challenging endeavor that researchers face.

2.8 Rationale for Development of Mini-tablets as Drug Delivery Systems

Mini-tablets are defined as tablets with a reduced diameter (2-3mm) in comparison to conventional tablets (Lennartz and Mielck, 1998). They have several advantages as oral drug delivery systems. These include: i) several mini-tablets can be used in combination to formulate a single dosage form either as a capsule or tablet, ii) act separately from the rhythm of food transport (Follonier, 1992), and iii) show repeatable coating with reduced amount of coating substance required due to the consistent area (Munday, 1994). Mini-tablets have various applications of which use as oral delivery systems are the most common. In a study, it was concluded that paracetamol could be tabletted in higher amounts if minitablets were produced Likewise, Lopes et al., (1996) developed and investigated biphasic delivery systems with a positive outcome. Recently, Tissen et al., (2011) produced mechanically robust 1 mm quinine hydrochloride mini-tablets for the first time, by direct compression (Figure 2.4). Taking the advantages into account, their initial use as oral systems led to the application of mini-tablets for ocular drug delivery.

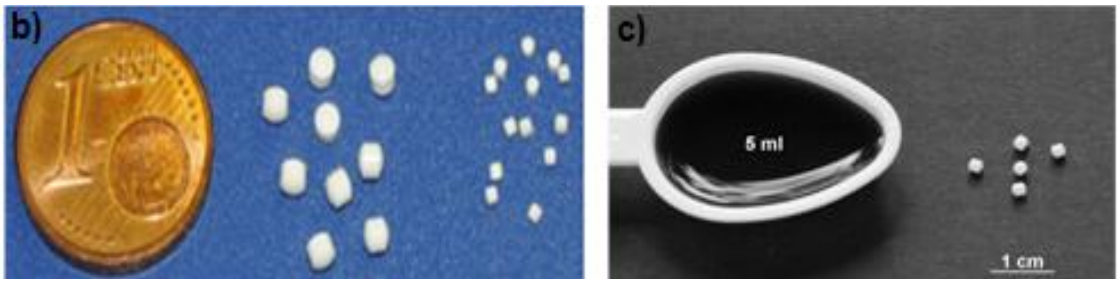


Figure 2,4: Diagram showing: a) difference in size between a one cent coin, mini-tablets (2mm) and mini-tablets (1mm) (Reproduced with permission from: Tissen et al., 2011) and b) 5 ml of a Brilliant Blue solution to simulate the required amount of hydrochlorothiazide (HCT) solution for a child weighing 5 kg (1 mg HCT/kg); right: five orally disintegrating mini-tablets (ODMT) with 1 mg HCT per mini-tablet (Reproduced with permission from: Stoltenberg and Breitkreutz, 2011).

2.9 Mini-tablets for Topical Ocular Drug Delivery

The shortcomings of and improvements made to eye drop formulations were outlined previously. Apart from improving contact time and bioavailability, patient compliance is an important factor to consider. The use of eye drops is convenient and ensures little discomfort for the patient. It remains the most common method of topical ocular delivery. However, patients often have difficulty instilling eye drops since they cannot focus the bottle and ultimately this leads to poor patient compliance ((Urtti and Salminen, 1995; Schwartz and Quigley, 2008). It is for this reason that a solid formulation will be more appropriate.

The following advantages of solid ophthalmic systems are apparent (Summarized from Saettone and Salimen,1995; Saettone et al., 1995; Diestelhorst et al., 1999):

- Ensuring accurate doses
- Systemic absorption reduction
- Improved patient compliance due to absence of continual instillation
- Longer residence times in cul-de-sac
- Less likely to be affected by nasolachrimal drainage system
- Reliability of drug release
- Lower incidences of visual and systemic side effects

Using the concepts of improving contact time and bioavailability of ocular preparations, mini-tablets for ocular drug delivery have been formulated. In terms of ophthalmic application, in the recent years, mini-tablets have gained momentum with early ophthalmic inserts prepared by

minitabletting to freeze dried sponge-like mini-tablets. Some advantages that these systems offer are outlined in Table 2.1:

Table 2.1. The advantages of mini-tablets as drug delivery systems for topical ocular use (Extracted from Refai and Tag, 2011; Ceulemans et al.,2001; Weyenberg et al., 2003; Weyenberg et al., 2005).

1. Easier patient administration due to absence of manipulating an eye drop bottle.
2. More convenient for elderly patients since they will not have to apply pressure to a bottle to expel the eye drop.
3. Avoids flushing out due to lachrymation and drainage once administered, since it is a solid form.
4. Increased corneal contact time due to the use of bioadhesive polymers.
5. Outer layers of mini-tablets swell when hydrated and as the liquid penetrates into the tablet gradual drug release occurs.
6. They are cost-effective and easily producible.
7. They do not result in irritation.

2.10 Commonly Employed Polymers in Ocular Mini-tablets

The initial approach for improving contact time in the field of ocular delivery was the selection of polymers that improves adhesion to the eye. Choice of polymers as drug carriers in mini-tablets is an important factor to consider since they contribute to the manner in which the delivery system operates and how drug is released. The increased viscosity of the polymers reduces drainage from the eye surface. Selected polymers employed should display certain properties for easier manufacturing and to avoid any harmful reactions or potential damage to the 'sensitive' eye ((Thakur and Kashiv, 2011). The following requisites are of importance:

- Biocompatible
- Biodegradable
- Non-toxic
- Inexpensive and readily available

Common polymers used in mini-tablets include: acrylates, celluloses, chitosan and drum dried waxy maize starch. Their advantages for ocular use are discussed below.

2.10.1 Cellulose derivatives

Cellulose polymers have been used artificial tear solutions and as viscosity-enhancing ophthalmic vehicles (Lin and Boehnke, 1999). These polymers display coil formation as temperatures increase and helix formation when temperatures are dropped (Calonge, 2001). Methylcellulose solutions form gels at higher temperatures (40-50°C), while

hydroxypropylmethyl cellulose (HPMC) displays this behavior at 75 and 90°C (Toda et al., 1996). Similarly, solutions of ethyl (hydroxyethyl) cellulose (EHEC) in also influenced by temperature but viscosity decreases with temperature (Ludwig, 2005). Apart from use in artificial tear formulations, these polymers have been employed in various ocular mini-tablets. Table 2 (a) depicts the structure of methylcellulose.

2.10.2 Acrylates

Poly(acrylic acid) and carbomers are mucoadhesive polymers employed in various ophthalmic formulations. Polyacrylates or carbomers are an example and have been proposed in the treatment of dry eye syndrome (Mortazavi et al., 2010). The mucoadhesive properties on the eye surface of these polymers are explained due to hydrogen bonding. The polymer interacts with mucin on the eye surface to form a hydrogel (Kumar and Himmelstein, 1995). Cross-linked poly (acrylic acid) (Carbopol®) is favourably and widely employed as a vehicle in the ocular field. (Table 2 (b)). In contrast to other polymers, Carbopol® displays excellent mucoadhesive effects on the eye surface. Ocular mini-tablets comprising Carbopol® 974P have been formulated and demonstrated good corneal adhesion (Davies et al., 1991).

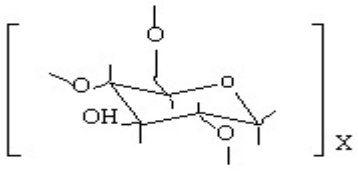
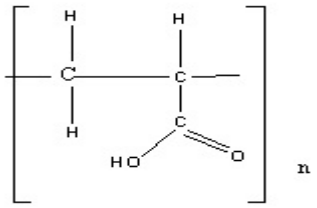
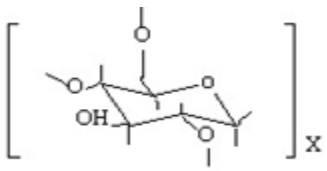
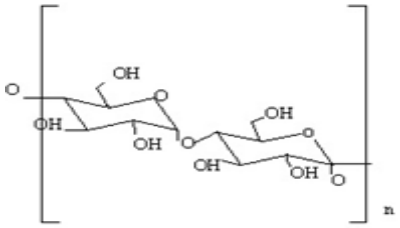
2.10.3 Chitosan

Chitosan is a naturally obtained cationic polymer that has been widely studied in ocular drug delivery due to its favourable properties (Motwani et al., 2008; Rajendran et al., 2010). It is a biocompatible, nontoxic mucoadhesive polymer that has shown good ocular tolerance. Its mucoadhesive feature is due to its positively charged amine groups which display an interaction with the negative sialic acid mucus layer and thus prolongs contact time with the eye surface (Dudhani and Kosaraju, 2010). A disadvantage of this polymer is its water insolubility. However by decreasing the molecular weight through depolymerization an improved solubility is achieved (Lehr et al., 1992). In addition, the antibacterial properties of chitosan are important for ocular use. Chitosan displays activity against a variety of organisms (yeasts, moulds, bacteria) and this depends on the type of chitosan used. For example, chitosan antibacterial properties are advantageous in conditions such as keratoconjunctivitis sicca. Chitosan mini-tablets were found to have good antimicrobial properties and bioadhesive strength as well as being a favourable sustained release drug delivery system in the eye (Gratieri et al., 2010). Table 2 (c) shows the typical chemical structure of chitosan.

2.10.4 Drum dried waxy maize starch (DDWMS)

The absorption of drugs has shown to be improved by the use of polymers that improve contact time between drug and the absorption site. These are usually high molecular weight hydrophilic, swellable polymers that contain hydroxyl, amine and carboxyl groups that favour adhesion (Gad, 2006). Polymer-mucus interaction occurs when they swell subsequent to water attraction. Starch is a carbohydrate comprising of several glucose units. Pure starch is water insoluble and consists of the linear helical amylase and branched amylopectin (Olayemi et al., 2008) (Table 2.2 (d)). Modified starch derivatives are prepared by modifying the native starch thereby changing their properties. Drying methods to make starch cold water soluble include drum drying, extrusion or spray drying (Yan and Zhengbiao, 2010). Improved absorption of insulin in rabbits has been demonstrated by Callens and co-workers (2003), with the use of DDWMS (amylopectin) via the nasal route. The use of ocular mini-tablets comprising drum dried waxy maize starch displayed increased residence time and good ocular tolerance.

Table 2.2. Chemical structures of common mini-tablet polymers

Polymer	Structure
a) Methylcellulose	
b) Carbopol®	
c) Chitosan	
d) Starch (amylopectin)	

2.11 Mini-tablets Developed for Topical Ocular Drug Delivery

2.11.1 Timolol-containing mini-tablets

Saettone et al. (1994), developed timolol maleate-loaded mini-tablets by compression in which they varied the acrylic coating to control the drug release. Acrylic polymers used to coat the mini-tablets resulted in the attainment of zero-order kinetics. Mini-tablets were prepared using glycerol palmito stearate and hydroxylpropyl-cellulose. They were tabletted using a single punch press of diameter 3.5mm. Mini-tablets contained either 0.34 or 0.68 mg of the active

respectively. Tablets were coated with 5%w/w of acrylic polymers. Uncoated mini-tablets showed diffusive or anomalous release. Samples that comprised coating which had a reduced permeability consisting of 80:20 Eudragit®-RS and Eudragit®-RL (ACR-RS/ACR-RL) showed zero-order kinetics, for which the release rate decreased with an increasing amount of coating. Coating with a low amount of the more permeable polymer mixture comprising 60:40 ACR-RS/ACR-RL, resulted in anomalous, non-Fickian release kinetics. Tablets containing hydroxypropylcellulose showed fast release of drug due to swelling effect in the dissolution medium. Mini-tablets were sterilized by gamma radiation and it was shown that drug content was unaffected by this process. The time taken to release 30% of TiM from type 1 and type 2 tablets was in the range of 1-47hours. Shortcomings of this study were that the tests were limited to *in vitro* tests only (i.e. there was no involvement of *in vivo* tests).

2.11.2 A Carbopol® and DDWMS mini-tablets

A polymeric combination containing Carbopol® 974P and DDWMS was developed by Ceulemans et al. (2001) (Figure 2.5). A Carbopol® 974P, Na-stearyl fumarate and DDWMS dispersion was formulated and compared to a mini-tablet. Sodium flourescein was used as a fluorescent marker for *in vivo* evaluation. The mini-tablet became fully hydrated after 2 hours and transformed into a concentrated gel. In comparison to the dispersion, the mini-tablet increased fluorescence in the anterior chamber. The mini-tablet was seen to be advantageous as a delivery system for infections of the anterior portion of the eye or glaucoma.

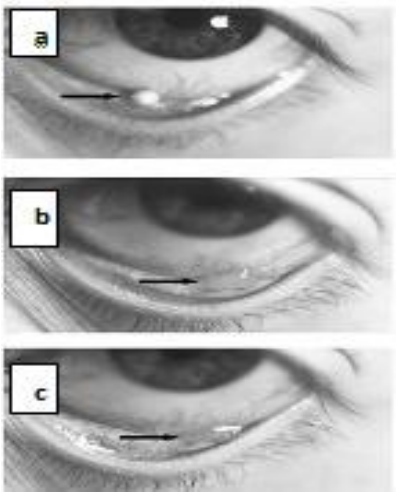


Figure 2.5: Image representing the hydration of the mini-tablet once inserted into the eye: a) 0 hours b) 2 hours and c) 4.5 hours after insertion (Reproduced with permission from: Ceulemans et al., 2001).

2.12 Evaluation of physical properties and irritation potential of Carbopol® 974 P and DDWMS mini-tablets

The effect of the force of compression on the physical properties, drug release and the *in vivo* results of mini-tablets was gauged by Weyenberg et al. (2003) (Figure 2.6). The bioerodible mini-tablets comprising of Carbopol® 974 P (5%w/w), DDWMS (92%w/w), sodium stearylfumarate (1%) and sodium fluorescein (2%w/w) were produced at different compression forces. Increasing the compression force caused an increase in crushing strength wheras a decreased friability, water uptake and porosity of the mini-tablets was noted. Mini-tablets made at higher forces resulted in a longer residence of sodium fluorescein in the tear film. The irritation potential of mini-tablets was determined by means of a slug mucosal-irritation (SMI) test by Weyenberg et al. (2003) Pharmacokinetics of lachrymal fluid of ciprofloxacin were determined in human volunteers after topical administration of a mini-tablet and a liquid eye drop preparation. Results of the mucosal-irritation test demonstrated non-irritating properties of the mini-tablet that it was well tolerated.

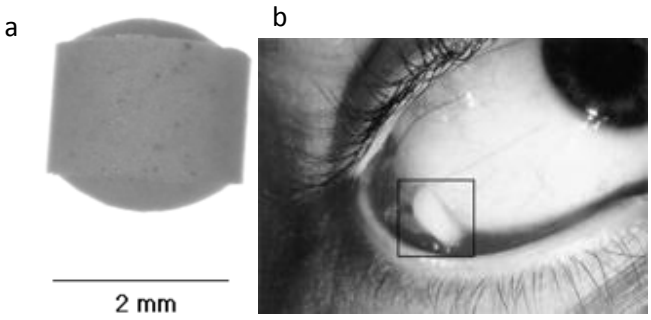


Figure 2.6: Schematic of: a) ocular minitablet (6mg weight, diameter 2mm) prepared with drum-dried waxy maize starch/Carbopol 974P/sodium stearylfumarate/ciprofloxacin hydrochloride (90.5/5/1/3.5, w/w) and b) macroscopic examination of the gelling minitablet in the eye, 4 hours after application (Reproduced with permission from: Weyenberg et al., 2003).

2.12.1 Ciprofloxacin-loaded granules compressed into minitablets

Weyenberg et al., (2005), prepared ciprofloxacin-loaded DDWMS and Carbopol® 974P granules for compression purposes in order to obtain ocular mini-tablets. To produce the mini-tablets in higher quantities, it was necessary to improve the flow properties of the powders. This was achieved through the dry granulation process by means of a roller compactor. The physical properties of the bioadhesive granules were optimized by adjusting the speed and force of the roller. Minimal flow time and friability properties were yielded by milling the maximum force and at the lowest speed. An improved compactibility correlated with smaller particle size since a

higher surface area was available for bonding if a finer particle size was employed. The tablet strength was significantly higher, at lower roller compaction forces, employed for the preparation of the granules. Based on the tablet strength, friability and dissolution results, a low compaction force and a high roller speed were shown to be preferable. The mini-tablets showed absence of mucosal irritation in volunteers. *In vivo* studies for this system are necessary for further insight.

2.12.2 Amioca® and Carbopol® mini-tablets

Weyenberg et al. 2006, evaluated new powder mixtures in tablets to obtain an improved fornix residence time, compared to the tablets containing DDWMS with 5%w/w Carbopol® 974P. Direct compression was used to form mini-tablets of diameter 2mm, consisting of sodium fluorescein as model active ingredient were manufactured and sterilized by gamma-irradiation. Carbopol® concentrations in the co-spray dried powder mixtures and gamma-irradiation had no significant influence on the crushing strength and friability of the mini-tablets evaluated but did affect the *in vitro* results. The slowest release was obtained with tablets containing 25% Carbopol 974P. In terms of co-spray dried Amioca® and 15%w/w Carbopol® 974P, a slower release was achieved compared to the physical mixtures of DDWMS or Amioca® starch with Carbopol® 974P. The mini-tablet was tolerated by humans and showed a lack of irritation. The gelling behavior of the mini-tablets was an advantage since it resulted in an extended residence time. (8hours). For the mini-tablets prepared with the physical mixture, fluorescein was measured only up to 6 hours, while with co-spray dried mini-tablets, the concentration in the tear film remained > 50 ng/mL between 4 and 11 hours after post insertion. The *in vivo* release of the ocular mini-tablets was prolonged by employing the co-spray dried mixture Amioca® starch with Carbopol® 974P instead of physical mixture of DDMWS.

2.12.3 Gentamicin ocular mini-tablets

Gasthuys et al. (2007), evaluated the behaviour of ocular mini-tablets compared to eye drops in ponies. The mini-tablets were 2mm in diameter and prepared by compression using DDWMS, Carbopol® 974P, sodium stearylfumarate and 5% gentamicin sulphate. Insertion of 2 mini-tablets into the bulbar conjunctiva of the right eye and liquid drops in the left eye were administered (Figure 2.7). The tablets swelled after insertion within 5 seconds. An increase in drug concentration occurred after the administration with subsequent reduction in all cases. The average drug concentration declined to 10.8lg/mL after 60 minutes, while a minimal concentration (<3lg/mL) was obtained after 2 hours. The mini-tablets were well tolerated and resulted in a high gentamicin sulphate levels in the lachrymal fluid during an 8 hour period



Figure 2.7: Digital image depicting *in situ* gelling after insertion of two ocular mini-tablets (arrow) on the ventral bulbar conjunctiva of the right eye in a sedated pony (Reproduced with permission from: Gasthuys et al., 2007).

2.12.4 Mucoadhesive microdiscs formulated in a rapidly dissolving tablet

Choy et al., (2008), synthesized microparticles < 10μm in diameter by an emulsification method with polymers poly(lactic-co-glycolic acid) (PLG) and poly(ethylene glycol) (PEG). Microdiscs were applied because their flattened surface can increase the contact area with the mucus surface of the front of the eye. A suspension and a tablet form of microparticles were formulated (Figure 2.8). The aim was to investigate the effect of the formulation on the ability of the microparticles to be retained on the eye surface. Mannitol tablets with mucoadhesive microdiscs had improved retention times than the other formulations. Fluorescence images depicted the the microdiscs remained in the fornix of the eye for approximately 1 hour. Thus, microdiscs formulated in a dry tablet form were able to have a prolonged residence time and thus were a potential opthalmic drug delivery system.

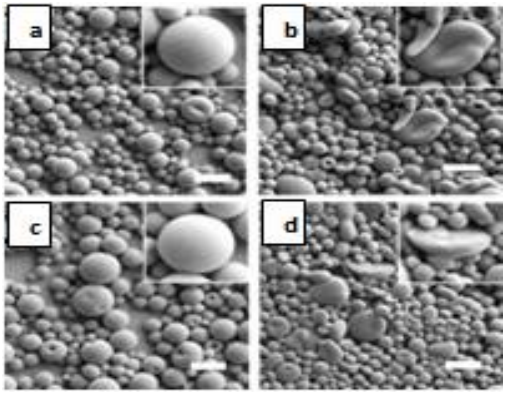


Figure 2.8: Scanning electron micrographs of microparticles prepared for ocular adhesion studies: a) PLG MS; b) PLG MD; c) PLG/PEG MS; d) PLG/PEG MD. (Scale bars 10 μm) (Reproduced with permission from: Choy et al., 2008). MS-microspheres MD-microdiscs.

2.12.5 Pregelatinized starch and Carbopol® mini-tablets

Bozdag et al. 2010 developed ocular bioadhesive mini-tablets containing gentamicin and vancomycin as model drugs. Pregelatinized starch (PS) and Carbopol® were used as polymers and they were either physical or cospray-dried mixtures. Granules were formed using the slugging method followed by mini-tablet compression (2mm diameter) and gamma irradiation sterilization at a dose of 25kGy. Irradiation sterilization did not have an effect on the property formulations and electron paramagnetic resonance (EPR) showed the presence of radicals up to one month post sterilization with no alteration of drug properties. The mini-tablets absorbed water to form a gel which slowed the drug release. Drug release results for preparations with physical powder mixtures of PS and Carbopol® 974P (96:4) were faster than the cospray-dried formulations of starch with Carbopol® 974P (95:5 and 85:15). Drug was detected up to 6 hours which is advantageous for a sustained release effect. The slug mucosal irritation (SMI) test indicated minimal irritant effects of the mini-tablet and *in vivo* evaluation is necessitated for confirmation of this.

2.12.6 Ocular mini-tablets for the treatment of microbial keratitis

Bioadhesive ocular gatifloxacin-loaded minitablets using sodium alginate, calcium gluconate and chitosan were prepared by Gilhotr et al. (2010). The resulting mini-tablets had a drug content of 4mg and a surface area of 50 mm^2. The ocular mini-tablets were sterilized by gamma radiation after packaging. The drug release of mini-tablets was improved by higher ratios of calcium gluconate. Mini-tablets containing 80%$^{w}/_{w}$ sodium alginate and 16%$^{w}/_{w}$ chitosan without calcium gluconate exhibited sustained drug release for the longest period of time which was 24 hours. The ocular tolerance studies indicated that the formulation was well tolerated in rabbits and can be safely administered to humans. The alginate-chitosan mini-tablet was found to have good antimicrobial activity. Formulations with higher chitosan content had improved bioadhesive strength and force of adhesion. It was concluded that this was a good vehicle for the treatment of bacterial keratitis and conjunctivitis.

2.12.7 Ciprofloxacin loaded mini-tablets

Mortazavi et al. (2010) prepared and evaluated ciprofloxacin-containing mini-tablets to obtain sustained and controlled release of the drug. Ciprofloxacin was used as the model drug and sustained released polymers such as hydroxypropylmethyl cellulose, sodium carboxymethyl cellulose, ethyl cellulose, and hydroxyethyl cellulose and Carbopol® 974P were used. Direct compression was used to obtain mini-tablets of 3mm diameter. Carbopol® increased the

adhesive nature in all the formulation and contributed to the integrity and compactness of the mini-tablets. Results indicated that the choice and concentration of cellulose derivatives used had affected the rate of drug released. *In vitro* studies showed that formulation containing 72%w/w ethyl cellulose, 4%w/w Carpobol® 974P, 1%w/w NaSF, 20%w/w mannitol and 3%w/w ciprofloxacin, demonstrated higher drug release over a period of 5 hours. *In vivo* studies were not carried out.

2.12.8 Sponge-like acyclovir mini-tablets

A novel freeze-dried chitosan ocular mini-tablet containing acyclovir was formulated by for keratitis therapy (Refai and Tag, 2011). The polymers tested were sodium carboxymethylcellulose (NaCMC), hydroxypropylmethylcellulose (HPMC), xanthan gum, chitosan and Carbopol® 943P. Tablets of 2mm diameter were prepared by forming solutions of different polymers followed by freezing and lyophilization of the product (Figure 2.9). Chitosan minitablet was selected as the candidate polymer due to its ability to sustain drug release and outstanding mucoadhesive property for animal studies in rabbits. The tablet showed a penetration across the corneal layer in comparison to a marketed Zovirax® eye ointment. Bokhara Trumpeter pigeons diagnosed with herpal infection of the eye were treated by insertion of one mini-tablet and within 2 days complete recovery of symptoms was observed. Thus, the use of the lyophilized matrices allowed for rapid hydration of the system and sustained drug release.

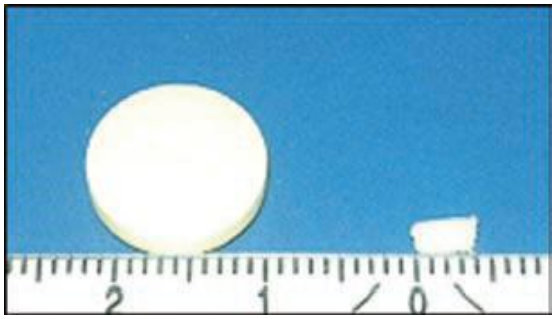


Figure 2.9: Digital images of: a) mini-tablet with a dimension of (4 × 2 mm) in comparison to a conventional oral tablet having a diameter of 12 mm (Reproduced with permission from: Refai and Tag, 2011).

2.13 Examples of Various Additional Solid Devices Developed for Topical Ocular Delivery

In addition to mini-tablets being fabricated for improved ocular drug delivery to the anterior eye, other solid devices have been investigated. Examples of these improved sophisticated systems are discussed in Table 2.3.

Table 2.3. Various additional solid ophthalmic devices

Device/insert	Description	Polymers	References
Bioadhesive ophthalmic drug inserts (BODI)	Adhesive rods containing gentamycin. Showed good tolerance, decrease expulsion, increased residence time and controlled drug release.	HPC, EC, PAA, Cellulose acetate phthalate (CAP)	Gurtler et al., 1995
Collagen shields	Collagen corneal shields allowed an increase in tobramycin penetration into the anterior chamber of the eye compared with hydrophilic soft contact lenses.	Crosslinked porcine sclera collagen	Unterman et al., 1988; O'Brien et al.,1988
Dry drops	Preservative-free freeze-dried device that hydrates in the tear film. The safety and lack of irritation were noted.	HPMC	Diestelhorst et al., 1999
Episcleral implants	LX201 (Lux Biosciences Inc., Jersey City, NJ, U.S.) is an episcleral implant designed to deliver cyclosporine A to the ocular surface for one year. The implant is flat on the bottom in contact with the episclera, and the top is rounded, in contact with anterior surface. It delivered continuously potentially therapeutic drug levels to the lacrimal gland.	Silicone matrix	Kim et al., 2005
Gelfoam	Absorbable gelatin sponge in the form of a matrix system. *In vivo* results showed that the device was more effective than two conventional pilocarpine dosage forms (eye drops and gel) in prolonging the duration of drug effect.	Cetyl ester wax in chloroform	Simamora et al., 1998
Lacrisert	Rod shaped water-soluble cul-de-sac insert (1.27 mm diameter, 3.5 mm long) indicated for moderate to severe dry eye syndrome. Lacrisert® has not been applied as a drug delivery vehicle.	HPC	Bawa, 1993 Kuno and Fujii, 2011
Minidisc or ocular therapeutic system (OTS)	Polymeric, monolithic, matrix-type device, which is a contoured disc with a convex front and concave back surface in contact with the eyeball. It offers the potential of resolving patient compliance issues of comfort and dosing frequency.	Hydrophilic or hydrophobic disc	Bawa, 1993
New or novel	Flag attached to paper-covered handle (Figure 10a). On	Polyvinyl alcohol (PVA)	Lawrenson et al., 1993

ophthalmic delivery system (NODS)	application, flag detaches, dissolves and releases the drug. Improved bioavailability by this system allows for reduced drug concentrations to be used.		
Ocuserts	Insoluble device with a matrix and reservoir (Figure 10b). Ocusert® provides uniform controlled release of pilocarpine..	Ethylene-vinyl acetate copolymer (EVA), pilocarpine in alginate gel, di-(ethylhexyl)phthalate	Quigley et al. 1975
Ophthalmic inserts	Rod-shaped mucoadhesive ophthalmic inserts fitting the upper or lower conjunctival fornix. The Inserts may be considered for ocular bacterial infections (e.g. trachoma)	Silicone elastomer,Sodium chloride,PAA, polymethylacrylic acid	Chetoni et al., 1998
Punctal plugs	Insertion of plugs into the puncta is an approach used to prolong the retention time and increase absorption and efficacy after instillation of eye-drops. They have been used for the treatment of dry-eye syndrome. QLT Inc. (Vancouver, Canada) and Vistakon Pharmaceuticals, LLC have developed punctal plugs for latanoprost and bimatoprost, respectively. Both have shown no dose-response for IOP reduction.	Silicone, collagen, acrylic polymers	Tai et al., 2002; ClinicalTrials.gov Safety and efficacy of a glaucoma drug delivery system
Soluble ocular inserts (SODI)	A small oval wafer that softens in the inferior cul-de- sac (10-15 seconds) and fits the shape of the eye globe.	Acrylamide, N-vinyl pyrroiidone, ethyl acrylate	Bawa, 1993
Subconjunctival Implants	A subconjunctival insert containing latanoprost (Latanoprost SR insert) in Phase I clinical study developed by Pfizer, Inc. (New York, NY, U.S.) is composed of a tube containing a latanoprost-core. One end of the tube is capped with an impermeable polymer, silicone, and the other end is capped with a permeable polymer. Duration of latanoprost release is designed for 3–6 months.	poly (DL-lactide-co-glycolide) (PLGA), (PVA)	ClinicalTrials.gov Safety study of latanoprost slow release insert (Latanoprost SR)

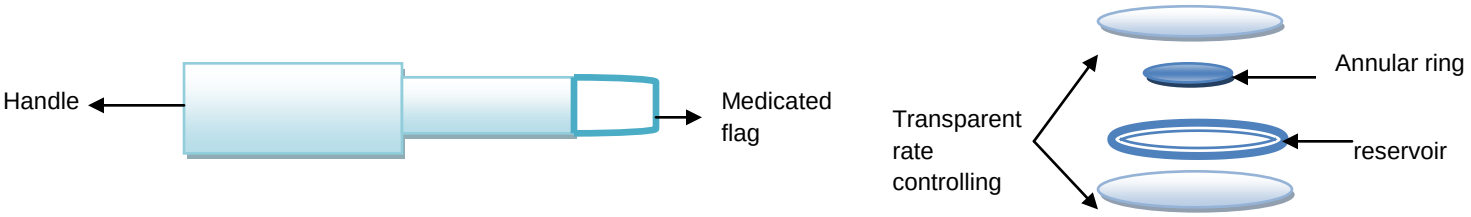


Figure 2.10: Schematic of: a) NODS device; and b) Ocusert (adapted from Bourlais et al., 1998).

2.14 Developments and Future Outlook

It is evident from this research that the eye poses a challenge to the drug delivery arena. Advanced systems are constantly being sought out and tested for improved topical ocular drug delivery. Innovations are necessary to assist in overcoming the limitations of current systems and offer hope in terms of treatment of debilitating ocular diseases. Examples of such forward steps include:

- Eye misters and microdroplets - Eye misters and microdroplets have been described reported to provide better ocular drug delivery than eye drops. A study revealed that higher levels of vitamin B12 were found in the aqueous humour due to the mist application to the eye by means of a nebulizer compared to an eye drop preparation (Kahn, 2005).
- Iontophoresis - This is a concept that moves charged compounds (e.g. low molecular weight drugs) into ocular tissue and studies have indicated significant increase of bioavailability compared to liquid drops (Eljarrat-Binstock and Domb, 2006).
- Drug-eluting contact lenses - Contact lenses have been shown to deliver drugs for longer periods and allowed improved residence time and drug levels in the anterior chamber in comparison to topical drop application (Ciolino et al., 2009).
- Nanoparticles - In a study conducted by Baba et al. (2011), nanoparticles of dye fluorescein diacetate (FDA) were shown to have high penetration rate into the cornea due to the small size of particles.

Although research efforts in improving topical ocular drug delivery has been an ongoing venture, commercialization of products has been minimal. For example, the commercialization of only one non-invasive insert (Ocusert®) developed by Alza corporation occurred in 1974. However, it was not widely used due to difficulty in inserting and ejecting the device from the eye, as well as irritation during insertion (Sihvola and PuustjÄRvi, 1980). This led to commercial failure which

amounted to the withdrawal of the product from the market (Weiner, 2010). In 1982, Lacrisert® was approved for dry eye treatment as discussed in table 3. As aptly pointed out by Kumaran et al. (2010), such setbacks may be attributed to factors such as reluctance of manufacturers, health care providers and receivers to move away from traditional systems, high cost implications and flaws of the delivery system itself at the application level. Numerous studies on advancements have been published with little marketed success. Although the technology-age dawns upon us, older, less complicated drug delivery systems are still successful on a commercial level. Modifications and improvements to simple dosage forms that are known to have beneficial properties, such as solid 'matriserts', may be the answer to consider.

2.15 Concluding Remarks

Topical drug delivery systems for treatment of conditions of the anterior segment of the eye remains the most common and convenient route for patients. On the other side of the coin, patients often find frequent instillation of medication challenging and results in poor compliance. Numerous systems have been developed and others are still being investigated as seen from this review. Solid ophthalmic dosage forms, display interesting and significant *in vivo* results and allow for therapeutic levels to be obtained over an extended period of time in the anterior chamber. As seen from this chapter, mini-tablets are favourable ocular drug delivery systems with mucoadhesive properties to treat infections and diseases that require continual eye drop instillation in order to maintain therapeutic drug levels. More and more people are faced with ocular conditions that affect vision that can ultimately lead to irreversible vision loss. Therefore, the development of novel ocular drug delivery systems, and more importantly, their success is of paramount importance and will surely benefit patients who suffer from ocular diseases.

CHAPTER 3
PREREQUISITE THEORETICAL CONSIDERATIONS AND PREFORMULATION INVESTIGATIONS

3.1 Introduction

In order to formulate a topical ocular drug delivery system several pivotal factors need to be taken into consideration. These are divided into three key areas namely: anatomical and physiological factors of the eye, properties of the drug delivery system and the constituents used and most importantly, patient considerations. These points were elaborated on in chapter 2 with the exception of the formulation considerations. These factors ultimately affect the performance of the final dosage form and should be explored for realization of barriers and understanding of solutions to overcome them.

The barriers to drug delivery to the eye were comprehensively explained in the previous chapter. Pertinent theoretical points were researched in order to gain a holistic view of taking steps toward the end point in a rational and logical manner. Preformulation studies can be described as the foundation phase of carrying out research through institution of biopharmaceutical concepts.

Logic dictates that the following points must be addressed by the investigator prior to conducting experiments:

1. Drug properties and dose
2. Polymer and excipient properties
3. Compatibility of constituents
4. The final dosage form and intended site of action

The optimum conditions for freeze-drying, physical structure, disintegration time and reproducibility of the formulations were noted in order to progress to more advanced analysis. This chapter aimed to consider important factors for development of topical ocular dosage forms followed by practical application for selection of candidate components. In order to formulate a rapidly disintegrating system by the freeze-drying technique, hydrophilic polymers and excipients were selected. The purpose of employing excipients was to aid in the formation of a robust and elegant structure.

Preformulation studies facilitate the initial stages and allows for time-effective progression to optimization.

3.1.1 Characteristics of topical ocular drug delivery systems

The determination and analysis of the properties and behaviour of any novel dosage form is of vital importance. Moreover, an ocular pharmaceutical system requires special attention due to the intricacy and sensitive nature of this organ. Figure 3.1 effectively brings to light the key factors that were taken into consideration.

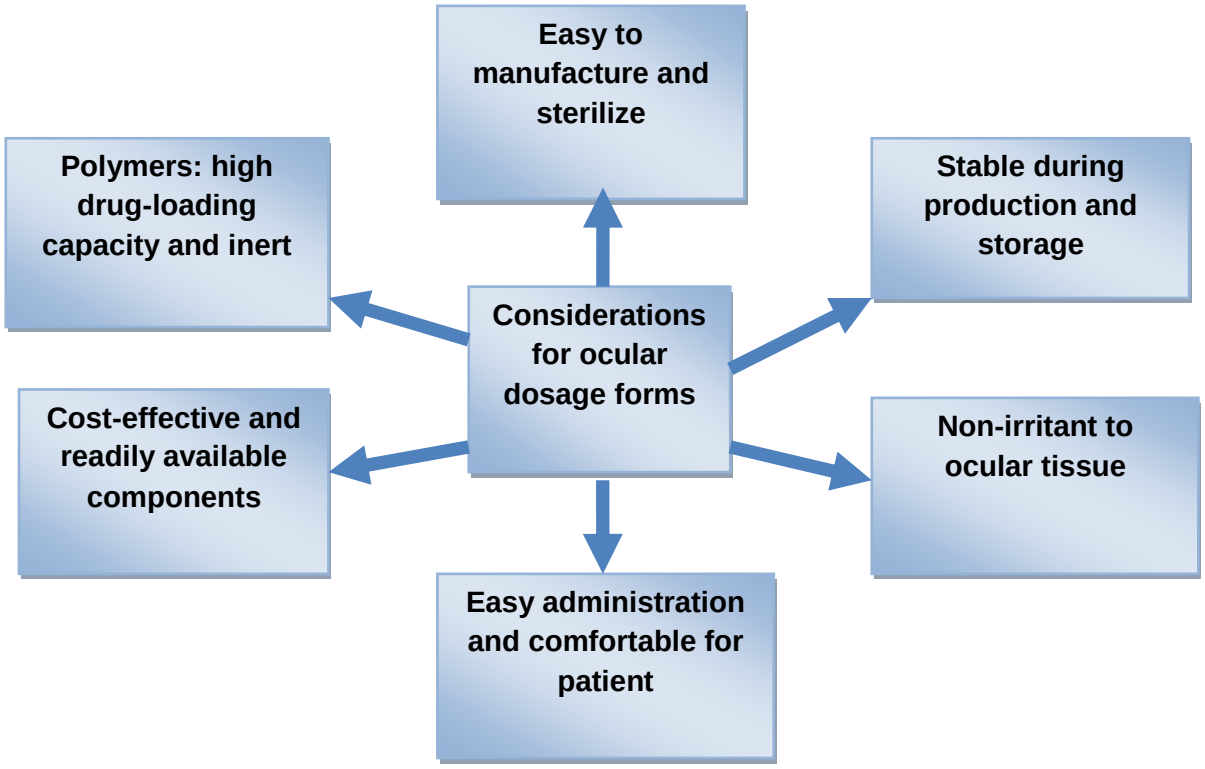


Figure 3.1: Schematic outlining important considerations in developing a novel ocular system (Information summarized from: Bawa, 1990; Ishikawa et al., 2001 and Conway, 2008).

3.2 Preliminary investigations for appropriate component selection

Various polymers and excipients were screened in order to ascertain the combinations that would allow for a rapidly disintegrating system. Polymer selection was based on literature reports for those suitable for ocular delivery (Kimura and Ogura, 2001; Ludwig, 2005; Najawande, 2007; Wagh et al., 2008). Key properties of suitable polymers included being eye compatible and rapidly disintegrating as exposed to aqueous media. Excipents are non-drug

components added to the formulation in order to serve additional functions such as improve the overall structure or appearance (Baheti et al., 2010).

Classification of excipients includes:

- Bulking agents - sugars, amino acids and polymers
- Buffering agents - pH adjusting agents
- Solubilizing agents – complexing agents, surfactants, co-solvents
- Other- tonocifying agents, collapse temperature modifiers, anti-microbial agents

Properties for choice of excipients were: to allow for system to remain sufficiently intact during handling processes, allow for rapid disintegration of system and ensure biocompatibility and compatibility with polymers and drug. Table 3.1 provides a summary of components. The model drug timolol maleate was selected for application in further chapters.

Table 3.1. Polymers and excipients selected for preformulation

Component	Description	Functions
Polymers		
Hydroxypropyl cellulose (HPC)	Hydrophilic, cellulose derivative	Polymer used to form matrix structure and applied as an ophthalmic lubricant
Pluronic® F68 (PF68)	Hydrophilic non ionic surfactant triblock copolymer	Polymer used to form matrix structure and applied as a viscosity enhancing agent to ophthalmic formulations
Carbopol® (C974P)	Cross-linked poly(acrylic acid)	Polymer used to form gel vehicle for ophthalmic formulations
Pluronic® F127 (PF127)	Hydrophilic non ionic surfactant, triblock copolymer	Polymer used to as vehicle in ocular formulations
Excipients		
Diglycine (DG)	Dipeptide of glycine	Collapse inhibitor
Polyacrylic acid sodium salt (PAA Na salt)	Anionic polyelectrolyte	Superabsorbant polymer (SAP), dissolution enhancer
Maltodextrin (MD)	Olligosaccharide produced from partial hydrolysis of starch	Lyoprotectant and improvement of hardness
Active ingredient		
Timolol maleate	Non-selective beta blocker	Employed as model opthalmic drug for treatment of glaucoma

3.3 Materials and Methods

3.3.1 Materials

Hydroxypropylcellulose (HPC) (Klucel®, Hercules Incorporated, Wilingtion, DE, USA), glycyl glycine (diglycine) (Fluka BioChemika, Belgium), Carbopol® 974p (Lubrizol Corporation, USA), poly(acylic acid sodium salt), maltodextrin (dextrose equivalent 16.5-19.5), Pluronic® F-68 and Pluronic® F-127 were all purchased from Sigma-Aldrich Corp. St. Louis, MO, USA. All other reagents were of analytical grade and purchased as used.

3.3.2 Preparation of polymeric solutions and synthesis of solid eye drops

Aqueous solutions of polymer were prepared in different concentrations in accordance with table 3.1. Components were dissolved in 100ml distilled water and agitated for 30 minutes until complete dissolution had occurred. 0.4mL of sample was placed in each mould of a blister pack. Samples were then frozen using a freezer (Sanyo Ultralow Temperature freezer, MDF-U73V, Sanyo Electric company, Japan) for 24 hours at -82ºC to solidify the product in a mould. The product was placed in a lyophilizer (Labconco Freeze-Dry Systems, Labconco Corp., Kansas City, MO, USA) for 48 hours to extract excess water. Figure 3.2 depicts the process.

Table 3.2. Components of the porous matrix and their concentrations (%$^{w/}_{v}$)

Formulation	PF127	C974P	HPC	PF68	DG	PAA Na-salt	MD
1		-	-	-	0.2	-	-
2		-	-	-	0.4	-	-
3		-	-	-	0.6	-	-
4		-	-	-	0.8	-	-
5		-	-	-	1	-	-
6		0.05	-	-	0.2	-	-
7		0.1	-	-	0.4	-	-
8		0.15	-	-	0.6	-	-
9		0.2	-	-	0.8	-	-
10		0.25	-	-	1	-	-
11		-	-	1	0.2	-	-
12		-	-	2	0.4	-	-
13		-	-	3	0.6	-	-
14		-	-	4	0.8	-	-
15		-	-	5	1	-	-
16		-	0.5	1	0.25	0.1	5
17		-	0.5	2	0.25	0.1	5
18		-	0.5	3	0.25	0.1	5
19		-	0.5	4	0.25	0.1	5
20		-	0.5	5	0.25	0.25	5
21		-	0.5	2.5	0.25	0.25	2.5
22		-	0.5	2.5	0.25	0.25	2.5
23		-	0.5	2.5	0.25	0.25	2.5
24		-	0.5	2.5	0.25	0.25	2.5
25		-	1	2.5	0.25	0.25	1.5
26		-	1	2.5	0.25	0.25	1.5
27		-	1	2	0.3	0.25	1.5
28		-	1	2	0.3	0.3	1.5
29		-	1	1	0.3	0.3	1
30		-	1	1	0.3	0.3	1

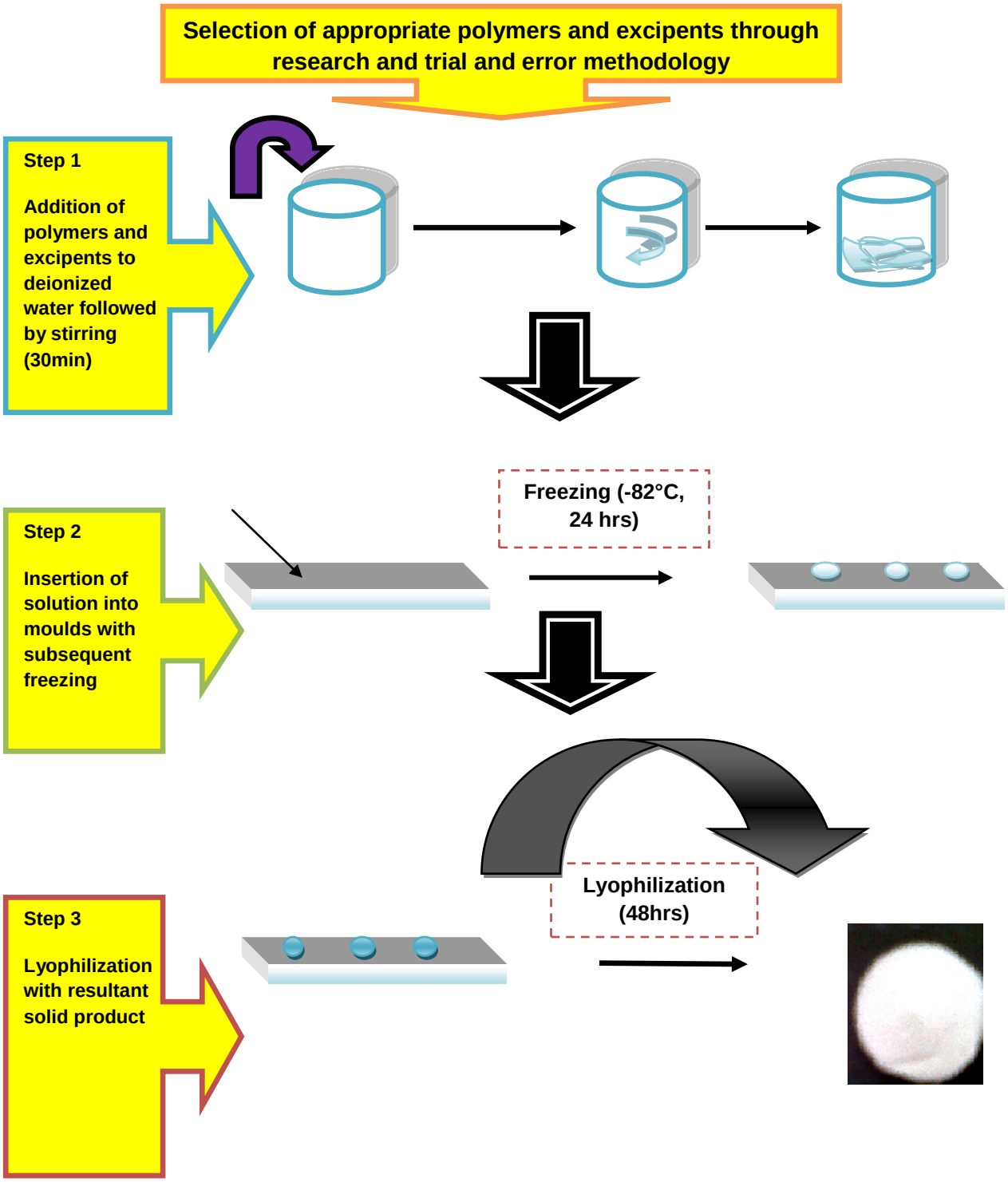


Figure 3.2: Schematic of method employed for preformulation studies.

3.3.3 Weight uniformity of matrices

Three randomly selected eye drops from each formulation batch were weighed individually and the average weight was determined.

3.3.4 Diameter and thickness of solid eye drop matrices

The thickness and diameter of drops were measured in triplicate using a manual vernier calliper (25X0.01mm capacity) (Taizhou hangyu tools gauge and blades Co., Ltd, Wenqiao, Zhejiang, China).

3.3.5 Disintegration time of the solid eye drops

The Petri-dish method for disintegration testing was employed (Gohel et al., 2004; Shailesh, et al., 2009) for preliminary studies. Distilled water (2mL) was placed in perspex petri dishes. The solid eye drops were placed in the centre of the dish. The disintegration time was taken as the time required for the eye drop to disintegrate entirely until no solid residue remained. As an initial preliminary investigation a digital stopwatch was used to determine the disintegration time.

3.3.6 Determination of the Friability of formulations

Friability was measured using a friabilator (Erweka D-63150, Heusenstamm, Germany). The drops were accurately weighed before being placed into the friabilator. A rotation time of 4 minutes at 25 rpm was used with 1% set as the upper limit of acceptability. Matrices were dusted off and re-weighed and the percentage weight loss was calculated using equation 1.1

$$WL_t = \frac{(W_0 - W_t)}{W_0} \times 100 \qquad \textit{Equation 3.1}$$

Where:

WL_t is the total weight loss is expressed as a percentage,

W_0 is the initial weight of the tablets and

W_t is the final weight of the tablets

3.4 Results and Discussion

3.4.1 Physical characteristics and weight uniformity

The ocular drops were successfully prepared by the lyophilization technique. They were white in appearance, light-weight yet robust enough to be handled. Weight of the drops ranged from

15.2-20mg. Average weight and appearance of three randomly selected drops from each batch are outlined in table 3.2. Figure 3.3 depicts the appearance of initial formulations.

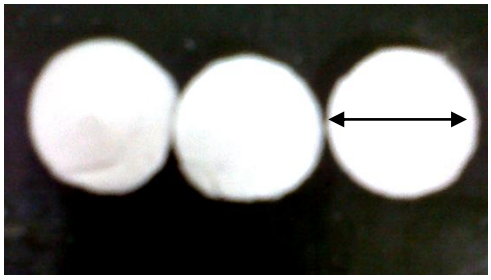


Figure 3.3: Digital image of top view of lyophilized drops of formulation 21 (diameter 11mm).

3.4.2 Diameter and thickness of the solid eye drop formulations

The consistency in size of drops is important to ensure uniformity. Samples were measured and found to have a diameter of 11mm and a thickness of 3mm.

3.4.3 Disintegration time

The absorption of water by the matrix is a key step for the disintegration process and ultimately the release of drug. The water soluble nature of the polymers allows for the rapid uptake of fluid with resultant dissolution (Refai and Tag, 2011). The disintegration times of the solid drops is outlined in table 3.2. HPC and PF68 were selected as ideal polymers for this system. After being placed in distilled water, the drops containing these polymers were hydrated and rapidly disintegrated within 2 seconds. Both HPC and PF68 are water soluble polymers which accounts for this behaviour. The other systems such as PF127 and C974P were not rapidly dissolving systems. They took a longer period of time to dissolve and formed gel-like residues despite the low concentrations used. For PF127, the slow disintegration time is due to the polymer swelling and forming a gel with increased temperatures (thermosensitive polymer) (Ricci et al., 2005). CP974P forms a gel when exposed to an increased pH which explains the slow process. Although these 2 polymers appeared to have an initial rapid disintegration time attributed to the fragile and poor structure of the matrix, the residue remained in the petri dish and did not dissolve completely.

3.4.4 Friability

Drops comprising HPC remained intact during and after the friability process. The individual C974P and PF127 drops displayed a tendency to crumble when removed from the mould and while being handled. As the C974P concentration increased, the drops displayed inadequate

mechanical properties. Weight loss ranged from 0.56-18.02% with formulations 21-30 displaying a favourable consideration (table 3.2). The addition of DG and MD noticeably assisted in formation of more stable structures.

Table 3.3. Results obtained from preformulation studies (N=3).

Formulation	Weight (mg)	Weight loss (%)	DT (s)	Appearance
1	17.2	4.07	32.5	Poor structure
2	17.3	6.35	33.2	Poor structure
3	17.4	7.47	38.9	Weak structure
4	16.1	3.11	40.8	Poor structure
5	16.5	13.93	52.1	Crumbled
6	17.4	18.97	31.0	Crumbled
7	16.3	12.88	30.2	Poor structure
8	15.9	17.6	30.1	Poor structure
9	17.2	18.02	30.5	Poor structure
10	18.2	10.98	10.6	Poorly formed
11	16.5	4.24	10.3	Fragile
12	16.6	7.83	10.4	Fragile
13	16.2	4.32	12.1	Fragile
14	17.4	2.3	3.2	Well formed
15	15.4	8.44	3.3	Well formed
16	17.2	5.23	3.6	Well formed
17	15.2	2.63	3.3	Well formed
18	17.4	2.30	3.1	Well formed
19	16.2	1.85	3.1	Well formed
20	17.0	1.18	2.8	Intact structure
21	17.2	0.58	2.3	Intact structure
22	17.4	1.16	2.5	Intact structure
23	16.9	0.56	2.3	Soft, well formed
24	17.2	0.60	3.2	Soft, well formed
25	17.7	1.13	3.5	Soft well formed
26	17.3	0.30	2.7	Soft, well formed
27	17.6	0.57	2.4	Soft, well formed
28	17.8	0.56	2.3	Soft structure
29	17.0	1.76	3.4	Soft structure
30	17.2	1.16	2.5	Soft structure

SD: weight ≤ 1.23, weight loss ≤0.64, DT ≤ 0.5

3.4.5 Effect of components on formulation properties

Results indicated that HPC and PF68 displayed behavior that was required for rapid dissolution as they are hydrophilic polymers, compared to the other 2 polymers which formed undesirable gel residues. The addition of DG promoted a more mechanically stable structure. High MD concentrations produced robust, hard and well formed matrices. The exclusion of DG and MD

resulted in poorly formed highly friable weakly formed structures. PAA Na salt at low concentrations (0.25%$^{w}/_{v}$) significantly enhanced the water uptake of samples with rapid dissolution due to the absorbent nature.

3.5 Ideal processing conditions for the development of solid eye drops

During initial investigations the following conditions were identified to be pertinent for formation of a rapidly disintegrating matrix of sufficient strength.

3.5.1 Duration required for complete dissolution of components

A time of 30minutes was found to be optimal for complete dissolution of the components at 600rpm at room temperature (25°C) until a clear solution was obtained.

3.5.2 Choice of moulds

Polyvinylchloride (PVC) blister packs (3mm diameter, 150uL volume) were selected as the most appropriate type of mould. The drops were easily removed without compromising their integrity. No lubricant was required and moulds were able to withstand the freezing and lyophilization processes. In the case of Perspex and Styrofoam wells, the drops adhered to the walls and were difficult to remove.

3.5.3 Type and concentration of constituents

After screening of various formulations HPC, PF68, DG, MD and PAA Na salt were henceforth selected as components most suitable to achieve the objective of the study. The formulation comprising (in $^{w}/_{v}$): 0.5% HPC, 2.5% PF-68, 2.5% MD, 0.25% DG and 0.25% PAA Na salt (Formulation 21) was seen to display rapid disintegration with sufficient strength as well as formulations 22-30.

3.5.4 Determination of Limits for variables of formulations

Lower and upper limits of variables were determined in the preliminary studies by the preparation of formulations of various concentrations (table 3.3). PF68 and MD concentrations were found to influence the formulation responses such as the time taken to dissolve and the overall strength.

Table 3.4. Formulation variables identified and response objectives.

	Limits	
Variables	Upper	Lower
PF68 (% $^{w}/_{v}$)	5	1
MD (%$^{w}/_{v}$)	5	1

3.5.4.1 PF68 concentration

The lower and upper limits were 1 and 5% respectively. Formulations above 3% had an increased disintegration time. This can be attributed to the gel forming nature of pluronics with increased concentration and temperature. Higher concentrations of PF68 resulted in higher matrix structure stability. Drug release was slower with higher concentrations again due to increased disintegration time and gelling nature of pluronics.

3.5.4.2 MD concentration

A concentration of 2.5%$^{w}/_{v}$ was sufficient to maintain the balance between the strength and rapid disintegration of the system. Higher concentrations showed a well-formed structure. However an overall harder surface was observed with higher concentrations and this was not appropriate for the sensitive ocular surface.

3.6 Concluding Remarks

This chapter aimed to formulate a quick dissolving system with enhanced strength through screening of components. Formulations 21-30 displayed interestingly acceptable results. Friability studies indicated that the matrices remained intact and were robust enough to be handled while the matrices dissolved in 3 seconds or less. The upper and lower limits were determined for further detailed evaluation. These findings provided an initial step in the fabrication of 1) a rapidly disintegrating system, 2) with substantial physical integrity and 3) furthermore, reproducibility and simplicity of the technique allowed for scale-up to be considered. The ideal manufacturing conditions identified were henceforth applied to the ideal size of the device and conditions specific to that of the eye surface. These studies assist the scientist to elicit the base of the goal and aids in identification of optimal components and conditions. Furthermore, it allows for anticipation of potential problems in the initial stages.

CHAPTER 4
CHARACTERIZATION AND STATISTICAL OPTIMIZATION OF THE ISED THROUGH INSTITUTION OF AN EXPERIMENTAL DESIGN

4.1. Introduction

Preformulation studies in Chapter 3 concluded that HPC, PF68, DG, MD and PAA-Na salt were components displaying ideal properties for an instantly soluble eye compatible matrix. Preliminary investigations provided a platform for determination of a prototype formulation and the aspects to be evaluated Trial and error methods were applied initially, however in order to conduct a scientifically sound experiment a design strategy was implemented. Design of experiments (DOE) is a mathematical strategy for setting up experiments in such a manner that the information required is obtained as efficiently and precisely as possible (Lewis et al., 1999; Anderson and Whitcomb, 2007). In terms of formulation development, DOE and statistical analysis have been applied in pharmaceutical areas for optimization and validation. The advantage of this in the formulation of products is that it enables factors to be evaluated simultaneously, systematically, it reduces the number of experimental runs allows for the detection of interactions between factors (Upasani and Banga, 2004). Once critical factors have been determined, the optimal formulation can be identified employing DOE and optimization. With the use of software that is specially programmed for the purpose, DOE is a critical method for improved pharmaceutical development (Bolton and Bon, 2004).

A response surface methodology (RSM) was chosen for DOE implementation in order to evaluate the formulation combinations to optimize the formulation. The RSM is employed to determine the acceptable formulation by prediction of responses through causal factors and polynomial equations (Takayama, 2008).

This method employs experimental designs and is based on:

- Identifying upper and lower limits of the formulation variables which are the independent variables
- Formulation of a design based on the limits
- Performing tests of various responses on the formulations derived from the design
- Regression analysis for coefficient evaluations
- Response prediction and validation for optimization of the formulation

A central composite design is useful in response surface methods for developing a model without the use of a complete three level factorial experiment. CCDs contain imbedded

factorial or fractional factorial matrix with centre points augmented with a group of star points or axial points that allow estimation of curvature (Late and Banga, 2010). They are flexible efficient designs with minimal runs required. Face centred composite designs contain star points at the centre of each factorial space (Figure 4.1).

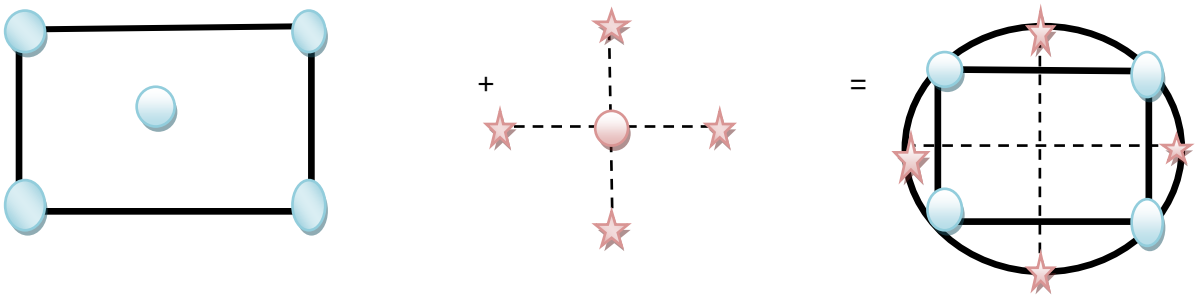


Figure 4.1: Schematic of FCCD.

Of the various designs, a 2 factor FCCCD was opted since MD and PF68 concentrations were the two factors displaying notable variations in responses during preliminary screening. A list of responses was identified for testing of the system.

A rapidly dissolving ocular system is a requisite necessity since it reduces foreign body sensation in the eye and will maintain higher drug levels in the eye due to the absence of flushing out effect as it is the case with traditional eye drops. A limitation of lyophilized systems as pointed out by Chandrasekhar and co-workers (2007) is the fragile nature of such systems.

Therefore, this chapter aimed to formulate and evaluate an instantly soluble solid eye drop by lyophilization technique with sufficient mechanical strength and a rapid disintegration time. Physicomechanical and drug release studies were carried out for characterization of the system. Timolol maleate was selected as the model drug since it is the standard treatment choice for common eye ailments namely, glaucoma. Tests carried out included: textural analysis, disintegration profiling, moisture content studies, scanning electron microscopy (SEM), stereomicroscopy, fluorescence microscopy, Drug Entrapment Efficiency (DEE), *in vitro* drug release and *ex vivo* permeation studies. Statistical analysis was conducted for optimization of the system.

4.2. Materials and Methods

4.2.1 Materials

Hydroxypropylcellulose (HPC) (M_w= 80 000 g/mol) (Klucel®, Hercules Incorporated, Wilington, Delaware, USA), glycyl-glycine (diglycine) (M_w= 132.12 g/mol) (Fluka BioChemika, Belgium), poly(acylic acid sodium salt) (PAA-Na salt) (M_w = 5100 g/mol), maltodextrin (dextrose equivalent 16.5-19.5), Pluronic® F-68 (M_w= 8400 g/mol), timolol maleate salt (M_w=432.49g/mol). fluorescein 5(6)-isothiocyanate (FITC) (M_w= 389.38 g/mol), phosphatidylethanolamine, and Dipalmitoyl-sulforhodamine B triethylammonium salt (rhodamine) (M_w= 1333.80g/mol) were all purchased from Sigma-Aldrich (St. Louis, Missouri, USA). All other reagents were of analytical grade and were used as supplied.

4.2.2 Development of an experimental design

A two-factor, three-level FCCCD was applied for the construction of a second order polynomial model describing the effect of formulation constituents on the characteristics of the system. Solid eye drop formulations of various combinations were prepared in accordance with the FCCCD. In order to determine the optimal formulation, several responses were tested: Textural characteristics, disintegration testing, *in vitro* drug release were responses measured. Constraint optimization predicted an optimized formulation, but a mathematical model was generated by regression analysis as several variables required simultaneous solving. The factors and levels are depicted in Table 4.1. The polynomial equation generated was:

$$y=b_0+b_1PF68+b_2MD+b_{11}PF68_2+b_{22}MD_2+b_{12}PF68MD \qquad \textbf{\textit{Equation 4.1}}$$

Table 4.1. Thirteen formulations generated from the FCCCD.

Formulation	PF68 (%$^{w}/_{v}$)	Maltodextrin (%$^{w}/_{v}$)
1	1	5
2	5	3
3	3	5
4	1	3
5	5	1
6	3	3
7	3	3
8	3	3
9	5	5
10	3	3
11	1	1
12	3	3
13	3	1

Specific responses and their respective objectives included:

- *Disintegration time (DT) (seconds)* **-** A minimum disintegration time corresponds to the fastest time of dissolution when in contact with fluid medium.
- *Matrix resilience (MR) (%)* **-** An increased resilience implies an overall improved strength of the matrix.
- *Mean Dissolution Time ($MDT_{50\%}$) (minutes)* **-** A minimum $MDT_{50\%}$ confers the fastest drug release attainable.

4.2.3 Preparation of polymeric solutions and synthesis of solid eye drops according to FCCCD

Aqueous solutions of polymer were prepared in various concentrations in accordance with the FCCCD. Table 4.1 depicts formulations generated from the design based on influential components as determined from preformulation studies. HPC 1%$^{w}/_{v}$, PAANa 0.25%$^{w}/_{v}$, DG 0.25%$^{w}/_{v}$ and variants in Table 1 were dissolved in 100mL deionized water and agitated for 30 minutes until complete dissolution had occurred. Samples of 150µL were injected into each mould of the polyvinyl chloride (PVC) blister packs. Samples were then frozen (Sanyo Ultralow Temperature freezer, MDF-U73V, Sanyo Electric company, Japan) for 24 hours at -82ºC to solidify the product. The product was placed in a lyophilizer (Labconco Freeze-Dry Systems, Labconco Corp., Kansas City, Missouri, USA) for 48 hours to extract excess water. The lyophilized samples were stored in glass vials in the presence of 2g desiccant sachets.

4.2.4 Determination of the physicomechanical properties of the solid eye drops by textural analysis

Textural analysis was used to characterize the compressibility of the solid drop using a Texture Analyzer (TA.XT*Plus*, Stable Microsystems, UK). Various tests were conducted in triplicate for characterization at room conditions (25°C), for determining the following textural properties employing the textural settings displayed in Table 4.2:

1. *Matrix Resilience (MR):* Resilience can be defined as the ability of a material to absorb energy when deformed upon exposure to an external stress and release of that energy post unloading. Resilience of the matrix provides an elucidation of the ability of the matrix to withstand an applied stress. The analyzer was fitted with a suitable 10mm diameter delcin probe for resilience measurement. Force-time profiles were generated and analyzed. The MR (%) was determined by finding the ratio between anchors 2 and 3 and between anchors 1 and 2 (Figure 4.2a).
2. *Energy of Absorption (EA):* The energy of absorption is an indirect indication of the porosity of the wafers. A highly porous wafer will exhibit a greater value for the energy of absorption because energy is accommodated within the voids in the matrix. The energy of absorption is calculated by determining the area under the curve (AUC) of a profile illustrating force (N) and distance (m) as depicted in Figure 4.2b.
3. *Matrix Yield Value (MYV):* Matrix yield value assists in the determination of strength of the surface structure of the matrix. This is determined by obtaining a gradient between anchors 1 and 2 of a force-distance profile (Figure 4.2b).
4. *Matrix Tolerance (MT):* Matrix tolerance indicates the overall matrix strength. The gradient between anchors 1 and 3 provides the matrix tolerance value. This is the point of total matrix collapse (Figure 4.2b).
5. *Brinell Hardness Number (BHN):* Hardness is described as the resistance of an object to permanent shape change when a force is applied. Brinell hardness is an indication of the force required to indent the surface of the matrix. Brinell hardness was assessed using a ball point probe. Force-distance profiles were generated and assessed (Figure 4.2c). The indentation hardness was represented by a conversion to the Brinell Hardness Number (BHN) (N/mm^2) using Equation 4.2:

$$BHN = \frac{2F}{\pi D\left(D - \sqrt{D^2 - d^2}\right)}$$ ***Equation 4.2***

Where:

F = force generated from indentation (N) obtained from maximum peak of curve,

D = diameter of ball probe indenter (3.125mm) and

d = indentation depth which is half the probe diameter (1.5625mm)

Table 4.2. Parameters employed for Textural analysis

Parameters	**MR[1]**	**BHN[2]**
Test mode	Compression	Force
Pre test speed	1.0 mm/sec	1.0mm/sec
Test speed	0.5 mm/sec	0.5mm/sec
Post test speed	1.0 mm/sec	1.0mm/sec
Compression force	-	40N
Trigger force	0.05N	0.05N
Load cell	5kg	5kg
Compression strain	50%	-
Compressive distance	-	1.5625mm

[1]*Matrix resilience*

[2]*Brinell hardness number*

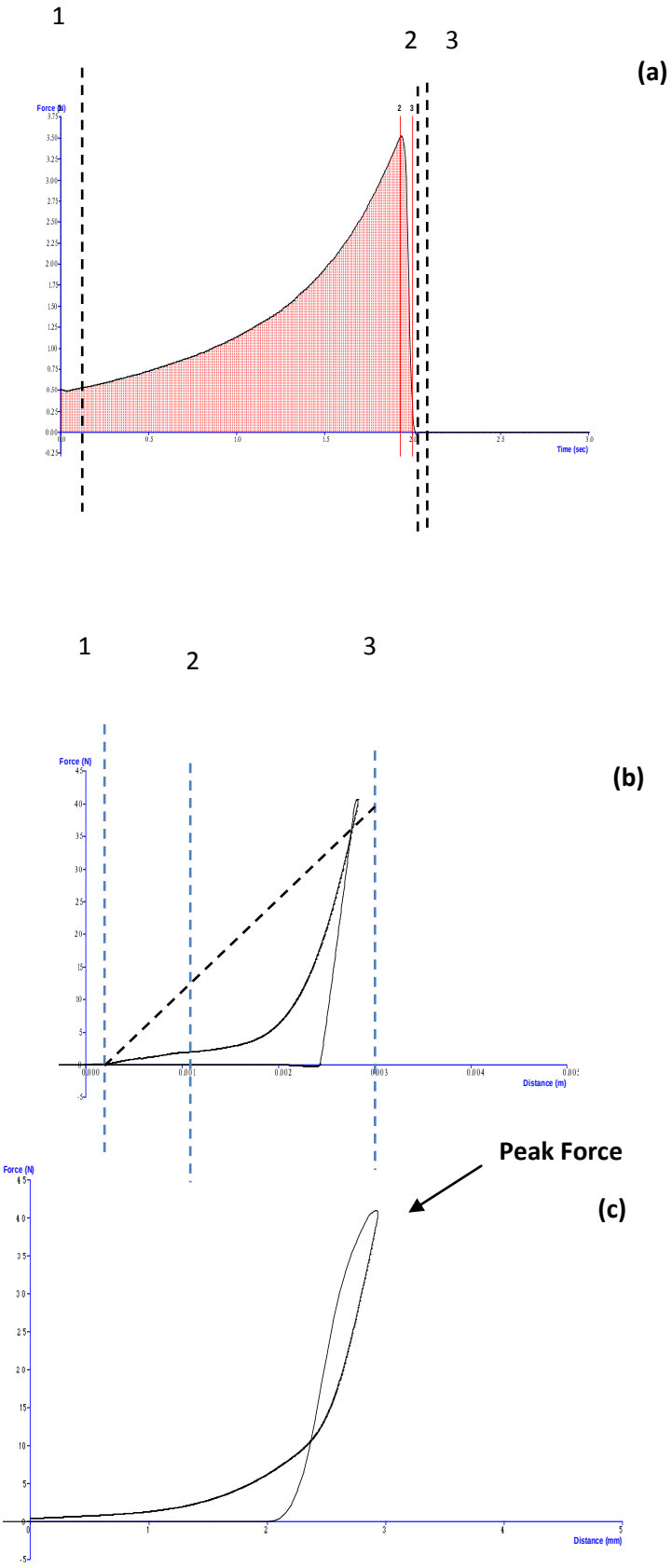


Figure 4.2: Typical: a) force-time profile for matrix resilience calculation; b) force-distance profile for the determination of matrix tolerance, yield value and energy of absorption; and c) force-distance profile for computation of BHN.

4.2.5 Disintegration profiling

Disintegration testing of fast dissolving systems is a vital test carried out for evaluation of the time taken for the system to dissolve. However, currently there is no standard test method in the British and United States Pharmacopoeias. Conventional oral tablet methods are employed but they pose certain limitations and may not always reflect ocular conditions *in vivo*:

- Fast dissolving tablets have a rapid disintegration profile and this is difficult to assess using conventional tablet methods which require the use of force.
- Tablet methods make use of large fluid volumes (900mL) for oral use and while the eye surface contains a minimal amount of fluid (7µl) (Shailesh et al., 2009).

Due to these limitations various methods have been proposed for testing. The Texture Analyzer method has been employed for the evaluation of disintegration of fast dissolving oral wafers (Dor et al., 1999; el-Arini and Clas, 2002; Fu et al., 2004). Advanced testing utilizing improved methods and parameter settings displayed in Table 4.3 was conducted employing a Texture Analyzer (TA) (Stable Micro Systems, Surrey, UK) with a flat, cylindrical probe. The probe head was magnetically attached to the shaft which was screwed onto the load cell carrier (Figure 4.3a and b). This allowed for preparation of 5 samples at a time and quick removal and interchanging of probe heads was done. The dry solid eye drop was attached to the probe head by means of a thin strip of double sided adhesive tape across its diameter. This was lowered into a perspex test vessel containing 2mL Simulated Lachrymal Fluid[4] (SLF, pH 7.4, 35°C) (Table 4.4). Upon entering the medium and quickly reaching an immersed perforated platform, the Texture Analyzer applied a minimal force (0.098N) for a chosen period of time. The clear vessel allowed for observation of the process. Typical distance-time profiles were generated from which disintegration rate (mm/sec) and end point disintegration time (s) were determined. Tests were carried out in triplicate. The following were determined from the graphs obtained (Figure 4.3c):

1. *Disintegration Rate* – the first gradient of the descending region from the onset of disintegration before the point of inflection where disintegration rate decreased or stopped.
2. *End Point Disintegration Time* – calculated using the interception of the slopes of the initial descending and final region.

Table 4.3. Parameters employed for disintegration profiling

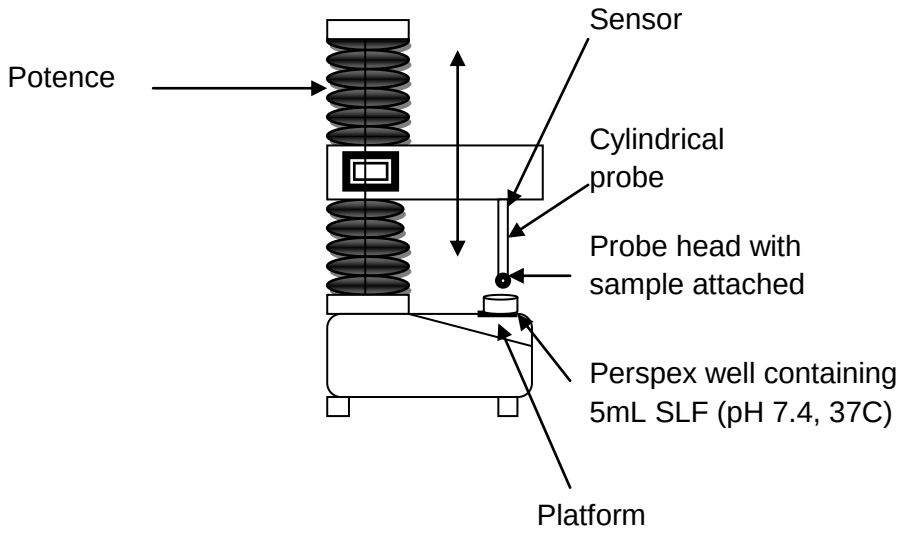
Parameters	Settings
Test mode	Compression Hold until reset
Pre test speed	2.0 mm/sec
Test speed	3.0 mm/sec
Post test speed	10.0 mm/sec
Force	0.098N
Trigger force	0.029N
Data Acquisition rate	500 points per second
Maximum tracking speed	5mm/sec

Table 4.4 Constituents used to prepare simulated lachrymal fluid (SLF) (Gonjari et al., 2009) and simulated aqueous humour (SAH) (Gianniola et al., 2007)

Components[a]	Quantity	Components[b]	Quantity
$NaHCO_3$	218mg	NaCl	6400mg
NaCl	678mg	KCl	750mg
$CaCl_2.2H_2O$	8.4mg	$CaCl_2$	480mg
KCl	138mg	$MgCl_2$	300mg
Deionized water	100mL	Sodium acetate	3900mg
		Sodium Citrate	1700mg
		Deionized water	1000mL

[a] *simulated lachrymal fluid (SLF)*[4]
[b] *simulated aqueous humour (SAH)*[5]

a)



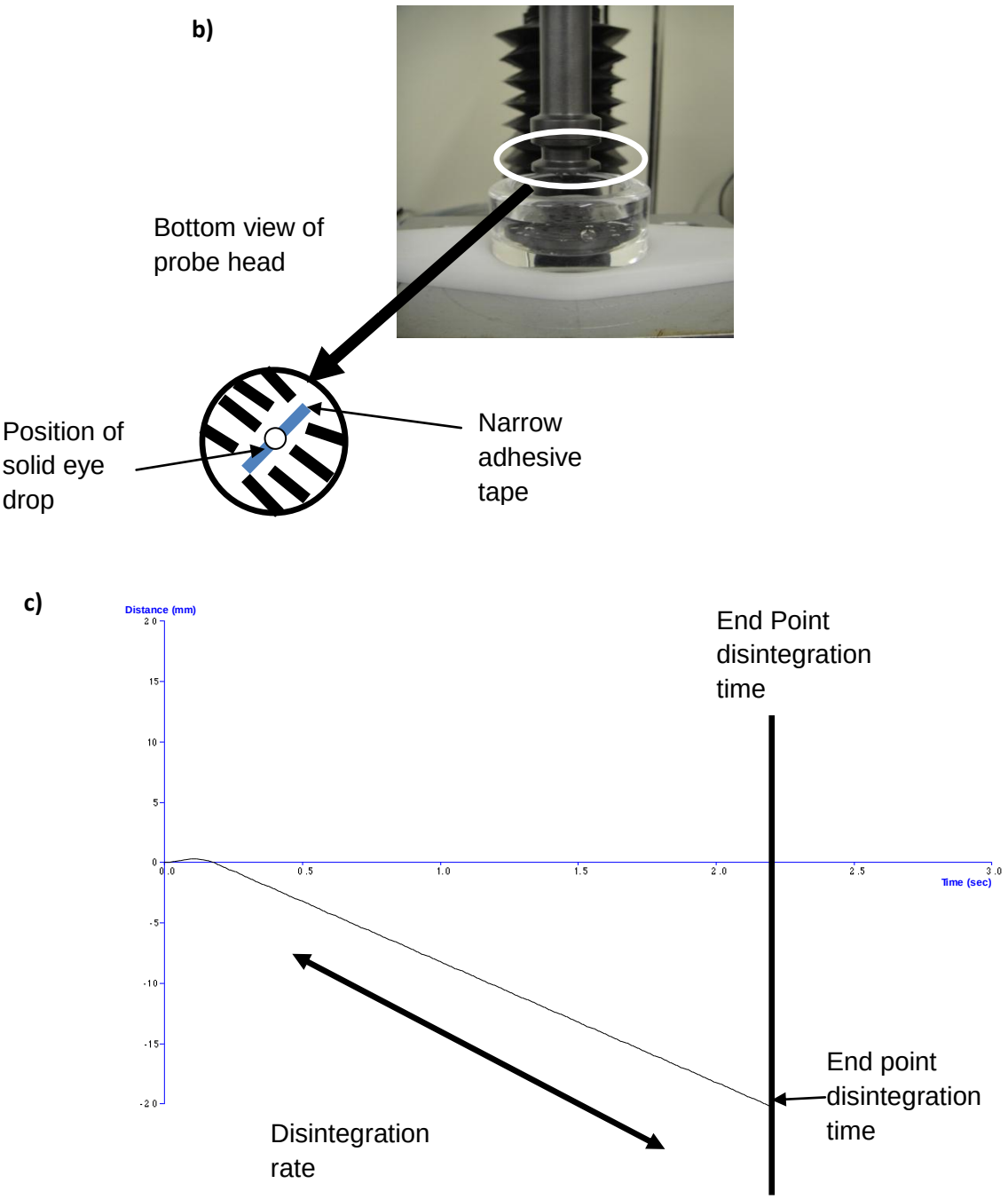


Figure 4.3: a) Texture analyzer employed for disintegration testing, b) digital image of the disintegration rig with 20mm diameter probe showing channeled geometry to allow fluid to flow above tablet to contact upper surface during the test **and c)** typical distance-time graph for disintegration profiling.

4.2.6 Determination of moisture content by Karl Fisher Titrimetry (KFT)

An essential test carried out for the determination of stability of rapidly disintegrating systems is water absorption studies. The moisture content was determined by Karl Fisher Titrator (Metler

Toledo, USA). This is a universal analytical chemistry method for the detection of trace amounts of water in samples and is based on the stoichiometric reaction of the Karl Fischer reagent with water present in the test sample. The amount of water equivalent to each milliliter of Karl Fischer reagent is determined using a methanol water solution as the standard. The determination is carried out in a closed titration cell containing a platinum electrode connected to a galvanometer in a dead stop endpoint circuit. The difference in the conductivity of the solution when any unreacted Karl Fischer reagent is present is used to determine the endpoint of the reaction. Samples were accurately weighed out and placed in the volumetric component of the titrator and moisture content was recorded. Parameters employed are outlined in Table 4.5. All tests were carried out in triplicate. Figure 4.4 depicts a typical plot obtained.

Table 4.5. Parameters employed for Karl Fisher Titration

Parameters	Settings
Titration standard	KF standard
Maximum time	60s
Drift	0.0µg/min
Temperature	25°C
Titrant	KF-1 comp 5K (5.33724mg/mL)

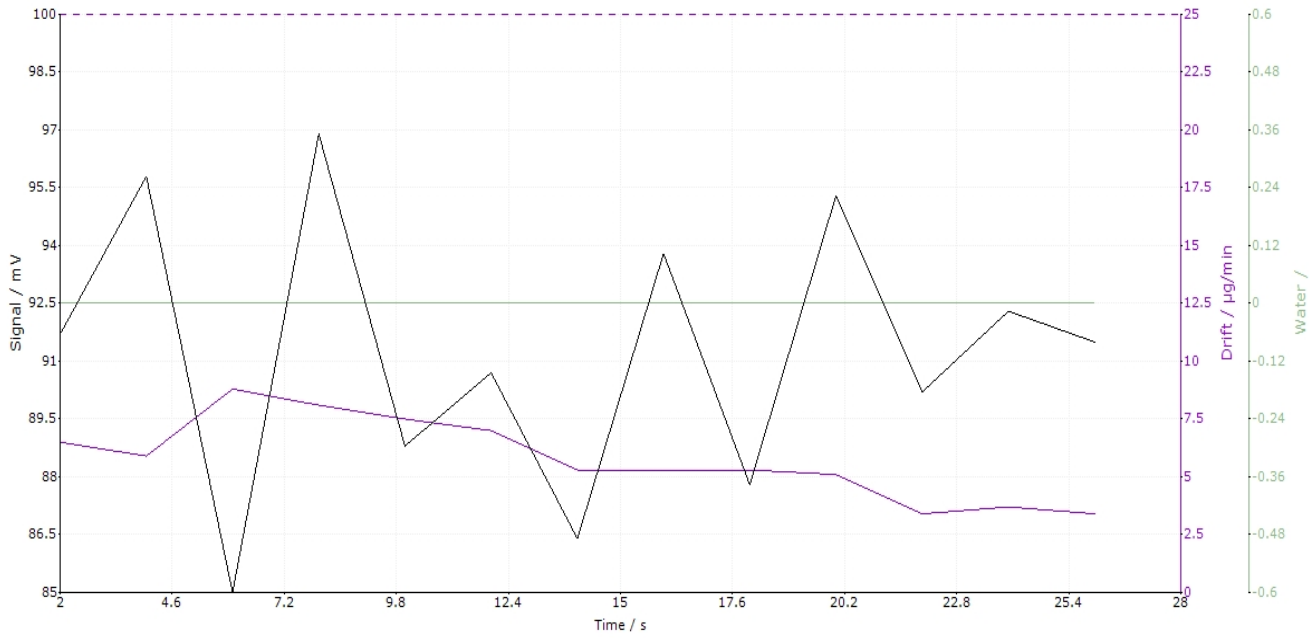


Figure 4.4: Typical graph obtained for KFT.

4.2.7 Surface morphology by scanning electron microscopy (SEM)

The in-depth surface morphology and internal structure of the matrix was visualized by the use of scanning electron microscopy (FEI Phenom™, Hillsboro, Oregon, USA). Samples were mounted on a spud and gold plated by the sputter-coater (SPI module™ sputter-coater and control unit, West Chester, Pennsylvania USA). Samples were then viewed under the SEM at different magnifications.

4.2.8 Visualization of dissolution process employing Stereomicroscopy

The visualization of the solubilization of the eye drop was determined by microscopy using light illumination for images in a 3-dimensional level. A stereomicroscope (Olympus SZX7 stereomicroscope, Olympus, Japan) connected to a digital camera (CC 12, Olympus, Japan) and image analysis system (AnalySIS® Soft Imaging System, GmbH, Germany) was employed. The unhydrated and hydrated samples were imaged to observe the entrance of fluid into the sample on a microscopic level.

4.2.9 Imaging of fluid ingression by Flourescence Microscopy

Flourescence microscopy was conducted to visualize the ingression of fluid into the polymeric matrix. The principle of flourescence microscopy involves the use of fluorescence for the generation of an image. A sample is illuminated by wavelength of light that excites fluorescence in the sample. Polymeric solutions were prepared as in section 2.2.1 and fluorescein (0.05mg) was added to the solutions pre-lyophilization. Flat discs were prepared and the yellow-stained eye drops were placed on a glass slide for microscopical examination employing a fluorescence microscope (Olympus BX41 flourescence microscope, Olympus, Japan) connected to a digital camera (CC 12, Olympus, Japan). Rhodamine stained water (1%) was allowed to ingress the wafer from one side and the samples analysed under the miscroscope.

4.2.10 Construction of calibration curve

A calibration curve was constructed by appropriate dilutions of TM. An R^2 value of 0.99 was obtained. Figure 4.5 shows the calibration curve of TM in SAH (pH7.4, 35°C) at 295nm.

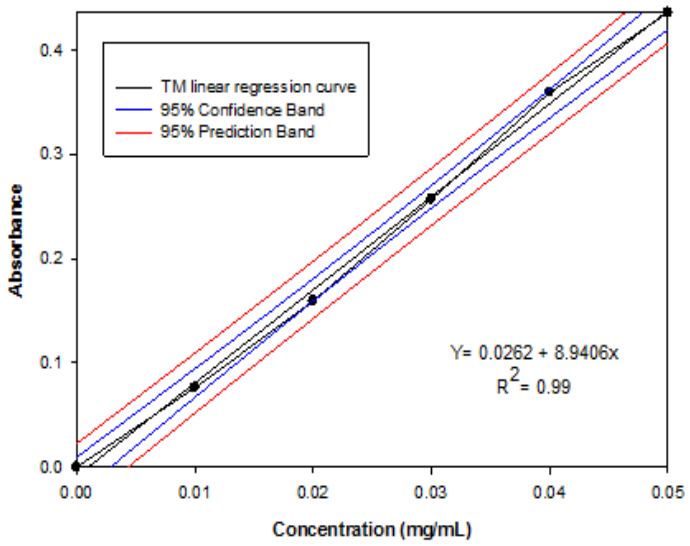


Figure 4.5: Calibration curve of TM in SAH (pH7.4, 37°C) at 295nm (SD≤0.0543).

4.2.11 Computation of Drug Entrapment Efficiency (DEE)

DEE was conducted by dissolving the solid drops in SLF and spectophometrically analyzing the solution at 295nm for determination of drug content. All tests were conducted in triplicate. Equation 4.3 was employed for the DEE calculation:

$$DEE = \frac{D_a}{D_t} x\ 100$$

Equation 4.3

Where:

DEE = Drug entrapment efficiency,

D_a = the actual quantity of drug (mg) measured by UV spectroscopy and

D_t = the theoretical quantity of drug (mg) added in the formulation.

4.2.12 *In vitro* drug release studies

The Franz diffusion cell is a method that can be used for studying the diffusion of drug from semisolid ocular dosage forms (Gorle and Gattani 2009; Gilhotr et al., 2010; Gilhotra and Mishra, 2011). A Franz diffusion cell consists of a donor chamber and a receptor chamber with a membrane clamped in between. Commercial cellophane membranes (M_w = 12000, Sigma-Aldrich Corp. St. Louis, Missouri, USA) were used to simulate the corneal epithelial barrier for ocular penetration of drug. Membranes were presoaked in dissolution media overnight. The diffusion cell donor chamber was filled with 2mL SLF (which was maintained

to simulate tear volume) solubilized with the solid eye drops. This solution was placed in the donor compartment in contact with the membrane. 12mL Simulated Aqueous Humour (SAH, pH 7.4, 37 °C) (Table 4.4) solution was contained in the receptor chamber. The membrane was placed such that the surface was in contact with the receptor solution which was continuously stirred by a magnetic stirrer at 20rpm to simulate blinking. Aliquots of 2mL were withdrawn from the receptor compartment at regular intervals (30, 60, 120, 180, 240 minutes and 24 hours after insertion) and replaced with an equal volume of dissolution medium. Samples were analyzed spectrophotometrically at 295 nm (Hewlett Packard 8453 Spectrophotometer, Germany) to determine the drug release. Tests were conducted in triplicate. The dissolution data was analyzed by calculation of the Mean Dissolution time (MDT). This is the sum of individual periods of time during which a fraction of the total drug is released (Pillay and Fassihi 1999; Govender et al., 2005). $MDT_{50\%}$ data point was selected for the design formulations. Equation 4.4 was used for the determination of MDT:

$$MDT = \sum_{t=1}^{n} t_i \frac{M_t}{M_\infty} \qquad \textbf{\textit{Equation 4.4}}$$

Where:

M_t = the fraction of dose released in time t_t

$t_t = (t_i + t_{i-1})/2$ and

M_∞ = loading dose

4.2.13 *Ex vivo* permeation studies

4.2.13.1 Tissue collection and storage

Enucleated rabbit eye balls were placed in phosphate buffered saline (PBS) (37°C, pH7.4) until the cornea was removed. The corneal layer was removed by making a slit employing a scalpel in the eye ball and cutting around carefully ensuring the cornea remained intact. Excess tissue was trimmed away (Figure 4.6a-c). The average thickness of corneas was measured to be 0.353±0.02mm using a vernier caliper (25x0.001mm capacity, Germany). Subsequently, the samples were snap frozen in liquid nitrogen and stored at -80°C for up to 2 months. This method of storage does not interfere with the permeation of the tissue (Fong et al., 1986; Araki et al., 1996; Dey et al., 2004). Samples were thawed when required for conduction of permeation studies. This involved rehydration of tissue in PBS (37°C, pH7.4) for 2 hours in order to retain the elasticity of the tissue.

4.2.13.2 Permeation test

Franz diffusion cell apparatus was used to conduct *ex vivo* permeation studies after the sample preparation process as outlined previously. Subsequent to rehydration, samples (11.83±0.04mm in diameter and area 3.0mm^2±0.01mm^2) were cut with the aid of surgical scissors and mounted on the Franz diffusion cell apparatus (Permagea, Arnie Systems, USA) connected to a heating bath system for temperature control (Figure 4.6d). Samples were placed in the donor compartment and the cumulative drug release (%) and drug flux were determined. Drug flux can be defined as the rate of drug permeation per unit area. Drug flux values were calculated at the steady state per unit area by regression analysis of permeation data. All tests were carried out in triplicate. A correction factor was appropriately applied in all cases where dilution of samples was required. The results of the analysis were used to calculate the cumulative amount (Q) of drug released per surface area of membrane using Equation 4.5:

$$Q = \{C_n V + \sum_{i-1}^{n-1} C_i \ S\}/A \qquad \textbf{Equation 4.5}$$

Where:

Q = Cumulative amount of drug released per surface area of membrane (µg/cm^2),
Cn = Concentration of drug (µg/mL) determined at nth sampling interval.
V = Volume of individual Franz diffusion cell n-1,
ΣCi = Sum of concentrations of drug (µg/mL),
i=1 determined at sampling intervals 1 through n-1,
S = Volume of sampling aliquot and
A = Surface area of sample well

Drug flux values were calculated employing the Equation 4.6:

$$J_s = \frac{Q_r}{A\ x\ t}$$

Equation 4.6

Where

J_s= drug flux (mg cm^{-2} min^{-1})
Q_r= amount of drug that passed through to the receptor compartment (mg)

A=Active cross-sectional area for diffusion (cm^2) and

t= time of exposure (min)

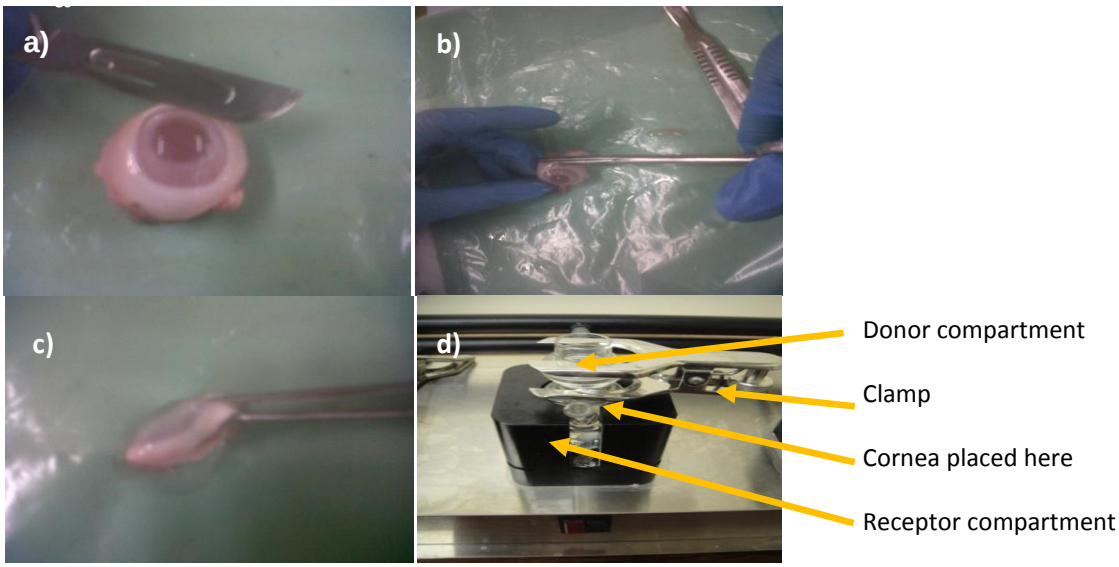


Figure 4.6: Digital images of: a) the enucleated eye ball, b) excision of the cornea, c) excised cornea and d) a single cell of Franz diffusion cell apparatus showing the set-up for permeation through corneal tissue.

4.2.14 Statistical evaluation of responses based on constraint optimization

A Central Composite Design (CCD) is useful in response surface methods for developing a model without the use of a complete three-level factorial experiment. Basically, CCD's contain imbedded factorial or fractional factorial matrix with centre points with a group of star points or axial points that allow for curvature estimation (Late and Banga, 2004). They are advantageous as minimal runs are required. FCCCD's contain star points at the centre of each factorial space. Of the various designs, a 2-factor FCCCD was opted for since MD and PF68 concentrations were the two factors displaying notable variations in responses during preliminary screening. Lists of responses were identified for testing of the system. All experiments were conducted in triplicate. Statistical comparisons were made using MINITAB® V14 (Minitab®, USA).

4.2.15 Mathematical modelling: numerical simulation of dissolution time

Mathematica (Wolfram Research of Champaign, Illinois) was used to simulate the dissolution of the proposed ISED. The problem was built employing a simplified model namely that of Fick's diffusion.

4.3. Results and Discussion

4.3.1 Physical properties of solid eye drops

The solid eye drops were successfully produced by the lyophilization process according to the FCCCD. The average weight ranged from 4.6-10.9mg (SD≤0.351), they were white in appearance and typically tablet shaped. Physically, they were resilient and robust matrices. The exception to this was with formulation 11 which displayed a poorly formed structure and was easily breakable when handled. This may be attributed to the low MD and PF68 concentrations which results in a poorly formed overall matrix despite the inclusion of collapse inhibitors. Thus, polymer concentration was seen to be a factor influencing the formation of the solid eye drops. A diameter of approximately 3mm and a thickness of 2mm were measured. Figure 4.7 depicts a digital image of typical solid eye drops produced. Noteworthy is that formulation 1 was desirably robust compared to formulation 11 which presented as a fragile matrix.

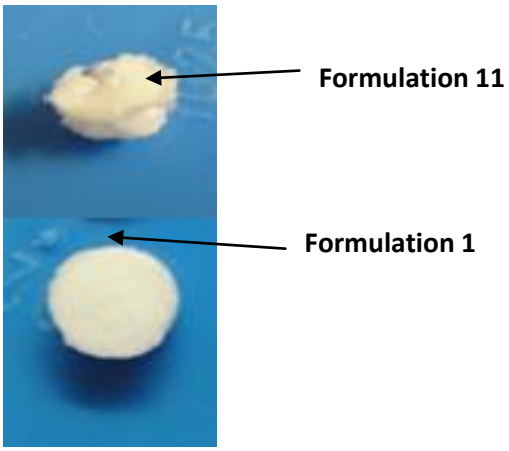


Figure 4.7: Digital image depicting the typical solid eye drops of formulation 1 and 11 produced from the FCCCD.

4.3.2 Textural profile analysis of solid eye drops

The physical characteristics of the solid eye drop as a dosage form are essential for determination of the stability during storage and use of the product in the eye. It provides an indication of the integrity of the formulations. The numerical values obtained from the analysis at room conditions are listed in Table 4.6. Low MD and PF68 concentrations resulted in solid eye drops that were fragile. Higher MD and PF68 concentrations produced well formed and easily removable eye drops. Higher MD imparted rigidity and improved hardness of the formulations. In addition, the presence of the protectant di-glycine in all formulations served to reduce collapsing of the structures. Glycine is an amino acid while di-

glycine or glycylglycine is the dipeptide of glycine (Dunn et al., 1932; Hakin et al., 1999). Glycine has been proposed to assist in maintaining the structure of the formulations during lyophilization process as well as storage (Seager 1998; Patel et al., 2007). Thus, the presence of its dipeptide conferred further consolidation of the formulations. Formulation 6, 7, 8, 10 and 12 comprised the same formulation combinations. Resilience can be described as the ability of a strained body to recovery in both size and shape after deformation on exposure to stress, derived from the Huber-Hencky Theory of Strength (Symonds et al., 1982, du Toit et al., 2007). An increase in matrix resilience is attributed to higher matrix strength and this is an important parameter to help understand the matrix characteristics. Resilience of these formulations was noted to be higher than other formulations ranging from 4.698 to 6.519 %. Elevated BHN values are due to higher stability characteristics. The BHN values did not vary much among the formulations. Highest BHN value was observed in formulation 1 (2.062N/mm^2). Energy of absorption was used as an assessment of porosity. Formulation 1 displayed the highest energy of absorption (0.026J) which indicates a superior stability between the surface and polymeric network and thus a more robust sample. More pores within a matrix enable more energy to be trapped and thus a higher energy of absorption was observed for formulation 1. Highest tolerance was noted for formulation 7 (19.531N/mm) which indicates a high overall matrix strength. In terms of yield value, the highest value was observed in formulation 1 (2.9180N/mm). The correlation between yield and tolerance values is such that initially a low yield value is observed and subsequent to fracturing of the matrix this energy is dissipated through the matrix resulting in complete collapse. This formulation contained a high amount of MD (5%) which is an amorphous saccharide. Yunxia and co-workers (1999) described this by the presence of ‘bridges’ in MD, conferring hardness to the formulation. Additionally, Corveleyn and Remon (2007) also concluded that maltodextrins were a beneficial component in formulating fast dissolving tablets made by freeze drying. Figure 4.8 shows the relationship between textural parameter

Table 4.6. Textural analysis results conducted on design formulations.

Formulation	Matrix yield value (N/mm)	Matrix tolerance (N/mm)	Matrix absorption energy (J)	Matrix resilience (%)	BHN (N/mm^2)
1	2.918	17.402	0.026	8.469	2.062
2	2.121	11.057	0.019	4.589	2.042
3	2.874	15.592	0.023	6.519	2.055
4	1.395	15.878	0.020	5.439	2.058
5	1.307	16.935	0.018	4.712	2.061
6	1.035	16.164	0.018	5.274	2.032
7	2.261	19.531	0.018	5.257	2.057
8	1.932	13.814	0.022	4.698	2.059
9	0.947	11.941	0.022	4.137	2.054
10	1.096	14.892	0.018	4.934	2.050
11	1.289	11.513	0.016	3.814	2.055
12	2.171	15.849	0.016	6.519	2.048
13	1.462	12.454	0.022	5.895	2.054

Results are expressed as the mean of at least three measurements, SDs obtained were within: yield value ≤0.010, tolerance ≤0.059, absorption energy ≤0.002, resilience ≤0.081, BHN ≤0.011.

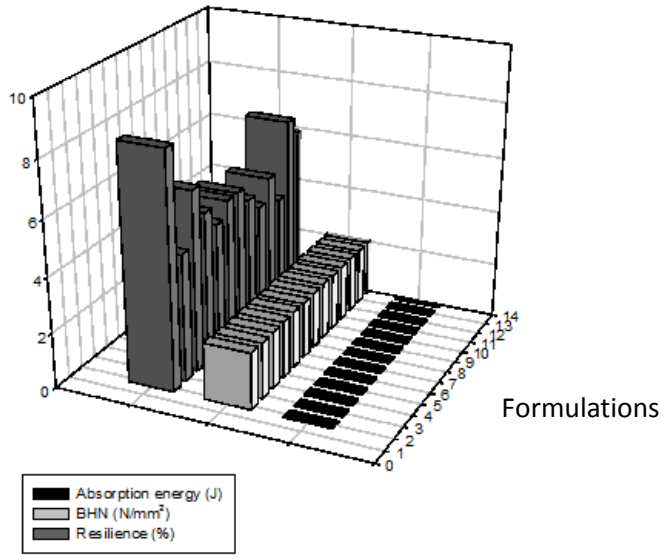


Figure 4.8: 3D bar graph of relationships observed for textural characteristics.

4.3.3 Disintegration testing

Disintegration times (DT) were determined by noting the end point on graphs. The DT was taken as the time taken for complete disintegration to occur as the system was immersed in SLF. Instantaneous disintegration was noted for all formulations due to the porous nature of the matrix and quick ingression of the fluid. This may purportedly be due to the polymers

HPC and PF68 being water-soluble. When placed in fluid medium these matrices absorbed water with subsequent dissolution. More importantly, the presence of the polyacrylic acid sodium salt PAANa (CH_2-CH(COONa)-]$_n$) contributed to the rapid dissolution of the solid eye drops (Figure 4.9b). The polymer is known as a superabsorbent polymer (SAP). SAP's, from the name, are polymers that absorb a large amount of liquid due to the ionic concentration of the solution in water (Chen et al., 2008). This may be explained by looking at the structure of the polymer. Water molecules move into the polymer by a diffusion gradient due to the neutralization of sodium. The polymer chains are prevented from straightening since cross-linking is present. Particle expansion occurs due to water and the water remains by means of hydrogen-bonding (Shakhashiri 1989; Thijs et al., 2007). On closer inspection, the carbonyl (COOH) and sodium (Na) groups are significant to the operation of the polymer. When in contact with water, Na dissociates from the carbonyl group creating two ions, carboxyl (COO-) and sodium (Na+). Repulsion occurs by like carboxyl groups and that causes the PAANa chain to uncoil or swell as shown in figure 4.9c and d (Lui and Guo, 2001; www. m2polymer. com/html/ superabsorbent_polymers.html). All formulations dissolved into liquid with the exception of formulations 2, 5 and 9. This was due to the higher PF68 concentration (5%). The polymer (PF68) displayed a tendency to form a gel-like residue with increasing concentration. This may be attributed to PF68 being a hydrophilic block co-polymer which upon heating and increased concentrations, displays a tendency to form a low viscosity gel-like substance (Maghraby and Alomrani, 2009). Formulation 11 displayed the fastest DT (0.200s) while formulation 9 had the slowest time (3.340s). Disintegration rate was taken as the first gradient of the descending region from the onset of disintegration. The highest disintegration rate was noted for formulation 11 (10mm/sec). This correlated with the highest disintegration time. This may be explained in terms of the low PF68 and MD concentration which produced a fragile matrix of formulation 11 and thus resulting in rapid breakdown of the matrix. From an ocular perspective, this rapid disintegration is advantageous since it would confer minimal irritation to the eye surface as the time taken to dissolve was under 1s for the majority of formulations. Table 4.7 depicts the values obtained from the study. Figure 4.9 a shows the correlation between DT and DR.

4.3.4 Moisture content studies

The lyophilization process has been established to improve the long-term stability of formulations. Karl Fisher titrimetry was conducted in order to determine the moisture levels in formulations. The significance of this method was that although stable, lyophilized matrices may display a tendency to be hygroscopic and this could compromise the integrity of the dosage form if stored under incorrect conditions. Fischer reaction, moisture in the

sample reacts with Karl Fischer reagent quantitatively. It is based on the oxidation of sulphur dioxide by iodine following the consumption of water as depicted in Equation 4.7.

$$I_2 + 2H_2O + SO_2 \rightarrow 2HI + H_2SO_4 \qquad \textit{Equation 4.7}$$

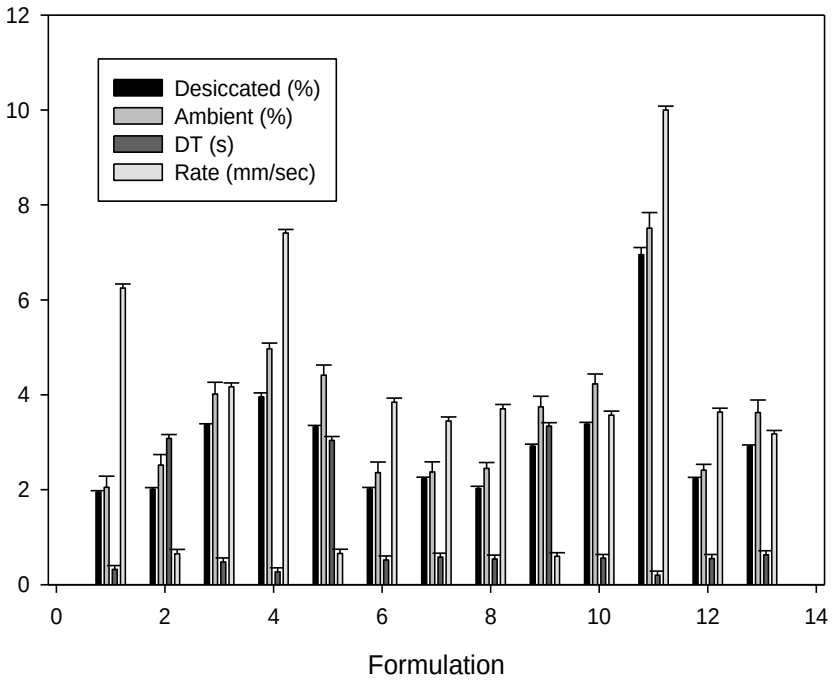
The endpoint of a titration represents a volume of the titrant needed for the reaction with the total amount of water present in the sample.[50] Moisture levels were determined under ambient (25°C, Relative humidity) and desiccated conditions (silica gel desiccant) after 24 hours. Moisture levels under ambient conditions ranged from 2.051-7.511%. Formulation 11 had the highest water content due to the fragility and highly porous structure. The voids allowed for moisture to be easily up-taken and thus a higher content was noted. Under desiccated conditions, moisture levels were reduced ranging from 1.950-6.953%. This suggested that exposure of the solid drops to ambient conditions did not influence the uptake of water to a great extent. Results indicate that a desiccant could contribute to lowering of moisture content levels. Moisture content values are listed in Table 4.7. Figure 4.9 is a graphical representation of the results.

Table 4.7. Moisture content of wafers under desiccated and ambient conditions

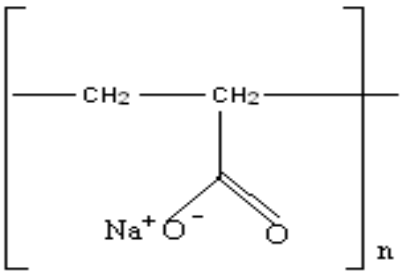
			Water content (%)	
Formulation	**EPDT (s)**	**Disintegration rate (mm/sec)**	**Desiccated conditions[1]**	**Ambient conditions[2]**
1	0.3200	6.250	1.950	2.051
2	3.0800	0.649	2.011	2.518
3	0.4800	4.167	3.367	4.015
4	0.2700	7.407	3.956	4.967
5	3.0400	0.658	3.324	4.415
6	0.5200	3.846	2.016	2.362
7	0.5800	3.448	2.231	2.376
8	0.5400	3.704	2.023	2.449
9	3.3400	0.598	2.921	3.747
10	0.5600	3.571	3.381	4.230
11	0.2000	10.00	6.953	7.511
12	0.5500	3.636	2.232	2.412
13	0.6300	3.175	2.915	3.626

[1]Silica gel (Vitapak®)
[2]Room conditions (25°C, Relative humidity)
Results are expressed as the mean of at least three measurements,
SDs obtained were within:EPDT≤0.171, DR≤0.509, dessicated≤0.151, ambient≤0.336.

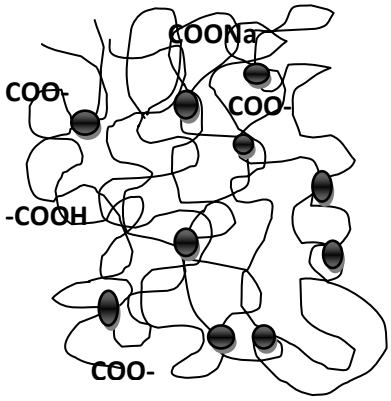
a)


Desiccated (%)
Ambient (%)
DT (s)
Rate (mm/sec)
0
2
4
6
8
10
12
14
Formulation

b)


CH2
CH2
Na+
O-
O
n

c)



d)

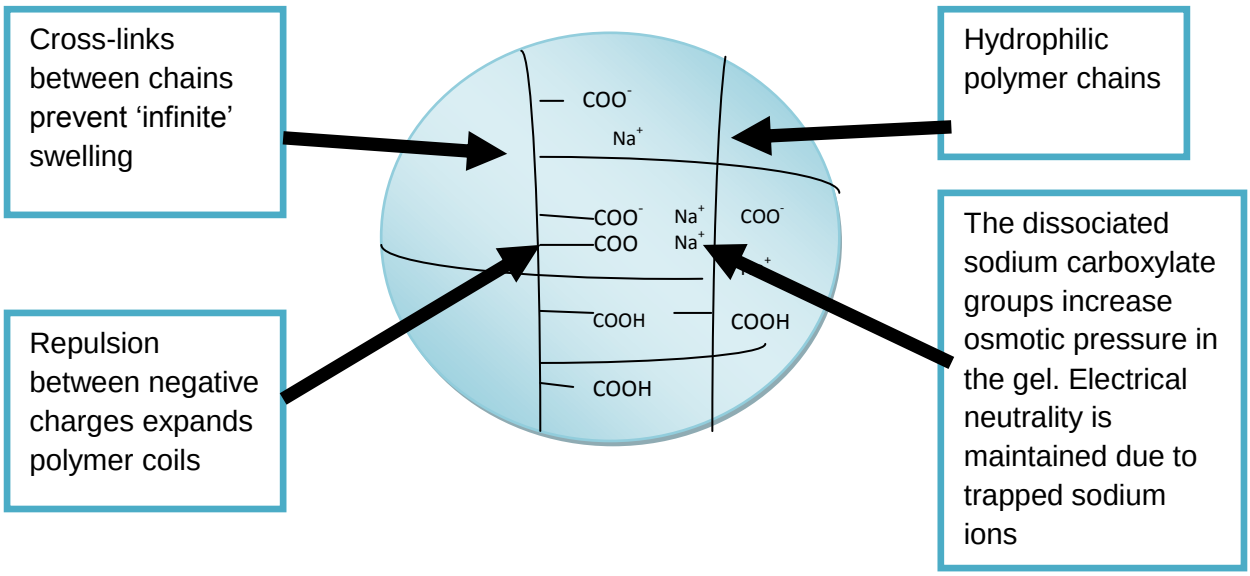


Figure 4.9: a) Horizontal bar graph depicting results from disintegration and moisture testing (error bars indicate standard deviation), b) chemical structure of PAANa, c) SAP network (adapted from www.m2polymer.com/html/superabsorbent_polymers.html) and d) process of charge repulsion resulting in polymer uncoiling and water interaction (adapted from www.watercampws.uiuc.edu/waterclear/*... /polymers _teacher_guide.p.*

4.3.5 Morphological structure of the solid eye drops matrices

The technology employed in the production of the solid eye drops was the lyophilization technique. This process involved freezing of the polymeric solution followed by freeze-drying which results in sublimation of water. Sublimation of the ice crystals results in the formation of pores in the matrix and determines the morphology of the resultant product.[51] SEM images of the matrix of formulation 1 were captured. The resultant product was, as expected, a porous solid matrix. The lyophilized matrix appeared to have a sponge-like surface and an interconnecting network with the presence of pores (Figure 4.10a). The pores were generally circular or asymmetrical across the matrix surface. Entrance of aqueous media into these pores allowed for rapid hydration and disintegration of the system.

It was noted that a relationship between pores and disintegration time existed. Matrices with a spongy pore appearance had a quicker disintegration time.

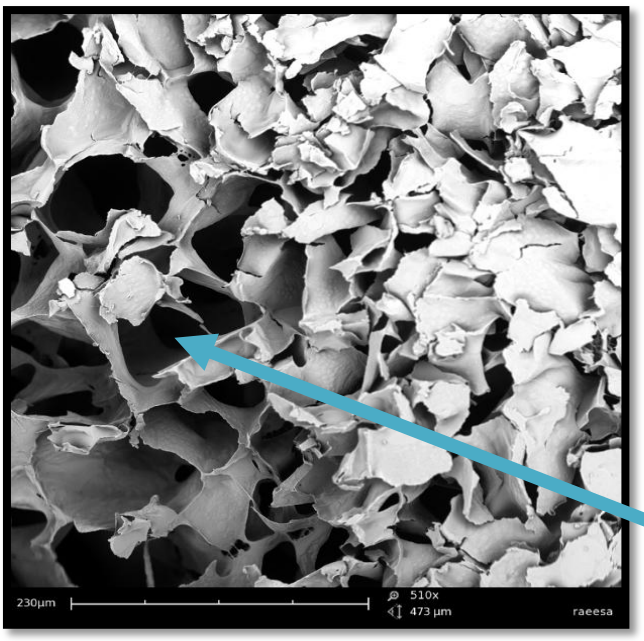
4.3.6 Stereomicroscopy of the solid eye drops matrices

Microscopic imaging of formulation 1 was performed to aid with visualization of the water uptake and rapid dissolution process (Figure 4.10b). This instantaneous process was apparent by the images captured. Initially, the unhydrated matrix and water front were distinctly separated. Upon addition of SLF, rapid ingression of the fluid was noted and the matrix dissolved in less than 1 second. The disintegration was consistent with the values obtained from disintegration profiling thus, confirming that the matrix was instantly soluble. Disintegration of the solid eye drops may be explained as being dissolution mediated whereby the disintegration process was due to dissolution of the available highly soluble components.

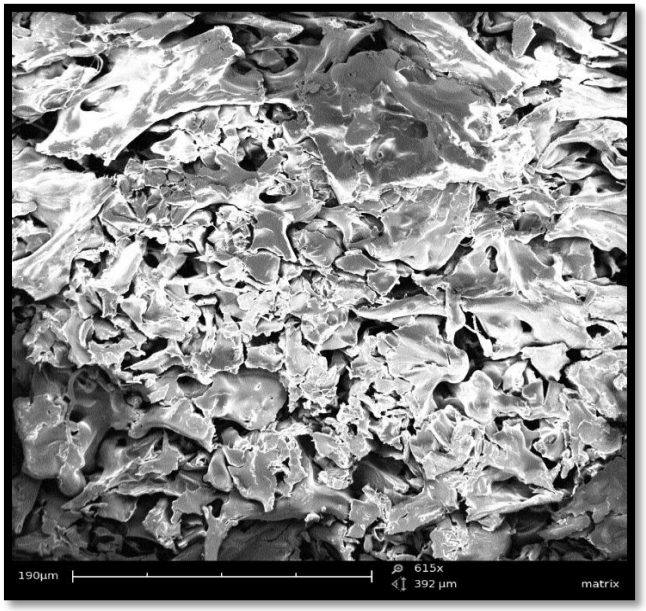
4.3.7 Fluorescent microscopy of the solid eye drops

Incorporation of this technique to the study of fast-disintegrating systems is fairly new. The use of organic dyes into solid matrices has useful applications. Improved photostability and fluorescence yield is noted in solids compared to liquids. Fluorescein is water soluble synthetic organic compound applied in microscopy. Rhodamine is a flourone dye that is used as a tracer in water for flow detection and due to the red colour and can be readily seen (Kolmakov et al., 2010). This test was carried out to view the actual fluid uptake by ingression of rhodamine-stained SLF (RSSLF) into the dry FITC-stained solid eye drop. Due to the rapid disintegration of the formulations it was noted that as the rhodamine was added, immediate dissolution occurred. The FITC-stained matrix appeared green in the image and as the RSSLF was added to the edge of the wafer, it was traced within the matrix and appeared red until the matrix was completely dissolved (Figure 4.10c). The significance of these results is that water uptake and hydration rate plays an important role in dissolution and ultimately affects drug release of the formulation.

a)



Pores allow for aqueous media to be imbibed into the matrix and results in rapid hydration and disintegration



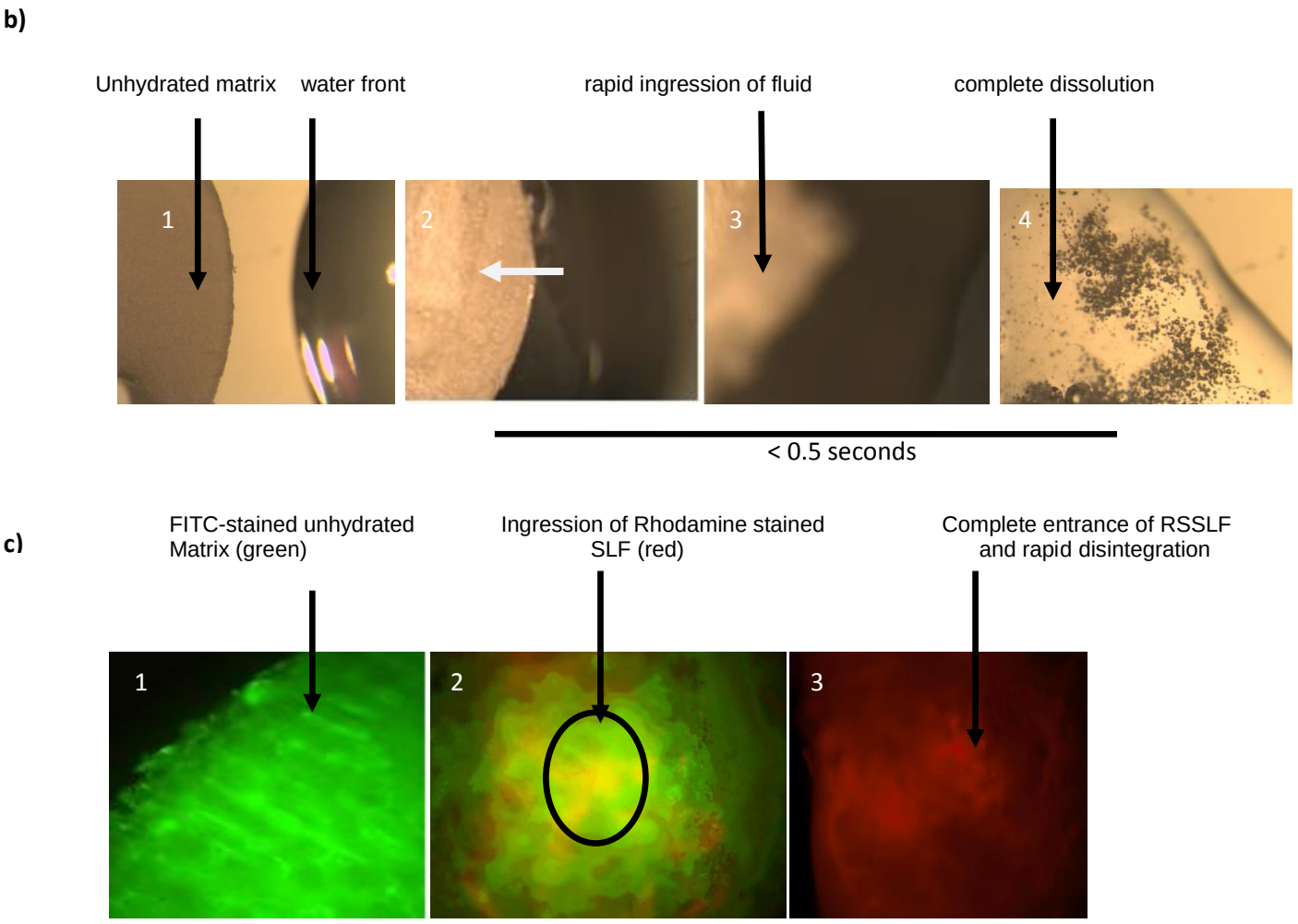


Figure 4.10: a) SEM images depicting the porous matrix surface of formulation 1 (510x and 615x magnification) and b) stereomicroscopy images for visualization of the rapid dissolution process (light and darkfield field 10x magnification); and c) Fluorescent images depicting fluid ingression into the matrix (10x magnification).

4.3.8 Drug entrapment efficiency

The prescribed dose of timolol as an anti-glaucoma agent is 0.25-0.5%$^{w}/_{v}$ as a solution (Aqil et al., 2010). Thus, this was used as an indication of the amount of drug that should be present in the formulations. Since it was a solid formulation, solid eye drops with approximately 0.68mg of timolol maleate (equivalent to 0.55mg timolol maleate base) were formulated (Saettone et al., 1995). The purpose of calculating the DEE was to determine the percentage of drug loaded into the formulations. This would ultimately affect the drug release profiles and a desirable attribute for the formulations are a high drug loading capacity. DEE for the dosage form ranged from 79-96%. Table 4.8 outlines DEE values calculated.

4.3.9 Drug release studies

Drug release studies for the solid eye drop formulations were determined. The plots of fractional drug release are depicted in Figure 4.11. The $MDT_{50\%}$ was calculated in order to determine the drug release characteristics (Table 4.8). This is the mean time for the drug to dissolve under *in vitro* conditions. With respect to drug release patterns, low $MDT_{50\%}$ values represent rapid release and high $MDT_{50\%}$ values indicate a prolonged release. Therefore, a low MDT was desirable since this was an immediate release formulation. All formulations showed initial burst release of the drug. This may be attributed to the porous nature of the system since it was instantaneously soluble upon contact with SLF due to the presence of hydrophilic polymers (PF68 and HPC) as well as the SAP PAANa, and therefore the drug contained was rapidly liberated. It is important to note that this instantaneous release was a desirable feature. Formulations 2, 5 and 9 which contained a higher concentration of PF68 (5%) showed a longer $MDT_{50\%}$ values of 54.5, 55.00 and 56.5 minutes respectively. This could be due to the gel-like properties of the polymer with increased concentration as explained previously.

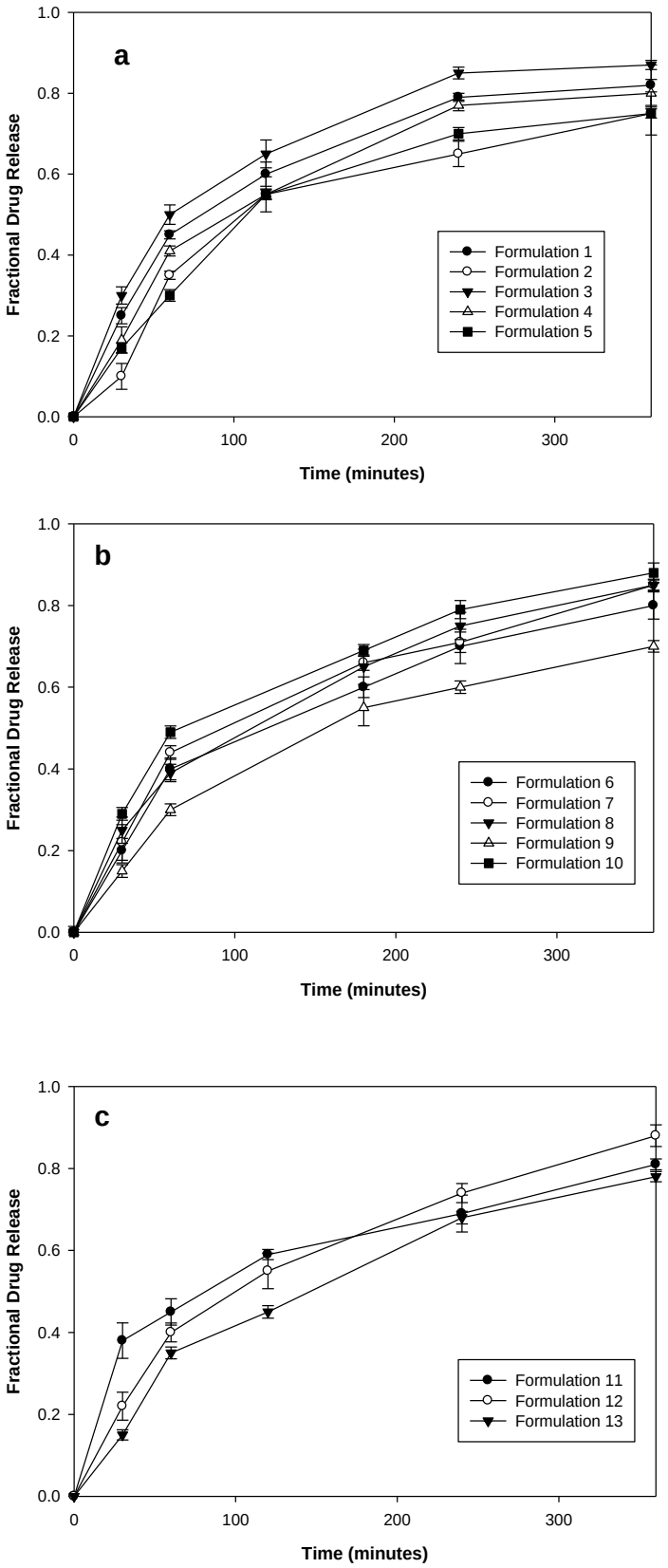


Figure 4.11: Drug release profiles for the design formulations (error bars indicate standard deviation).

Table 4.8: Mean dissolution times calculated for drug release characteristics

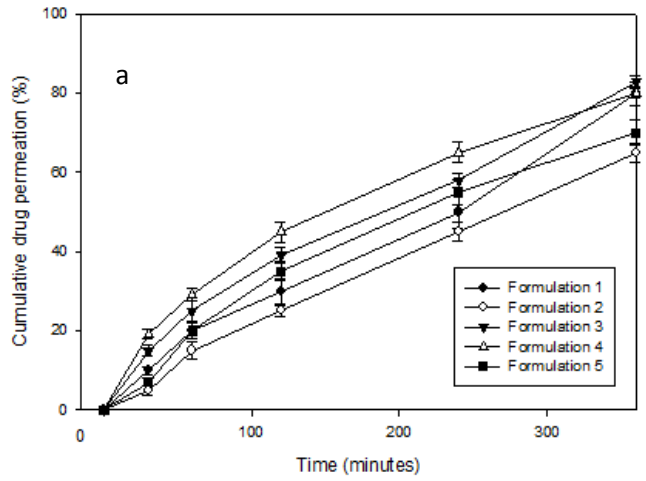
Formulation	DEE (%)	$MDT_{50\%}$ (minutes)
1	81.573	25.0000
2	83.295	54.5000
3	94.451	42.1000
4	93.262	27.2500
5	88.227	55.0000
6	85.987	49.5000
7	90.139	49.0000
8	95.225	48.7500
9	91.293	56.5000
10	89.982	48.2000
11	78.922	21.2000
12	96.132	48.1000
13	92.918	45.2500

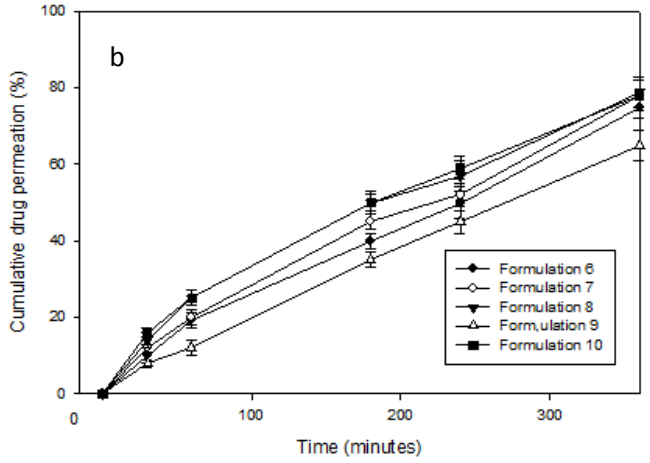
Results are expressed as the mean of three measurements, SD's obtained were within: DEE ≤2.517 and MDT ≤0.430.

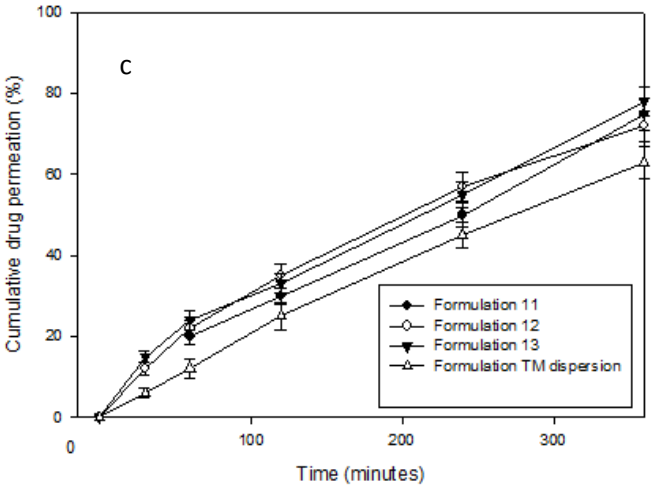
4.3.10 *Ex vivo* permeation studies

The effect of formulation components on corneal permeation of TM was investigated. This was compared to a pure TM dispersion (TMD) formulated in saline (0.9% NaCl). The cumulative drug permeated (%) and cumulative flux at 360 minutes ($mg.cm^{-2}.min^{-1}$) were determined for the formulations. Results indicated that increased cumulative permeation values were noted for formulations 1, 3, 7, 8, 10, 11, 12 and 13 (Figure 4.12a-c). Overall, the formulations displayed an improved permeation capability compared to the pure drug. This can be attributed to the properties of selected polymers. HPC has been used in ocular formulations as viscosity enhancers. This improves the muco-adhesive properties and allows for better corneal interaction (Qui et al., 2009). Similarly, PF68 also displays a tendency to interact with the cornea. This can be explained due to hydrophobic and hydrophilic nature which simulates the action of mucin (a glycoprotein) on the eye surface. Furthermore, both PF68 and HPC are water soluble polymers and in the presence of water or biological fluid they imbibe and can assist in enhancing residence time of the drug by corneal interaction as opposed to liquid formulations. Formulations 2, 5 and 9 displayed lower cumulative permeation values. This could be on account of the increased PF68 concentration which resulted in increased residence time and slower drug release compared to the other formulations. In terms of the drug, TM is a nonselective β-blocker and is both a hydrophilic and lipophilic drug. TM is proposed to pass the cornea mainly via passive diffusion through the transcellular pathway. These mechanisms may have contributed to the permeation of drug across the tissue. Flux values for the solid eye formulations ranged from 0.00039-0.00052$mg.cm^{-2}.min^{-1}$ (Figure 4.12d). The drug dispersion showed a lower flux of 0.000378 $mg.cm^{-2}.min^{-1}$. Thus, it is certainly evident that the drug dispersion into the polymeric

structure may have an advantage of improving the residence time by circumventing barriers of the eye such as the rapid washout due to lachrimation and drainage.







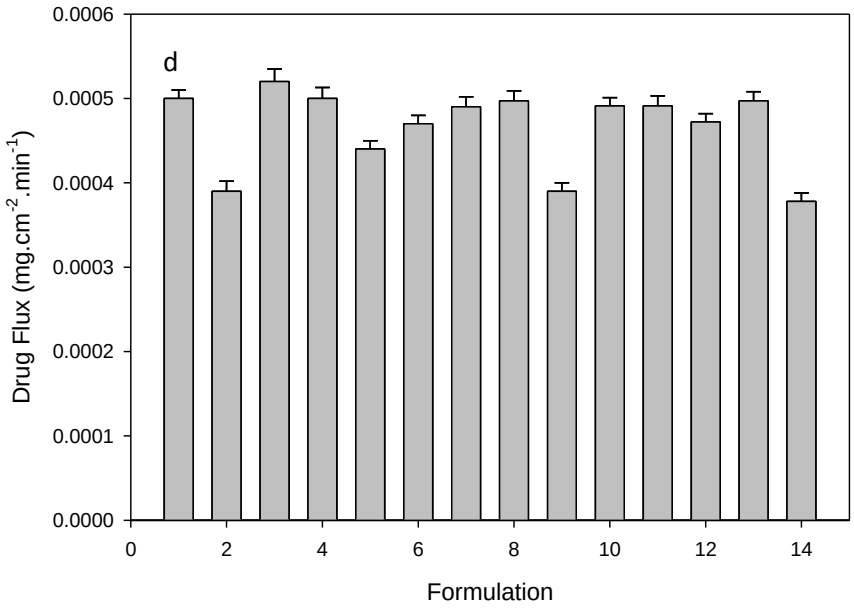


Figure 4.12: Graphs depicting cumulative drug permeated (%) of: a) formulations 1-5, b) formulations 6-10, c) formulations 11-13 including TM dispersion and flux ($mg.cm^{-2}.min^{-1}$) calculated at 360 minutes for: d) formulations 1-13 including TM dispersion (error bars indicate standard deviation).

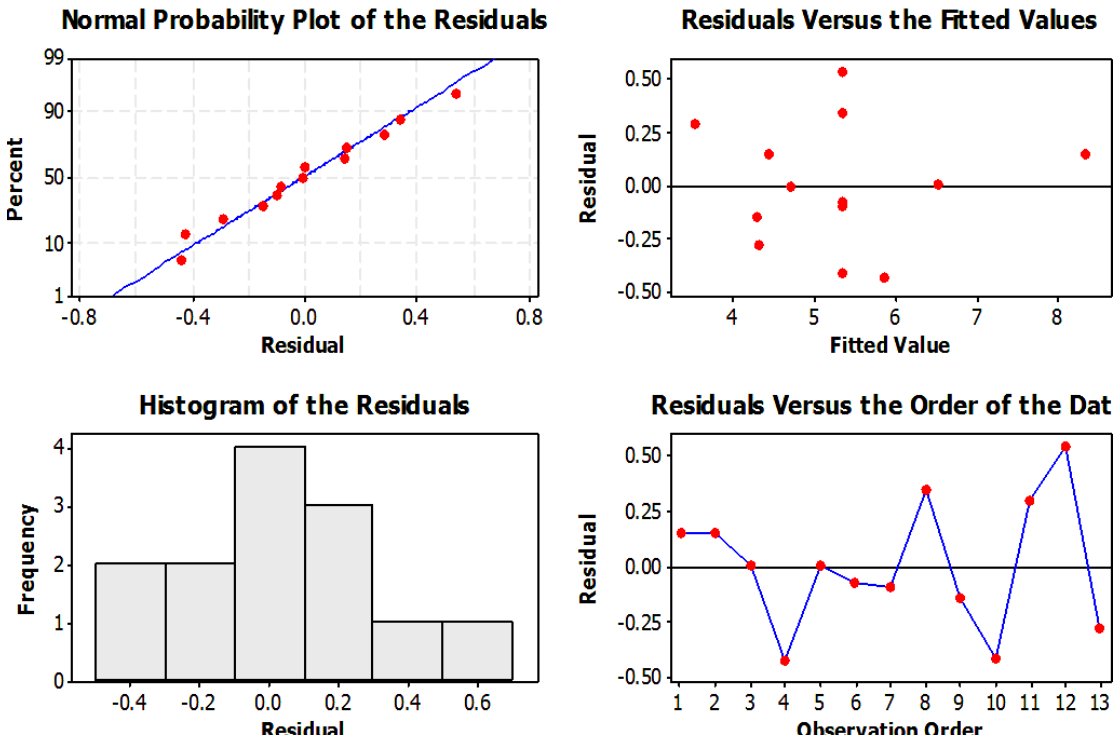
4.3.11 Statistical Analysis

4.3.11.1 Residual plots

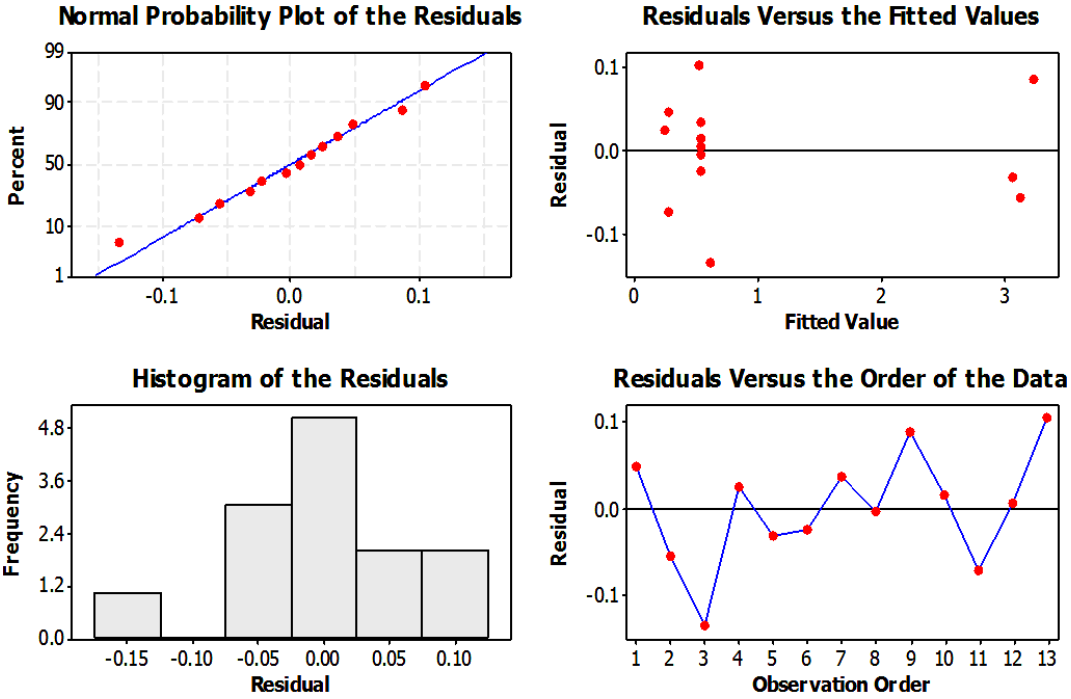
Residual plots indicate the difference between the predicted and actual values. The plot for MR suggested that most of the residuals follow a normal distribution as majority of the points fall on the 45° line (Figure 4.13a). It also suggests that there were no significantly unusual data points in the data set. Two outliers were noticed, none of which were influential points. These are unusual points and do not change the fact that the data is normally distributed. The histogram is used to check whether residuals are normally distributed. A symmetric bell-shaped histogram which is evenly distributed around zero indicates that the normality is likely to be true. From the residuals vs. fitted plot, it can be noted that the variance is constant as residuals are random about zero. This suggests that the assumption that the relationship is linear is reasonable. A horizontal-band pattern suggests that the variance of the residuals is constant. In terms of DT, residual plots displayed a random scatter (Figure 4.13b). This showed that none of the assumptions of regression were majorly violated. The normal probability plots fell on the straight line indicating that the data was normally distributed. The residuals roughly form a "horizontal band" around the 0 line. This suggests that the variances of the error terms are equal. The histogram indicated that random error was not normally distributed and this suggested that the model's underlying assumptions

may have been violated. For MDT, fairly random scatter for residuals was noted (Figure 4.13c). There are a few outliers but one possible outlier with a potential influential point that will affect the regression**.** This indicates that there could have been no constant variance. The histogram shape did not follow a symmetrical bell-shape suggesting that underlying assumptions of the model may have been violated. Residual values increased as the size of the fitted value increased. Thus, the residual cloud was observed to be "funnel shaped" with the larger end toward larger fitted values. This means the residuals had larger scatter as the value of the response increased. From the residual vs order of the data, a positive serial correlation among error terms was observed. The plot suggests that the assumption of independent error terms was violated. The residuals and standardized residuals indicate that the response surface model adequately fit most cases. Predicted and observed values for the responses showed close correlation for MR, DT and $MDT_{50\%}$ with R^2 values 0.904, 0.995 and 0.968 respectively.

a)


Normal Probability Plot of the Residuals
Percent
Residual
Residuals Versus the Fitted Values
Residual
Fitted Value
Histogram of the Residuals
Frequency
Residual
Residuals Versus the Order of the Dat
Residual
Observation Order

b)


Normal Probability Plot of the Residuals
Percent
Residual
Residuals Versus the Fitted Values
Residual
Fitted Value
Histogram of the Residuals
Frequency
Residual
Residuals Versus the Order of the Data
Residual
Observation Order

c)

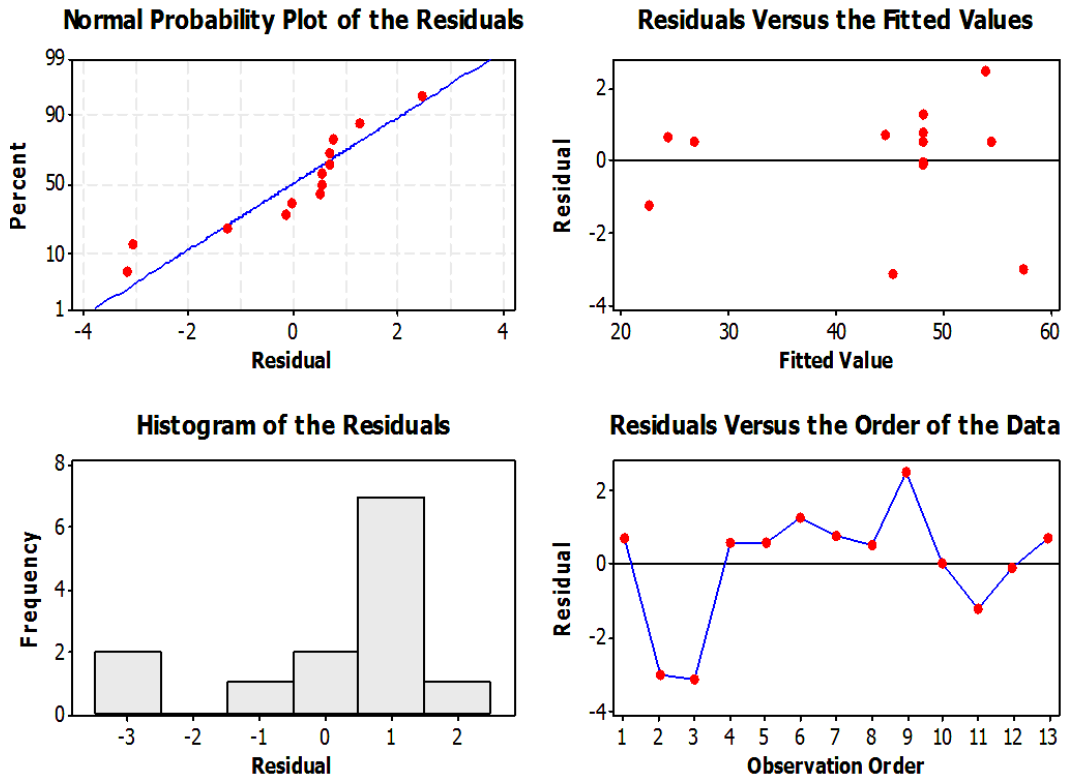


Figure 4.13: Residual plots for a) MR, b) DT and c) MDT_{50}

4.3.11.2 Basic statistical t-test and F-test for determination of variable effects on responses

The plots generated verified regression assumptions of constant variance of residuals and the added assumption of normality. The t and and F- tests were implemented for further explanation:

- T-test: tests whether a single predictor included in the model can actually predict the response variable.
- F-test: Tests if all predictors collectively are capable of predicting the response.

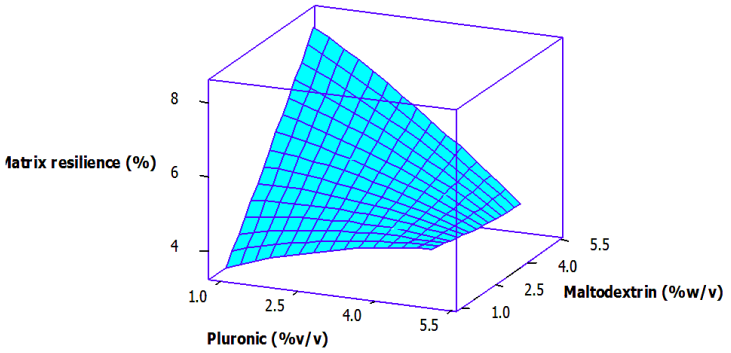
At a 5% significance level: PF68 (p=0.046), MD (p=0.007), and PF68*MD (p=0.000) were all significant in predicting the response. $PF68^2$ was not a significant variable. However, this was tested in a model which included all variables. Basically, this implied that $PF68^2$ did not assist in the variables of the response while the other variables (PF68, MD, PF68*MD and MD^2) were present. This could infer that one (or more) of the other predictors were better at predicting $PF68^2$ itself, that $PF68^2$ was marginilized. MD^2 was also insignificant.

4.3.11.3 Response surface analysis

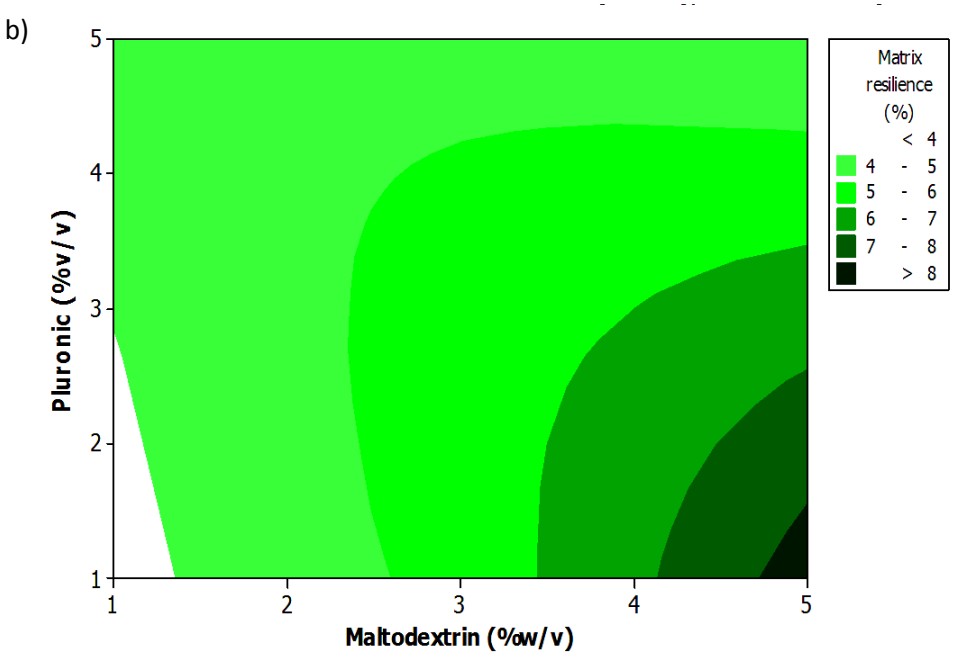
From these plots, the effect of the independent variables and their mutual interaction on the responses can be observed via the maxima and minima. Both MD and PF68 showed an effect on MR (p=0.000), however only a significant effect was noted for an increase in MD concentration. Increased PF68 concentrations showed a slight increase in MR. Higher MD concentrations yielded a more robust matrix thus a higher resilience. The ability of this excipient to contribute to overall stability of formulations is highlighted here. As explained previously, this saccharide as an excipient has the ability to serve as a lyoprotectant thus increasing the hardness of lyophilized matrices. Figure 4.14a accentuates that MR was highest at high levels of MD and low levels of PF68. In terms of DT, the effect of PF68 (p=0.000) and MD (p=0.567) were noted. Higher PF68 concentration resulted in an increased disintegration time. This can be due to the inherent property of this polymer forming a gel-like residue upon contact with increasing temperatures. Higher MD concentrations also showed an increase in disintegration time purportedly due to the conferring of overall strength. However, although a decreased disintegration time was desirable; all formulations displayed a tendency to dissolve in less than one second. Lowering PF68 and MD concentrations would ultimately result in a rapid disintegrating system with poor strength, an undesirable feature. The general fast disintegration times for all formulations can be attributed to the presence of the PAANa. This agent is hygroscopic and draws liquid into the formulation thus showing a good *wicking action* (Late and Banga,

2004). The influence of variable concentrations on DT is elicited in Figure 4.14b. The $MDT_{50\%}$ was influenced by both MD (p=0.033) and PF68 (p=0.000) concentrations (Figure 4.13c). Higher PF68 concentrations resulted in increased MDT since these formulations took slightly longer to dissolve and thus drug was retained in the residue rather than being immediately liberated for permeation. Figure 4.14 g provides a 3D scatter plot of the relationship between MD and MR.

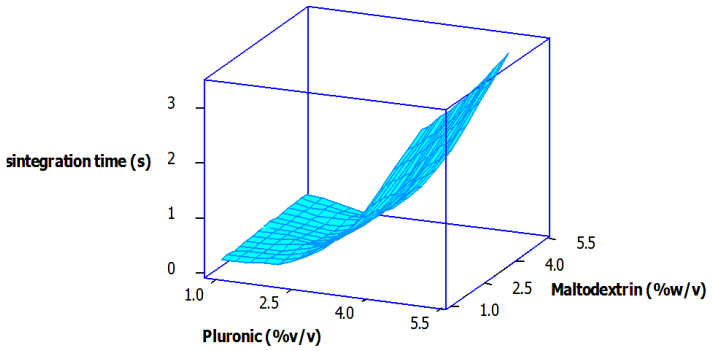
a)



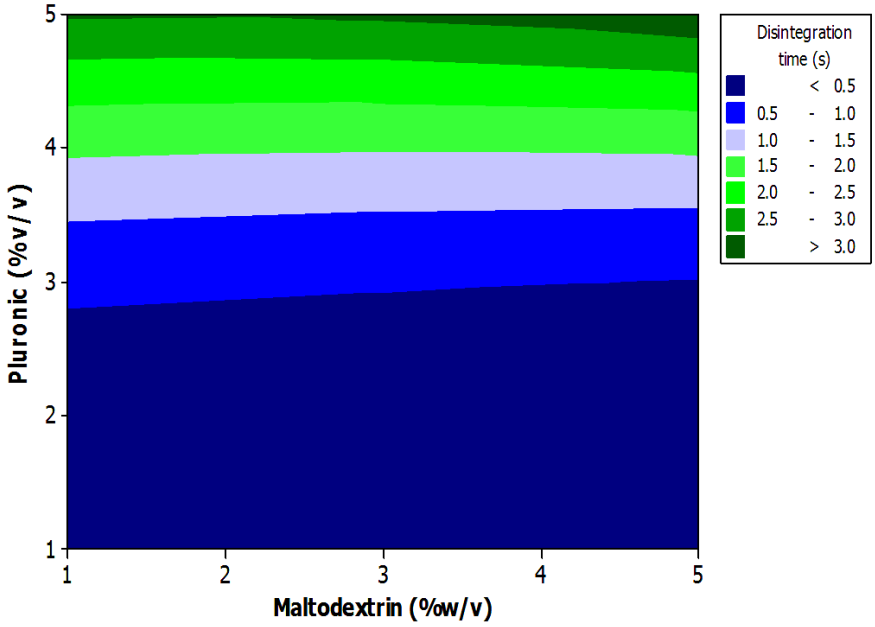
b)



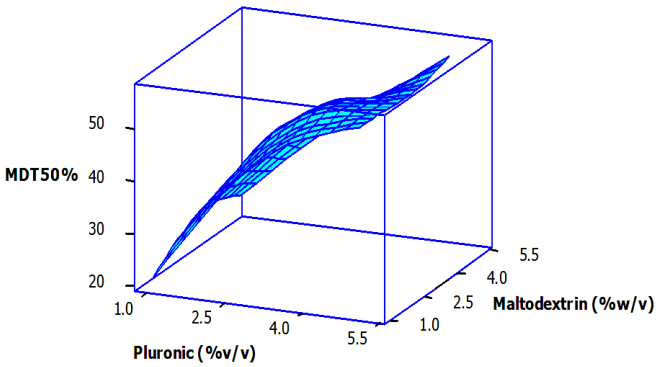
c)


sintegration time (s)
3
2
1
0
1.0
2.5
4.0
5.5
Pluronic (%v/v)
1.0
2.5
4.0
5.5
Maltodextrin (%w/v)

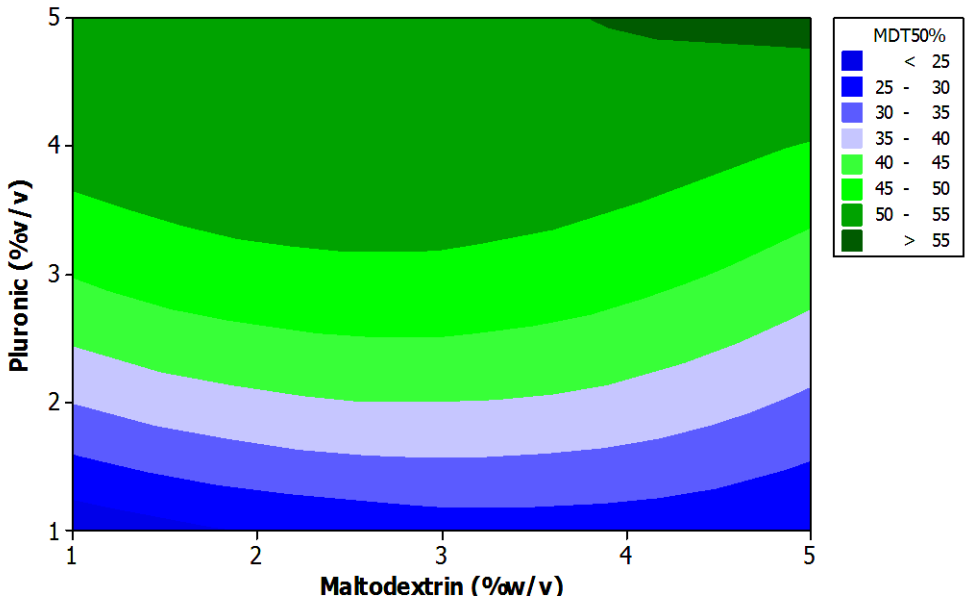
d)


Pluronic (%v/v)
5
4
3
2
1
1
2
3
4
5
Maltodextrin (%w/v)
Disintegration time (s)
< 0.5
0.5 - 1.0
1.0 - 1.5
1.5 - 2.0
2.0 - 2.5
2.5 - 3.0
> 3.0

e)



f)



g)

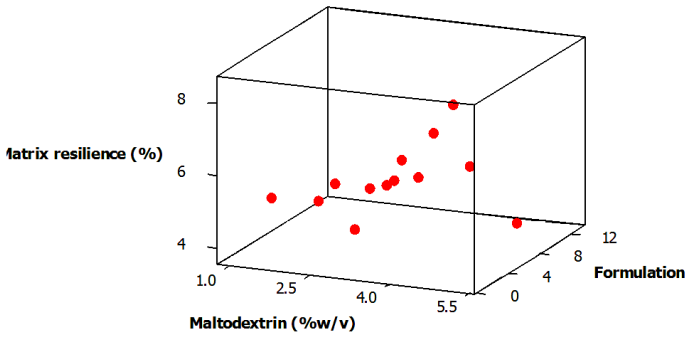
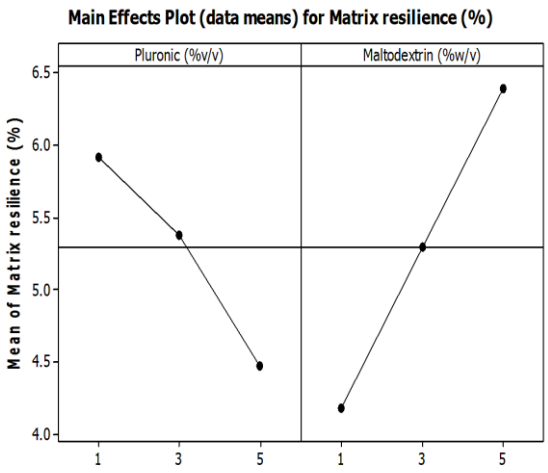


Figure 4.14: Response surface plots and corresponding contour plots for: a),b) MR vs PF68 and MD; c),d) DT vs MD, PF68; and e), f) MDT vs MD, PF68 and g) 3D scatter plot showing the relationship between MR and MD.

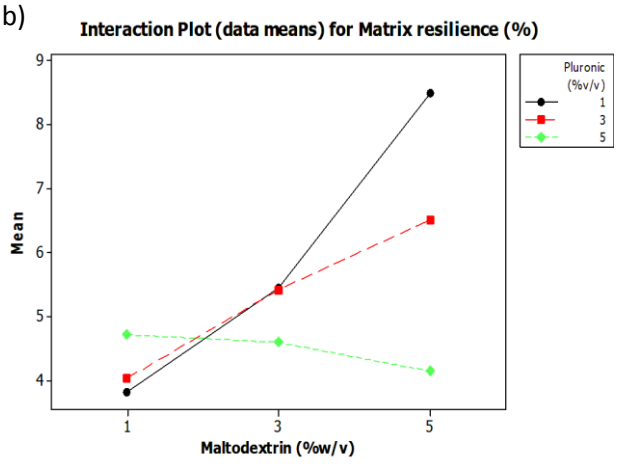
4.3.11.4 Main and interaction effects on responses

An interaction plot is a line graph for examining interactions between variables. The interaction effects are estimated by subtracting mean positive response values from the mean negative response values. A “main effect” is the effect of the independent variables on the dependent variable (Bakeman, 2005). The main effects plot depicts a horizontal line drawn at the grand mean. The effects are the differences between the means and the reference line. With respect to matrix resilience, MD had a more significant effect than PF68 (Figure 4.15a). The interaction plots (Figure 4.15b) depicted that there was an interaction since the lines were nonparallel. Greater deviation of the lines from the parallel implies a higher degree of interaction. This means that both PF68 and MD had a combined effect on MR. In terms of DT, the main effects plot showed that PF68 had an increased effect as opposed to MD (Figure 4.15c). The parallel line of MD in the interactions plot indicated no interaction between variables on this response (Figure 14d). PF68 at 5 $\%^{w}/_{v}$ was seen to be influential on DT. In the main effect plot for MDT it was observed that PF68 had a greater effect, while the interaction plot revealed that an interaction was present with both variables (Figure 4.15 e and f).

a)



b)



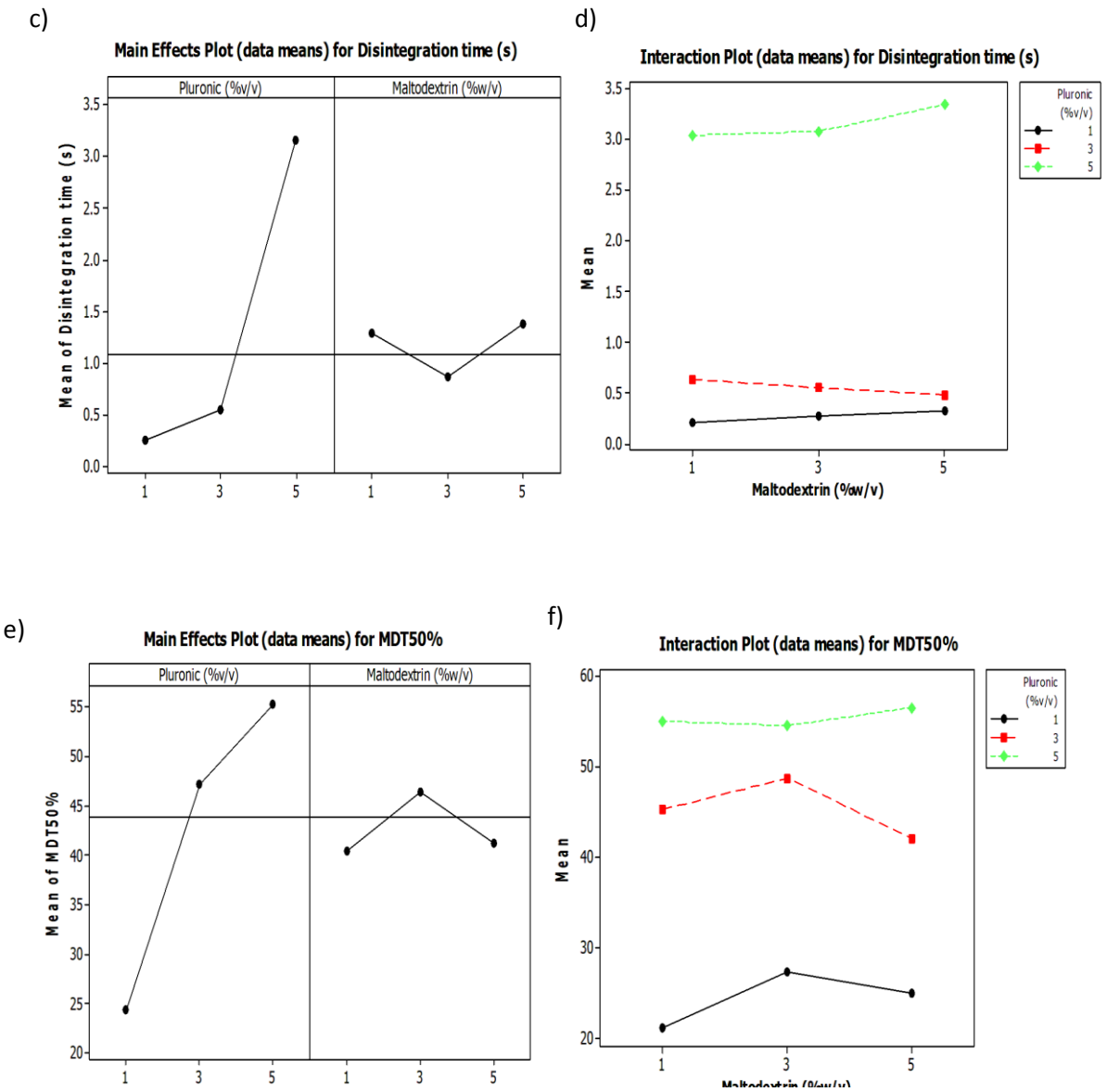


Figure 4.15: Typical: a) main effects plot for MR; b) interaction of the response values for MR; c) main effects plot for DT; d) interaction of the response values for DT; e) main effects plot for MDT; and f) interaction of the response values for MDT.

4.3.11.5 Agreement between Experimental vs. Predicted values

The predicted and observed values obtained were in close agreement for MR (R^2 0.904), DT (R^2 0.995) and MDT (R^2 0.968). Regression analysis therefore indicated that the models and surface plots generated were applicable. Cook's distance (CD) is an important diagnostic tools for detecting influential observations (Zhu et al., 2012). A few unusual observations were noticed. If CD is greater than 1, then the data point is worthy of further investigation. If CD is greater than 4, then the data point is influential. In terms of MR, the CD for formulation 11 (1.72577) stood out compared to the other results and this can be seen as influential. Formulations 9 and 11 showed a CD greater than 1 for DT as well as MDT. In addition, the Pearson product-moment correlation coefficient (r) was inspected. This is a

measure of the strength of linear dependence between two variables. The correlation coefficient ranged from −1 to 1. A value of 1 implies that a linear equation describes the relationship. The R^2 (0.944, 0.997, 0.998) and R^2-adjusted values (0.904,0.995,0.968) for the MR, DT and MDT models were satisfactory. A statistical Chi-squared (Cs) test was used to determine the goodness of fit between theoretical and experimental data. Greater differences between expected and actual data produce a larger (Cs) value. For MR, DT and MDT the Cs values were 1, 1 and 0.99 respectively. Values of 1 indicated a moderate fit and less than 1 indicated a good fit. Table 4.9 depicts the results for experimental and predicted values obtained while Figure 4.16 is a graphical representation of the agreement.

Table 4.9: Correlation between experimental and predicted values.

Formulation	MR			DT			MDT		
	E	P	CD	E	P	CD	E	P	CD
1	8.4960	8.3510	0.4307	0.3200	0.2720	0.9298	25.0000	24.315	0.3155
2	4.5890	4.4380	0.0501	3.0800	3.1360	0.1352	54.5000	57.536	0.6674
3	6.5190	6.5160	$2x10^{-5}$	0.4800	0.6160	0.8055	42.1000	45.270	0.7273
4	5.4390	5.8750	0.4176	0.2700	0.2460	0.0263	27.2500	26.686	0.0230
5	4.7120	4.7150	0.0002	3.0400	3.0720	0.4238	55.0000	54.449	0.2046
6	5.2740	5.3550	0.0019	0.5200	0.5440	0.0032	49.5000	48.216	0.0156
7	5.2570	5.3550	0.0027	0.5800	0.5440	0.0075	49.0000	48.216	0.0058
8	5.6980	5.3550	0.0337	0.5400	0.5440	$8x10^{-5}$	48.7500	48.216	0.0027
9	4.1370	4.2850	0.4485	3.3400	3.2520	3.1395	56.5000	54.015	4.1542
10	4.9340	5.3550	0.0506	0.5600	0.5440	0.0015	48.2000	48.216	0.0000
11	3.8140	3.5230	1.7258	0.2000	0.2720	2.1274	21.2000	22.449	1.0489
12	5.8950	5.3550	0.0836	0.5500	0.5440	0.0002	48.1000	48.216	$1.3x10^{-4}$
13	4.0290	4.3170	0.1822	0.6300	0.5260	0.4788	45.2500	44.553	0.03518

E- Experimental
P-Predicted
CD-Cook's distance

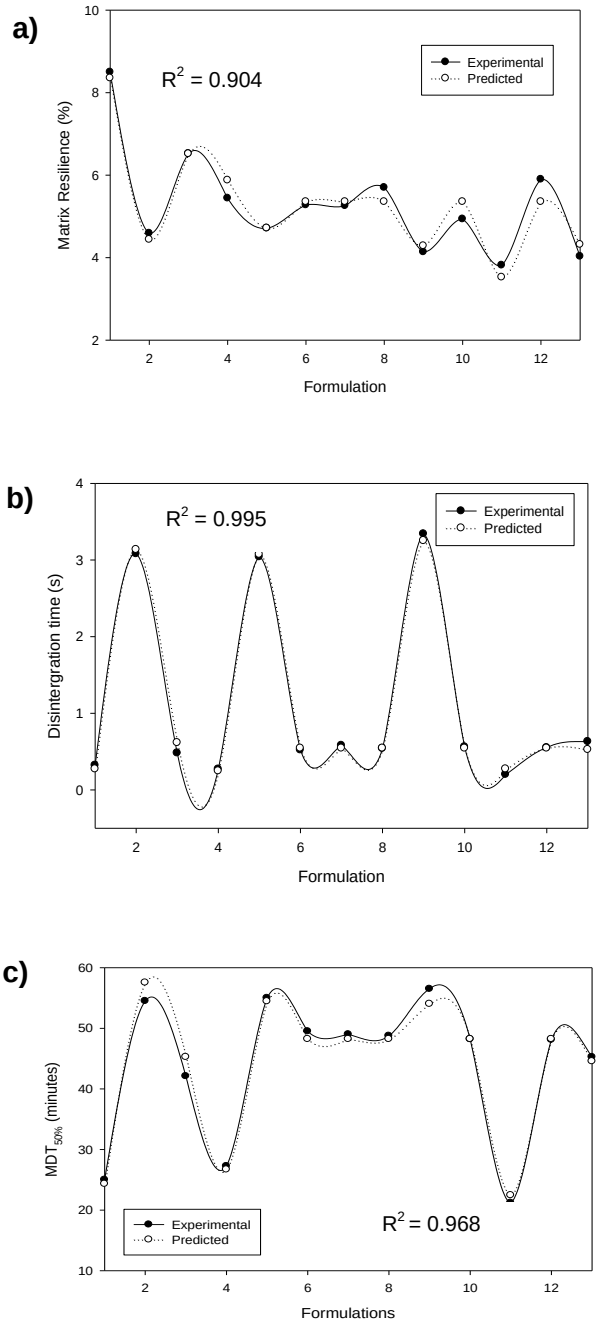


Figure 4.16: Agreement between experimental and predicted values for: a) MR; b) DT; and c) MDT.

4.3.11.6 Analysis of variance (ANOVA)

ANOVA was conducted on the input variables of the solid eye drops to determine which input variables had a significant effect on the recorded output properties of the solid eye drops. Points for the output variable indicated that for MR and MD, concentration had a

significant effect ($p<0.05$). PF68 concentration had a significant effect on DT and MDT ($p=0.000$). Therefore, the selected responses were reliable measures that would discern between the effects of different input variables on optimization of the solid eye drop formulation. Polynomial regression co-efficients relating the variables to the responses were generated and the estimated p-values for responses are outlined in Table 4.10 while full ANOVA results are depicted in Table 4.11.

Table 4.10. Estimated p-values for MR, DT and MDT

Term	p-value		
	MR	**DT**	**MDT**
Constant	0.072	0.000	0.616
PF68	0.046	0.000	0.000
MD	0.007	0.567	0.033
$PF68^2$	0.418	0.000	0.002
MD^2	0.796	0.620	0.035
PF68*MD	0.000	0.328	0.603

p value: significance

Table 4.11. ANOVA for dependant variables of the FCCCD

	DF	SS	MS	F
MR				
Regression	5	17.3688	3.47376	23.69
Linear	2	3.4991	1.74955	11.93
Square	2	0.1089	0.05446	0.37
Interaction	1	6.9090	6.90901	47.12
Residual error	7	1.0264	0.14663	
Lack of fit	3	0.4398	0.14659	1.00
Pure error	4	0.5866	0.14666	
Total	12			
DT				
Regression	5	16.87453	3.37491	459.65
Linear	2	1.12010	0.56005	76.28
Square	2	4.32613	2.16306	294.60
Interaction	1	0.00810	0.00810	1.10
Residual error	7	0.05140	0.00734	
Lack of fit	3	0.04940	0.01647	32.93
Pure error	4	0.00200	0.00050	
Total	12			
MDT				
Regression	5	1634.989	326.998	73.51
Linear	2	375.060	187.530	42.16
Square	2	205.312	102.656	23.08
Interaction	1	1.322	1.322	0.30
Residual error	7	31.139	4.448	
Lack of fit	3	29.797	9.932	29.60
Pure error	4	1.342	0.335	
Total	12			

SS-sum of squares
DF- degrees of freedom
MS- mean squared
F- value

Full regression equations for MR, DT and MDT are given by:

$$MR\ (\%) = 1.51979 + 0.92352\,[PF68] + 1.44252\,[MD] - 0.04951\,[PF68^2] + 0.01594\,[MD^2] - 0.32856\,[PF68*MD] \quad \textit{Equation 4.8}$$

$$DT\ (s) = 1.0503 - 1.03134\,[PF68] - 0.5134\,[MD] + 0.28668\,[PF68^2] + 0.00668\,[MD^2] + 0.01125\,[PF68*MD] \quad \textit{Equation 4.9}$$

$$MDT_{50\%}\ (min) = 2.0774 + 17.3002\,[PF68] + 5.5669\,[MD] - 1.5261\,[PF68^2] - 0.8261\,[MD^2] - 0.1437\,[PF68*MD] \quad \textit{Equation 4.10}$$

4.3.11.7 Response optimization procedure and identification of the optimum ISED formulation

The optimization levels were obtained employing software (MINITAB®, V14, Minitab, USA). Simultaneous constraint optimization of the responses were carried out for obtaining a formulation that would have a mechanically robust structure and capable of rapid disintegration and instantaneous drug release. The constrained settings utilized are shown in Table 4.12. A single formulation was developed following constraint optimization. Statistical desirability of the formulation was 0.958 (Figure 4.17). The optimal formulation predicted comprised of: 5%$^{w}/_{w}$ MD and 2.94%$^{w}/_{w}$ PF68. Agreement between the experimental and predicted values for the optimized formulation was satisfactory (Table 4.12). Thus, the response surface methodology allowed for the generation of the formulation with the desired characteristics.

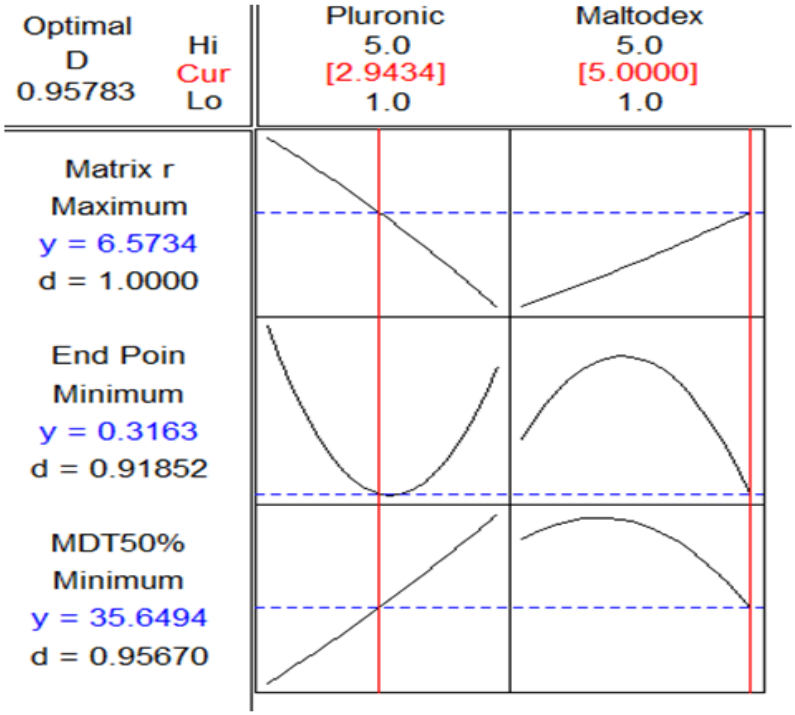


Figure 4.17: Desirability plot depicting factor settings and desirability values for the variables and responses

Table 4.12. Constraints for the optimal formulation and experimental and predicted response values for the optimized formulation

Constraint	Level
PF68(%$^{w}/_{w}$)	1-5
MD(%w/w)	1-5
MR	5-6.5
DT	0.3-0.5
MDT	25-50

Measured Response	Predicted	Experimental	Desirability
MR	6.574	8.625	1.00
DT	0.316	0.350	1.00
MDT	35.65	30.21	0.847

4.3.11.8 Mathematical modeling

Mathematical modeling was used to simulate the dissolution of the ISED in the eye in terms of mathematics. The thin film features and advective properties of the tear fluid were neglected. Additionally, the eye ball was treated as flat. The model considered dissolution as taking place radially outward (with azimuthal symmetry) and neglects any variation of dissolution in the direction of the tear thickness (vertically for an eye looking up). Using the physical parameters of the eye as well as the time measured for dissolution in the experiment a dimensionless diffusions equation was solved using mathematics. The full partial differential equation is given by equation 4.11:

$$\frac{\partial c}{\partial t} = \frac{\alpha}{r}\frac{\partial}{\partial r}\left(r\frac{\partial c}{\partial r}\right) \qquad \textit{Equation 4.11}$$

Where:

C = concentration of ”wet” drug,

t = time,

α^2 = ratio of the diffusivity coefficient of the ”wet” drug and the scale time over the radius of the eye (the scale time is just the time for dissolution as measured by experiment)

r = radius from the centre of the eye surface (i.e. the middle of the pupil).

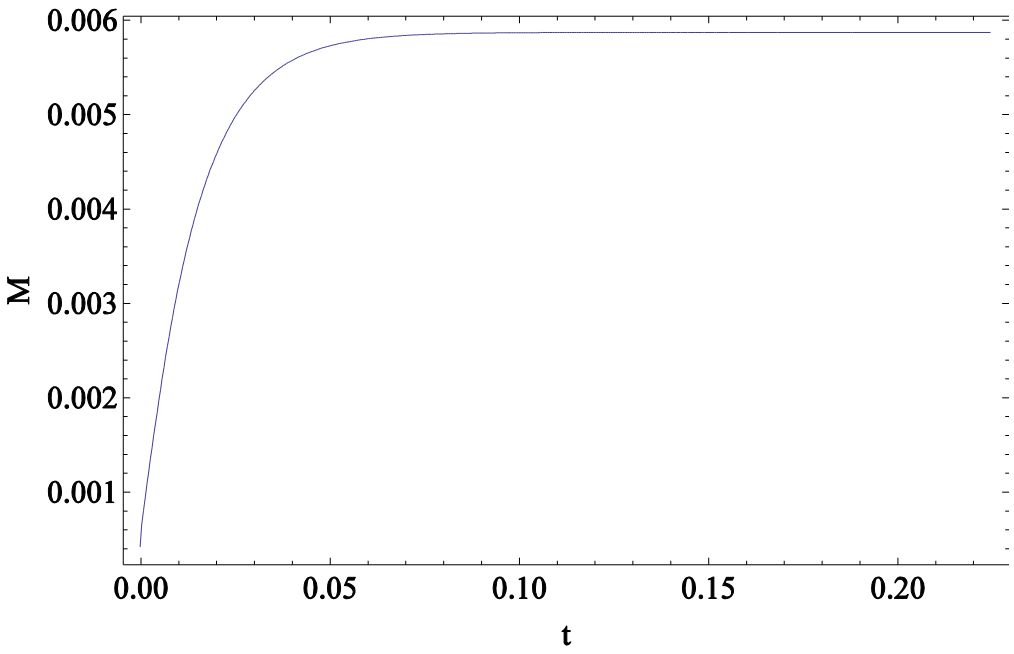
The initial and boundary conditions are now mentioned by equation 4.12:

$$c(0,r) = \theta\left(\frac{1}{5} - r\right),\ c(t,0) = 1,\ \left.\frac{\partial c}{\partial r}\right|_{r=1} = 0 \qquad \textbf{\textit{Equation 4.12}}$$

The first boundary condition signifies that as dissolved ISED is carried away it is replaced by more ISED. This condition must change once the entire ISED has been dissolved. Although the equation above has been solved numerically some analytical properties can be mentioned in terms of the geometry chosen in the model. In the current model (using cylindrical geometry) the analytical solution can be given in terms of a decaying Bessel function while if spherical geometry is used (assuming a fixed radius and azimuthal symmetry) the solution may be written as a decaying Legendre function.

A finite volume method was implemented to solve the modeling equation. Below is given a plot of the mass of the ISED deposited into the tear layer as a function of time (Figure 4.18a). Additionally, the concentration profile at different times is shown (Figure 4.18b). 500 000 iterations were run in the simulation with 150 grid points.

a)



b)

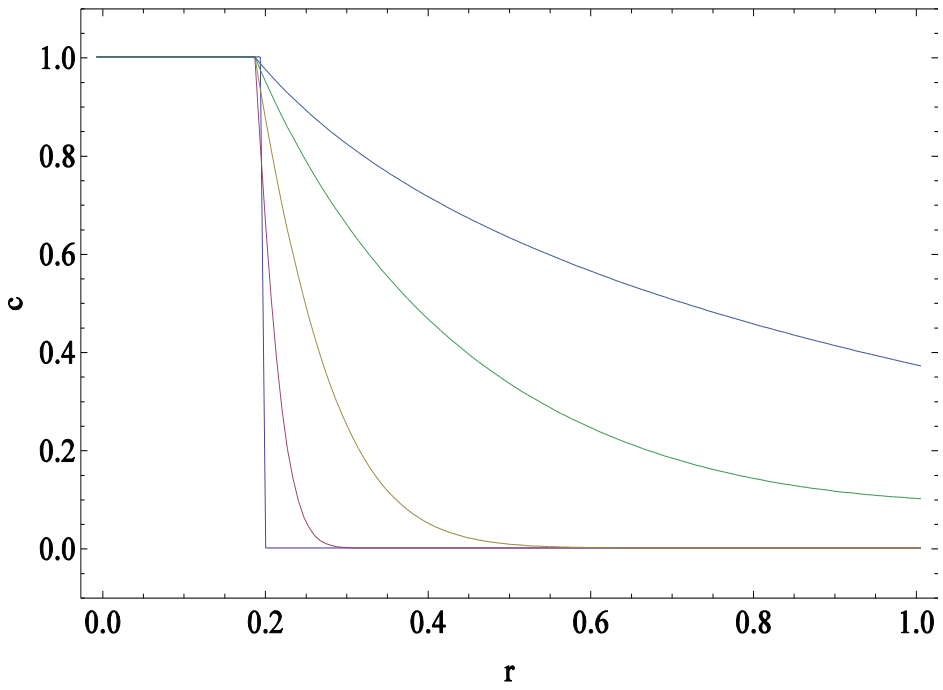


Figure 4.18: Plots depicting: a) the mass increase of the ISED in the tear layer and b) concentration profile at several times.

4.4 Concluding Remarks

This chapter aimed at formulating a rapidly disintegrating system with sufficient strength. Textural analysis revealed a robust matrix was formed. Disintegration testing demonstrated that instant dissolution was achieved signifying that rapid liberation of drug was possible. Surface morphology allowed for visualization of the porous surface of the formulations. Flourescence and Stereomicroscopy confirmed the rapid and complete ingression of fluid into the system. From drug release analysis, it could be deduced that rapid release was achieved for most formulations. *Ex vivo* permeation studies showed that the solid eye formulations had an improved drug permeation compared to a pure dispersion of the drug. Guidance by the implementation of the FCCCD methodology for the generation of a significant mathematical model allowed for efficacious optimization of the system. The fitted responses displayed a high degree of correlation between the predicted values and experimental data which indicates that the design was reliable. These findings provide an initial step in the formulation of versatile instantaneously disintegrating systems with enhanced physical properties. Rapidly dissolving systems are cost-efficient and are simple to manufacture and this allows for further advancements in terms of drug delivery in the ocular field. The optimized formulation was generated for further analysis.

CHAPTER 5
ELUCIDATION OF THE IN DEPTH PHARMACEUTICAL CHARACTERISTICS OF AN OPTIMIZED RAPIDLY DISINTEGRATING OPTHALMIC DRUG DELIVERY SYSTEM

5.1 Introduction

New and innovative drug delivery systems are required to undergo extensive *in vitro* and *ex vivo* evaluation prior to proceeding to *in vivo* stages. Moreover, an ocular pharmaceutical system requires special attention due to the intricacy and sensitive nature of this organ. The focus of the present chapter was to gauge the in-depth pertinent pharmaceutical properties of the optimized instantly soluble solid eye drop formulation.

Lyophilized systems often operate via the rapid intake of fluid with almost immediate disintegration and drug liberation. However, the process of lyophilization may have an impact on the physical properties, thermal behavior and chemical stability of the polymers involved (Guo et al., 2000). Therefore, detailed pharmaceutical analysis of the final product is mandatory in order to verify its stability. Additionally, the porosity of a freeze-dried system is significant since the voids within a matrix often display a relationship with the appearance and *in vitro* behavior of the dosage form (Sznitowska et al., 2005).

In terms of drug release, kinetics on dosage forms are undertaken since the drug may display varied release patterns, depending on the dosage form and final intended application. Several models have been proposed for the drug release mechanism from fast disintegrating systems. The purpose of model fitting is to actuate the mechanism of the release of drug from the specific dosage form employing mathematical models. Examples of models include: zero order, first order, Higuchi, Hopfenberg, Hixon-Crowell, Weibull, Baker-Lonsdale and Korsmeyer-Peppas (Costa and Lobo, 2001). Ultimately, the results will indicate which model best fits the drug release profile from the specific dosage form extracted from *in vitro* data.

Of crucial importance is the toxicity of an ocular formulation. As pointed out by Vargas and co-workers (2007), in order to evaluate novel drug delivery systems, the use of animal models is required but has the disadvantage of being costly, difficult and time-consuming. Apart from this, legal and ethical issues pertaining to animal use have to be taken into account. Thus, alternative means have to be delved into with methods that can be compared to those expected under *in vivo* conditions. The Hens Egg Choriollointic membrane test (HET-CAM) is a substitute to the

Draize rabbit eye test for the assessment of potential ocular irritants and has been applied in various ocular studies (Gorle and Gattani, 2009; Gilhotra and Mishra, 2012). The Draize test is a highly controversial and criticized test due to the harmful effects inflicted on the test subjects. Thus, the HET-CAM test can be used as a pre-screening test in order to understand the potential behavior of the dosage form. The advantage of this test is the sensitivity, rapidity and cost-effectiveness (Schrage et al., 2010). This test has been accepted in Europe and documented in the current EU guidance to The UN Globally Harmonized System of Classification and Labeling of Chemicals (UN GHS) (European Union. 2009; Scheel et al., 2011).

The above-mentioned tests are all of value for the characterization of the system and ultimately the performance. Polymers such as HPC and PF68 have been found to be compatible with the eye surface and offer advantageous effects such as good corneal adhesion and safety. Therefore, the aim of this chapter was to evaluate the properties of the optimized lyophilized solid eye drops. Optimized eye drops were obtained from Chapter 4 employing DOE and constraint optimization. Thermal analysis, molecular transitions, surface morphology, porosity studies, kinetic drug evaluation (zero-order, first order and Hopfenberg models), ocular tolerance safety testing and *ex vivo* permeability across rabbit corneas were conducted.

5.2. Methods and Materials

5.2.1 Materials

Hydroxypropylcellulose (HPC) (M_w= 80 000 g/mol) (Klucel®, Hercules Incorporated, Wilingtion, DE, USA), glycyl-glycine (diglycine) (M_w= 132.12 g/mol) (Fluka BioChemika, Belgium), poly(acylic acid sodium salt) (PAA-Na salt) (M_w = 5100 g/mol), Maltodextrin (dextrose equivalent 16.5-19.5), Pluronic® F-68 (M_w= 8400 g/mol), Sodium Dodecyl Sulphate (SDS) (M_w= 288.38g/mol) and Timolol maleate salt (M_w=432.49g/mol) were all purchased from Sigma-Aldrich (St. Louis, MO, USA). All other reagents were of analytical grade and used as supplied.

5.2.2 Attainment of an optimized formulation

A two-factor, three-level Face Centred Central Composite Design (FCCCD) was applied for the construction of a model describing the effect of formulation constituents on the characteristics of the system. Solid eye drop formulations of various combinations were prepared in accordance with the FCCCD. In order to determine the optimal formulation, several responses were tested: Textural characteristics, disintegration testing and *in vitro* drug release. Constraint optimization

predicted an optimized formulation of MD and PF68 concentrations with sufficient strength and rapid disintegration as carried out in chapter 4 using Minitab®.

5.2.3 Preparation of polymeric solutions and synthesis of solid eye drops according to optimized constraints

Aqueous solutions of polymer were prepared in accordance with the optimized formulation components obtained using: HPC 1%$^{w}/_{v}$, PAANa 0.25%$^{w}/_{v}$, DG 0.25%$^{w}/_{v}$, MD 5%$^{w}/_{w}$ and PF68 2.94%$^{w}/_{w}$. Components were dissolved in 100mL deionized water and agitated for 30 minutes until complete dissolution had occurred. Samples of 150µL were injected into each mould of the polyvinyl chloride (PVC) blister packs. Samples were then frozen (Sanyo Ultralow Temperature freezer, MDF-U73V, Sanyo Electric company, Japan) for 24 hours at -82ºC to solidify the product. The product was placed in a lyophilizer (Labconco Freeze-Dry Systems, Labconco Corp., Kansas City, MO, USA) for 48 hours to extract excess water. On attainment of the samples they were stored in glass vials in the presence of 2g desiccant sachets. Figure 5.1 provides a visual depiction.



Figure 5.1: Digital image of a batch of optimized ISED.

5.2.4 Determination of the molecular vibrational transitions

Fourier transform infrared (FTIR) spectroscopy is used for the detection of interactions between native polymers and blends as well as the specific groups found in all components. FTIR was carried out to detect vibration characteristics of chemical functional groups in response to infrared light interactions. A Perkin Elmer Spectrum 2000 FTIR spectrometer with a MIRTGS detector, (PerkinElmer Spectrum 100, Llantrisant, Wales, UK) was used. Samples were be prepared as pellets against a blank ZnCn pellet background at a wave number ranging from 4000 – 650 cm^{-1} and a resolution of 4. The spectrum software (Spectrum 100) was used for interpretation of the results.

5.2.5 Determination of thermophysical and supplementary properties via temperature modulated differential scanning calorimetry (TMDSC) and Thermal Gravimetric analysis (TGA)

Thermal analysis was carried out to determine the thermal properties of the formulations. A Temperature Modulated Differential Scanning Calorimeter (TMDSC) (Mettler Toledo, DSC1, STAR^{e}System, Swchwerzenback, ZH, Switzerland) equipped with software for computation of evaluation numerical values was used. The glass transition temperature (T_g), melting temperature (T_m) and temperature of crystallization (T_c) were determined. Temperature calibration was attained by a melting transition of 6.7mg indium. Samples (10mg) were weighed out on aluminium crucibles, sealed and tested within a temperature gradient of 0-300°C under constant N_2 purge to reduce the oxidation rate of 1°C/min. Supplementary thermal characterization was conducted using a Thermogravimetric analyser (TGA) (PerkinElmer, TG-IR 8000, Llantrisant, Wales, UK) in order to determine weight variations of samples as a function of temperature. The instrument was purged with N_2 (to prevent the occurrence of any undesirable reactions). Samples were placed in a pan using tweezers followed by heating between 50-550°C at a rate of 10°C/min. Weight vs. temperature plots were generated and analysed using Pyris^{TM} software.

5.2.6 Complementary surface morphology and porositometric analysis

The in-depth surface morphology and internal structure of the matrix was visualized. This was done by the use of scanning electron microscopy (FEI Phenom™, Hillsboro, Oregon, USA). Samples were mounted on a spud and gold plated by the sputter-coater (SPI module™ sputter-

coater and control unit, West Chester, Pennsylvania USA).Samples were then viewed by the SEM at different magnifications. In addition, the visualization of the surface of the eye drop was determined by microscopy using light illumination for images in a 3-dimensional level. A stereomicroscope (Olympus SZX7 stereomicroscope, Olympus, Japan) connected to a digital camera (CC 12, Olympus, Japan) and image analysis system (AnalySIS® Soft Imaging System, GmbH, Germany) was employed. The porosity of the eye drop was determined by employing a porositometer (Micromeritics ASAP 2020, GA) with the use of Brunauer-Emmett-Teller (BET) isotherm of adsorption/desorption of nitrogen. The process involved:

1. *Degassing* of samples was carried out which involves an evacuation and heating phase, parameters of which are outlined in Table 5.1. Samples were inserted into tubes and underwent this phase.
2. *Asdorbtive properties* were then determined.

Data analysis

- *BET calculation*: obtained from determination of the volume of adsorbed gas.
- *T-plot calculation*: analysis of area and total volume due to micropores
- *Barrett-Joiner-Halenda (BJH)*: mesopore volume/area distribution

Table 5.1. Parameters employed for degassing phase of wafers

Parameters	Settings
a) Degassing conditions (evacuation)	
Temperature ramp rate	10°C/min
Target temperature	30°C
Evacuation rate	50.0 mmHg/s
Unrestricted evacuation from	30.0 mmHg
Vacuum set-point	500 mmHg
Evacuation time	60 min
b)Degassing conditions (heating)	
Ramp rate	10°C/min
Hold temperature	30°C
Hold time	900 min
Hold pressure	100 mmHg
c)Analysis conditions (adsorptive)	
Adsorptive	Nitrogen gas (N_2)
Maximum manifold pressure	925 kPa
Nonideality factor	0.0000620
Density conversion factor	0.0015468
Hard sphere diameter	3.860 A˚
Molecular cross-sectional area	0.162 nm^2

5.2.6 Kinetic modelling of release data

A release model describes the release pattern of a drug. The kinetics of TM released from the ISED was determined by finding the best fit of the curves to the zero-order, first order and Hopfenberg models as described below. DDSolver® (Microsoft Excel add-in) was used to analyze data.

A first order system describes a system where drug release is dependent on its concentration. This is given by:

$$Q = k_1 \, t^{1/2} \qquad \textit{Equation 5.1}$$

Where:

Q_1 = the amount of drug remaining at time (t),

Q_∞ = the total amount of drug present initially,

k_1 = first-order rate constant.

A zero order system indicates the release is independent of drug concentration. The following equation describes this:

$$Q_t - Q_0 = K_O\, t \qquad \textit{Equation 5.2}$$

Where*:*

Q_t = amount of drug released in time (*t*),

Q_0 = is the amount of drug dissolved at time zero and

k_0 = the zero-order release constant.

Hopfenberg (1976) described the release of drugs from surface eroding devices such as slabs, spheres and cylinders by:

$$\frac{M_t}{M_\infty}\ 1 - \left[1 - \frac{k_0\ t}{C_0 a_0}\right]^n \qquad \textit{Equation 5.3a}$$

$\frac{M_t}{M_\infty}$ = fraction of drug dissolved

k = erosion rate constant

C_0 = initial concentration of drug in the matrix

a_0 = initial radius for a sphere or cylinder or the half-thickness for a slab

n = 1 for a slab, 2 for a cylinder, and 3 for a sphere

Modification of this model as implemented by El-Arini and Leuenberger (1998) is denoted by :

$$\frac{M_t}{M_\infty} = 1 - [1 - k_1\, t\ (\mathrm{t} - \mathrm{l})]^{\mathrm{n}} \qquad \textit{Equation 5.3b}$$

Where:

$k_1 = \frac{k_0}{C_0 a_0}$

l = lag time at the beginning of drug release

5.2.7 Ocular tolerance testing employing modified Hen Egg Chorioallontoic (HET-CAM) test

5.2.7.1 Assay preparation and procedure

The methodology involved using hen's eggs (50-60g) that were fertile and purchased from a local hatchery (Bruce Hatcheries, South Africa) and less than a week old. The eggs were placed in commercial incubators (Surehatch, Brakenfell, South Africa) and rotated every 12 hours. On day 3, a hole was made and the albumin was removed. The eggs were sealed by sterile heated parafilm and left in an equatorial position. On day 5 and everyday thereafter eggs were candled for viability and non-viable ones were discarded. On day 10, a window (2x2cm) was made and 2-3mL saline (0.9% NaCl) was added and eggs were returned to the incubator. The following samples were prepared for testing: Standard solution: 1% sodium dodecyl sulphate (SDS), test sample: test sample drug-loaded ISED dissolved in 0.9% NaCl, Placebo sample: drug-free ISED dissolved in 0.9% NaCl, Control: 0.9% NaCl. The eggs were then dosed with 0.3mL of samples and observed for 5 minutes for any effects of injury in accordance with table 5.2 and this was noted. Saline was used as a control for comparison purposes. Eggs were scored for severity of any reaction and time taken to occur (Table 5.2). At the end of the assay the embryos were discarded immediately by placing the eggs into a freezer -80°C. The following features were used for observation of injury: hemorrhage, vascular lysis and coagulation. Figure 5.2 depicts the procedure for the test.

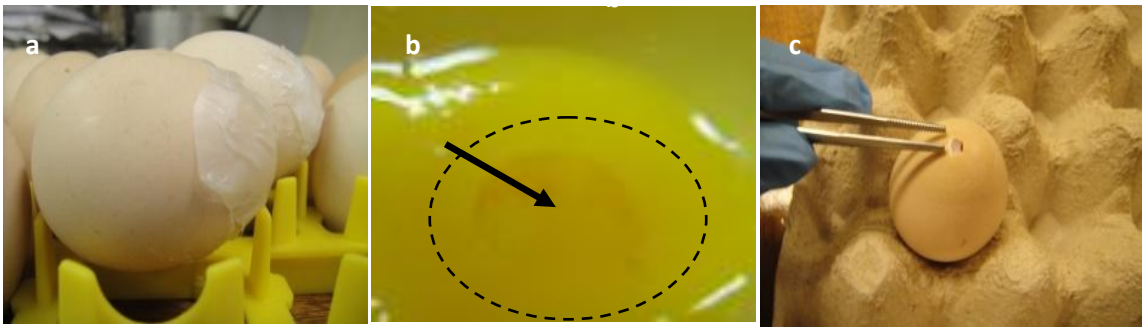


Figure 5.2: Digital images of: a) eggs placed in an equatorial position after albumin removal, b) observation of embryo formation on day 3 and c) preparation of egg for sample testing.

Table 5.2. Scoring chart employed for the HET-CAM test (Velpandian et al., 2006**)**

Effects	Score	IS ranges	Inference
No visible haemorrhage	0	0-0.9	Non-irritant
Visible membrane discoloration	1	1-4.9	Mildy-irritant
Structures covered due to partial haemorrhage/discolouration	2	5-8.9	Moderately irritant
Structures covered fully due to haemorrhage/discolouration	3	9-21	Severely irritant

IS = irritation score

The period taken for any untoward reaction to occur was noted and the irritation threshold was determined (highest concentration of samples required for a minimal reaction to occur). The irritation score was calculated by means of the following equation:

$$IS = \frac{301 - secH.5}{300} + \frac{301 - secL.7}{300} + \frac{301 - secC.9}{300}$$

Equation 5.4

Where:
IS = irritation score
Sec = onset of reaction in seconds
H = hemorrhage
L = lyses
C = coagulation

5.2.8 Treatment of dissolution data by comparison of release profiles of the optimized ISED and a commercial product

A model independent approach was used for mathematical analysis of dissolution data (Rinaki et al., 2003). According to the US FDA, the similarity and difference factors are significant to identify for this purpose.

Two factors were determined with the time point set at 360 minutes.

1. Difference factor (*f*1) – measurement of percentage error of two curves at each time point. Curves are similar if *f*1 is close to 0.

$$f_1 = \frac{\sum_{j=1}^{n} |R_j - T_j|}{\sum_{j=1}^{n} R_j}$$ ***Equation 5.5 a***

2. Similarity factor (*f*2) - logarithmic transformation of th sum-squared error of differences between test and reference products over all time points. Curves are considered similar when *f*2 is between 50 -100.

$$f_2 = 50\, x \log\left\{\left[1 + \left(\frac{1}{n}\right)\sum_{j=1}^{n} |R_j - T_J|^2\right]^{-0.5} x\ 100\right\}$$ ***Equation 5.5 b***

Where:
n = sampling number
R and T = reference and test products at each time point j

5.2.2.9 *Ex vivo* permeation studies of the optimized formulation in comparison to a commercial anti-glaucoma product

Franz diffusion cell apparatus was used to conduct *ex vivo* permeation studies. Excised rabbit corneas (11.83±0.04mm in diameter and area 3.0mm^2±0.01mm^2) were mounted on the Franz diffusion cell apparatus (Permagea, Arnie Systems, USA) connected to a heating bath system for temperature control. The diffusion cell donor chamber was filled with 2mL Simulated tear fluid (SLF) (which was maintained to simulate tear volume). 12mL Simulated Aqueous Humour (SAH, pH 7.4, 37 °C) solution was contained in the receptor chamber. The cornea was placed such that the surface was in contact with the receptor solution which was continuously stirred by a magnetic stirrer at 20rpm to simulate blinking. Samples of one optimized formulation. pure drug dispersion and one drop of marketed product (0.5% timolol maleate) were tested in triplicate for comparison purposes. Aliquots of 1mL were withdrawn from the receptor compartment at regular intervals (30, 60, 120, 180, 240 minutes and 24 hours after insertion) and replaced with an equal volume of dissolution medium. Samples were then subjected to the quantification of drug through spectrophotometric analysis at 295 nm (Hewlett Packard 8453 Spectrophotometer, Germany) to determine the drug release and flux (rate of drug permeation per unit area). Drug flux values were calculated at the steady state per unit area by regression analysis of permeation. Drug flux values were calculated employing the Equation 5.6a:

$$J_s = \frac{Q_r}{A\ x\ t}$$

Equation 5.6a

Where:

J_s= drug flux (mg cm^{-2} min^{-1})
Q_r= amount of drug that passed through to the receptor compartment (mg)
A=Active cross-sectional area for diffusion (cm^2) and
t= time of exposure (min)

The permeability co-efficient can be described as the velocity of drug diffusion through the cornea based on its mathematical unit. Equation 5.6b was used to calculate this:

$$kp = \frac{J_s}{C_d}$$

Equation 5.6b

Where:
Kp = permeability co-efficient ($cm.min^{-1}$)
J_s = Flux at steady state (mg cm^{-2} min^{-1})
C_d = drug concentration in donor compartment ($mg.cm^{-3}$)

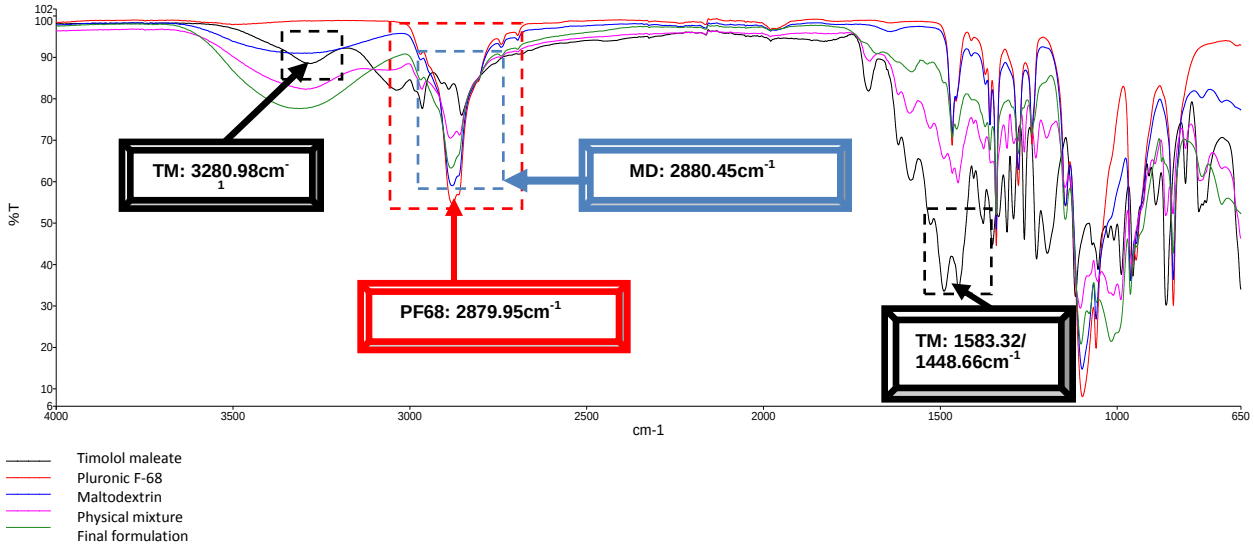
5.3. Results and Discussion

5.3.1 Molecular vibration transitions

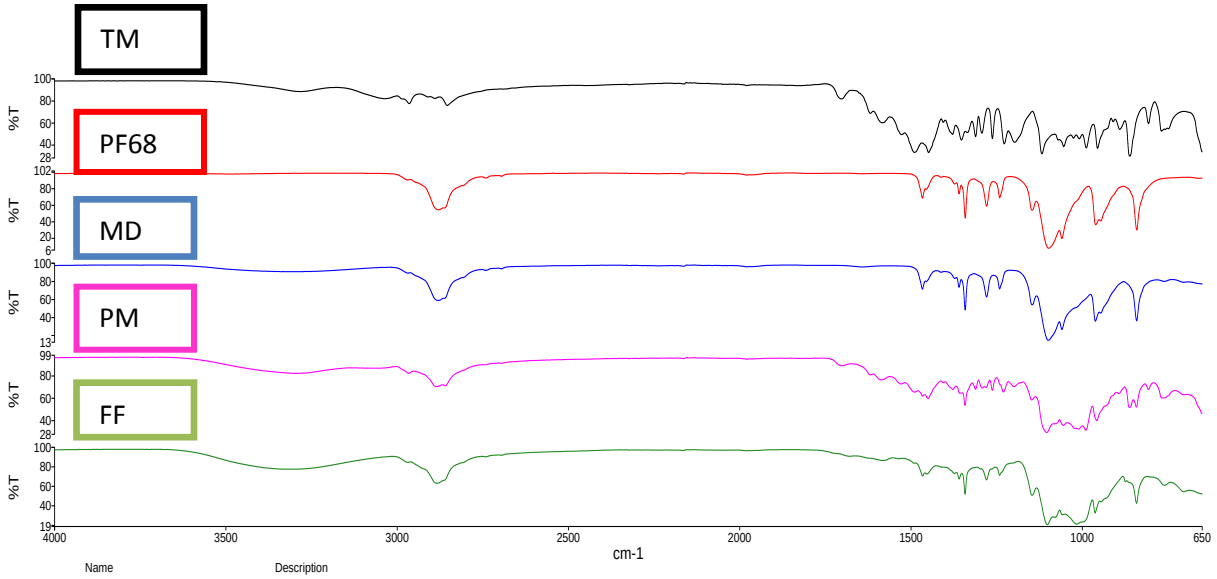
FTIR spectroscopy is employed for the detection of interaction of polymers or drugs as well as observation of important groups found in constituents. The vibrational bands highlight changes on a molecular level. FTIR spectra of the pure drug TM, individual MD and PF68, a physical mixture and the drug-loaded final formulation were analyzed for possible interactions with corresponding structures (Figure 5.3a-e). From the spectrum of pure drug the major peaks were observed thus confirming that the drug was timolol maleate. A quaternary ammonium peak (N-H) was found at 3280.98cm^{-1}. Presence of an OH group was seen at 3037.96cm^{-1}. Also, C-O-C stretching (1702.51cm^{-1}) and C=C aromatic ring (1583.32cm^{-1} and 1448.66cm^{-1}) were noted. Furthermore, CH stretching and CH bending were observed at 1352.7cm^{-1} and 2964.98cm^{-1} respectively. The broad peak at 2879.95cm^{-1} was attributed to the OH moeity present in PF68. Additionally, C-O stretching occurred at 1145.98cm^{-1}. For MD, OH stretching occured around 3304.07cm^{-1}. C-O stretching of MD corresponds to peaks at 1059.52cm^{-1} and 961.79cm^{-1}. All major peaks of pure drug appeared in the physical mixture indicating that no interaction occurred (3294.94cm^{-1}, 1586.96cm^{-1}). For the final formulation, drug peaks were not clearly defined and this could be attributed to the homogenous dispersion within the matrix. In terms of the final formulation, the major components were PF68 and MD. Since no major shifts in peaks

were observed, it can be proposed that the absence of any appreciable variations or chemical interaction between polymers or drug was noted and the components maintained their initial structure. The peaks occurring in the region of >3000cm^{-1} could be attributed to the summation of peaks associated with polymer HPC (3423.75cm^{-1}), excipients DG (3283.1cm^{-1}) and PAANa (3285.27cm^{-1}). Hence, this assisted in confirming that the formulation remained stable during the preparation procedure. Table 5.3 outlines the peaks and their respective assignments.

a)



b)



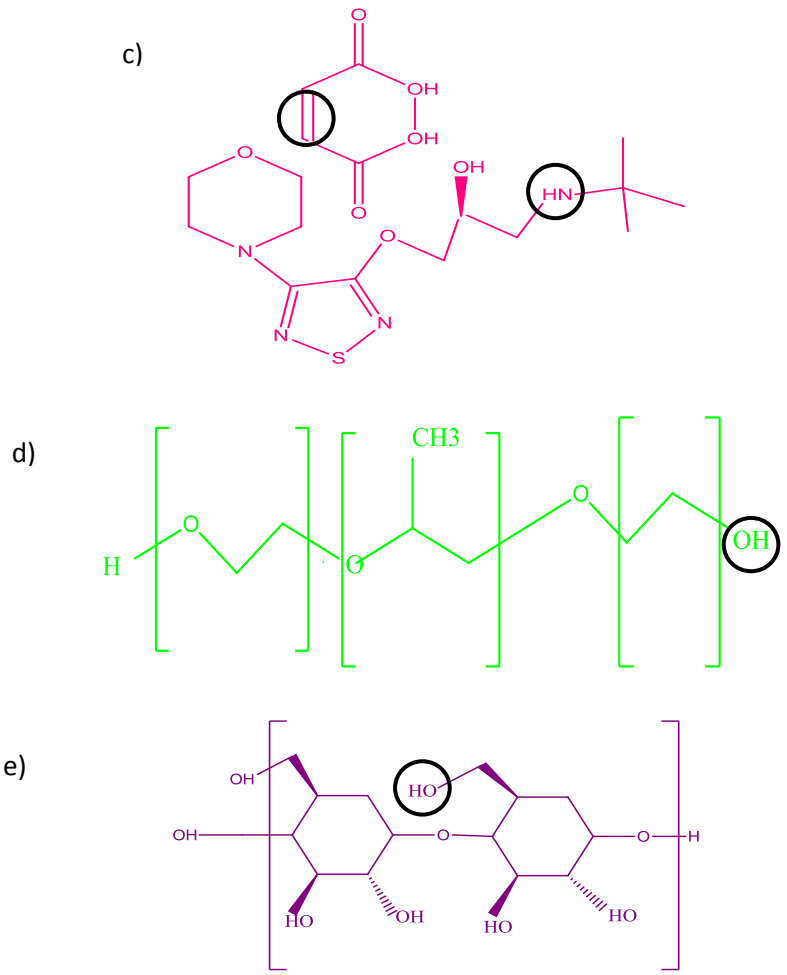


Figure 5.3: Schematics of a) superimposed FTIR spectra of components, physical mixture and final formulation, b) separated peaks of components, c) structure of TM, d) structure of PF68, and e) structure of MD, with respective observed groups highlighted.

Table 5.3. Interpretation of vibrational bands obtained from FTIR analysis

TM	MD	PF68	PM	FF	Assignment	Transmittance of peaks (%)				
						TM	MD	PF68	PM	FF
3280.98			3294.94		N-H/-N-	88.54			82.25	
3037.96	2280.45	2879.95	2885.45	3306.55	OH stretch	82.09	59.04	54.76	70.53	77.65
				2884.13	CH stretching *(Aromatic)*	77.67				63.3
2964.98					CH stretching *(Aliphatic)*					
	1059.5	1145.98			C-O stretching		26.8	54.15		
1583.32/1448.66			1586.96	1581.87	C=O				76.56	86.53
1352.7					C=C aromatic	60.34/33.7				
1702.51					C-H bend	44.71				
					C-O-C stretch (ether)	81.89				

TM = Timolol maleate

MD = maltodextrin

PF68 = Pluronic F-68

PM= Physical mixture

FF= Final formulation

5.3.2 Thermal analysis

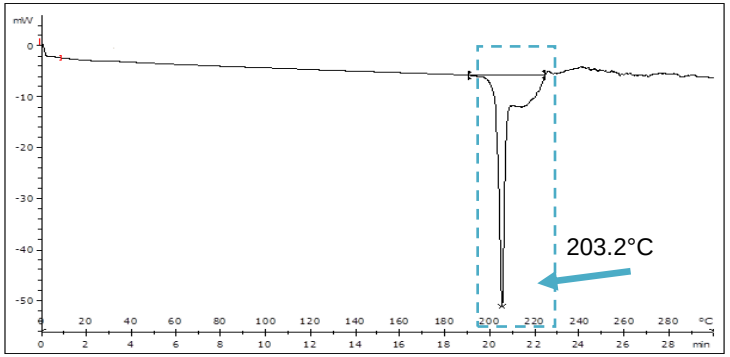
Thermal analysis of lyophilized systems is of key importance in order to gather the significant characteristics of the sample. Specifically, the 'collapse temperature' which is the temperature over-which the sample displays loss of its structure and collapses during the lyophilization process (Pikal, 1990). This is critical in terms of manufacturing and storage. Testing provides information regarding the possibility of drug-polymer interactions. Analysis was conducted via DSC and thermal curves of the pure drug TM and a drug-loaded final formulation were investigated. In terms of the pure drug a single defined endothermic peak was observed at 203.2°C confirming its crystalline nature (Figure 5.3a). This corresponded to the melting peak (T_m) of the drug which is the transition from a solid to liquid state with subsequent degradation. In terms of the drug-loaded formulation, PF68 and MD were the major components. Native PF68 produced a distinguishable single step endothermic degradation at 53.9°C (Figure 5.3b). For pure MD, peaks that occur before 220°C (106.51°C) (Figure 5.3c) were possibly due to the elution of water (Elnaggar et al., 2010). The T_m of MD was observed as a broad peak at 230.98°C. In terms of the physical mixture, a less defined broad TM peak in the region of 193.89°C was seen confirming the presence of the drug (Figure 5.3d). TM uniformly dispersed within the final optimized formulation as well as increased polymer and excipient concentration compared to drug, possibly contributed to the diminished broad T_m of the drug (Figure 5.3e). Furthermore, Simon and co-workers (2003), reported that a lower endothermic peak of lyophilized samples when compared to the individual components may be due to a decrease in thermal conductivity. This may be as a result of the presence voids/pores within the matrix. Additionally, the endothermic peak was reduced in the final formulation, postulated due to MD (16.5-19.5 dextrose equivalence). It has been investigated to be a lyoprotectant (lyophilization stabilizer) by being amorphous and displaying a diluting ability during the lyophilization process (Corveleyn and Remon, 1996).

Further investigation was conducted on the final formulation by Temperature modulated differential scanning calorimetry (TMDSC) or Alternating Differential Scanning Calorimetry (ADSC) at range of 20-100°C. The usefulness of this is that it is a confirmatory technique that allows for the separation of overlapping peaks (Wunderlich et al, 1994; Wang et al., 2000). Analysis showed a broad endothermic peak which corresponds to the loss of water. The following can be gathered from ADSC curve (Figure 5.3f): 1) reversing peak gives the T_g and 2) non-reversing and total heat-flow curves depict the melting point (endothermic, downward peak,

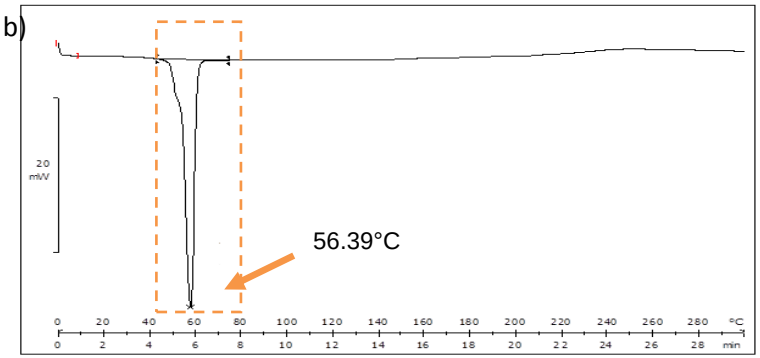
Cp outphase) and crystallization peaks (exothermic, upward peak, Cp inphase). A decreased T_m (total heat flow curve) for the final formulation could also be as a result of reduced water after lyophilization (Sobral et al., 2001; Patel, 2005). For the final formulation, the temperature ranges were not significantly alterered thus indicating no incompatibility between formulation components and drug. This was congruent with FTIR findings.

TGA was utilized in order to assist in interpretation of thermal properties of the samples using heat and stoichiometric ratios in determination of the percent by mass of solute. Pure TM displayed a definate weight loss in the region comprising an extrapolated onset of 200°C and an endset of 350°C which can be explained as the decomposition temperature (Figure 5.3g). A sharp endothermic peak is observed in this area which is in agreement with the findings of Joshi and co-workers (2009). The derivative curve of TM shows weight loss corresponding to a three step pattern at 231.14°C, 260°C and 313.95°C respectively. In terms of the optimized formulations, similar weight loss patterns were noticed. For both DF and DL formulations, weight sharp loss occurred in the region of 200°C-450°C (Figure 5.4h and i). Additionally, in the derivative curves for both formulations, 3 points of degradation were noted at approximately 230-240°C, 305-310°C and 411-413°C. It is explicable that incorporation of drug did not alter the thermal properties.

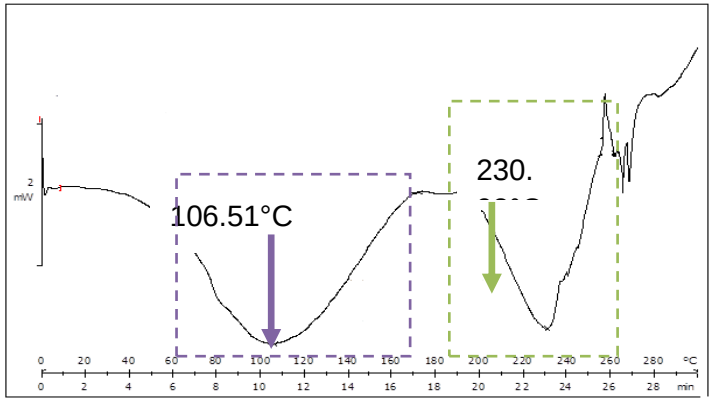
a)


mW
0
-10
-20
-30
-40
-50
203.2°C
0 20 40 60 80 100 120 140 160 180 200 220 240 260 280 °C
0 2 4 6 8 10 12 14 16 18 20 22 24 26 28 min

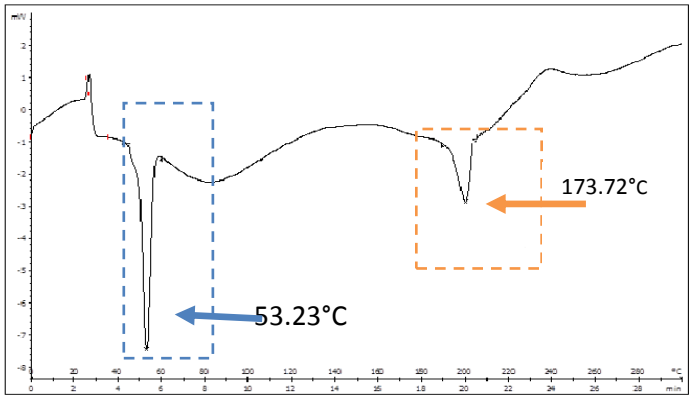
b)


20
mW
56.39°C
0 20 40 60 80 100 120 140 160 180 200 220 240 260 280 °C
0 2 4 6 8 10 12 14 16 18 20 22 24 26 28 min

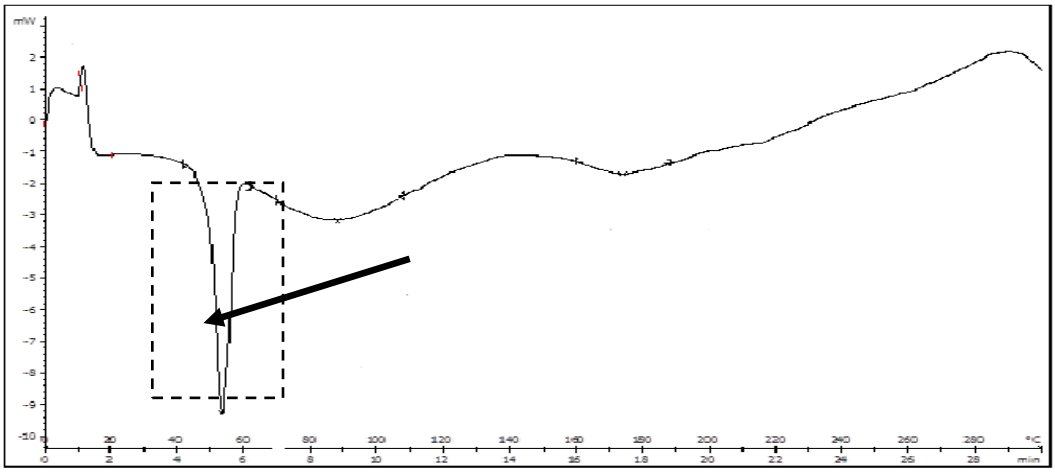
c)


2
mW
106.51°C
230.
0 20 40 60 80 100 120 140 160 180 200 220 240 260 280 °C
0 2 4 6 8 10 12 14 16 18 20 22 24 26 28 min

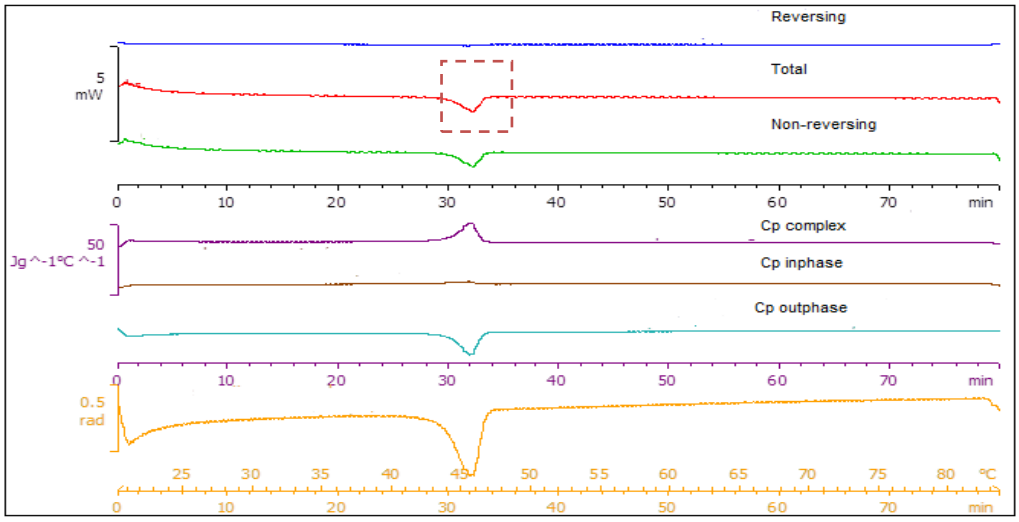
d)


mW
2
1
0
-1
-2
-3
-4
-5
-6
-7
-8
173.72°C
53.23°C

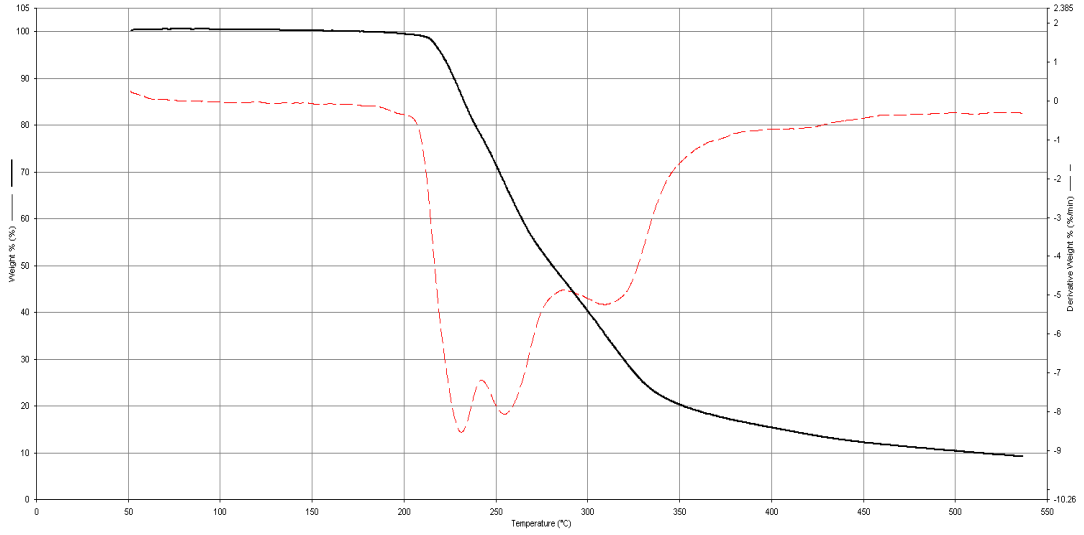
e)


mW
°C
min

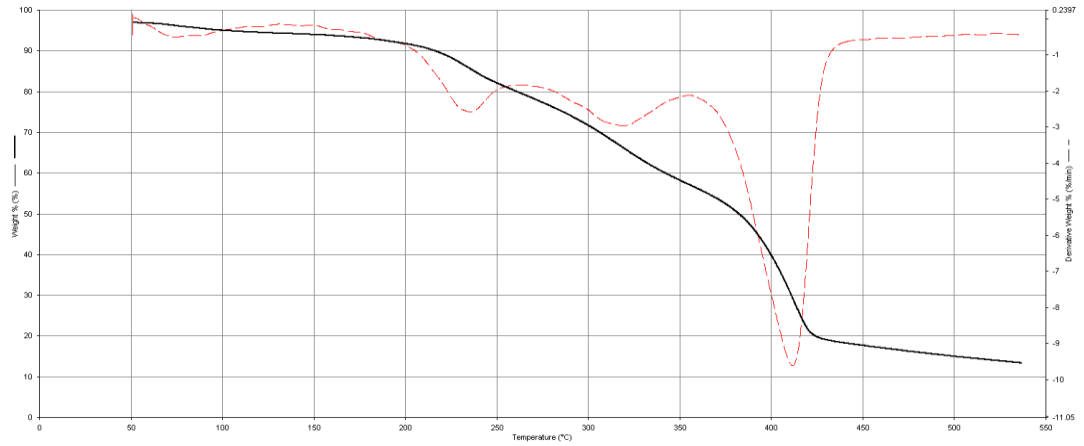
f)


Reversing
Total
Non-reversing
5
mW
Cp complex
Cp inphase
Cp outphase
50
Jg^-1°C^-1
0.5
rad
min
°C

g)



h)



i)

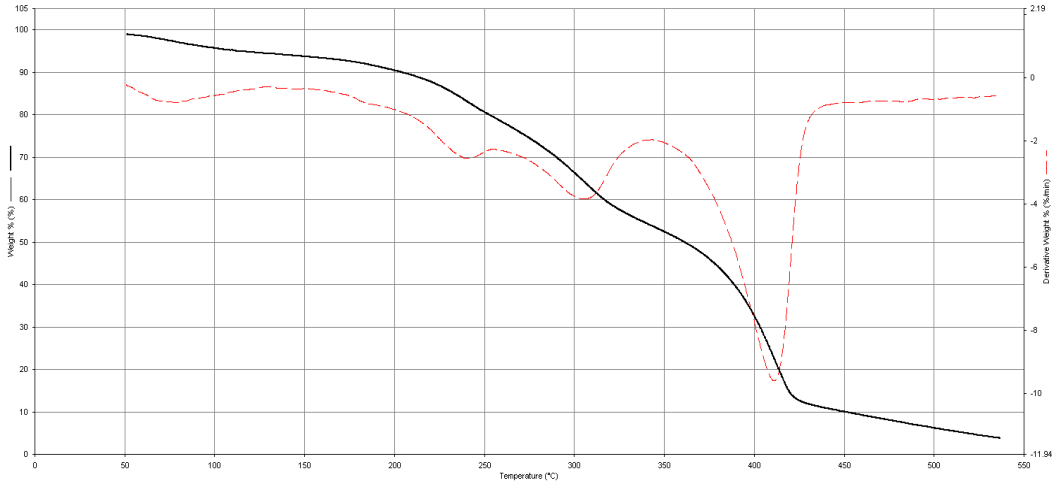


Figure 5.4: DSC thermograms of a) pure drug timolol maleate, b) native PF68, c) native MD, d) physical mixture, e) DL final formulation f) ADSC graph of drug-loaded formulation, g) TGA graph of pure TM, h) DF formulation and i) DL formulation (N= 3 in all cases).

5.3.3 Porositometric and surface imaging analysis comparison

Porosity can be described as the measurement of the voids/spaces within a sample. With regards to lyophilized matrices, the resultant product is often porous due to the sublimation of water post-freezing. This can be quantified in terms of porosity analysis and visualization by SEM. The basic principle behind this method is the adsorption of nitrogen gas on a material's surface or on the pores, if present. A degassing linear isotherm and the Brunauer-Emmet-Teller (BET) surface area plots are depicted in Figures 5.5a and b respectively. The linear plot indicates that degassing occurred since the adsorption and desorption isotherms are noted. The presence of a hysteresis loop was noted since a difference in the adsorption and desorption curves were seen as per definition of the loop. The loop infers nitrogen evaporation from pores (Guirguis and Moselhey, 2012). A type 3 hysteresis loop (H3) can be possibly classified due to the isotherms sloping. This implies the presence of slit-like pores. This sample can thus be described as mesoporous (pore diameter between 2-50A) and macroporous (pore diameter > 50A) according to the IUPAC definition (Condon, 2000).

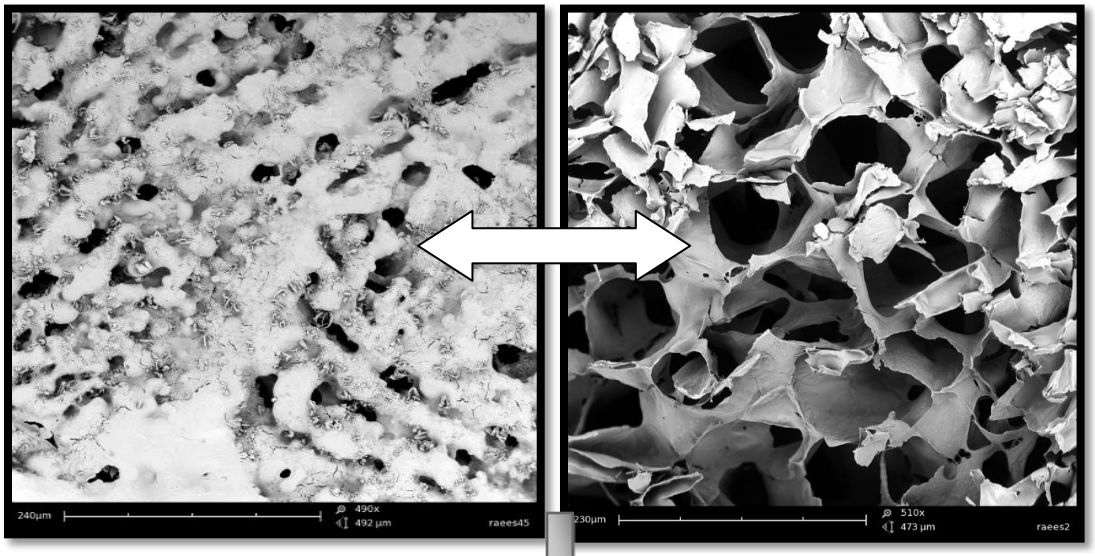
Corresponding SEM images for qualitative analysis enumerated the findings of porosity analysis and allowed for visualization of the surface and pore distribution. Pores were demarcated, interconnecting and circular to assymetrical over the matrix surface. BET plots indicated that a positive value was obtained (27.2052m^2/g, R^2=0.99). Explanation of the BET concept is of the assumption that there is a uniform surface exposure and that nitrogen is more attracted to the surface then other nitrogen molecules. BET-C ranges between 5-100. Values <5 implied that the gas-gas affinity was competing with the gas-solid affinity as a result of the significantly reduced surface area and minimization of pores (Everett, 1972; Siminiceanu, 2008). A value of 4.785274 was obtained for the formulation tested. A method for determination of pore volume or surface area as a function of pore diameter was proposed by Barret, Joyner and Halender (Barrette al., 1951). BJH adsorption plots, BJH Desorption dV/dlog(D) Pore volume plots with implementation of the Halsey-Faas correction and are seen in Figures 5.5 c and d (Halsey, 1948). The average pore size for BJH adsorption and desorption were 46.644Å and 53.949Å respectively. The large pore distribution can explained be on account of the entrapped air spaces within the matrix as a result of the freeze-drying methodology for production. Figure 4 e displays t-plots based on Lippins, Linsen and de Boer (Lippins et al., 1964). This is used for the determination of micropore or mesopore presence < 20Å. Positive BET values enabled the computation of the t-plot. The micropore volume is obtained by extrapolation of the isotherm. A t-plot micropore volume of -0.010393cm^3/g was obtained indicating the presence of micropores.

Hence, these findings emphasized that the lyophilization process significantly contributed to the porous nature of the samples and ultimately results in a light structure that rapidly disintegrates. This explains the possible method of disintegration and drug release i.e via fluid filling into the pores of the matrix with subsequent dissolution. Table 5.4 computes results obtained for optimized drug-loaded samples.

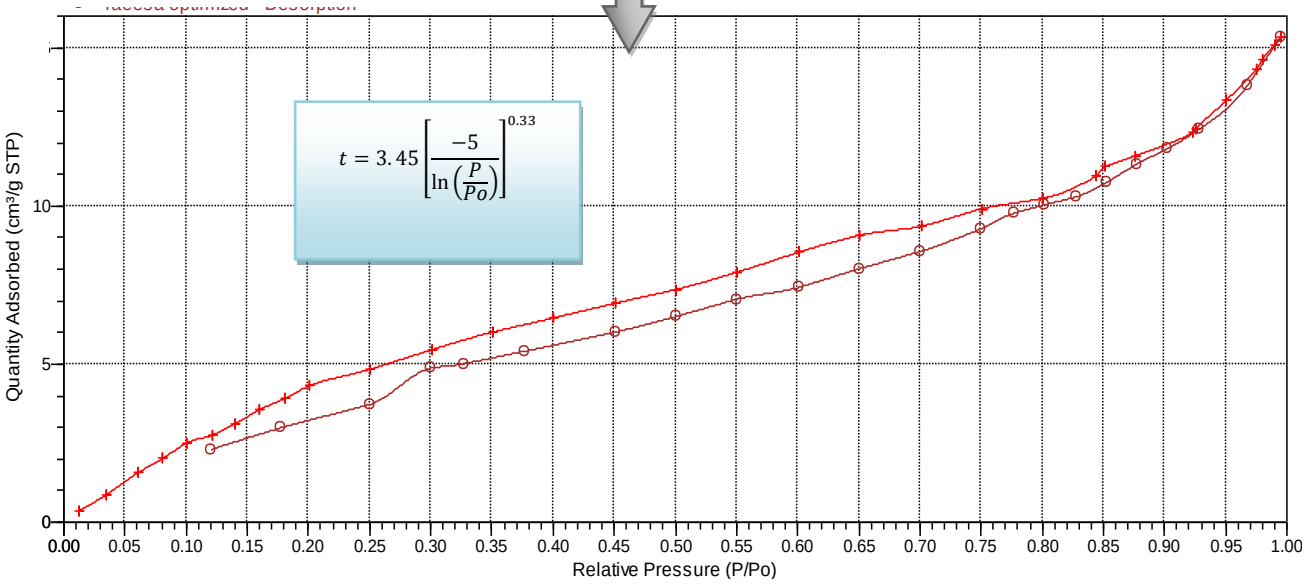
Table 5.4. Results obtained from porosity analysis

Parameter	DL ISED
BET total surface area (m^2/g)	27.2052
BET-C	4.785274
Qm (cm^3/g STP)	6.2495
BET slope(g/cm^3 STP)	0.126575 ± 0.007612
BET y-intercept (g/cm^3 STP)	0.033439 ± 0.001053
R^2 (BET plot)	0.99
Micropore volume (cm^3/g)	-0.010393
External surface area (m^2/g)	38.5234
R^2 (t-plot)	0.99
t-plot slope (cm^3/g.Å STP)	2.490519 ± 0.099199
t-plot y-intercept (cm^3/g STP)	-6.718757 ± 0.403672
Pore diameter range (Å)	7-3000
Pore thickness range (Å)	3.5-5
BJH adsorption pore size (Å)	46.644
BJH desorption pore size (Å)	53.949

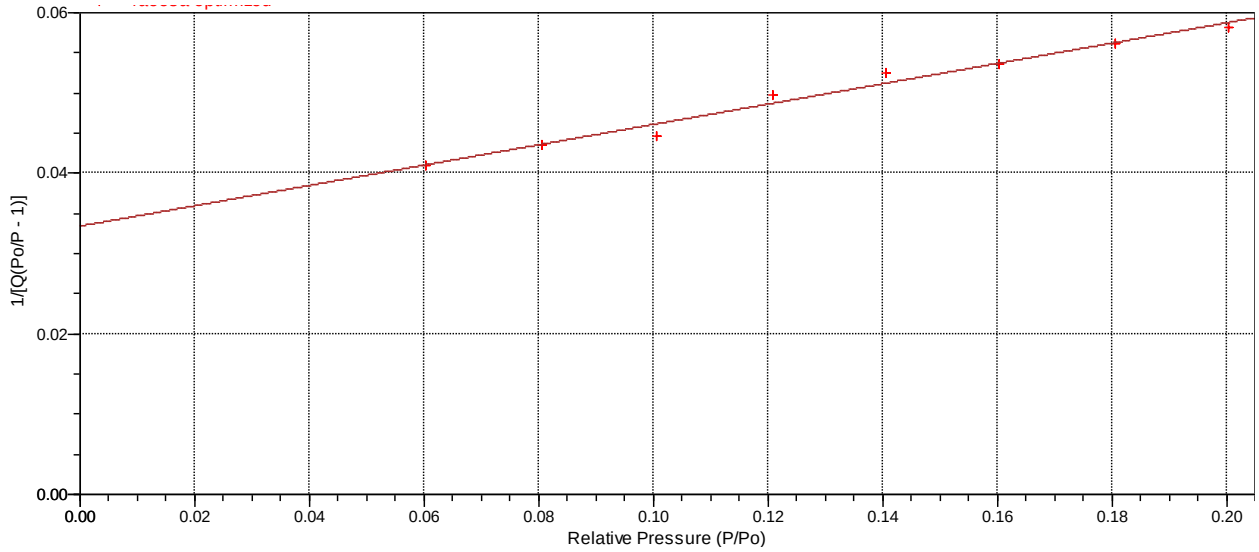
DL= drug-loaded
BET-C = intensity of the N_2-surface interaction
Qm = monolayer surface capacity


240µm
490x
492 µm
raees45
230µm
510x
473 µm
raees2

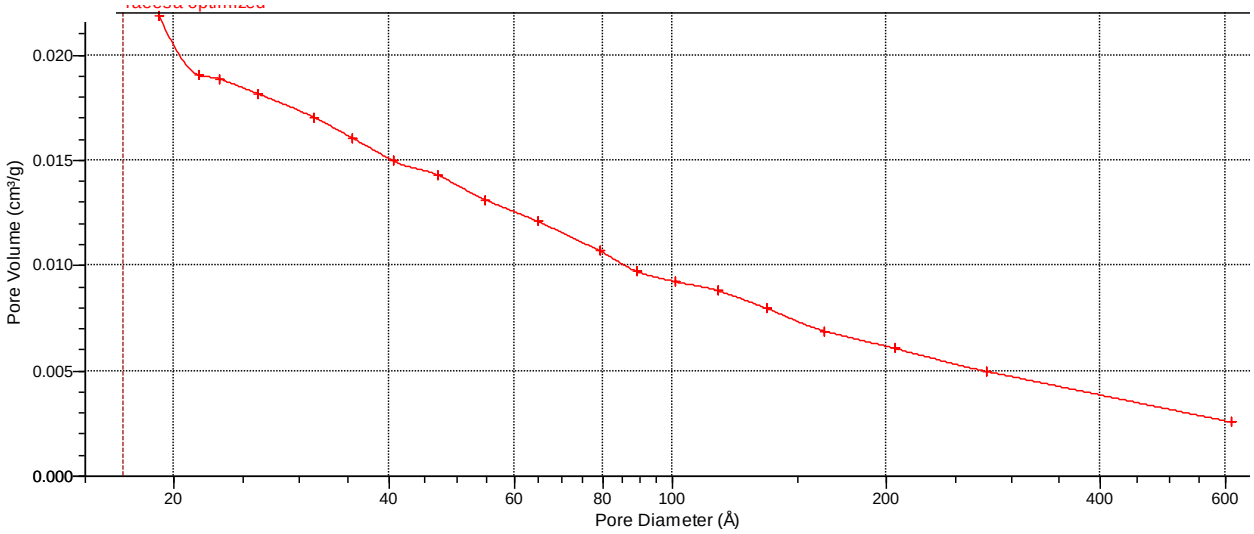
a)


$t = 3.45\left[\frac{-5}{\ln\left(\frac{P}{Po}\right)}\right]^{0.33}$
Quantity Adsorbed (cm³/g STP)
Relative Pressure (P/Po)
0
5
10
0.00
0.05
0.10
0.15
0.20
0.25
0.30
0.35
0.40
0.45
0.50
0.55
0.60
0.65
0.70
0.75
0.80
0.85
0.90
0.95
1.00

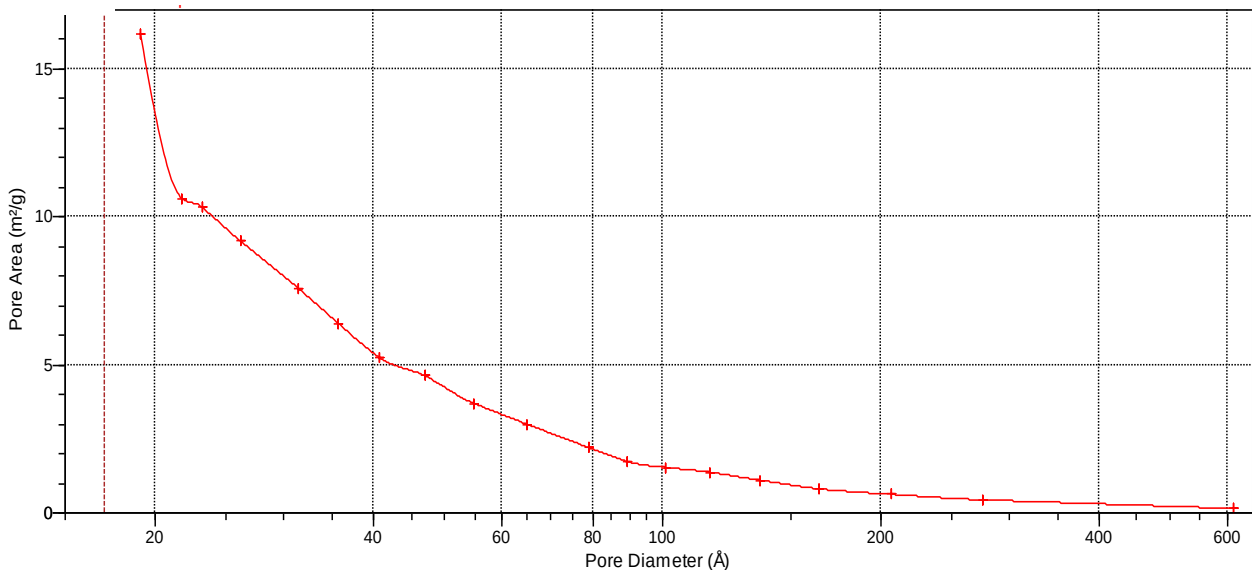
b)


0.06
0.04
0.02
0.00
1/[Q(Po/P - 1)]
0.00
0.02
0.04
0.06
0.08
0.10
0.12
0.14
0.16
0.18
0.20
Relative Pressure (P/Po)

c)


0.020
0.015
0.010
0.005
0.000
Pore Volume (cm³/g)
20
40
60
80
100
200
400
600
Pore Diameter (Å)

d)



e)

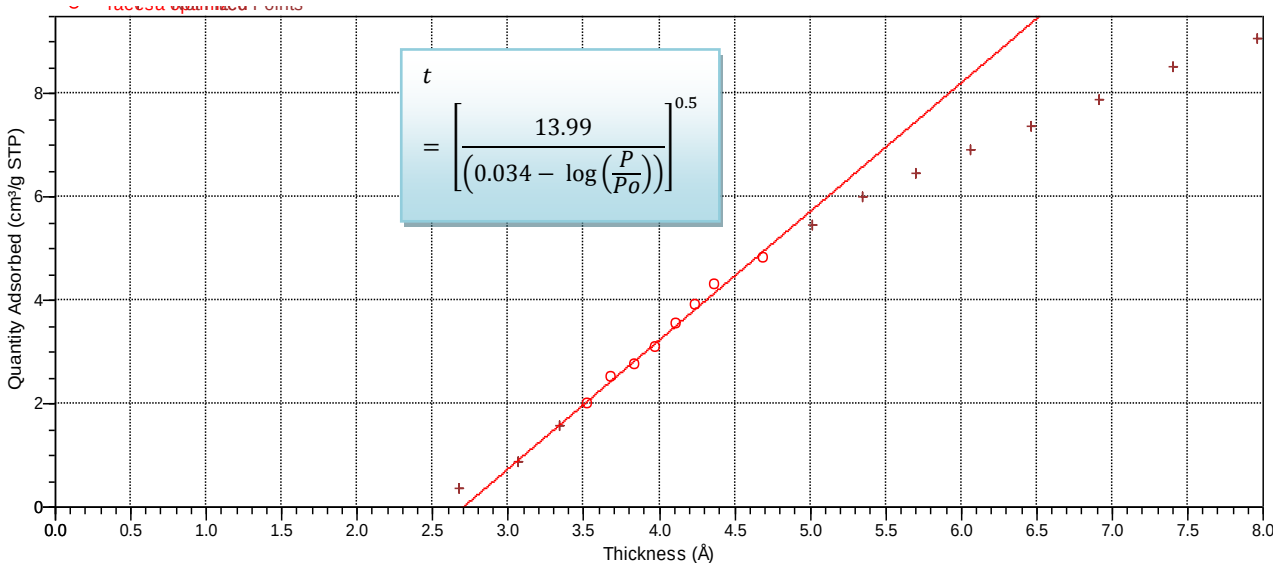


Figure 5.5: Porosity analysis plots and corresponding SEM images of drug-loaded optimized formulation: a) Linear isotherm, b) BET surface area, c) BJH adsorption cumulative pore volumes, d) BJH desorption cumulative dA/dD pore areas, e) typical t-plot.

5.3.4 Drug release kinetics

Modeling of the dissolution profile was conducted in order to ascertain the best model of fit. The significance of this is for analysis of experimental results using equations for an improved understanding of the mechanisms that govern the drug release from a dosage form. Zero order, first order and Hopfenberg models were employed for this purpose from the composite drug release curve (Figure 5.6). Results obtained from the modeling were in terms of Akaike information criteria (AIC) and Model selection criteria (MSC). The MSC is a criterion gaining popularity for model selection from the data provided while the AIC measures the goodness of fit of a model (Zhang et al., 2010). The MSC is an adapted reciprocal value of the AIC and is given by the following equation:

$$\ln\left(\frac{\sum_{i=1}^{n} w_i \cdot \left(y_{i_obs} - y_{_obs}\right)^2}{\sum_{i=1}^{n} w_i \cdot \left(y_{i_obs} - y_{i_pre}\right)^2}\right) - \frac{2p}{n} \qquad \textit{Equation 5.7}$$

Where:

Wi = weighting factor (1)

yi_obs = ith observed y value

yi_pre = ith predicted y value

y obs = the mean of all observed y-data points

p = number of parameters in model

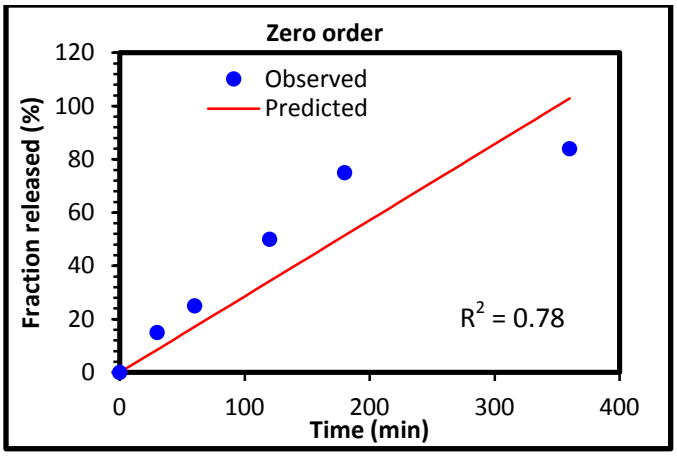
n = number of data points

Results indicated that the first order model provided the best fit (R^2 = 0.98). In terms of interpretation, low AIC and large MSC (> 2-3) values correspond to the best fitted models. In this case, the first order model had the lowest value of 31.27 indicating suitability of this model, while the zero order model displayed the highest value of 44.8. Numerical values that supported these models are shown in table 5.5 Zero-order model implies that the process of drug release depends on the drug concentration. Thus, the predominant mechanism of drug release from the matrix was first order release.

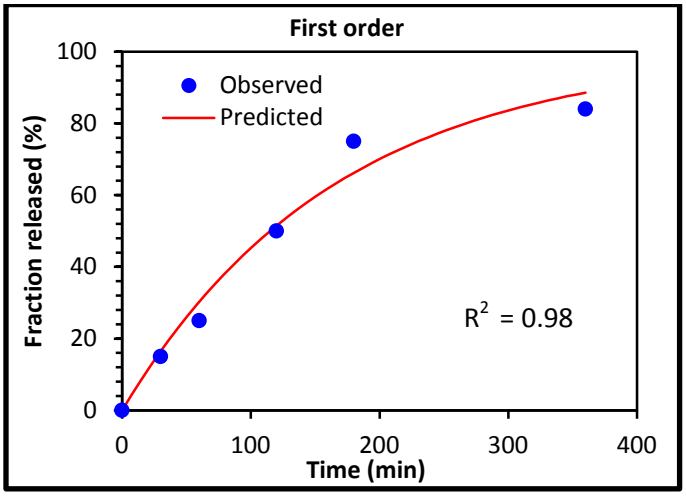
Table 5.5. Release data obtained from various models

Model	k_0	k_1	n	k_{HB}	AIC	MSC
Zero order	0.286				44.8	0.81
First order		0.006			31.27	3.07
Hopfenberg			44.18	0	33.27	2.74

a)



b)



c)

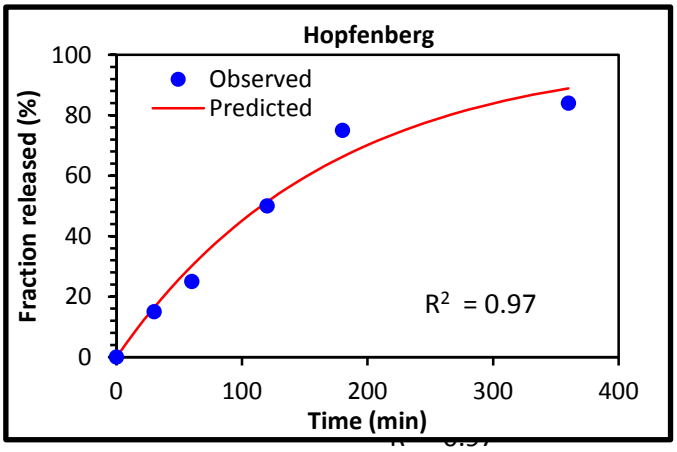


Figure 5.6: Dissolution profiles compared to a) Zero order, b) first order and c) Hopfenberg models.

5.3.5 Ocular toxicity evaluation

The purpose of employing this test was due to the CAM being tissue that is vascularized (arteries, veins and capillary plexus). The occurrence of any injury with inflammation due to a test substance is an indication of the damage that can occur and be compared to that of the eye surface *in vivo* and served as the rationale for this test (Speilman et al., 1991). The HET CAM test acts as an alternative to the use of mammalian tissue and application of the highly controversial and harmful Draize-irritancy test performed on live animals. In addition, the HET CAM test is rapid and cost-effective for the evaluation of novel drug-delivery systems. Testing was carried out according to Globally Harmonized System of classification and labeling of chemicals (GHS) guidelines for testing of chemicals (UN, 2009). Results indicated that after exposing the CAM to samples (300uL) for 5 minutes, drug-free and drug-loaded samples were practically non-irritant and therefore well-tolerated with a mean score of 0. This can be attributed to the constituents of the formulation. They are ocular-compatible, biodegradable polymers (HPC and PF68) and have been previously studied for ocular application and thus showed no adverse effects. Furthermore, the drug itself TM, is a standard treatment for glaucoma and its presence displayed no untoward reaction to the CAM. Saline, employed as a control also displayed a score of 0 implying no irritation potential as expected. SDS used as a positive control, showed a score of 2.5 inferring considerable toxicity with disruption of the CAM. It is an organic compound and non-ionic surfactant known to cause cell lysis and is often used for comparison purposes in studies.

Equation 5.4 was used to determine the IS of formulations (0 - 21). An IS of 0 for NaCl, DF and DL formulations were obtained while in contrast, 10.4 for SDS. Notably, NaCl and optimized formulations were virtually non-irritant even at higher concentrations while SLS displayed toxicity at low concentrations. Table 5.6 outlines results obtained. The CAM remains unaffected when tested with the optimized formulation while disruption is clear with SDS (Figure 5.7). Thus, this study revealed that both drug-loaded and drug-free solid eye drops were non-irritant to the membrane and can be considered safe for use on the eye surface. It is a pre-requisite for ocular systems to have no adverse reaction on the eye, thus the selected polymers and excipients were suitable for the intended application.

Table 5.6. Results obtained for the HET-CAM test

Substance	Score	Inference	IS
Negative control			
NaCl	0	Non-irritant	0
Positive control			
SDS	2.5	Severe	10.40
Samples			
DF	0	Non-irritant	0
DL	0	Non-irritant	0

Results expressed as a mean of 3 values
NaCl= saline, DF= Drug free, DL= drug loaded, SLS= sodium lauryl sulphate

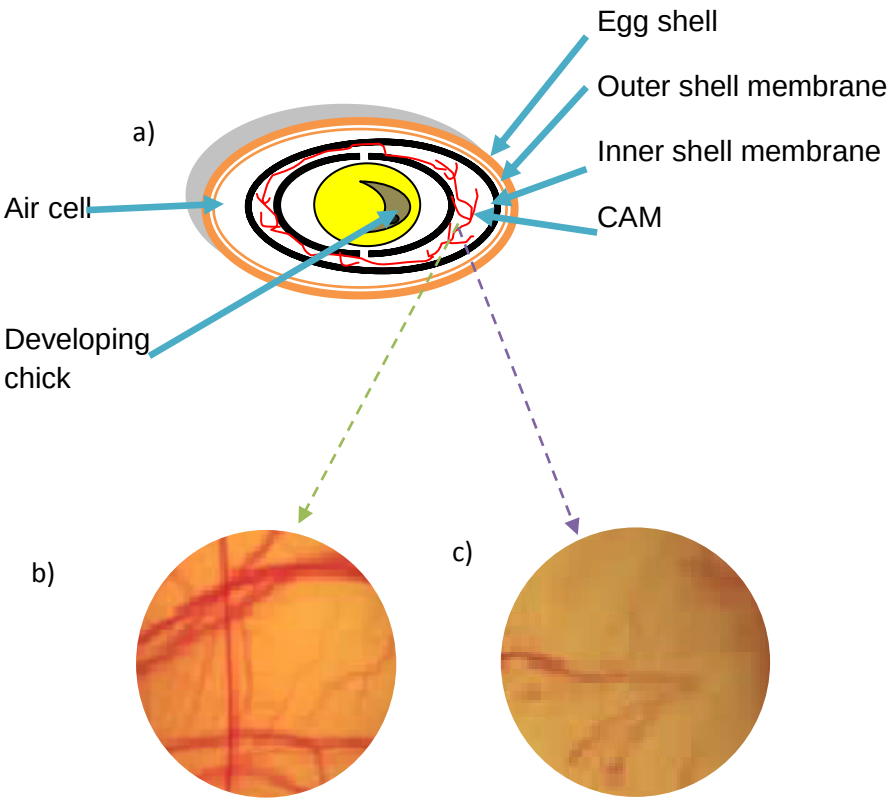


Figure 5.7: a) schematic of CAM (adapted from Vargas et al., 2007), b) CAM after exposure to optimized sample and c) after exposure to SDS.

5.3.6 Comparison of dissolution data

Both formulations, since immediate release dosage forms, displayed initial burst release. However, the ISED displayed a superior result than the eye drops. The level of similarity was

evaluated by means of the similarity and difference factors. A *f*1 value of 13.69 and a *f*2 of 61.61 were obtained. A f1 of 0 - 15 indicates that there are minor differences between the samples tested and f2 between 50 - 100 indicates the sameness of the samples. Figure 5.8 depicts the profiles. Results indicated a similar trend in the profiles. This can be used as a surrogate before conducting *in vivo* studies.

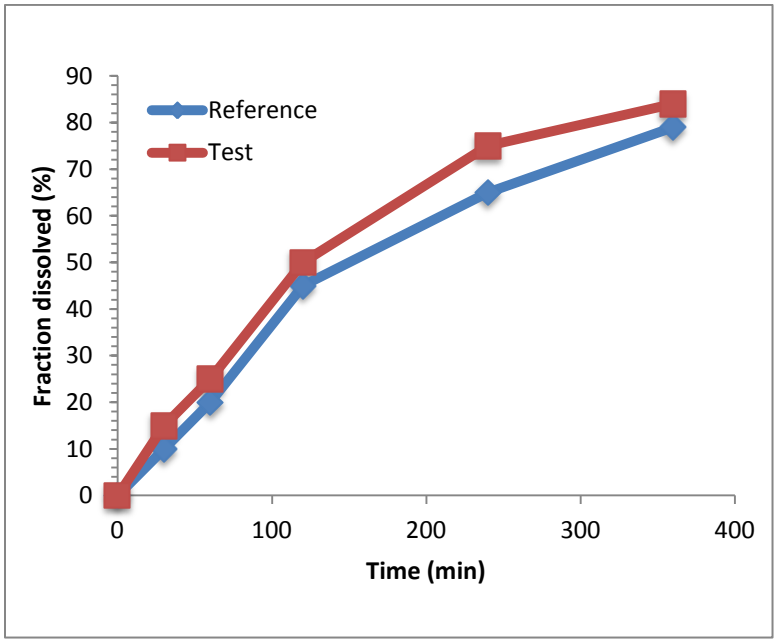


Figure 5.8: Graph of drug release of ISED and commercial formulation.

5.3.7 Determination of *ex vivo* permeation in comparison to a marketed product

Permeation capabilities of the optimized formulation compared to the pure drug dispersion of TM and marketed eye drops were tested across excised rabbit cornea samples. Results had a positive outcome indicating that an improved steady state flux was noted for the optimized formulation 1 (0.00052mg.cm^{-2}.min^{-1}) compared to pure drug 2 (0.000378mg.cm^{-2}.min^{-1}) and eye drops 3 (0.00039mg.cm^{-2}.min^{-1}) (Figure 5.9) . This can be attributed to the polymers employed in the formulation. PF68 forms a slight gel-like substance due increased temperature of SLF which assists in increases the corneal contact time. Also, HPC is a non-ionic surface-active viscosity adjusting polymer that favours pre-corneal retention thus influencing the drug permeation. A low concentration of the polymers were incorporated to promote rapid disintegration of the device, avoidance of a highly viscous gel-like residue yet allowance of sufficient corneal contact. The

influx of fluid in the pores influenced the matrix disentanglement flowed by rapid dissolution and drug liberation. Pure drug solution is diluted and remains in the SLF or on the corneal surface as it is dispersed within a liquid (saline) and thus drug takes longer period to diffuse across the corneal epithelium as opposed to a polymeric device that favours adhesion and corneal interaction. The kp calculated for the samples differed, and this disparity is likely to be due to the difference in composition. As an oral drug, timolol has been classified as a class 1 drug according to Biopharmaceutics Classification system (BCS) (Kasim et al., 2004; Dahan et al., 2009). This infers that it is a highly permeable and soluble drug across the intestinal tissue. On the eye surface, across the corneal epithelium, it also displays favorable permeability due to the advantageous hydrophilic and lipophilic property. The polymers and excipients employed in the optimized formulation are all hydrophilic thus rapid drug liberation and permeation was attained and thus this was suitable for immediate drug release. Table 5.7 shows differences in kp values.

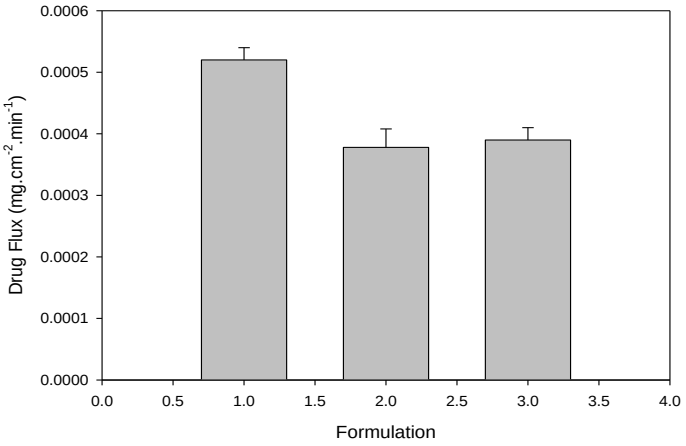


Figure 5.9: Graphical representation of drug flux of the optimized formulation and TM drug dispersion (error bars indicate standard deviation)

Table 5.7. Results obtained for permeability co-efficients

Sample	Kp ($cm.min^{-1}$)
Optimized formulation	$1.7x10^{-4}$
Pure drug dispersion	$1.2x10^{-4}$
Marketed eye drops	$1.3x10^{-4}$

Results expressed as a mean of 3 values

5.8 Concluding Remarks

Chapter 5 provided an extensive pharmaceutical analysis of an optimized instantly soluble eye drop device previously developed via statistical analysis. Molecular transition studies and

thermal analysis revealed that no incompatibility between drug, polymers and excipients existed. Porosity and morphological examination confirmed the porous-nature of the formulation. First-order release was determined to be the predominant release mechanism as indicated by kinetic analysis. Ocular toxicity studies via the HET-CAM test proved to be efficient for evaluation of samples and determined that the device was non-noxious and thus considered safe for topical ophthalmic application. Comparison with a pure drug dispersion and marketed eye drops for trans-corneal permeation revealed that the optimized formulation had an improved drug flux and permeability co-efficient attributed to the rapid disintegration and presence of hydrophilic adhesive polymers. Due to the common occurrence of topical eye ailments, advances in therapy are required. From this investigation, evidently, the optimized formulation was concluded to be stable and can thus be considered for potential *in vivo* verification.

CHAPTER 6

IRRADIATION STERILIZATION AND SUBSEQUENT CHARACTERIZATION OF THE OPTIMIZED ISED

6.1 Introduction

Of major importance is to ensure that any novel drug delivery system is rendered sterile before proceeding to *in vivo* analysis. This goes without saying, since contamination must be avoided specifically with regards to the eye surface. This is also a requirement of Good Manufacturing Practice (GMP) for pharmaceuticals. Sterilization is a process that destroys any form of micro-organisms within the dosage form. In general, several methods of sterilization of ophthalmic pharmaceutical products have been proposed as summarized in Table 6.1. Of note in selection of a method is that the procedure should ideally be validated and not impinge on the quality and properties of the product intended for sterilization.

Table 6.1. Methods of achieving sterilization of ophthalmic products (summarized from Weyenberg, 2004, Weiner 2010 and Kumar,2012)

Method	Description	Examples
Irradiation	Use of non-radiation methods such as ultraviolet light for surface sterilization and radiation methods by penetrating gamma rays	Ocular minitablets/solid devices or inserts
Filtration	Use of membrane filters for removal of micro-organisms (0.22um)	Aqueous eye drop preparations
Aseptic conditions	Formulations prepared under a laminar-flow unit that reduces the risk of airborne contamination	Liquid eye drop preparations

For purposes of this study, gamma (γ)-irradiation was employed. Commonly, this method has been used for ocular systems such as mini-tablets, implants and gels (Petrich and Rosen 1995, Weyenberg et al., 2006; Choonara, 2010). This involves the use of γ rays which are highly penetratable and commonly used as they kill organisms by destroying bonds of bacterial deoxyribonucleic acid (DNA). The rays are a type of high energy electromagnetic radiation emitted from the decay of Cobalt 60. Figure 6.1 provides a summary of the process. The

purpose of selecting this method was due to the apparent advantages such as: safety, simplicity, controlled conditions and importantly, no residual activity after the process. Furthermore as stated by Sinco, (1999): ‘’Gamma radiation has been recognized since the 1950’s as a safe and effective method of sterilizing medical products.’’ The use of this method is recognized by the American National Standards Institute (ANSI), the American Association of Medical Instrumentation (AAMI) and the International Standards Organization (ISO) (Martin, 2012).

To determine if the selected method is successful a sterility test is conducted. Sterility testing can be explained as a test conducted on a sterilized product to determine if it is free from any contamination i.e confirmation of the effectiveness of the process. A direct inoculation method for sterility testing was executed. This involves introducing the test product into media followed by incubation.

Products that remain in storage may have a tendency to change depending on the conditions under which they remain. The shelf-life of a product is the period that it remains stable under specified conditions (International Conference on Harmonisation of Technical Requirements for Registration of Pharmaceuticals for Human Use (ICH), 2003). Accelerated stability studies were done to determine the ISED stability.

This chapter investigated the sterilization procedure and post-sterilization characterization tests undertaken to confirm the safety and efficacy of the method. Pre and post-sterilization analysis via DSC, FTIR, confirmation of sterility through microbiological studies. Accelerated stability studies were conducted to ascertain the effects of storage on the ISED..

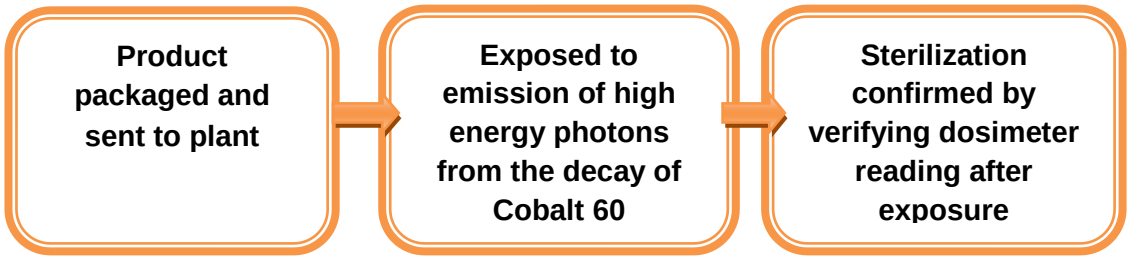


Figure 6.1: Summary flow diagram of the gamma sterilization process.

6.2 Materials and Methods

6.2.1 Materials

As in *Chapter 5, Section 5.2.1 Materials*

6.2.2 Gamma irradiation sterilization of the optimized ISED

DF and DL samples were prepared and packaged into labelled glass polytops sealed with a plastic lid. Samples were transported to Isotron (Pty) Ltd. (Isando, South Africa) and irradiated at a dose of 25KGy (sufficient for sterilization without biological validation according to the European Guideline, 1992) (Appendix D1).

6.2.3 Determination of molecular vibrational transitions and complementary thermal analysis of optimized ISED

Samples were analyzed according to the method in *Chapter 5, Sections 5.2.2.3 Determination of the molecular vibrational transitions and 5.2.2.4 Determination of thermophysical and supplementary properties via temperature modulated differential scanning calorimetry (TMDSC) and Thermal Gravimetric analysis (TGA).*

6.2.4 Determination of sterility efficacy through microbiological techniques

Microbiological tests were conducted in order to confirm the effectiveness of the selected sterilization procedure. A modified USP XXIV Method II sterility testing was employed as a guideline (El-Bagory et al., 2010). The following agar samples were used:

- Thioglycolate medium for anaerobic microbial testing (negative control)
- Triptone soya medium for fungal and bacterial testing (negative control)
- Thioglycolate medium with *Escheria coli* for microbial testing (positive control)
- Triptone soya medium with *Candida albicans* for fungal testing (positive control)
- Thioglycolate medium containing DL and DF ISED for anaerobic microbial testing (test sample)
- Triptone soya medium with DL and DF ISED for fungal and bacterial testing (test sample)

A layer of the nutrient agar (20ml) was solidified in glass petri dishes. Negative controls containing only medium were prepared. Under aseptic conditions by use of a horizontal laminar flow unit (Airstream® horizontal laminar flow cabinet, ESCO technologies, USA), the sterilized DF and DL devices were dissolved in 10mL of sterile water and vortexed for 30 seconds (Figure 6.2a,b). A sterile micropipette was used to transfer 0.1mL of the solution to the centre of the

petri dish (Figure c,d). A bent glass rod was used to spread the solution around the agar (Figure 6.2e). Petri dishes were covered, appropriately labeled and incubated at 37°C for 14days to determine the occurrence of any growth. In the case of the thioglycolate medium, anaerobic conditions were created by placing the petri dishes in sealed a glass jar with a burning candle (Figure 6.2f). Once the candle was extinguished, indicating depletion of oxygen, the jar was incubated.

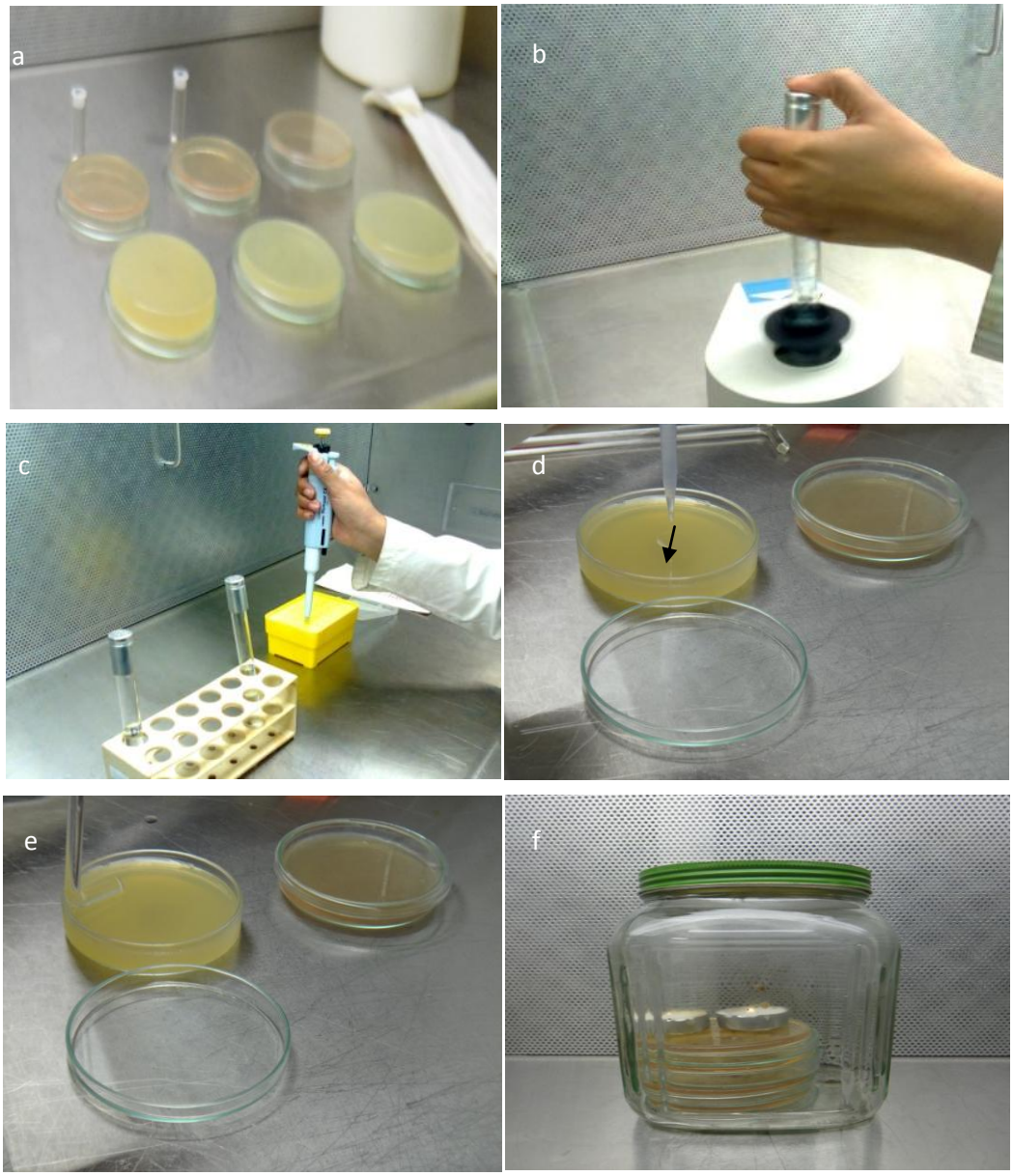


Figure 6.2: Digital images depicting: a) the agar plates of different media, b) vortexing the solutions, c) preparing the pipette, d) transferring the solution to the plates, e) spreading the solution using the glass rod and f) candle jar.

6.2.5 Accelerated stability studies

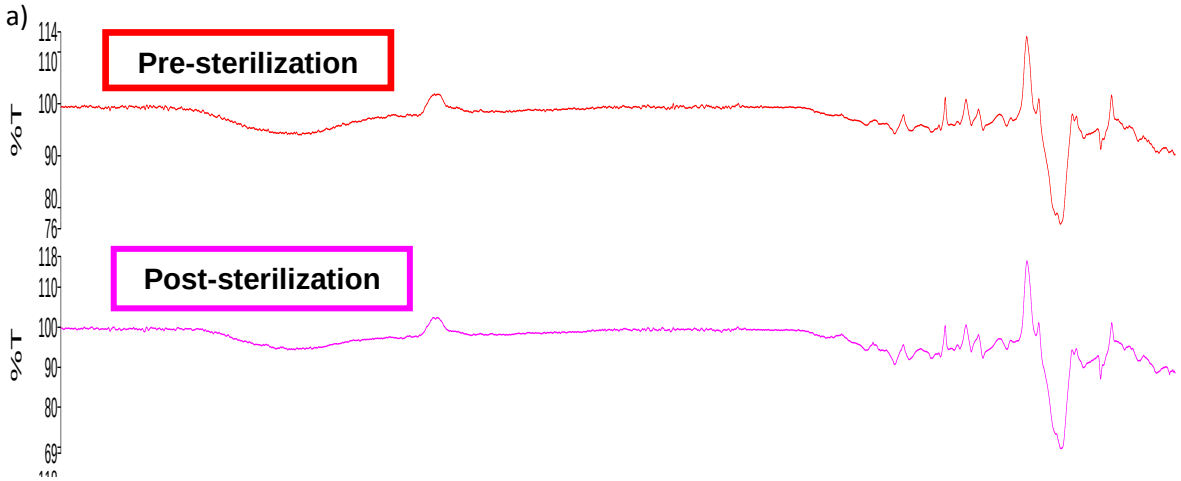
Accelerated stability studies were undertaken in order to gauge the stability of the device after storage. Moisture content, disintegration testing, matrix resilience, drug content and drug release were determined after 0 and 3 months at 40°C 75% RH according to the methods outlined in *Chapter 4, Sections 4.2.2.3 Determination of the physicomechanical properties of the solid eye drops by textural analysis, 4.2.2.4 Disintegration Profiling, 4.2.2.5 Determination of moisture content by Karl Fisher Titrimetry (KFT), 4.2.2.9 Computation of Drug Entrapment Efficiency (DEE) and 4.2.2.10 In vitro drug release studies.*

6.3 Results and Discussion

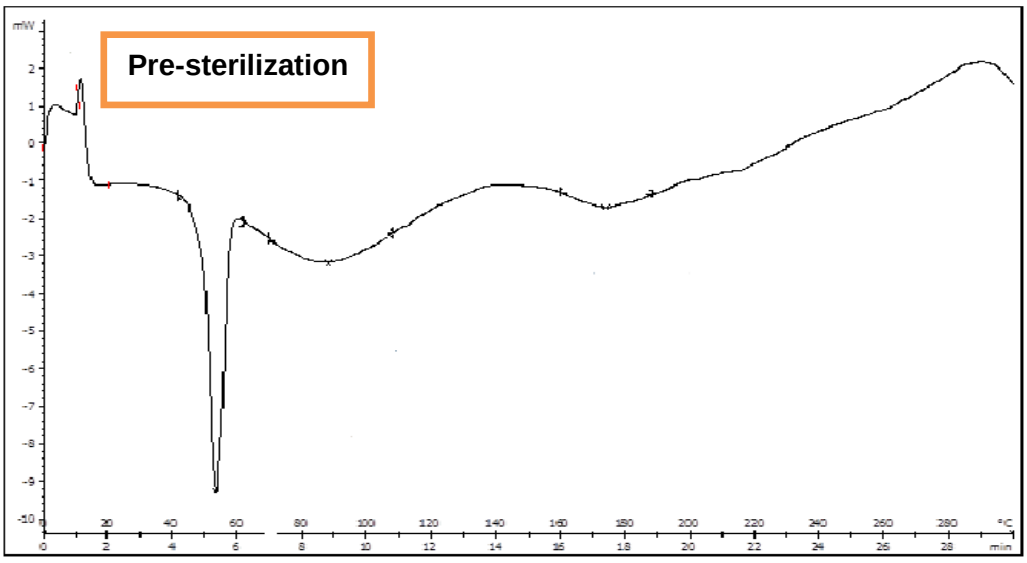
6.3.1 Chemical transitions and thermal analysis of ISED

This favourably proves that radiation did not affect the maintenance of thermal properties.

FTIR results showed that no changes were evident as both graphs depicted similar bands as explained in chapter chapter 5 (Figure 6.3a). This confirms that γ-irradiation sterilization did not alter the chemical structure of polymers and drug. Thermal analysis was conducted to view any alterations in thermal events. Temperature ranges of peaks remained similar in both ISED devices as explained in chapter section. The T_g was fairly stable in both cases (Figure 6.3b,c).



b)



c)

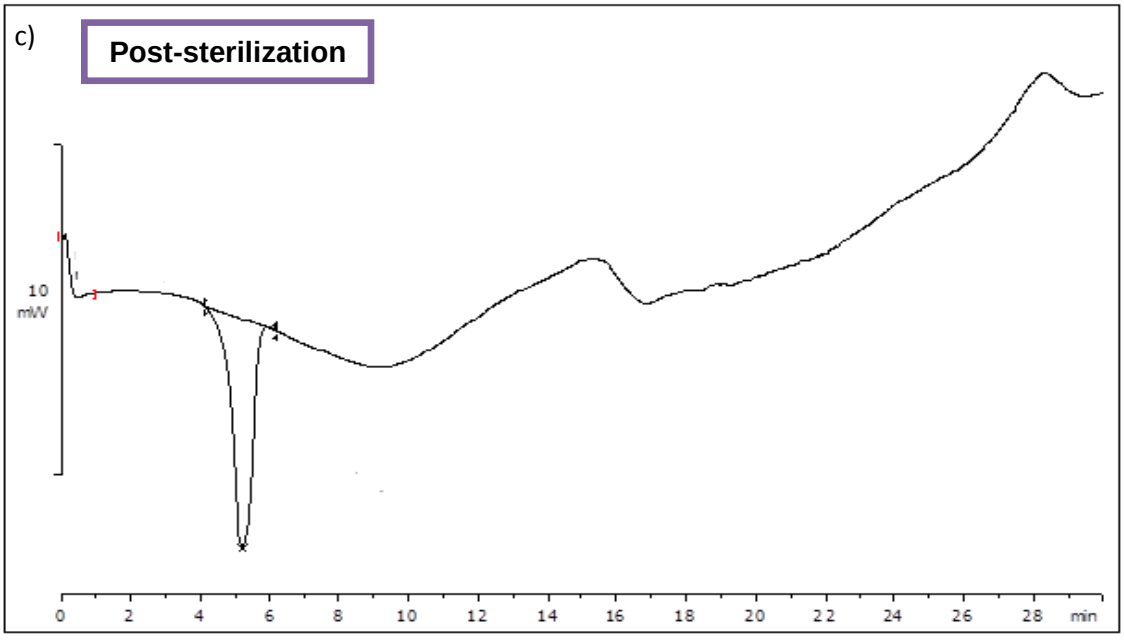


Figure 6.3: FTIR graphs depicting: a) unsterilized ISED, b) sterilized ISED, DSC thermographs of: c) unsterilized ISED and d) sterilized ISED.

6.3.2 Sterility confirmation of ISED

The purpose of this study was to determine if any contamination occurred upon incubation of the plates as the media serves as a substrate to allow for bacterial and fungal growth (Hartman,

2011). The outcome revealed that no growth occurred in the case of test samples. This was a positive outcome and served to confirm the reliability of γ-irradiation for ensuing effective and importantly safe sterilization of the ophthalmic devices. Figure 6.4 a and b elicits the absence of any visible contamination of the positive and negative controls respectively.

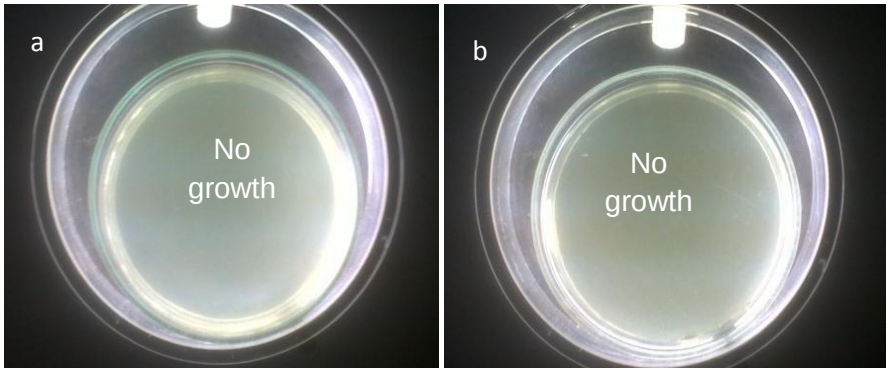
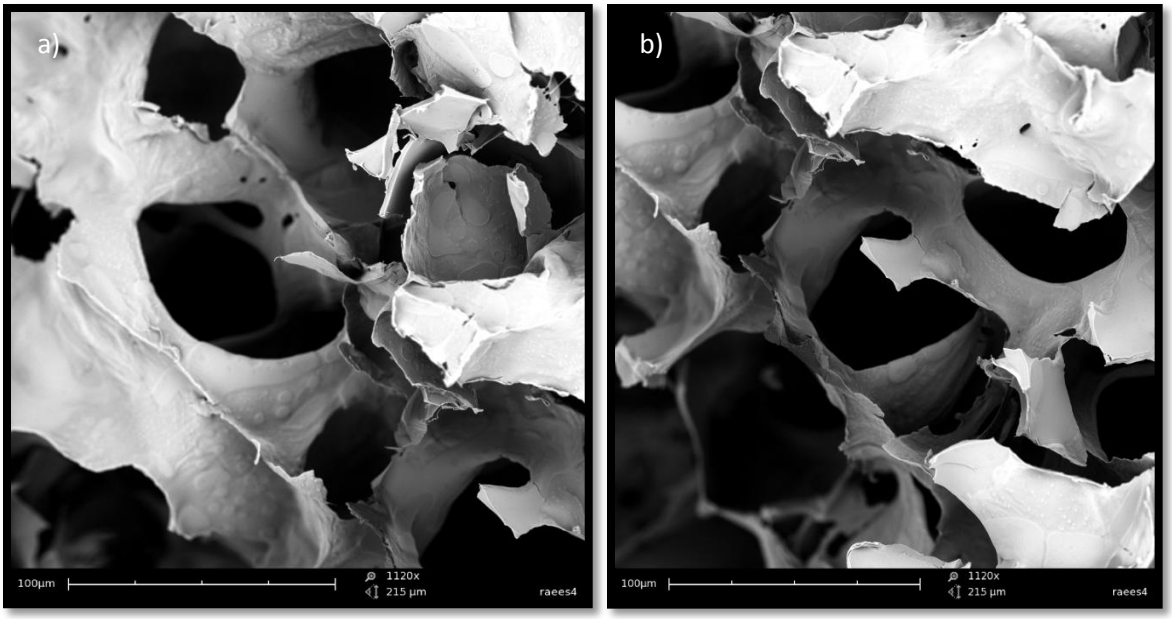


Figure 6.4: Digital images of a) a test sample and b) a negative control of sterile media after incubation.

6.3.3 Stability studies

Stability studies were undertaken to determine whether storage had any impact on the ISED. Results indicated that no significant changes occurred in terms of visual appearance as a robust structure was maintained. Slight yellowing discolouration of the devices was noticed as this is seen with polymers exposed to γ-radiation. The degree of discolouration is usually proportional to the dose received, although this does not seem to affect the properties of the polymers (Croonenborghs et al, 2007). SEM images revealed no difference in morphological structure and presence of spherical to asymmetrical widely distributed pores across the surfaces of matrices was observed (Figure 6.5a and b). Matrix resilience value of 8.512% was obtained with no significant difference compared to the initial result (Figure 6.5c). In terms of the moisture content a slight increase in moisture content was noted (3.321%) which could be attributed to the porous hydrophilic nature of the matrix with a tendency to be hygroscopic upon storage. Disintegration time was not majorly altered with a value of 0.311s compared to 0.350s at 0 months and an immediately soluble structure was favorably maintained. DEE was 93.2% indicative of fairly consistent drug level. MDT calculated from drug release data was fairly consistent (30.21min). Therefore, data was suggestive of overall stability of the formulation. Results are shown in table 6.2.



c)

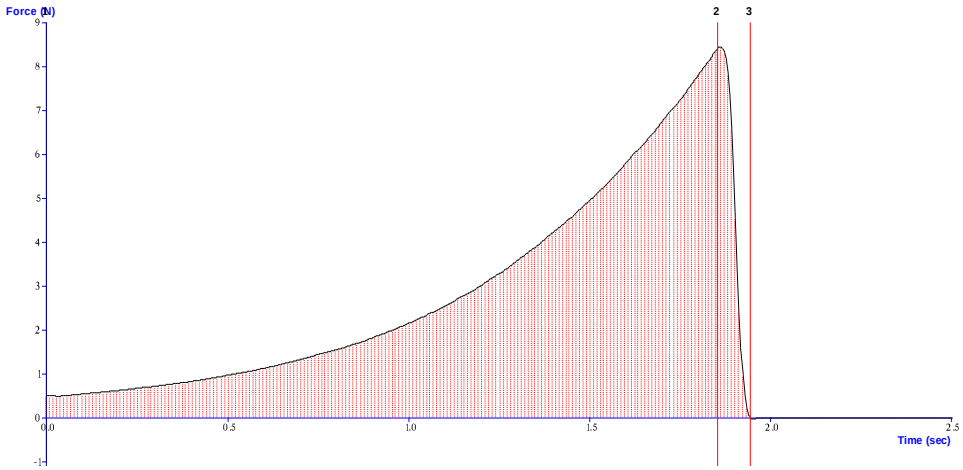


Figure 6.5: SEM images of: a) ISED at 0 months, b) ISED at 3months and c) typical resilience graph.

Table. 6.2: Data obtained for accelerated stability studies at 0 and 3 months (37°C,75%RH).

Time interval (months)	Matrix resilience (%)	Disintegration time (s)	Moisture content (%)	Drug content (%)	$MDT_{50\%}$ (minutes)
0	8.625	0.350	2.051	94.4	30.21
3	8.512	0.311	3.321	93.2	30.10

Results are expressed as the mean of at least three measurements, SDs obtained were within: MR ≤0.010, DT ≤0.059, MC ≤0.002, DC ≤0.081, $MDT_{50\%}$ *≤0.011.*

6.4 Concluding Remarks

This chapter sought to determine the effect of γ-irradiation sterilization on and the overall stability of the optimized ISED. Gamma irradiation served as an effective terminal sterilization procedure for the ISED. Thermal and molecular transitional analysis complemented each other by depicting no appreciable variability in the properties of post sterilized devices. Microbiological tests were a valuable research tool in confirming the efficacy of the sterilization method with absence of contamination. Accelerated stability studies revealed the chemical and physical stability of the ISED were uncompromised and thus the inherent integrity of the device was desirably maintained. A sterile and stable ISED was favourably confirmed by the outcome of the above-mentioned studies.

CHAPTER 7

DEVELOPMENT OF A NOVEL DRUG DETECTION METHOD AND *IN VIVO* ANALYSIS OF AN OPTIMIZED ISED IN THE RABBIT MODEL

7.1 Introduction

Previous chapters of this dissertation conducted extensive *in vitro* analysis of the ISED. In light of the interesting results obtained thus far, *in vivo* studies become necessary. Acquiring *in vivo* data from ISED used in the animal model is essential to corroborate the feasibility of the device in human patients. For detection of the drug, developing a method is required. The application of Ultra Performance Liquid chromatography (UPLC) for analysis is advancement in the field of chromatography and offers a time-effective and highly sensitive detection process (Novakova et al, 2006).

The rabbit or primate (monkey) is commonly selected for ocular experiments. The reason is that animal models are selected for is that human trials create an issue on an ethical level. Frequent sampling can take place which may not be possible in humans. Furthermore, reduced variability can be an advantage in animal models (Craig, 1993).

Pharmacokinetics studies the relationship of the drug in the body. It allows for a mathematical means to interpret data obtained from *in vivo* analysis. However, from an ocular perspective, this is the study of absorption, distribution and elimination of drug after topical instillation on the eye surface (Mayers et al., 1991).

In vitro in vivo correlation (IVIVC) is a concept that has been described by the Food and Drug administration FDA as model that shows the relationship between the *in vitro* drug dissolution and *in vivo* absorption results. *In vivo* absorption can be determined by means of model independent Wagner Nelson method (one compartment model) or Loo-Riegelmin (multi-compartment model). There are mainly 4 levels of IVIVC i.e A, B, C and multiple C. These levels are based on the ability to reflect the complete plasma time profile of which Level A provides a point-point to point relationship and is often preferred. IVIVC serves to support a dissolution method and assists in quality control during manufacturing (Leeson,1995).

The crux of this research and aim of this chapter was to develop a novel UPLC method for the detection of TM in aqueous humour and to determine the pharmacokinetic parameters of *in vivo* release of the ISED in comparison to a marketed eye drop preparation in the New Zealand Albino rabbit eye. Finally, the compatibility of the ISED with the ocular tissue via histology was assessed.

In summary the objectives of this chapter were:

- Aqueous humour aspiration for determination of drug concentration
- To determine the pharmacokinetic parameters of *in vivo* release in the rabbit eye
- To determine the biodegradability and biocompatibility of the ISED by histological toxicity studies

7.2 Materials and methods

7.2.1 Materials

Timolol maleate (M_w = 432.49g/mol), diclofenac sodium (M_w = 318.13g/mol) were purchased from Sigma Aldrich, ammonium acetate (M_w = 77.09 g/mol, Saarchem, Muldersdrift, South Africa), glacial acetic acid (Associate chemical enterprises, southdale, Johannesburg), acetonitrile 200, perchloric acid and methanol (UPLC grade, ROMIL^{TM}, Johannesburg), Glaucosan$^{®}$ 0.5% eye drops (Hexal Pharma (SA)(PTY)(LTD) and double deionized water was obtained by use of a Millipore filter (Millipore water purification system, Millipore, Molsheim, France).

7.2.2 Instrumentation

The equipment consisted of an ultra-performance liquid chromatography (ACQUITY™ Ultra Performance LC, UPLC, Waters, coupled with PDA detector and ELC detector). Data acquisition and interpretation was conducted using Waters Empower software.

7.2.3 Chromatographic conditions

Analysis was performed with ammonium acetate (AA): acetonitrile (ACN) (49:51 v/v) as a mobile phase which was pumped at flow rate of 0.25ml/min in isocratic mode employing a C_{18} column (1.7µm; 1×100mm) at 25°C. The wavelength was kept at 295nm for detection of TM and 2ul of sample was injected for analysis. The run time was set at 3minutes.

7.2.4 Sample preparation

a) Filtration:

Reagents were filtered using 0.22um membranes (Sterile Millipore filter, Millipore Corporation, Bedford, MA, USA) and degassed prior to use. These included:

1. Methanol 100%
2. ACN 100%
3. Strong wash 90/10 ACN/WATER
4. Weak wash 10/90 ACN/WATER

b) Priming

The UPLC was primed according to standard methods before use employing the abovementioned reagents. It involved washing out of the system before use.

c) Mobile phase

AA buffer was prepared by dissolving 7.7g in 100ml water as solvent A. pH was adjusted to 4.5 with glacial acetic acid in a drop-wise manner. ACN 100% was employed as solvent B

d) Stock solutions of analytes and internal standards

TM and internal standard (IS) were prepared (0.34mg/ml). Solutions were kept in amber glass vials until use. Standard solutions of drug and IS were prepared and calibration curves were constructed. A mixture in a 1:1 ratio of analyte and IS were prepared. Samples were filtered (0.22um) and injected into 2mL vials for analysis. Figure 7.1 provides a summary of the process.

e) Aqueous humour collection and drug extraction via liquid-liquid procedure

Enucleated rabbit eye balls were collected and punctured for blank aqueous humour sample aspiration (200uL). Samples were stored in plastic eppendorf tubes at -80°C until used for analysis. Samples were thawed out (200uL) and spiked with standard solutions of analytes. An equal volume of IS was added and samples were vortexed for two minutes. An equal volume of 6%$^{v}/_{v}$ perchloric acid and methanol were added for deproteination. Samples were centrifuged for 10min at 1500rpm (MSE minor laboratory centrifuge, Scientific instruments, West Palm

Beach, Florida, USA) and the clear supernatant was removed. This was made up to a volume of 2mL with mobile phase.

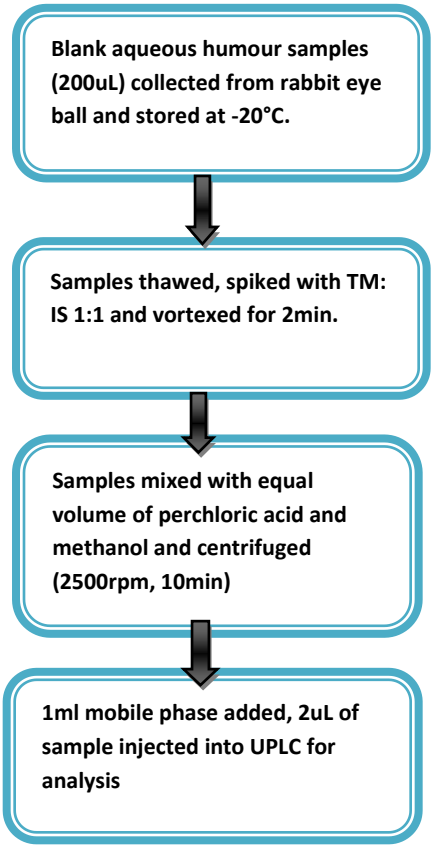


Figure 7.1: Schematic depicting the methodology of liquid-liquid extraction method *in vitro* UPLC analysis process.

f) Construction of calibration curve

Samples were prepared and analyzed as explained above and a calibration curve was constructed (Figure 7.2). The lowest standard concentration of the calibration curve was regarded as the lowest limit of quantification (LOQ). Calibration curve obtained for TM in blank aqueous humour samples was constructed. R^2 of 0.99 was obtained.

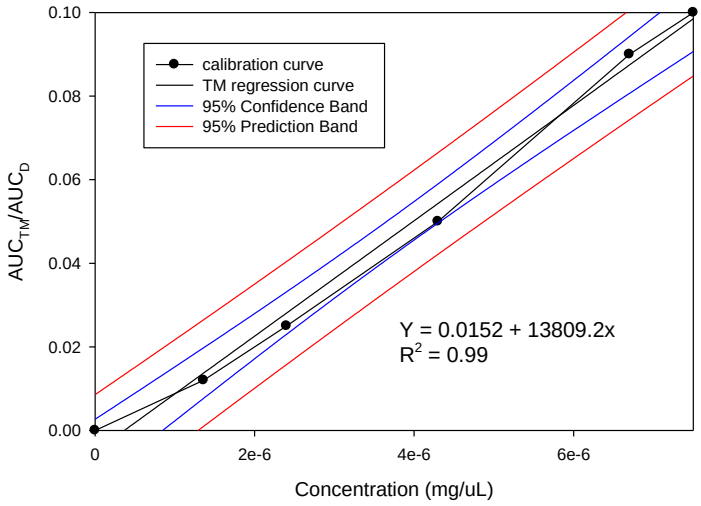


Figure 7.2: Calibration curve obtained in blank aqueous humour samples.

g) Determination of precision, accuracy and stability of TM

Calibration standards were repeated in 3 assay runs. 2 calibration standards were additionally constructed at each concentration. Results were analyzed using single way ANOVA analysis. Recovery of TM was assessed through replicate analysis (N = 5) and compared to those generated from aqueous solutions. Periodic analysis of TM was conducted to determine its stability after being stored in amber bottles and after being frozen.

7.2.5 Preparation of the ISED

The optimized ISED was prepared as outlined in *chapter 5, section 5.2.2.2 Preparation of polymeric solutions and synthesis of solid eye drops according to optimized constraints.*

7.2.6 Sterilization of the ISED

Sterilization by means of gamma irradiation was carried out as explained in *chapter 6, section 6.2.2.1 Gamma irradiation sterilization of the optimized ISED.*

7.2.7 *In vivo* characterization of the ISED in the rabbit model

a) Selection of an appropriate animal model

The operation, safety and the release of drug from the ISED across simulated ocular conditions was determined. However, the use of *in vitro* data, which only simulates the *in vivo* environment,

is not sufficient. An *in vivo* model provides for more accurate pharmacokinetic and pharmacodynamic data as well as more realistic clinical correlation.

Reasons for the animal model in this study:

- Rabbits are a frequently used animal model in opthalmological testing (Barar et al., 2009).
- The rabbit eye is such that it is large enough for accurate ocular injections or delivery by other methods (Short, 2008).
- Certain histological structures can be compared to that of the human eye (Tsonis, P. A., 2008).

Morphometric comparisons and differences of the rabbit eye:

- Rabbit lens a 'fish-eye' to accommodate peripheral vision
- Absence of ciliary muscle results in fixed focal length
- Lens and anterior chamber are larger in rabbit
- Ratio of vitreous to globe is 0.3 in rabbits and 0.6 in humans

Figure 7.3 provides a visual representation of the differences.

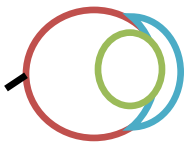
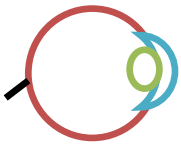
Rabbit	Primate
	

Figure 7.3: Comparison of the rabbit and primate globes (adapted from Short, 2008).

b) Study Protocol

Ethics clearance was obtained from the Animal Ethics Clearance (AEC) committee, University of the Witwatersrand (Appendix C1). All animals and biological tissue were handled according to Standard Operating Procedures (SOP) of the Central Animal Services (CAS). Furthermore, guidelines of Association for Research in Vision and Ophthalmology (ARVO) Resolution on the Use of Animals in Ophthalmic Research and Vision Research (Rockville, MD, USA) were

followed. Cage activity by means of observation for 1 hour periods daily were used to assess state of well-being. Assessment of wellbeing was determined with the use of a score sheet (Appendix E1). Score sheets can be used for routine monitoring and thus contribute to the welfare of the animals.

7.2.7.1 Experimental procedures

A total of 66 New Zealand Albino rabbits of weight ≈2.25kg were used. An initial pilot study was conducted on (6 rabbits). The remaining 60 rabbits were randomly assigned to 2 groups with 30 rabbits each for group 1 and 2. Rabbits were divided into the respective groups (test/placebo group 1 and comparison group 2). A pilot study was conducted on 6 rabbits (1 rabbit for each sampling point) in order to collect samples after ISED insertion. The following groups were assigned:

1. *Pilot study (6 rabbits):* To determine ease of administration at the defined site and presence of any untoward reactions in the rabbit eye following visual assessment after insertion.
2. *Test and Placebo group 1 (30 rabbits):* Rabbits in this group received a drug-loaded ISED containing in the cul-de-sac of the left eye. Drug-free devices were inserted into the right eye for the placebo effect.
3. *Comparison group 2 (30 rabbits):* Rabbits in this group received eye drops of a commercial product (Glaucosan®, 0.5%) in the cul-de-sac of the left eye.

Rabbits were anaesthetized with an intramuscular combination of ketamine hydrochloride (40mg/kg) and xylazine (10mg/kg) for ocular delivery of the drug-loaded ISED in the left cul-de-sac at time 0. Placebo ISED was inserted into the opposing eye (right). Samples were withdrawn at 30, 60, 120, 240, 360 minutes and 24 hours after insertion. At each sampling point each animal was euthanised with an overdose of IV sodium pentobarbitone (> 50 mg/kg, ~2 mL) with consequent enucleation (surgical removal of the eyeball). The aqueous humour (≈200ul) was aspirated (paracentesis/tapping) employing an insulin syringe fitted with a 26 gauge needle inserted parallel to the iris (Lee and Robinson, 1979). The aqueous humor samples was frozen immediately and stored at -80° C. Figure 7.3 is a schematic of the procedure while Figure 7.4 provides digital images of the process.

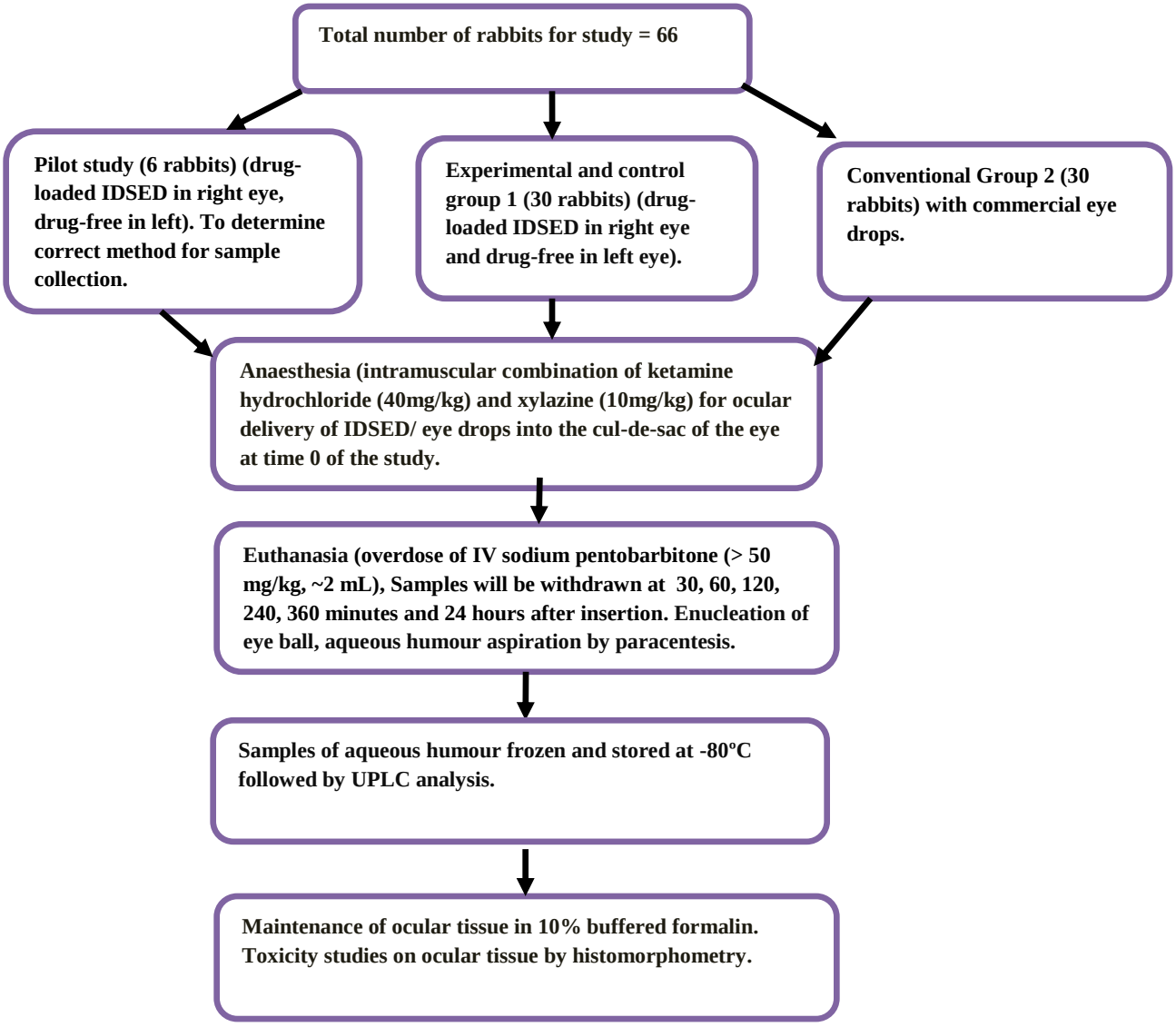


Figure 7.4: Schematic of the procedure of experimental animal studies that will be conducted on rabbits.

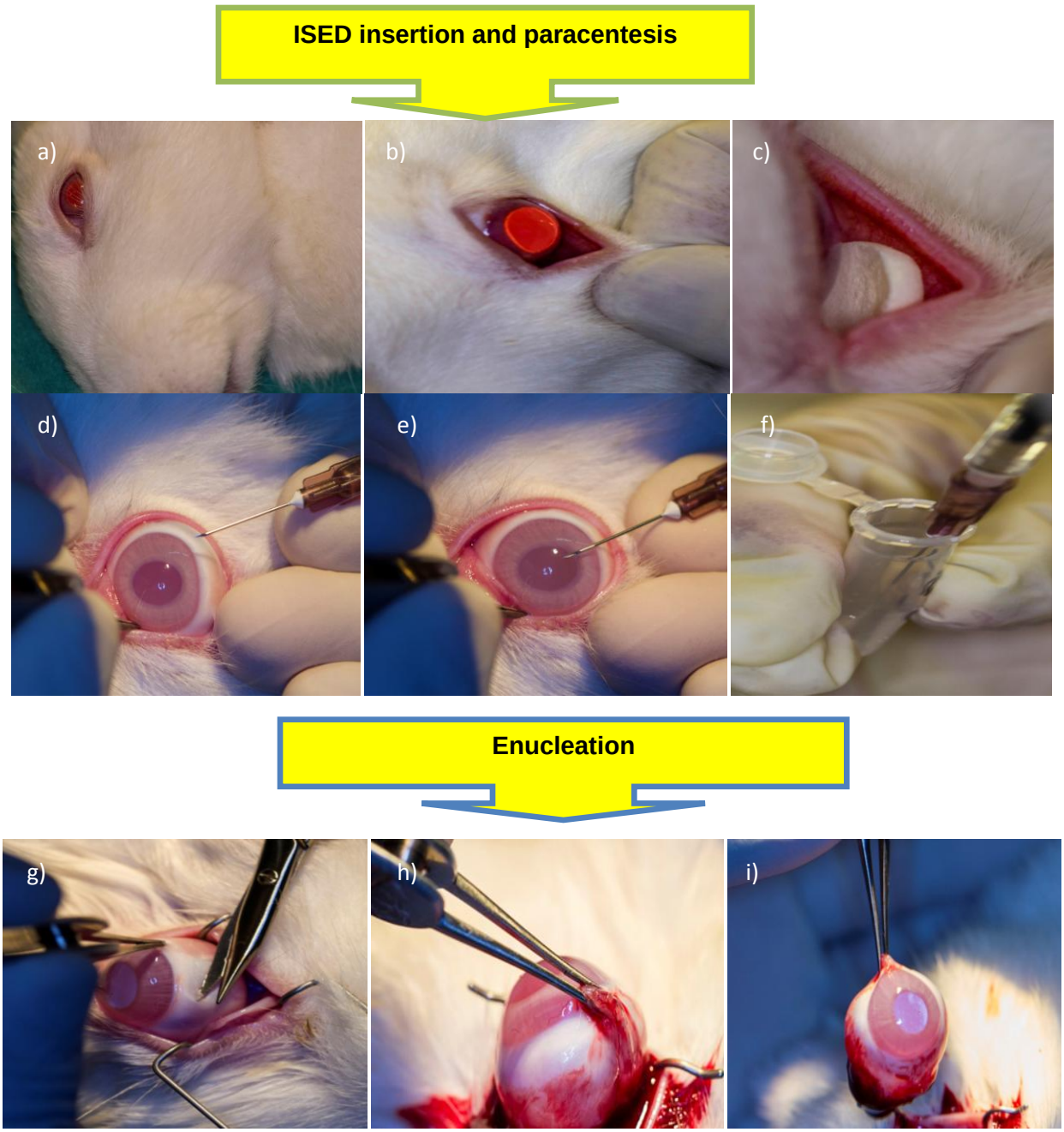


Figure 7.5: Digital images outlining the step-wise *in vivo* studies: a) Left eye of New Zealand Albino Rabbit, b) cul-de-sac of the eye, c) insertion of ISED into the cul-de-sac, d) insertion of the needle for paracentesis, e) aqueous humour aspiration, f) sample collection into a plastic eppendorph, g) removal of surrounding tissue, h) enucleation of the eyeball, i) complete removal of the eye.

7.2.7.2 Post-insertion assessment of the effect of the ISED on the eye surface

Rabbit eyes were assessed using through observation on a macroscopic level. This involved observing any possible effects of the ISED on the eye with reference to Table 7.1. Evaluation of

irritation was conducted according to a 0 (absence) to 3 (highest) clinical evaluation scale of discharge, conjuctival chemosis and conjuctival redness. The untreated eye served as a control. Overall irritation was calculated by addition of the total clinical evaluation scores (A, B, C) (Mishra and Gilholtra, 2008).

Table 7.1. Clinical evaluation scale of irritation (adapted from Mishra and Gilholtra, 2008)

A. Conjunctival redness
Normal vessels 0
Injected vessels 1
Diffuse crimson red vessels 2
Diffuse beefy red 3
B. Conjunctival chemosis
No swelling 0
Swelling above normal 1
Swelling with partial eversion of lids 2
Swelling with half closed lids 3
C. Discharge
No discharge 0
Slight discharge without moistness out of eye 1
Discharge with moistness just adjacent to lids 2
Discharge with moistness on an area around the eye 3

7.2.7.3 Analysis of aqueous humour samples

Analysis of samples was carried out as delineated in *section 7.2.2.2 Chromatographic conditions, e) Aqueous humour collection and drug extraction via liquid-liquid procedure.* Area under the curve (AUC) was calculated from the chromatographs obtained. Figure 7.5 depicts the methodology.

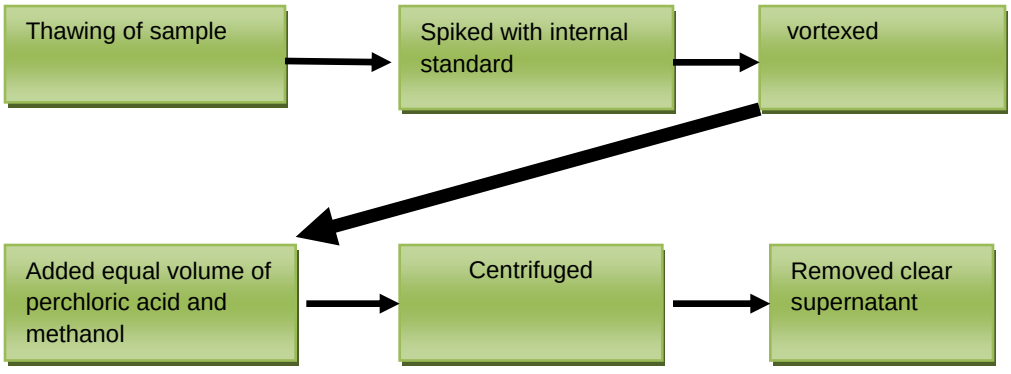


Figure 7.6: Schematic of process for drug extraction procedure.

7.2.8 Data analysis

A one-compartmental pharmacokinetic model (PK) was used for the assessment of ocular results (Mishma, 1981; Lee et al., 1991). This proposes that the drug distributes to a central compartment (aqueous humour) initially followed by a peripheral compartment (Figure 7.7).

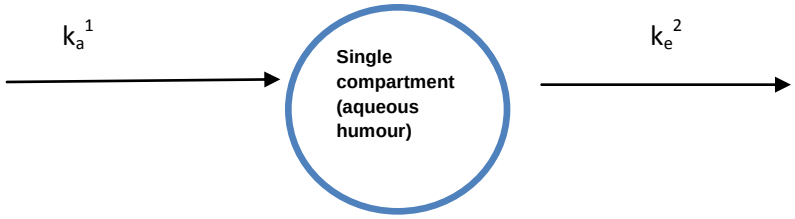


Figure 7.7: Schematic of a one compartmental model of the eye.
[1]Apparent absorption rate constant (ka)
[2]Apparent elimination rate constant (ke)

PKsolver (Microsoft Excel add-ins) was used for analysis. The following pertinent Pk parameters were determined:

1. Apparent absorption rate constant (k_a)
2. Apparent elimination rate constant (k_e)
3. Peak TM concentration (C_{max})
4. Area under the concentration vs. time curve (AUC)
5. Area under the zero and first moment curves from the last sampling time to infinity ($AUC_{t-\infty}$)
6. Area under the moment curve (AUMC)
7. Peak time (t_{max})
8. Mean residence time (MRT)

The following diagnostic criteria were used to determine suitability of the selected model:

1. Co-efficient (R)
2. Weighted sum squares of residuals (SS)
3. Standard error of residuals (SE)
4. Akaike's information criteria (AIC)
5. Schwarz criteria (SC)

7.2.9 *In vitro in vivo* correlation (IVIVC)

A mathematical model for the relationship between an *in vitro* property and *in vivo* response was developed using R-console (version 2.15.3, R foundation for statistical computing) with ivivc

package (0.1.6). Input data was the drug release data from the optimized ISED as well as *in vivo* pK data obtained from UPLC analysis. Level A correlation was selected for IVIVC. 2 steps were followed:

1. *Deconvolution:* fraction of absorbed drug (observed) estimated with Wagner-Nelson method. pK parameters were estimated by nonlinear regression. IVIVC model was developed using fraction of absorbed drug (observed) and drug dissolved.
2. *Convolution:* predicted fraction of absorbed drug was convoluted to predicted aqueous humour concentrations. The prediction error (%PE) between observed and predicted concentrations was calculated (difference in C_{max} and AUC_{∞}).

7.2.10 Histological evaluation of ISED ocular-compatibility

Each eye was cut in a sagittal section and each select block of the eye was placed in a histological cassette and processed in an automated tissue processor according to procedures. Following automated tissue processing, wax blocks were prepared and sections of 6µm were cut on a microtome. The prepared sections were stained in an automated Haematoxylin and Eosin stainer. After staining, the specimen was mounted and the slides examined.

7.3 Results and discussion

7.3.1 Preparation of the ISED

The optimized ISED was prepared as outlined previously. Figure 7.8 below depicts the actual size of the ISED in comparison to a South African R5 coin (diameter 26mm, thickness 3mm).



Figure 7.8: Digital image of the ISED in comparison to a R5 coin.

7.3.2 Visual assessment of ISED effect on ocular tissue

During *in vivo* studies, observations were made to determine the effect of the ISED on the ocular surface. No negative effects were noticed and this served to confirm the results from the HET-CAM test. Table 7.2 provides the results obtained from scoring.

Table 7.2. Score for clinical assessment of ISED on ocular tissue

Effect	Score DL	Score DF
Conjunctival rednesss	0	0
Conjunctival chemosis	0	0
Discharge	0	0

7.3.3 Drug detection

Figure 7.7 depicts the 2D and 3D chromatographs of TM and IS DS obtained from UPLC 1hour after analysis. TM was eluted at 0.594 minutes and DS at 1.595 minutes. Intra- and inter-day precision and accuracy and drug recovery were seen as satisfactory (R^2 = 0.98). The developed method used perchloric acid and methanol in order to de-proteinate samples. The mobile phase maintained at a pH of 4.5 was acceptable to allow for drug retention and peak separation. No difference in retention times of TM and DS in blank samples was noted.

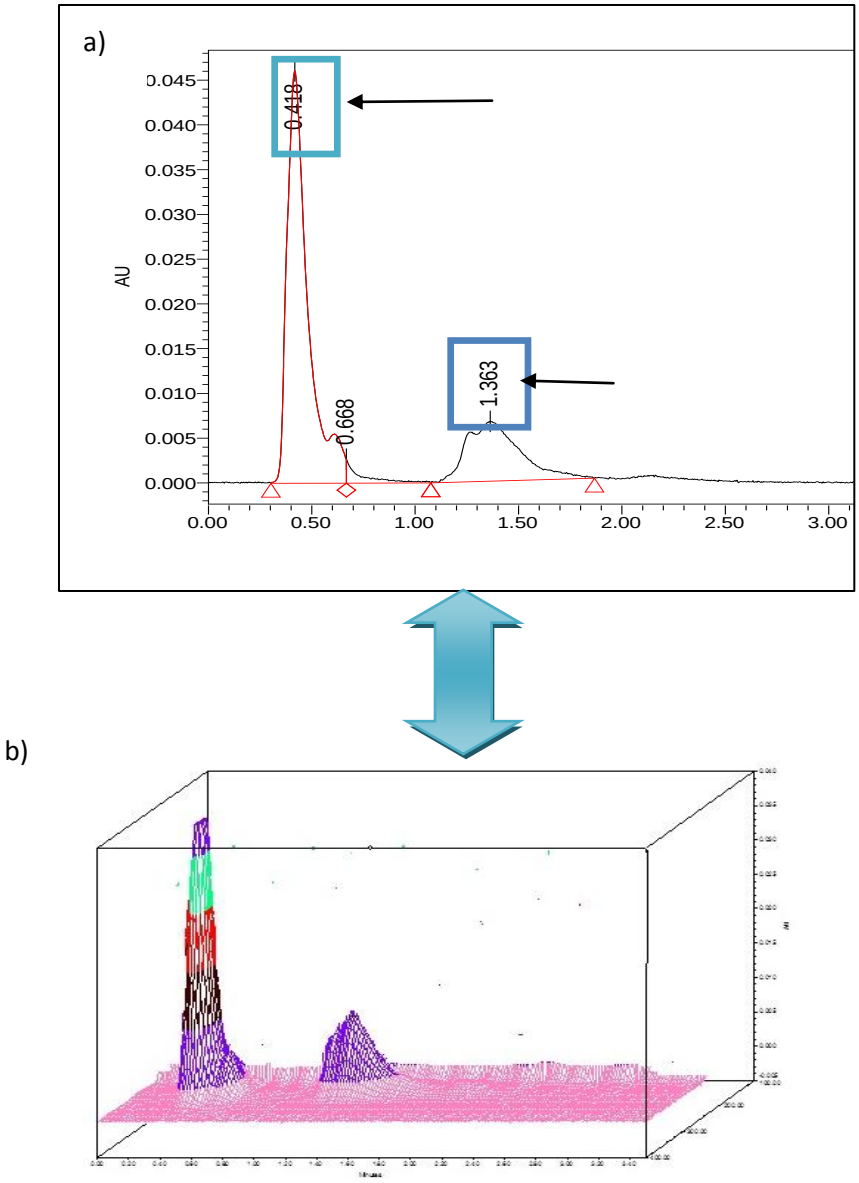
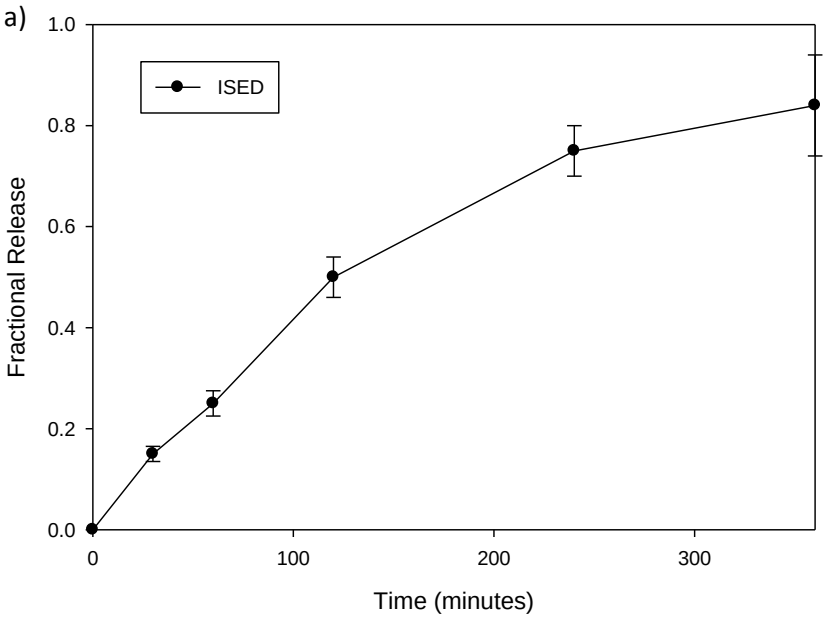


Figure 7.9: 2D chromatograph of: a) TM and DS and corresponding 3D graph of b) TM and DS.

7.3.4 *In vivo* results from the ISED in comparison to marketed eye drop preparation

Results, as confirmed in previous studies, indicated that peak TM concentrations were achieved around 60 - 100 minutes in the aqueous humour (Phillips et al., 1985). For the ISED a peak concentration was reached at around 104.9minutes. In the case of the eye drops a lower C_{max} was obtained (1.97ug/mL). As expected, the optimized ISED displayed a better drug release profile compared to the eye drops (Table 7.3). Diagnostic criteria for 'goodness of fit' of the selected model revealed that low AIC and SC values showed a good model fit. Reasons for the

improved ISED behaviour can be attributed to the following: the eye surface contains hydrophilic glycoproteins termed ocular mucins. As explained by Mantelli and Argüeso (2008), these mucins have the function of stabilizing the tear layer to postpone the break-up of this layer. Mucins are found on the cornea as well as the cul-de-sac and polymers have the tendency to bind non-covalently to these mucins. This allows for localization of drug to a specific area and reduces the possibility of drainage as in the case of the drug within a liquid vehicle. HPC is a surface-active polymer that assisted in alteration of the elimination of the drug instilled by means of the ISED. Similarly, the inclusion of PF68 allowed for pre-corneal interaction when exposed to the increased eye temperature (Wahg et al., 2008). Figure 7.10 displays the *in vivo* and *in vitro* drug release curves for the ISED as well as the eye drops while Figure 7.11 shows graphs from PK analysis.



b)

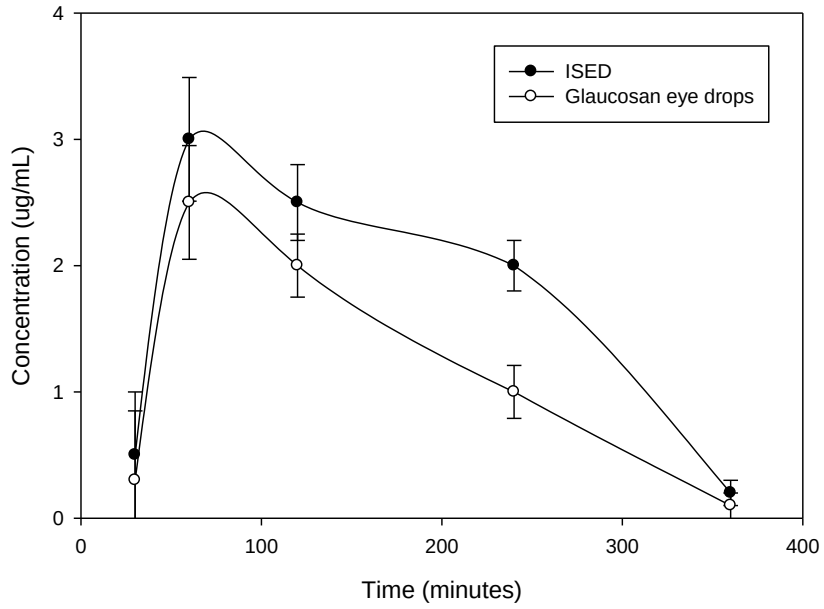
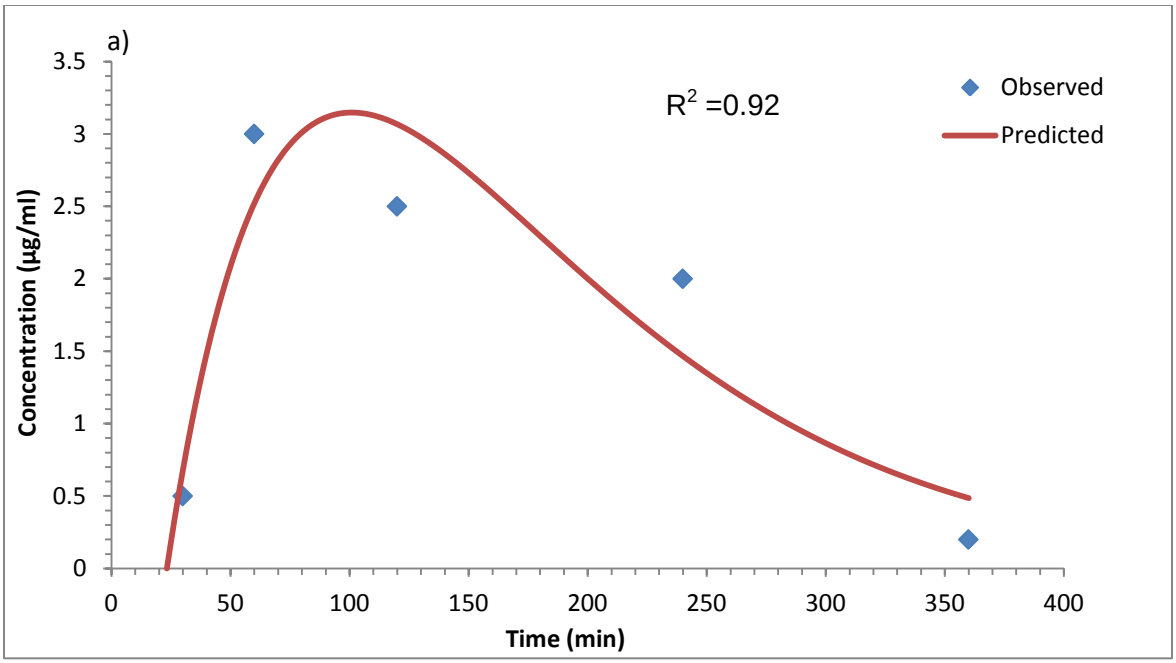


Figure 7.10: Graph depicting: a) *in vitro* ISED drug release results and b) *in vivo* ISED and commercial eye drop drug concentrations.

Table 7.3 PK parameters and diagnostic criteria for ''goodness of fit'' of TM in the aqueous humour following topical application

Parameters	ISED	Eye drops
Pk parameters		
K_a (min^{-1})	0.012	0.011
K_e (min^{-1})	0.013	0.01
T_{max}(min)	100.09	92.2
C_{max}(ug/mL)	3.14	1.97
AUC_{0-t}(ng/ml)	628.39	447.03
$AUC_{t-\infty}$	664.77	496.78
AUMC ($ug/ml/min^{-2}$)	103272.52	91924.99
MRT(min)	155.34	185.04
Diagnostic criteria		
R obs pred	0.92	0.86
SS	0.94	1.50
SC	6.17	6.86
SE	1.007	0.866
AIC	7.74	8.032



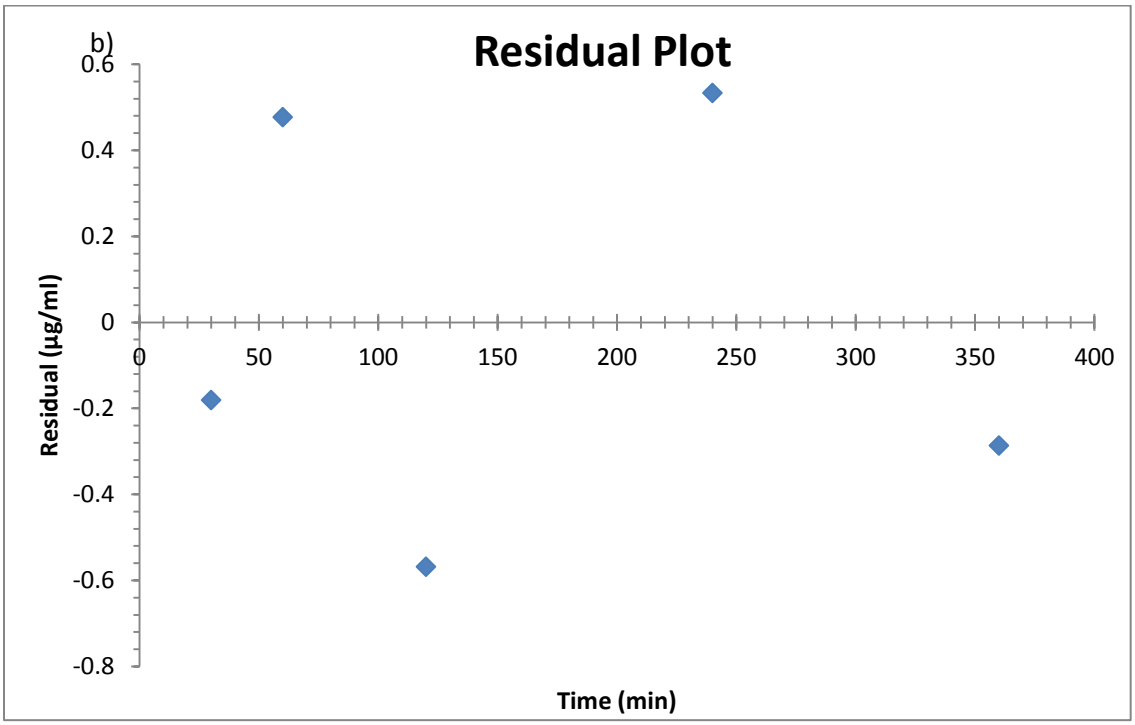


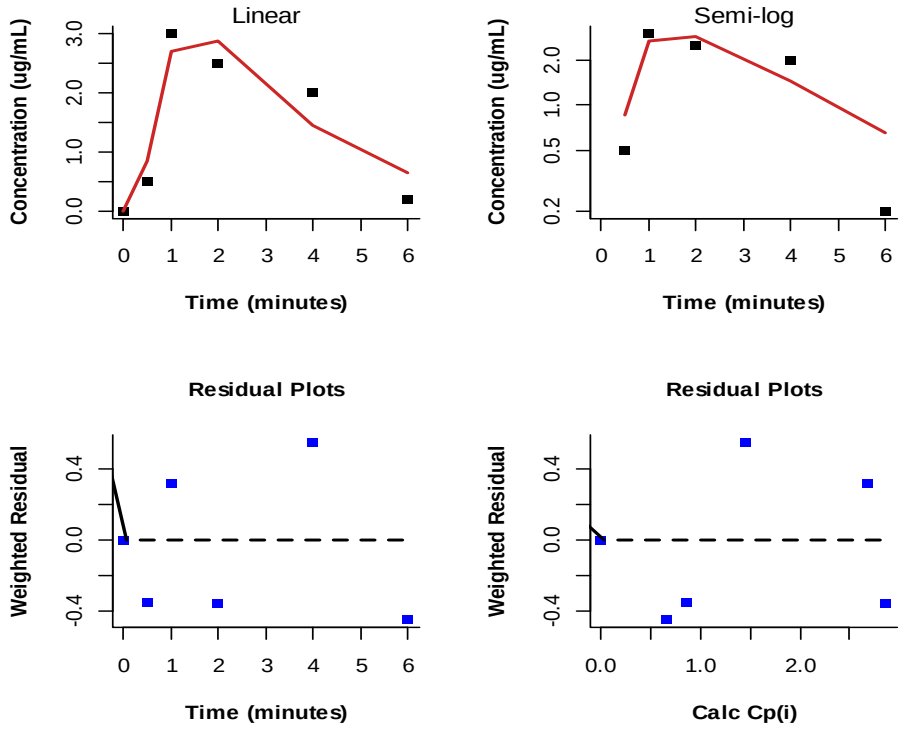
Figure 7.11: Graphs depicting: a) concentration vs time of ISED, b) residual plot of ISED.

7.3.5 In vitro in vivo correlation (IVIVC)

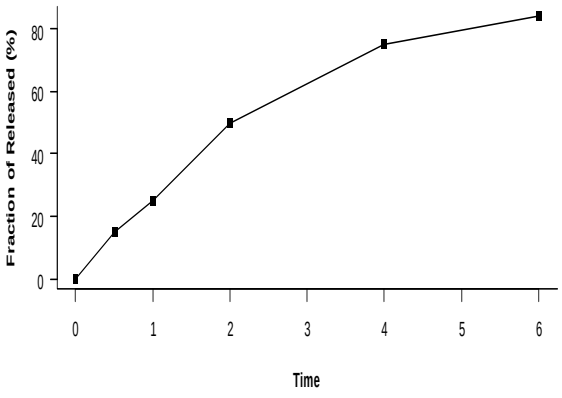
Figure 7.12 (a-d) provides a graphical representation of the data obtained. A Wagner Nelson method was employed to calculate the *in vivo* drug release. Level A point-to-point IVIVC plots

indicated a R^2 value of 0.84. This serves to imply that the *in vitro* dissolution data can be compared to and may serve as a surrogate to that of *in vivo* pK data.

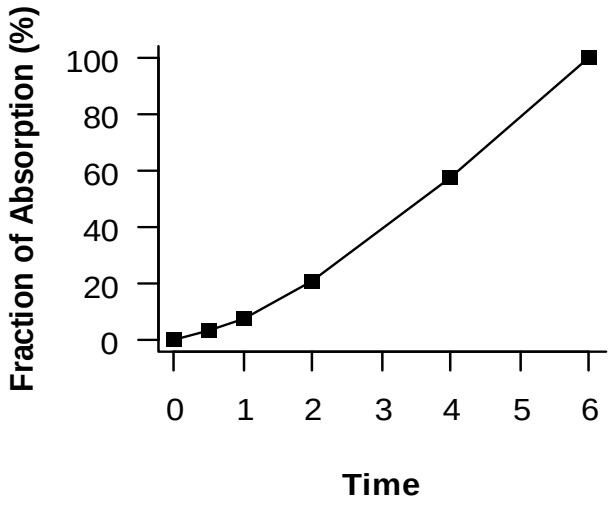
a)



b)



c)



d)

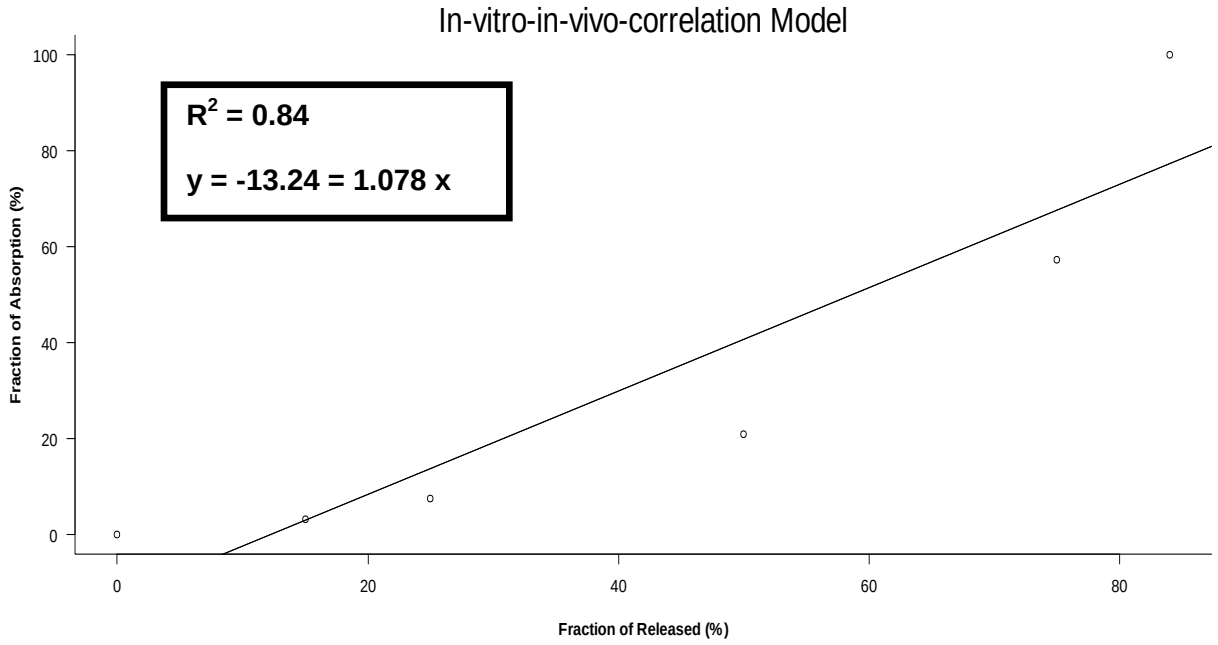


Figure 7.12: Graphs depicting: a) residuals plots, b) *in vitro* release, c) *in vivo* absorption and d) point-to-point Level A IVIVC model plot.

7.3.6 Histological assessment

Histological analysis was performed to assess the safety of the ISED in the eye surface. The corneal topographical findings from the drug-loaded and placebo specimens from the eyes of the rabbits were recorded. The presence of heterophils as well as the heterophil exocytosis into the conjunctival epithelium appeared minimal. Heterophils are usually indicative of sub-acute or chronic inflammation (Gervais et al., 2011). Absence of defects or inflammation was noticed.

Based on the findings, there was minimal pathology or any marked changes and irritation due to the insertion of a drug-loaded device as well as from the placebo administration. Figure 7.13 provides images of the corneal layer at different time points.

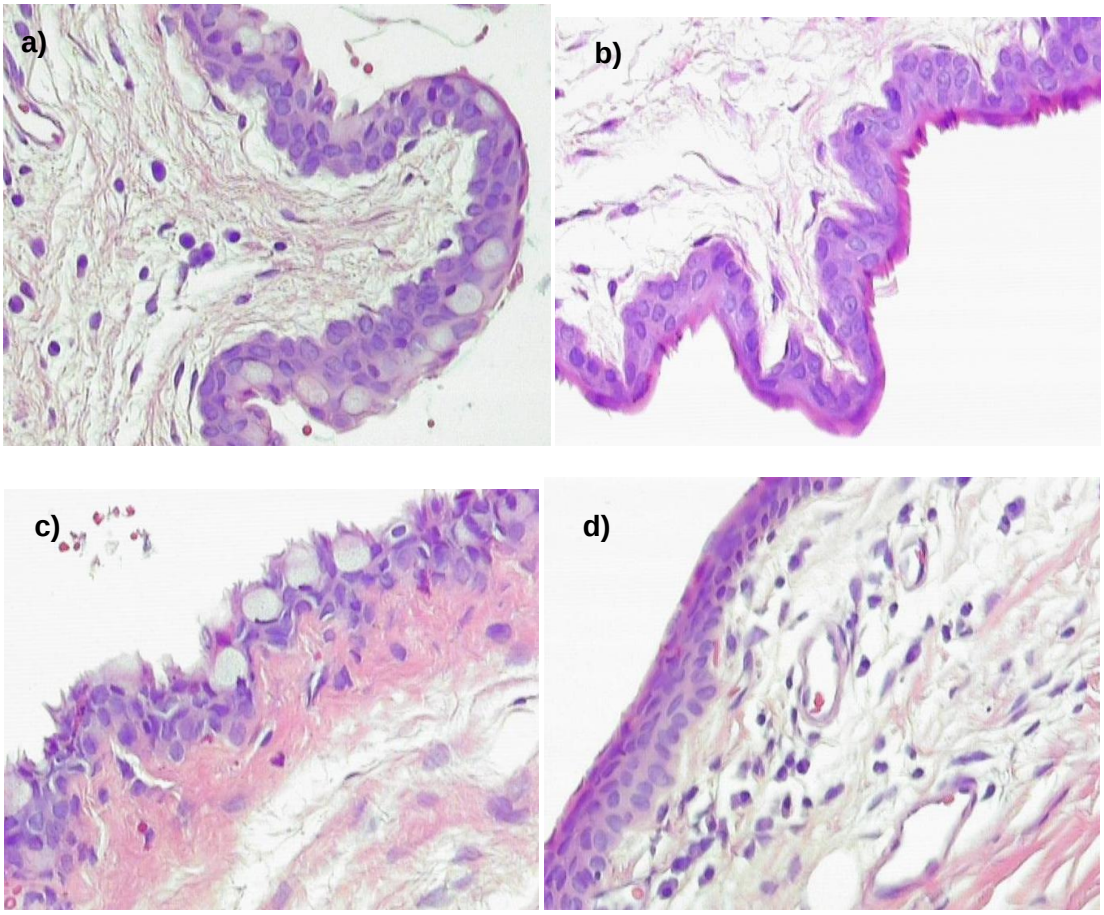


Figure 7.13: Digital images depicting corneal layer with a) DL ISED at 30 minutes and b) with DF ISED at 30 minutes, c) DL ISED at 240 minutes and d) DF ISED at 240 minutes.

7.4 Concluding remarks

The application of UPLC for drug detection allowed for an advantageous development of a novel and sensitive method. *In vivo* assessment indicated that the ISED had improved drug levels in the aqueous humour in comparison to the eye drops. The inclusion of polymers in the ISED allowed for improved corneal adherence and absence of drug drainage as in the case of liquid eye drops. Level A IVIVC correlation indicated an R^2 value of 0.84. Histological assessment revealed the safety of the device as seen from observational studies. Thus, results from this chapter showed that the ISED was concluded to display advantageous behavior and considered safe for the eye surface.

CHAPTER 8

PRELIMINARY INVESTIGATION OF AN ISED WITH ENHANCED PERMEABILITY CAPABILITIES

8.1 Introduction

Up to this point, thorough investigation was conducted on the ISED on an *in vitro* and *in vivo* level. Enhanced permeability compared to pure drug dispersions as well as eye drops was achieved by use of bioadhesive polymers that served to promote corneal interaction and adhesion as opposed to being drained away in the case of a liquid. A step further, was to investigate the possibility of a device that specifically demonstrates improved drug permeation and corneal compatibility. Furthermore, the inclusion of this additional layer could serve as an extra matrix for drug incorporation in circumstances that require more than one active pharmaceutical ingredient.

Permeation enhancers are substances that allow for better movement of drug through the cornea via increase of corneal cell membrane permeability or opening of tight junctions between cells (Manish et al., 2009). Some of these include: bile salts (Sodium deoxycholate SDC, calcium chelators (ethylene diamene tetra acetic acid EDTA), preservatives (benzalkinium chloride BAC), surfactants (Tween 80) (Figure 8.1). However, a few of these enhancers have a tendency to display negative effects on the cornea. For example, BAC is known to result in changes of the corneal morphology (Saettenoe et al., 1996), while saponin causes irritation and increases rabbit blinking rate (Furrer and Mayer, 2002). Thus, the ocular permeation of drugs is improved with the unfortunate increase in corneal irritation and damage. The risk benefit ratio has to be certainly considered.

Advances in research resulted in the application of cyclodextrins. These are molecules with a hydrophilic surface on the outside and an inner lipophilic cavity. They form inclusion complexes of poorly water soluble drugs to allow for corneal penetration (e.g. hydroxypropylbetacyclodextrin HPBCD) (Gaudana et al., 2009). For example, oral drug acetazolamide used for glaucoma displayed improved water solubility in a HPBCD solution and thus could be prepared as an eye drop formulation. They are well tolerated and improve formulation stability however, in some instances may retard permeation of highly soluble poorly permeable drugs (Loftsson et al, 2005). Apart from this, if cyclodextrins are not used in the correct ratios, the permeation is further affected. Time-consuming methods and solubility testing

are required in order to form inclusion complexes with drugs and determine the appropriate concentrations.

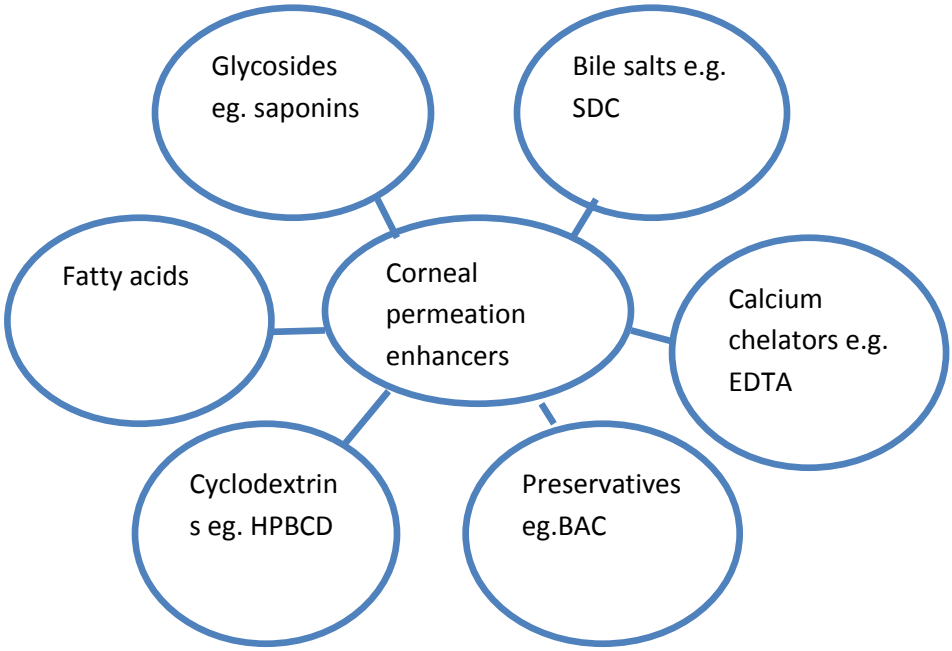


Figure 8.1: Schematic of classes of permeation enhancers.

Aside from specific permeation enhancers, polymers themselves have also been known to assist in improving trans-corneal drug movement. Evidently, one such polymer is chitosan. This is a cationic polysaccharide that is employed in ophthalmic formulations due to favourable bioadhesive, mucoadhesive, antimicrobial and ocular-compatible properties. Furthermore, the major advantage noticed is the permeation enhancing ability. This operates by tight junction opening and allows for drug crossing through the paracellular route (Rabea et al., 2003; de Campos, 2004; de la Fuent et la., 2010). Low water solubility is a limiting factor of chitosan but this drawback can be overcome by a reduction its molecular weight. This is achieved by enzymatic or acidic hydrolysis to prepare the degraded derivatives (Xia et al., 2010). Low molecular weight chitosans (LMWC) have been investigated for topical ocular use. Fairly recently, Tian and co-workers (2012), showed that lipid nanostructures with water soluble chitosan prepared by partial deacytylation had good permeability across excised corneas as well as non-irritating properties. It can be noted that this polymer offers beneficial results for ocular drug delivery and water soluble derivatives have an added advantage.

Chitosan oligosaccharides (COS) (~10 daltons (kDa) (where 1000g/mol = 1kDa)) are another example of a derivative that shows good water solubility. COS have drawn interest in both the

food and pharmaceutical area due to their variety of benefits. These include: biocompatibility, use in cancer therapy, wound healing and antimicrobial properties (Lee et al., 2008; Mourya et al., 2010; Xia et al., 2010). The application to the eye has also been looked into with this material seen as an excellent candidate. Li and co-workers (2009), reported that liposomes coated with COS (8kDa), demonstrated an improved apparent permeability co-efficeint (P_{app}) of diclofenac sodium across rabbit corneas compared to that of uncoated samples. Excellent mucoadhesive effects and safety were also noted.

Thus, reasons for selection of this polymer for testing as gathered from research include:

1. Ocular-compatible and non-toxic
2. Enhanced corneal permeation capabilities
3. Mucoadhesive effects
4. Water soluble

In order to follow a planned process, a Plackett Burman design (PB) was used. PB designs are screening tools for determination of the influence of independent variables on the responses. They allow for minimal number of runs and are thus economical (Plackett and Burman, 1946). A PB design was implemented in order to decipher the important variable effects on responses.

This chapter served as a mini-study to explore the possibility of using COS as a solid lyophilized system for potential ocular application. Determination of corneal drug permeability and $MDT_{50\%}$ through the application of a PB screening experimental design was undertaken.

8.2 Materials and Methods

8.2.1 Materials

Glycyl-glycine (diglycine) (M_w= 132.12 g/mol) (Fluka BioChemika, Belgium), (hydroxypropyl)methyl cellulose (40-60 Cp medium viscosity), chitosan oligosaccharide lactate (M_w = 5000g/mol) and timolol maleate salt (M_w=432.49g/mol were purchased from Sigma-Aldrich (St. Louis, Missouri, USA). All other reagents were of analytical grade and were used as supplied.

8.2.2 Preliminary screening and development of an experimental design

Initial studies revealed an upper and lower limit of 1 and 5 %w/v of chitosan oligosaccharide (COS). Concentrations below 1 produced a fragile poorly formed structure. In the case of DG an amount above 0.2%w/v contributed to the improvement of the structural integrity. HPMC was selected due to its water solubility and concentrations between 0.5 - 3% were suitable for a defined matrix to be formed. Higher concentrations tended to result in increased viscosity. Table 8.1 outlines variable concentrations.

Variables included:

- COS concentration (1 - 5 $\%^{w}/_{v}$)
- DG concentration (0.2 - 1 $\%^{w}/_{v}$)
- HPMC concentration (0.5 - 3 $\%^{w}/_{v}$)

Table 8.1. Formulations generated from the PB design

Formulation	COS ($\%^{w}/_{v}$)	DG ($\%^{w}/_{v}$)	HPMC ($\%^{w}/_{v}$)
1	1	0.2	0.50
2	1	1.0	3.00
3	1	0.2	0.50
4	5	1.0	0.50
5	5	1.0	0.50
6	5	0.2	3.00
7	1	0.2	3.00
8	5	0.2	0.50
9	1	1.0	3.00
10	5	1.0	3.00
11	3	0.6	1.75
12	5	0.2	3.00
13	1	1.0	0.50
14	3	0.6	1.75

Specific responses included:

- **Permeability (P) (kp) -** A higher permeability value corresponds to a faster movement of drug across the cornea.
- **Mean Dissolution Time ($MDT_{50\%}$) (minutes) -** A minimum $MDT_{50\%}$ confers the fastest drug release attainable.
- **Matrix resilience (MR) (%) -** An increased resilience implies an overall strength of the matrix.

8.2.3 Preparation of the solid eye drop

Aqueous solutions of polymers and excipients were prepared in various concentrations in accordance with the PB design. Components were dissolved in 100mL deionized water and stirred for 30 minutes. Samples were injected into each mould of the polyvinyl chloride (PVC) blister packs. Samples were then frozen for 24 hours at -82ºC to solidify the product and lyophilized for 48 hours to extract excess water.

8.2.4 Surface morphology

Surface morphology was determined according to the method in *chapter 4 section 4.2.2.6 Surface morphology by scanning electron microscopy (SEM).*

8.2.5 Matrix resilience

This was determined as in *chapter 4, section 4.2.2.3 Determination of the physicomechanical properties of the solid eye drops by textural analysis.*

8.2.6 Disintegration time

DT was conducted according to the methods in *chapter 4, section 4.2.2.4 Disintegration Profiling.*

8.2.7 Drug release

Drug release was determined as in *chapter 4, section 4.2.2.10 In vitro drug release studies.*

8.2.8 Corneal permeability

The permeation and calculations were conducted and calculated as in *chapter 4, section 4.2.2.11 Ex vivo permeation studies and chapter 5, section 5.2.2.8 Ex vivo permeation studies of the optimized formulation in comparison to a commercial anti-glaucoma product.*

8.3 Results and Discussion

8.3.1 Physical features and surface appearance

Formulations 2, 4, 5, 6, 7, 8, 9, 10, 11, 12 and 14 appeared well-formed while other remaining samples were slightly fragile. This was expected due to the low polymer and excipient concentrations. SEM revealed structures with circular pores well distributed over the matrix. Figure 8.1 depicts a typical SEM image.

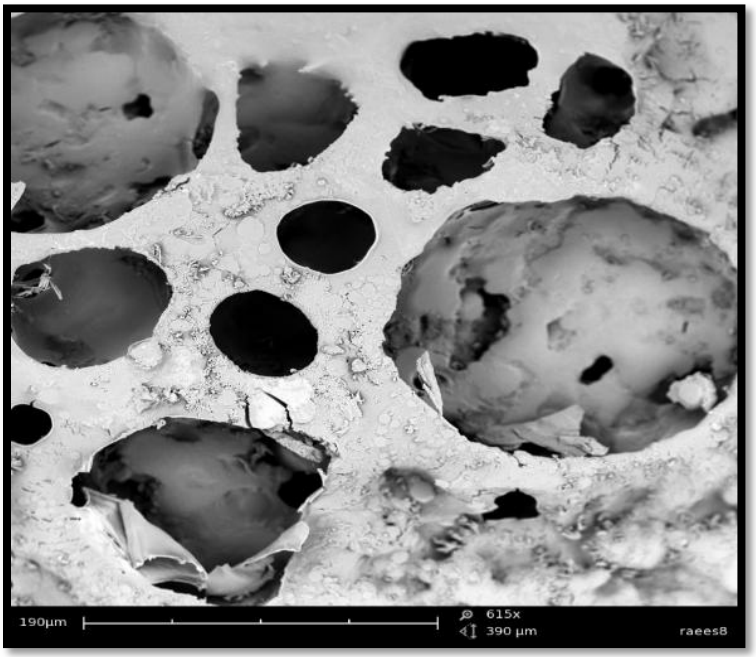


Figure 8.2: SEM image of formulation 1 (magnification 615x).

8.3.2 Matrix resilience

MR results identified that well formed structures as explained above correlated with higher MR values. Formulation 10 had the highest value of 7.7264%. To an extent higher DG levels contributed to higher MR however the polymer concentrations seemed to be more significant in this regard while DG influenced the ability of the structure to be held together rather than the overall strength.

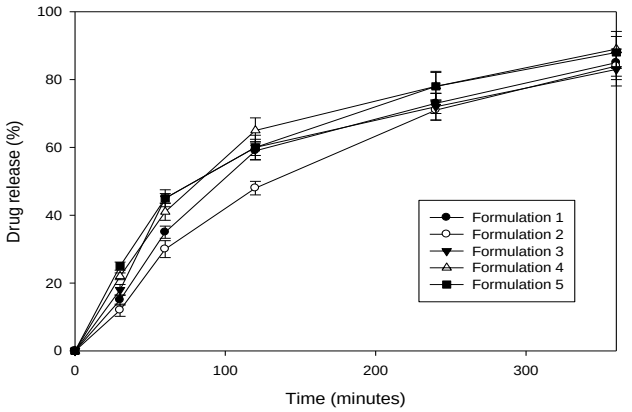
8.3.3 Disintegration time

The disintegration times of formulations ranged from 3.530-7.713s. Lower COS and HMPC concentrations resulted in higher disintegration times as expected but overall rapid solubility was observed due to the high degree of water solubility of both polymers. HPMC tends to display an increased viscosity when higher amounts are added and thus formulations with increased HPMC dissolved slower compared to the other formulations.

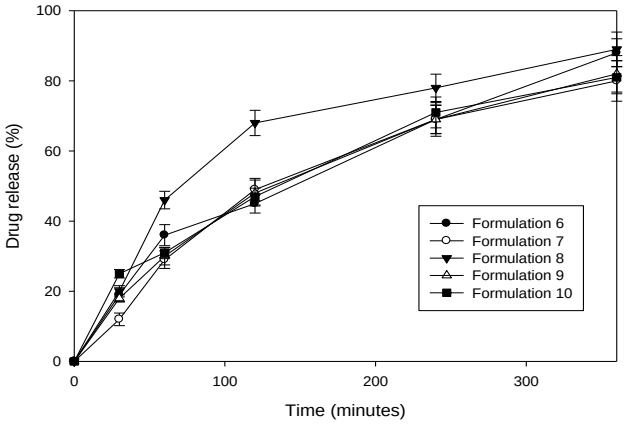
8.3.4 Drug release

In vitro drug release revealed that a higher HPMC concentration corresponded to slower release due to the slow movement of drug from the viscous system. Conversely, the lower polymer concentrations allowed for a faster drug release due to rapid disintegration. Although high COS concentrations were present in some formulations, the presence of high HPMC levels slowed the drug release and consequent permeation. Figure 8.2 elicits the results.

a)



b)



c)

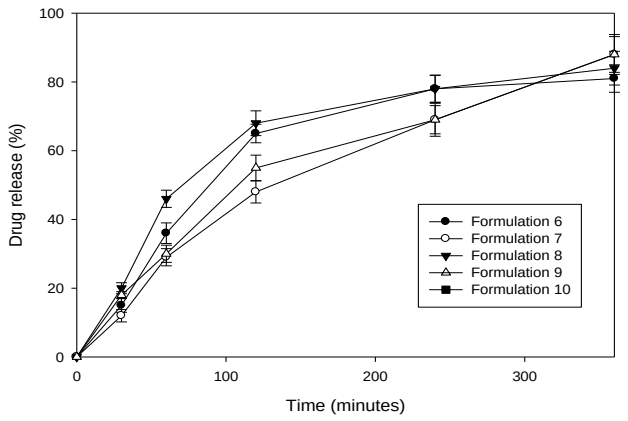


Figure 8.3: Drug release curves for the 14 formulations.

8.3.5 Permeability

Permeation values provided an interesting revelation that confirmed the ability of COS to act as a corneal penetration enhancer. Formulations 4, 5, 6, 8, 12 and 14 had the highest kp values. As mentioned before, this can be connected to the higher COS amounts incorporated. It is established that the chitosan polymer has good interaction with the cornea. The mechanism of permeation has been described through the paracelular pathway of the cell membrane. To explain further, the presence of amino groups on the polymer (positive charge) has some sought of interaction with the cellular membrane and epithelial tight junctions (negative charge) (de la Fuente 2010). This then results in opening of the junctions which allows for drug movement. Another point worth mentioning is that although an increase in COS resulted in enhanced permeation this effect is saturable process (Alonso and Sanchez, 2003). The remaining formulations still had a better permeation value than that of a pure drug dispersion as reported in chapter 4 and this can be attributed to the presence of COS. Table 8.2 depicts a comprehensive summary of results obtained from analysis.

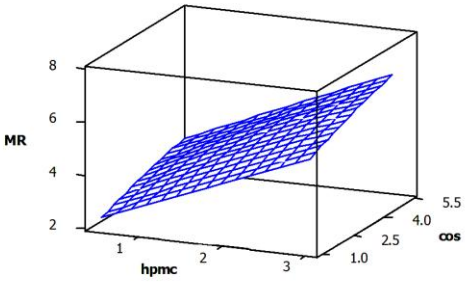
Table 8.2. Data generated from analysis of the novel ISED

Formulation	MR(%)	DT(s)	$MDT_{50\%}$(min)	k_p(cm.min^{-1})
1	2.281	6.243	25.00	1.9 x 10^{-4}
2	5.232	3.530	34.00	1.8 x 10^{-4}
3	2.412	3.645	24.00	1.9 x 10^{-4}
4	3.612	5.712	21.00	2.6 x 10^{-4}
5	3.153	6.683	23.00	2.5 x 10^{-4}
6	6.271	6.832	35.00	2.1 x 10^{-4}
7	5.162	6.973	32.00	1.8 x 10^{-4}
8	3.589	5.545	21.00	2.6 x 10^{-4}
9	5.831	3.913	35.00	1.8 x 10^{-4}
10	7.726	3.672	36.00	1.9 x 10^{-4}
11	4.912	7.532	25.00	1.9 x10^{-4}
12	6.145	3.692	35.00	2.0 x10^{-4}
13	2.315	3.642	25.00	1.9 x10^{-4}
14	4.453	7.713	28.00	2.0 x 10^{-4}

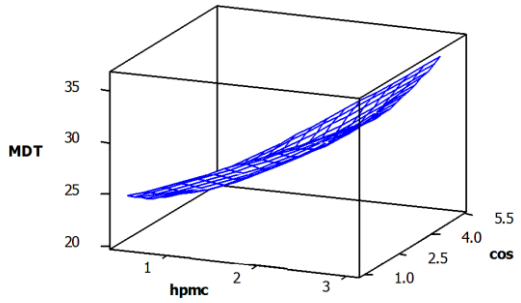
8.3.6 Response surface analysis

Factorial analysis revealed that for the response MR, COS and HPMC displayed the most influential effects (p=0.001 and p=0.000 respectively). Increased concentrations of these polymers contributed to higher strength. HPMC displayed a significant effect on MDT, while the other 2 components were insignificant. This is due to the fact that this polymer dissolves faster at lower concentrations and thus drug is released faster. Finally and most importantly kP was affected mainly by COS as expected (p=0.001). HPMC was also a factor (p=0.003) but not directly on permeation. Higher HPMC amounts retarded drug release and thus reduced kP values were obtained despite high COS concentrations. DG did not contribute to responses in a Surface plots are shown in Figure 8.3.

a)



b)



c)

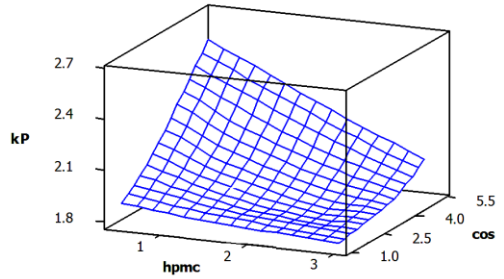


Figure 8.4: Surface plots of a) MR vs. COS, HPMC, b) MDT vs. COS, HPMC and c) Kp vs. COS, HPMC.

8.3 Preliminary insight into the design of a bi-layered ISED

A step further was to consider the possibility of an ISED comprising more than one layer. These are termed multilayered systems. Numerous studies on multilayered tablets for oral use have been reported. The reasons for conceptualization of these ideas are concisely summarized in Table 8.3.

Table 8.3. Summary of the characteristics of multi-layered tablets (Extracted from Kulkarni and Bhatia, 2009; Vaithiyalingam and Sayeed, 2010; Divya et al., 2011; Askok and Kumar 2012; Pujara et al., 2012).

Reasons for design	Advantages	Disadvantages/ Challenges	Ideal properties
Incorporation of more than one active ingredient in a single unit Separation of incompatible actives Fixed dose drug combinations Development of novel delivery systems e.g. chewable or gastro-retentive devices To modify or control the release of actives	Enhance patient compliance through reduced dose frequency Lower cost compared to general oral dosage forms Chemical stability Possible for large-scale manufacture	New challenges in formulation and production Regulatory control Certain drugs resist compression, require coating May be difficult to swallow e.g. pediatrics, geriatrics and unconscious patients	Elegant appearance Sufficient mechanical strength Release of actives reproducibly and predictably Chemical stability

In order to get a better understanding into the concept a selected example of an advanced multilayered oral tablet is hereby explained. This osmotic technology termed OROS®, developed by Alza corporation, consists of the analgesic hydromorphone is an extended release dosage form (24 hours). Basically, this comprises bi-layered core which has the drug layer and another push- layer of excipients and osmotic agents. When water from the GIT passes through over the membrane the water insoluble drug forms a suspension and the push layer releases drug through a hole formed by lazer drilling (Divya et al., 2011). Figure 8.4 provides a visual representation.

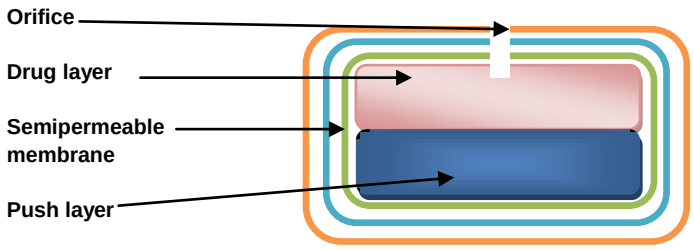


Figure 8.5: Schematic of OROS technology (adapted from Plangio et al., 2002).

Multilayered fast disintegrating tablets have been developed; however, they have been prepared mainly through conventional tableting procedures. For example, Kulkarni and Rhagvendra (2011), reported that a fast disintegrating aclofenac-loaded tablet was attempted by direct compression. This tri-layered tablet displayed an enhanced surface area, rapid drug release and superior properties when compared to marketed tablets. Thus, it can be seen that the lyophilization technique has not been given much attention.

To our knowledge, a multilayered fast disintegrating system prepared by freeze-drying for ocular use has been minimally researched. This sub-section aimed to prepare a bi-layered ISED (BLISED) comprising the optimized ISED from chapter 4 and the COS ISED of this current chapter.

8.3.1 Methodology for BLISED preparation

The COS ISED solution was prepared according to methods outlined in chapter 8. A modification was the addition of half the volume of the polymeric solution into the blister pack followed by freezing. After 24 hours, the blister pack was removed from the freezer and allowed to stand for a period of 5 minutes which allowed for slight melting of the top of the frozen solution. The second solution of the ISED (prepared according to methods in chapter 5) was injected into the mould and this allowed for interaction of the layers but still maintained separation. The formulation was frozen for 24 hours followed by lyophilization.

8.3.2 Results and discussion

A fairly stable BLISED was formed with identification of the distinct layers (Figure 8.5). Separation of the layers did not occur. The BLISED dissolved within time frame of 0.2s for the ISED and 3 seconds for the COS component. The advantage of this system is that it can be applied in cases where more than one medication is required. Combination therapy for

glaucoma is quite popular e.g. timolol and latanprost eye drops. This will be convenient for the patient as one dose will be necessary and avoid the complications attached to liquid eye drops.

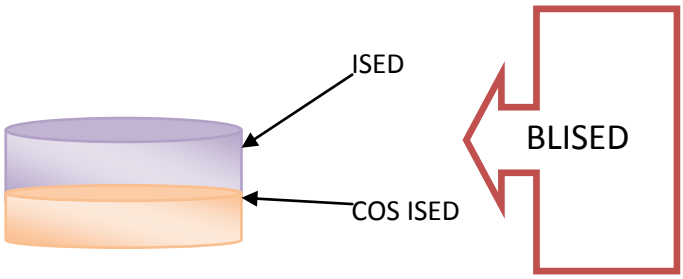


Figure 8.6: Schematic of bilayered ISED.

8.4 Concluding Remarks

Evidently, from this chapter, the favourable properties of COS were confirmed. In addition, the use of COS further added the benefit of increased water solubility and thus quicker dissolving time. A porous structure with enhanced permeation was fabricated. This mini-study served to function as the basis of advancements to the ISED by means of enhanced penetration. Furthermore, the idea of a BLISED may be beneficial for inclusion of other actives in multiple drug regimens. In depth characterization and further studies are obviously necessitated.

CHAPTER 9

CONCLUSIONS AND RECOMMENDATIONS

9.1 Conclusions

We are at a point to realize that the increasing prevalence of eye diseases is at an obviously shocking level. The availability of treatment and drugs are present, yet these diseases seem to display a lack of control. This is possibly as a result of the lack of patient adherence which stems from a variety of factors as elaborated on in this dissertation. Patient-friendly drug delivery systems that are effective and cheap could be a way forward.

According to the South African Glaucoma Society (2006), glaucoma is one such ocular disease that can be regarded as chronic as well as a major cause of complete vision loss in this country. Thus, it is seen as a burden to the health of this nation and requires urgent plan. Glaucoma is only one example of a variety of anterior ocular conditions, and is mentioned due to the rife occurrence and poor prognosis.

This study was initiated with the aim in mind of developing a simplified, effective ocular drug delivery system and thoroughly testing it under laboratory and body conditions. The main goal was to assist patients with the administration of the system particularly older and impaired individuals, who already suffer from a number of ailments. Treatment has to be individualized and the social and financial mileu of patients are of major importance.

The objectives described were achieved through fabrication of the rapidly soluble eye drop that allowed for easy instillation and improved drug bioavailability. The eye drops were optimized to form a matrix in order to yield a stable yet fast release system. Studies under simulated ocular conditions showed the safety and effectiveness of the system. Furthermore, *in vivo* studies served to confirm these results.

Adding on to the research, the concept of developing a system with enhanced permeability capabilities was touched on. By employing ocular compatible polymers as opposed to specific permeation enhancers interesting results were seen. The simple freeze-drying technique employed to develop the eye drops could be considered as an alternative to the use of liquid eye drops which have a variety of concerns.

9.2 Recommendations

In vivo studies conducted provided a holistic and in depth view of the performance of the device. The possibility of clinical trials would allow for further progression and insight for a true reflection of the system's'' behaviour. However due to the strenuous conditions under which the investigator and animals are put, a suggestion of development of alternative models that would closely be correlated with human conditions and would avoid the use of animals is proposed.

At a manufacturing level, a feasible and viable system is evident with simple 3 step procedure employing cheap and available components. The thought of a bi-layered system could assist in the treatment of conditions that require more than one drug such as an antibiotic and analgesic for infections or combination therapy. This would minimize the need for frequent administration.

9.3 Challenges observed

During *in vivo* studies insertion of the ISED was fairly simple in comparison to the eye drops as it was noticed the liquid eye drops were easily forced out. However, in some instances if the ISED was not placed correctly and movement in and around the eye was noticed.

9.4 Future outlook

The completion of this research aimed to help improve patient compliance in terms of drug administration for diseases of the anterior eye. Elderly and arthritic patients will have a convenient means of drug administration since eye drops are difficult to apply. The proposed ISED may also prove to be a suitable device for the delivery of other anti-glaucoma agents as well as other actives. Dry eye syndrome, infections or other 'front of the eye' problems can be target conditions. The superior properties of the ISED would allow for the development of a suitable delivery system that could be used as a platform for delivery of drugs to various other sites. For example, the technology and methodology can be implemented to the oramucosal route can be considered as an area for other conditions requiring oral therapy.

This research involved conducting progressive ocular drug delivery system development that may lead to further advancements in the future. Fulfillment of the objectives will allow for new publications of more advanced drug delivery systems. Publications arising from this work will serve to boost the academic field and marketing of such systems will ultimately contribute to the economy and development of this country.

REFERENCES

Abduljalil, K., Diestelhorst, M., Doroshyenko, O., Lux, A., Steinfeld, A., Dinslage, S., Süverkrüp, R., and Fuhr, U., (2008). Modelling ocular pharmacokinetics of fluorescein administered as lyophilisate or conventional eye drops. *European Journal of Clinical Pharmacology*, **64**, 521–529.

Ahmed, I., (2003). The noncorneal route in ocular drug delivery. In: Mitra AK, eds. *Ophthalmic drug delivery systems*. New York: Marcel Dekker, 335-363.

Ahmed, I.S., and Aboul-Einien, M.H., (2007). In vitro and in vivo evaluation of a fast-disintegrating lyophilized dry emulsion tablet containing griseofulvin. *European Journal of Pharmaceutical Sciences*, **32**, 58-68.

Ali, M., Horikawa, S., Venkatesh, S., Saha, J., Hong, J. W., and Byrne, M. E., (2007). Zero-order therapeutic release from imprinted hydrogel contact lenses within in vitro physiological ocular tear flow**.** *Journal of Controlled Release*, **124** ,154–162.

Allan, B.D., and Dart, J.K.G., (1995). Strategies for the management of microbial keratitis. *British Journal of Ophthalmology,* **79**, 777–786.

Alonso, M.J., and Sa´ nchez, A., (2003). The potential of chitosan in ocular drug delivery. *Journal of Pharmacy and Pharmacology*, **55**,1451–1463.

Anderson, M.J., and Whitcomb, P.J., (2007). DOE Simplified – Practical tools for effective experimentation (2nd Ed). Productivity Press, New York, NY, USA.

Andres-Guerrero, V., and Herrero-Vanrell, R., (2008). Ocular drug absorbtion by topical route. Role of conjunctiva. *Archivos de la Socidied Espanola de Oftalmologia*, **83**, 683-686.

Anumolu, S.S., Singh, Y., Gao, D., Stein, S., and Sinko, S.J., (2009). Design and evaluation of novel fast forming pilocarpine-loaded ocular hydrogels for sustained pharmacological response. *Journal of Controlled Release,* **137**,152–159.

Araki, K., Ohashi, Y., Sasabe, T., Kinoshita, X.S., Hayashi, K., Yang, X.Z., Hosaka, Y., Aizawa, S., Handa, H., (1993). Immortalization of Rabbit Corneal Epithelial Cells by a SV40-Adenovirus Vector. *Investigative Ophthalmology and Visual Science*, **18**, 2665-2671.

Ashok, H.P., and Kumar, T. A., (2012). A novel approach for bi layer tablet technology: a review. *International research journal of pharmacy*, **3**, 44-49.

Baba, K., Tanaka, Y., Kubota, A., Kasai, H., Yokokura, S., Nakanishi, H., and Nishida, K., (2011). A method for enhancing the ocular penetration of eye drops using nanoparticles of hydrolyzable dye. *Journal of Controlled Release,* **153**, 278–287.

Baheti, A., Kumar, L., and Bansal, A.K., (2010). Excipients used in lyophilization of small molecules. *Excipients and Food Chemicals,* **1**, 41-54.

Bakeman, R., (2005). Recommended effect size statistics for repeated measures designs. *Behaviour Research Methods*, **37**, 379-384.

Barar, J., Asadi, M., Mortazavi-Tabatabaei, S.A., and Omidi, Y., (2009). Ocular Drug Delivery; Impact of in vitro Cell Culture Models. *Journal of Ophthalmic and Vision Research*, **4**, 238-252.

Barar, J., Asadi, M., Mortazavi-Tabatabaei, S.A., Omidi, Y., (2009). Ocular Drug Delivery; Impact of in vitro Cell Culture Models. *Journal of Opthalmic and Visual Research*, **4**, 238-252.

Barrett, E.P., Joyner, L.G., and Halenda, P.P., (1951). The determination of pore volume and area distributions in porous substances. Computations from nitrogen isotherms. *Journal of the American Chemical Society*, **73**, 373-380.

Bawa, R., (1993). Ocular inserts. In: Mitra, AK, eds. *Opthalmic Drug Delivery Systems*. New York: Marcel Dekker Inc., 223-260.

Boateng, J.S., Auffret, A.D., Matthews, K.H., Humphrey, M.J., Stevens, H.N.E., and Ecclestona, G.M., (2010). Characterisation of freeze-dried wafers and solvent evaporated films as potential drug delivery systems to mucosal surfaces. *International Journal of Pharmaceutics*, 389, 24-31.

Bolton, S., and Bon, C., (2004). Pharmaceutical Statistics – Practical and Clinical. Applications (4th Ed). Marcel Dekker, Inc. New York.

Bourlais, C.L., Acar, L., Zia, H., Sado, P. A., Needham, T., and Leverge, R., (1998). Ophthalmic Drug Delivery Systems-Recent advances, *Progress in Retinal Eye Research,* **17**, 33–58.

Bozdag, S., Weyenberg, W., Adriaens, E., Dhondt, M. M., Vergote, V., Vervaet, C., De Prijck, K., Nelis, H.J., De Spiegeleer, B., Ludwig, A., and Remon, J.P., (2010). In vitro evaluation of gentamicin- and vancomycin-containing minitablets as a replacement for fortified eye drops. *Drug Development and Industrial Pharmacy,* **36**, 1259-1270.

Callens, C., Pringels, E., and Remon, J. P., (2003). Influence of multiple nasal administrations of bioadhesive powders on the insulin bioavailability. *International Journal of Pharmaceutics*, **2**, 415-422.

Calonge, M., (2001). The treatment of dry eye. *Survey of Ophthalmology,* **45**, 227–239.
Carpenter, J.F, Pikal, M.J., Chang B.S., Randolph TW., (1997). Rational design of stable lyophilized protein formulations: some practical advice. Pharmaceutical Research, **14**, 969–975.

Carpenter, J.F., Pikal, M.J., Chang, B.S., and Randolph, T.W., (1997). Rational design of stable lyophilized protein formulations: some practical advice. *Pharmaceutical Research*, **14**, 969–975.

Ceulemans, J., Vermeire, A., Adriaens, E., Remon, J.P., and Ludwig, A., (2001). Evaluation of a mucoadhesive tablet for ocular use. *Journal of Controlled Release,* **77**, 333–344.

Chandrasekhar, R., Hassan, Z., Al Husban, F., Smith, A.M., and Mohammed, A.R., (2009). The role of formulation excipients in the development of lyophilized fast-disintegrating tablets. *European Journal of Pharmaceutics and Biopharmaceutics*, **72**, 119–129.

Chang, J.N., (2010). Recent Advances in Ophthalmic Drug Delivery. In: Kulkarn VS eds. *Handbook of Non-Invasive Drug Delivery Systems* New York: William Andrew Publishing**,** 165-192.

Chen, Y., Lui, Y., and Tan, H., (2008). Preparation of macroporous cellulose-based superabsorbent polymer through precipitation method. *Biological Research*, **3**, 247-254.

Chetoni, P., Di Colo, G., Grandi, M., Morelli, M., Saettone,, M. F., and Darougar, S., (1998). Silicone rubber/hydrogel composite ophthalmic inserts: preparation and preliminary in vitro/in vivo evaluation. *European journal of Pharmaceutics and Biopharmaceutics*, *46*, 125-132.

Choonara, Y.E., 2011. An *in vitro* study of the design and development of a novel donut-shaped minitablet for intraocular implantation. A thesis submitted to the Faculty of Health Sciences, University of the Witwatersrand in fulfillment of the requirements for the degree of Doctor of Philosophy.

Chowhan, M., Weiner, A.L., Bhagat, H., (2002). Drug delivery – ophthalmic route. In: Swarbrick J Boylan JC eds. *Encyclopedia of Pharmaceutical Technology* New York: Marcel Dekker, 863–870.

Choy, Y. B., Park, J., McCarey, B. E., Edelhauser, H, F., and Prausnitz, M.R., (2008). Mucoadhesive Microdiscs Engineered for Ophthalmic Drug Delivery: Effect of Particle Geometry and Formulation on Preocular Residence Time. *Investigative Ophthalmolology and Visual Science,***11**, 4808-4815.

Ciolino, J. B, Dohlman, C. H, and Kohane, D. S., (2009). Contact lenses for drug delivery. *Seminars in Ophthalmology*, **24**, 156–160.

Ciper, M., and Bodmeier, R., (2006). Modified conventional hard gelatin capsules as fast disintegrating dosage form in the oral cavity. *European Journal of Pharmaceutics and Biopharmaceutics,* **62**, 178-184.

Ciper, M., Bodmeier, R., (2006). Modified conventional hard gelatin capsules as fast disintegrating dosage form in the oral cavity. *European Journal of Pharmaceutics and Biopharmaceutics*, **62**, 178-184.

ClinicalTrials.gov Safety and efficacy of a glaucoma drug delivery system. http://clinicaltrials.gov/ct2/show/study/NCT00824720?term=vistakon&rank=49
[Accessed 7 March 2012].

ClinicalTrials.gov Safety study of latanoprost slow release insert (Latanoprost SR). http://clinicaltrials.gov/ct2/show/NCT01180062
[Accessed 7 March 2012].

Condon, J.B., (2000). Equivalency of Dubinin-Polanyi equations and QM based sorption isotherm equation. B. Simulations of heterogeneous surfaces. *Microporous Mesoporous Materials,* **38**, 359–383.

Conway, B.R, (2008). Recent patents on ocular drug delivery systems. Recent Patents Drug Delivery Formulation, **2**, 1-8.

Corveleyn, S., Remon, J.P., (1996). Maltodextrins as lyoprotectants in the lyophilization of a model protein, LDH. *Pharmaceutical Research*, **13**,146-50.

Costa, P., and Lobo, J.M.S., (2001). Modeling and comparison of dissolution profiles. European Journal Pharmaceutical Sciences, **13**, 123-133.

Craig, W., (1993). Relevance of animal models for clinical treatment. *European Journal of Clinical Microbiology*, **12**, 55–7.

Croonenborghs, B., Smith, M.A., Strain, P., (2007). X-ray versus gamma irradiation effects on polymers. *Radiation Physics and Chemistry*, **76**, 1676–1678.

Cunha-Vaz, J., (2004). The blood–retinal barriers system. Basic concepts and clinical evaluation. *Experimental Eye Research,* 78, 715–721.

Dahan, A,, Miller, J.M., and Amidon, G.L., (2009). Prediction of Solubility and Permeability Class Membership: Provisional BCS Classification of the World's Top Oral Drugs. *AAPS J*, **11**, 740-746.

Davies, N.M., (2000). Biopharmaceutical considerations in topical ocular drug delivery. *Clinical and Experimental Pharmacology and Physiology,* **27**, 558-562.

Davis, J. L., Gilger, B. C., and Robinson, M. R., (2004). Novel approaches to ocular drug delivery. *Current Opinion in Molecular Therapeutics,* **6,** 195-205.

de la Fuente, M., Raviña, M., Paolicelli, P., Sanchez, A., Seijo, B., Alonso, M.J., (2010). Chitosan-based nanostructures: A delivery platform for ocular therapeutics. *Advanced Drug Delivery Reviews,* **62**,100–117.

Dey, S., Gunda, S., and Mitra, A.K., (2004). Pharmacokinetics of Erythromycin in Rabbit Corneas after Single-Dose Infusion: Role of P-Glycoprotein as a Barrier to in Vivo Ocular Drug Absorption. *AAPS PharmSciTech*, **11**, 1627-35.

Diebold, Y., and Calonge, M., (2010). Applications of nanoparticles in ophthalmology. *Progress in Retinal Eye Res*earch, **29**, 596-609.

Diestelhorst, M., Grunthal, S., and Suverkrup, R., (1999). Dry Drops: a new preservative-free drug delivery system. *Greafes Archive Clinical and Experimental Ophthamology,* **237**, 394-398.

Diestelhorst, M., Grunthal, S., and Süverkrüp, R., (1999). Dry Drops: a new preservative-free drug delivery system. *Graefes Archive of Clinical and Experimental Ophthalmology*, **237**,394-398.

Ding, S (1998). Recent developments in ophthalmic drug delivery. *PSTT*, 1, 328-35.

Divya, A., Kavitha, K., Kumar, M.R., Dakshayani, S., Singh, J., (2011). Bilayer tablet technology: An overview. *Journal of Applied Pharmaceutical Science*, **1**, 43-47.

Dor, J.M., Fix, J.A., and Johnson, J.I.. (1999). A New In Vitro Method to Measure the Disintegration Time of a Fast-Disintegration Tablet. *Proc Intl Symp Control Rel Bioact Mater*, **26**, 939–940.

du Toit, L.C., Pillay, V., Danckwerts, M.P., and Penny, C., (2008). Formulation and Statistical Optimization of a Novel Crosslinked Polymeric Anti-Tuberculosis Drug Delivery System. *Journal of Pharmaceutical Sciences*, **97**, 2176–2207.

Dudhani, A.R., and Kosaraju, S.L., (2010) Bioadhesive chitosan nanoparticles: Preparation and characterization. *Carbohydrate Pol*ymers, **81**, 243–251.

Dunn, M.S,, Butler, A.W., and Deakers, T., (1932). The synthesis of glycylglycine. *Journal of Biological Chemistry*. **99**, 217-220.

Edwards, A., and Prausnitz, M.P., (2001). Predicted Permeability of the Cornea to Topical Drugs, *Pharmaceutical Research*, **11**, 1497-1508.

el-Arini, S., and Clas, S., (2002). Evaluation of Disintegration Testing of Different Fast Dissolving Tablets Using the Texture Analyzer. *Pharmaceutical Development and Technology,* **7**, 361–371.

El-Bagory, I.M., Bayomi, M.A., Mahrous, G.M., Alanazi, F.K., and Alsarra, I.A., (2010). Effect of Gamma Irradiation on Pluronic Gels for Ocular Delivery of Ciprofloxacin: in Vitro Evaluation. *Australian Journal of Basic and Applied Sciences*, **4**, 4490-4498.

Eljarrat-Binstock, E., Domb, A.J., (2006). Iontophoresis: a non-invasive ocular drug delivery. *Journal of Controlled Release,* **110**, 479–489.

Elnaggar, Y.S.R., El-Massik, M.A., Abdallah, O.Y., Ebian, A.R., (2010). Maltodextrin: A Novel Excipient Used in Sugar-Based Orally Disintegrating Tablets and Phase Transition Process. *AAPS Pharm Sci Tech*, **11**, 645-651.

European Guideline 3AQ4a, (1992). The use of ionizing radiation in the manufacture of medicinal products. Official Publications in the European Communities, London

European Union (2009). EU Guidance to Regulation (EC) No 1272/2008 on classification, labelling and packaging (CLP) of substances and mixtures. ECHA Reference: ECHA-09-G-02-EN, p. 245ff.

Everett, D.H., (1972). IUPAC Manual of Symbols and Terminology, Appendix 2, part 1. *Pure Applied Chemistry*, **31**, 578-638.

Follonier, N., (1992). Biopharmaceutical comparison of oral multiple-unit and single-unit sustained-release dosage forms. *Pharmaceutical Sciences*, **2**, 141–158.

Fong, L.P., Hunt, C.J., Taylor, M.J., Pegg, D.E., (1986). Cryopreservation of rabbit corneas: assessment by microscopy and transplantation. *British Journal of Ophthalmology*, **70**, 751-60.

Fu, Y., Yang, S., Jeong, S.H., Kimura, S., Park, K., (2004). Orally Fast Disintegrating Tablets: Developments, Technologies, Taste-Masking and Clinical Studies. *Therapeutic Drug Carrier Systems*, **21**, 433–475.

Furrer, P., and Mayer, J.M., (2002). Ocular Tolerance of Absorption Enhancers in Ophthalmic Preparations. *AAPS PharmSciTech,* 4, 6-10.

Gad, S.C., (2008). *Schematic of Amylopectin structure Pharmaceutical manufacturing handbook: production and processes*. New Jersey: John Wiley and sons Inc. Hoboken.

Gasthuys, F., Pockelé, K., Vervaet, C., Weyenberg, W., De Prijck, K., Pille, F., Vlaminck, L., Nelis, H., and Remon, J.P., (2007). Evaluation of the in vivo behaviour of gentamicin sulphate ocular mini-tablets in ponies. *Journal of Veterinary Pharmacology and Therapeutics*, **30**, 470-476.

Gaudana, R., Jwala, J., Boddu, S.H.S., and Mitra A.K., (2009). Recent Perspectives in Ocular. *Pharmaceutical Research*, **26,** 1197-216.

Gaudana, R., Jwala, J., Boddu, S.H.S., and Mitra, A.K., (2009). Recent perspectives in ocular drug delivery. *Pharmaceutical Research,* **26**,1197-16.

Gayton, J.L., (2009). Etiology, prevalence, and treatment of dry eye disease. *Clinical Ophthalmology,* **3**, 405–412.

Geroski, D.H., and Edelhauser, H.F., (2000). Drug delivery for posterior segment eye disease. *Investigative Ophthalmolology Visual Science,* **41**, 961–964.

Gervais, F., Liberge, P., Palate, B., Legrand, J. CiToxLAB France, Evreux. The most common ocular histology lesions observed in rabbits and minipigs after intravitreal injection during toxicology studies. www.google.co.za/#hl=en&q=The+most+common+ocular+histology +lesions+observed+in+rabbits+and+minipigs+after+intravitreal+injection+during+&oq=The+most+

common+ocular+histology+lesions+observed+in+rabbits+and+minipigs+after+intravitreal+injection+during+&gs_l=serp.12...2961.5055.0.6546.1.1.0.0.0.0.0.0..0.0.les%3B..0.0...1c.1.6.serp.UtJjcPNvF8Y&bav=on.2,or.&fp=33e6a56f3d937244&biw=1093&bih=494
[Accessed 1 March 2013].

Giannola, L., De Caro, V., Giandalia, V., Siragusa, M.G., and Cordone, L., (2007). Ocular Gelling Microspheres: In Vitro Precorneal Retention Time and Drug Permeation Through Reconstituted Corneal Epithelium. *Journal of Ocular Pharmacology and Therapeutics*, **24**,186-196.

Gilhotr, R.M., Gilhotra, N., and Mishra, D.N., (2010). A hydrogel–forming bioadhesive ocular minitablet for the management of microbial Keratitis. *Asian Journal of Pharmaceutical Sciences*, **5**,19-25.

Gilhotra, R., and Mishra, D.N. Polymeric Systems for Ocular Inserts. at: www.Pharmainfo.net. [Accessed December 11, 2011]

Gilhotra, R., Mishra, D.N. Polymeric Systems for Ocular Inserts. : www.Pharmainfo.net.

Gohel, M., Patel, M., Amin, A., Agrawal, R., Dave, R., Bariya, N., (2004). Formulation Design and Optimization of Mouth Dissolve Tablets of Nimesulide Using Vacuum Drying Technique. *AAPS PharmSciTech,* 5, 10-15.

Gonjari, I.D., Hosmani, A.H., Karmarkar, A.B., Godage, A.S., Kadam, S.B., and Dhabale, P.N., (2009). Formulation and evaluation of *in situ* gelling thermoreversible mucoadhesive gel of fluconazole. *Drug Discovery and Therapeutics,* **3***,* 6-9.

Gorle, A.P., and Gattani, S.G., (2009). Design and evaluation of polymeric ocular drug delivery system. *Chemical and Pharmaceutical Bulletin*, **57**, 914-9.

Govender, S., Pillay, V., Chetty, D.J., Essack, S.Y., Dangor, C.M., Govender, T., (2005). Optimisation and characterization of bioadhesive controlled release tetracycline microspheres. *International Journal of Pharmaceutics*, **306**, 24–40.

Gratieri, T., Gelfuso, G. M., Rocha, E. M., Sarmento, V. H., de Freitas, O., and Lopez, R. F. V., (2010). A poloxamer/chitosan in situ forming gel with prolonged retention time for ocular delivery. *European Journal of Pharmaceutics and Biopharmaceutics*, **75**, 186–193.

Grieshaber, M.C., and Flammer, J., (2010). Is the medication used to achieve the target intraocular pressure in glaucoma therapy of relevance? – An exemplary analysis on the basis of two beta-blockers. *Progress in Retinal and Eye Research,* **29**, 79–93.

Guirguis, O.W., Moselhey, M.T.H., (2012). Thermal and structural studies of poly(vinyl alcohol) and hydroxypropyl cellulose blends. *Natural Science*, **4**, 57-67.

Guo, Y., Byrn, S.R., and Zografi, G., (2000). Effects of lyophilization on the physical characteristics and chemical stability of amorphous quinapril hydrochloride. *Pharmaceutical Research*, **17**, 930-5.

Gupta, H., Aqil, M., Khar, R.K., Ali, A., Bhatnagar, A., Mittal, G., and Jain, S., (2009). Development and Characterization of 99mTc-timolol Maleate for Evaluating Efficacy of In Situ Ocular Drug Delivery System. *AAPS Pharm Sci Tech*, **10**, 540-546.

Gurtler. F., Kaltsatos, V., Boisrame, B., Gurny, R., (1995). Long-acting Bioadhesive Opthalmic Drug Insert (BODI) containing gentamicin for veterinary use: optimization and clinical investigation. *Journal of Controlled Release,* **33**, 231-236.

Hakin, A.W., Daisley, D.C., Delgado, L., Liu, J.L., Marriott, R.A., Marty, J.L., and Tompkins, G., (1999). Volumetric properties of glycine in water at elevated temperatures and pressures measured with a new optically driven vibrating-tube densimeter. *Journal of Chemical Thermodynamics,* **30**, 583–606.

Halsey, G.D., (1948). Physical adsorption on non-uniform surfaces. *Journal of Chemical Physics*, **16**, 931-937.

Hartman, D., (2011). Perfecting Your Spread Plate Technique. *Journal of Microbiology & Biology Education*, **12**, 204-205**.**

Hornof, M., Toropainen, E., and Urtti, A., (2005). Cell culture models of the ocular barriers, *European Journal of Pharmaceutics and Biopharmaceutics,* **60**, 207–225.

Hosoya, K., Lee, V.H., Kim, K.J., (2005). Roles of the conjunctiva in ocular drug delivery: a review of conjunctival transport mechanisms and their regulation. *European Journal of Pharmaceutics and Biopharmaceutics*, **60**, 227–240.

How do superabsorbent polymers work? www. m2polymer.com/ html/superabsorbent _polymers.html
[Accessed 1 July 2012]

Hunek, B., Cheng, A., Capettini, J., (2007). Increasing Lyophilization Productivity,Flexibility,and Reliability Using Liquid Nitrogen Refrigeration. *BioPharm International* Part 1, 54-61.

ICH (2003). Stability testing for new drug substances and products. Geneva www.biopharminternational.com /biopharm/article/articleDetail.jsp?id=76722
[Accessed 1 March 2013]

Ishikawa, T., Mukai, B., Shiraishi, S., Utoguchi, N., Fujii, M., Matsumoto, M., and Watanabe, N., (2001). Preparation of rapidly disintegrating tablet using new types of microcrystalline cellulose (PH-M Series) and low substitutedhydroxypropylcellulose or spherical sugar granules by direct compression method. *Chemical & Pharmaceutical Bulletin*, **2**, 134-139.

Janoria, K.G., Gunda, S., Boddu, S.H., and Mitra, A.K., (2007). Novel approaches to retinal drug delivery. *Expert Opinion Drug Deliv*ery, **4**, 371–388.

Järvinen, T., and Järvinen, K., (1996). Prodrugs for improved ocular drug delivery. *Advanced Drug Delivery Reveiws*, 19, 203-224.

Joshi, G.V., Kevadiya, B.D., Patel, H.A., Bajaj, H.C., Jasra, R.V., (2009). Montmorillonite as a drug delivery system: Intercalation and in vitro release of timolol maleate. *International Journal Pharmaceutics*, **374**, 53–57.

Kasim, N.A., Whitehouse, M., Ramachandran, C., Bermejo, M., Lennernas, H., Hussain, A.S., Junginger, H.E., Stavchansky SA, Midha KK, Shah VP, Amidon GL. Molecular properties of WHO essential drugs and provisional biopharmaceutical classification. *Molecular Pharmaceutics*, **1**, 85-96.

Kahn, M., (2005). Bioavailability of vitamin B using a small-volume nebulizer ophthalmic drug delivery system. *Clinical and Experimental Ophthalmology,* 33, 402–407.

Kasper, J.C., and Friess, W., (2011). The freezing step in lyophilization: Physico-chemical fundamentals, freezing methods and consequences on process performance and quality attributes of biopharmaceuticals. *European Journal of Pharmaceutics and Biopharmaceutics*, **78**, 248–263.

Kikuchi, T., Suzuki, M., Kusai, A., Iseki, K., Sasaki, I., and Nakashima, K., (2005). Mechanism of permeability-enhancing effect of EDTA and boric acid on the corneal penetration of 4-[1-hydroxy-1-methylethyl]-2- propyl-1-[4-[2-[tetrazole-5-yl]phenyl]phenyl] methylimidazole-5-carboxylic acid monohydrate (CS-088). *International Journal of Pharmaceutics*, **299**, 107–114.

Kim, H., Csaky, K.G., Gilger, B.C., Dunn, J.P., Lee, S.S., Tremblay, M., de Monasterio, F., Tansey, G., Yuan, P., Bungay, P.M., Lutz, R.J., Robinson, M.R., (2005). Preclinical evaluation of a novel episcleral cyclosporine implant for ocular graft-versus-host disease. *Investigative Ophthalmology and Visual. Science,* **46**, 655-662.

Kimura, H., Ogura, Y., (2001). Biodegradable polymers for ocular drug delivery. *Ophthalmologica.* , **215**, 143-55.

Kolmakov, K., Belov, V.N., Bierwagen, J., Ringemann, C., M_ller, V., Eggeling, C., and Hell, S.W., (2010). Red-Emitting Rhodamine Dyes for Fluorescence Microscopy and Nanoscopy. *Chemistry*,**16**,158 – 166.

Kompella, U.B., Kadam R.S., and Lee, V.H.L., (2010). Recent advances in ophthalmic drug delivery. *Therapeutic Deliv*ery, **1**, 435-456.

Kubota, N., Tatsumoto, N., Sano, T., and Toya, K., (2000). A simple preparation of half N-acetylated chitosan highly soluble in water and aqueous organic solvents. *Carbohydrate Research*, **324**, 268–274.

Kulkarni, A., and Bhatia, M., (2009). Development and evaluation of bilayer floating tablets
Kulkarni, U., and Raghavendra, N.G., (2011). Design and Development of Aceclofenac Novel Multi-layer Fast Dissolving Tablets: A Modified – release Drug Delivery Technology. *Journal of Pharmacy Research*, **4**, 2230-2232.

Kumar, K.P.S., Bhowmik, D., Paswan, S., and Srivastava, S., (2012). Recent Challenges and Advances in Ophthalmic Drug Delivery System. *The pharma Innovation*, **1**, 1-15.

Kumar, S., Haglund, B. O., and Himmelstein, K.J., (1994). In situ-forming gels for

Kumar, S., Himmelstein, K.J., (1995). Modification of in situ gelling behavior of carbopol solutions by hydroxypropyl methylcellulose. *Journal of Pharmaceutical Sciences,* **84**, 344-8.

Kumaran, K.S.G.A., Karthika, K., and Padmapreetha, J., (2010). Comparative review on conventional and advanced drug delivery formulations. *International Journal of Pharmacy and Pharmaceutical Sciences*, **2**, 1-5.

Kuno, N., and Fujii, S., (2011). Recent Advances in Ocular Drug Delivery Systems. *Polymers*, **3**, 193-221.

Lang, J.C., (1995). Ocular drug deliveRy conventional ocular formulations. *Advanced Drug Delivery,* **16**, 39-43.

Late, S.G., and Banga, A.K., (2004). Response surface methodology to optimize novel fast disintegrating tablets using β cyclodextrin as diluent. *Journal of Pharmacology and Experimental Therapeutics*, **311**, 246–255.

Lawrenson, J. G., Edgar, D. F., Gudgeon, A. C., Burns, J. M., Geraint, M., Nas, B. A., (1993). Comparison of the efficacy and duration of action of topically applied proxymetacaine using a

novel ophthalmic delivery system versus eye drops in healthy young volunteers. *British Journal of Ophthamology,* **77**, 771-775.

Lee, V.H.L., Luo, A. M., Li, S., Podder, S. K., Chang, J. S. C., (1991). S. Ocular Pharmacokinetic Modeling of intraocular pressure lowering in timolol combinations. *Investigative Ophthalmology and Visual Science,* **32**, 2948–2957.

Lee, D., Xia, W., and Zhang, J., (2008). Enzymatic preparation of chitooligosaccharides by commercial lipase. *Food Chemistry*, **111**, 291–295.

Leeson, L.J., (1995). In vitro/ In vivo correlations. *Drug Information Journal,* **29**, 903-915.

Lehr, C.M., Bouwstra, J. A., Schacht, E. H., and Junginger, H. E., (1992). In vitro evaluation of mucoadhesive properties of chitosan and some other natural polymers. *International Journal of Pharmaceutics,* **78**, 43–48.

Lennartz, P., and Mielck, J.B., (1998). Minitabletting: improving the compactability of paracetamol powder mixtures. *International Journal of Pharmaceutics*, **173**, 75–85.

Lewis, G.A., Mathieu, R., Phan-Tan-Luu., (1999). Pharmaceutical Experimental Design, Marcel Dekker, New York.

Lin, C.P., and Boehnke, M., (1999). Influences of methylcellulose on corneal epithelial wound healing, *Journal of Ocular Pharmacology and Therapeutics,* **15**, 59–63.

Lippins, B.C., Linsen, B.G., and de Boer, J.H., (1964). Pore systems in catalysts. I. Adsorption of nitrogen apparatus and calculation. *Journal of Catalysis*, **3**, 32-37.

Loftsson, T., Jarho, P., Másson, M., and Järvinen, T., (2005). Cyclodextrins in drug delivery. *Expert Opinion on Drug Delivery,* **2**, 335-51.

Loftssona, T., Jarvinen, T., (1999). Cyclodextrins in ophthalmic drug delivery. *Advanced Drug Delivery Reviews*, **36**, 59-79.

Lopes, C. M., Lobo, J. M. S., Pinto, J. F., and Costa, P., (2006). Compressed mini-tablets as a biphasic delivery system. *International Journal of Pharmaceutics*, **323**, 93-100.

Ludwig, A., (2005). The use of mucoadhesive polymers in ocular drug delivery. *Advanced Drug Delivery Reviews*, **57**, 1595–1639.

Lui, M., and Guo, T., (2001). Preparation and Swelling Properties of Crosslinked Sodium Polyacrylate. *Journal of Applied Polymer Science*, **82**,1515–1520.

Luo, Q.,, Zhao, J., Zhang X., Pana, W., (2009). Nanostructured lipid carrier (NLC) coated with Chitosan Oligosaccharides and its potential use in ocular drug delivery system. *Journal of Materials Science: Materials in Medicine*, **20,** 1057–1079.

Lux, A., Maier, S., Dinslage, S., Süverkrüp, R., and Diestelhorst, M., (2003). A comparative bioavailability study of three conventional eye drops versus a single lyophilisate. *British Journal of Ophthalmology*, **87**, 436-440.

Lux, A., Maier, S., Dinslage, S., Süverkrüp, R., and Diestelhorst, M., (2003). A comparative bioavailability study of three conventional eye drops versus a single lyophilisate. *British Journal of Ophthalmology,* **87**, 436-440.

Macdonald, E.A., and Maurice, D.M., (1991). Loss of fluorescein across the conjunctiva. *Experimental Eye Research*, **53**, 427–430.

Maghraby, G.M., and Alomrani A.H., (2009). Synergistic Enhancement of Itraconazole Dissolution by Ternary System Formation with Pluronic F68 and Hydroxypropylmethylcellulose. *Scientia Pharmaceutica*, **77**, 401–417.

Manish, K., Kulkarni, G.T., (2012). Recent advances in ophthalmic drug delivery. *International Journal of Pharmacy and Pharmaceutical Sciences,* **4**, 387-394.

Mannermaa, E., Vellonen, K., and Urtti, A., (2006). Drug transport in corneal epithelium and blood–retina barrier: Emerging role of transporters in ocular pharmacokinetics. *Advanced Drug Delivery Reviews*, **58**, 1136–1163.

Mantelli, F., and Argüeso, P., (2008). Functions of ocular surface mucins in health and disease. *Current Opinion in Allergy and Clinical Immunology*, **8**, 477–483.

Martin, J., (2012). Understanding Gamma Sterilization. *Biopharm*, **2**, 18-22.

Mayers, M., Rush, D., Madu, A., Motyl, M., Miller, M., (1991). Pharmacokinetics of Amikacin and Chloramphenicol in the Aqueous Humor of Rabbits.Antimicrobial agents and Chemotherapy, **35**, 1791-1798.

Mediero, A., Alarma-Estrany, P., and Pintor, J., (2009). New treatments for ocular hypertension. *Autonomic Neuroscience: Basic and Clinical,* **147**, 14–19.

Mishima, S., (1981). Clinical pharmacokinetics of the eye. *Investigative ophthalmology and Visual Sciences*, **21**, 504-541.

Mizumoto, T., Masuda, Y., Yamamoto, T., Yonemochi, E., Terada, K., (2005). Formulation design of a novel fast disintegrating tablet. *International of Journal of Pharmaceutics*, **306**, 83–90.

Mortazavi, S. A., Jaffariaza, Z., and Damercheli, E., (2010). Formulation and *In-Vitro* Evaluation of Ocular Ciprofloxacin-Containing Minitablets Prepared with Different Combinations of Carbopol 974P and Various Cellulose Derivatives. *Iranian Journal of Pharmaceutical Research* , **9**, 107-114.

Motwani S.K., Chopra, S., Talegaonkar, S., Kanchan Kohli, K., Ahmad, F.J., Roop K. Khar R.K., (2008). Chitosan–sodium alginate nanoparticles as submicroscopic reservoirs for ocular delivery: Formulation, optimization and in vitro characterization. *European Journal of Pharmaceutics and Biopharmaceutics*, **68**, 513–525.

Mourya, V.K., and Inamdar, N.N., (2010). Trimethyl chitosan and its applications in drug delivery. *Advanced Drug Delivery Reviews*, **62**, 100–117.

Munday, D.L., (1994). A comparison of the dissolution characteristics of theo-phylline from film-coated granules and mini-tablets. *Drug Development and Industrial Pharmacy*, **20**, 2369–2379.

Nanjawade, B. K., Manvi, F.V., and Manjappa, A. S., (2007). In situ-forming hydrogels for sustained ophthalmic drug delivery. *Journal of Controlled Release,* **122**,119–134.
nanoparticles as new ocular drug delivery systems: in vitro stability, in vivo fate, and cellular toxicity. *Pharmaceutical Research*, **21**, 803–810.

Noecker, R., (2001). Effects of common ophthalmic preservatives on ocular health. *Advances in Therapy*, **18**, 205–215.

Nov´akov´a, L., Matysov´a, L., and Solich, P., (2006). Advantages of application of UPLC in pharmaceutical analysis. *Talanta*, **68,** 908–918.

O'Brien, T. P., Sawusch, M. R., Dick, J. D., Hamburg, T. R., Gottsch, J. D., (1988). Use of collagen corneal shields versus soft contact lenses to enhan ce penetration of topical tobramycin . *Journal of Cataract and Refractive Surgery*, **14**, 505-507.

Ohdo, S., and Grass G.M., (1991). Pharmacokinetic Basis for Nonadditivity of Intraocular Pressure Lowering in Timolol Combinations. *Investigative Ophthalmology & Visual Science*, **32**,

Olayemi, O. J., Oyi, A. R., and Allagh T . S., (2008). Comparative evaluation of maize, rice and wheat starch powders as pharmaceutical excipients. *Nigerian Journal of Pharmaceutical Sciences*, **1**, 131-138.

Palangio, M., Northfelt, D., Portenoy, R.K., Brookoff, D., Doyle, R.T., Dornseif, B.E., and Damask, M.C., (2002). Dose Conversion and Titration with a Novel, Once-Daily, OROS® Osmotic Technology, Extended-Release Hydromorphone Formulation in the Treatment of Chronic Malignant or Nonmalignant Pain. *Journal of Pain and Symptom Management,* **23**, 355-368.

Park, B.K., and Kim, M., (2010). Review Applications of Chitin and Its Derivatives in Biological Medicine. *International Journal of Molecular Science,* **11**, 5152–5164.

Pascolini, D., Mariotti, S.P.M., (2011). Global estimates of visual impairment: 2010. *British Journal Ophthalmology*. doi:10.1136/bjophthalmol-2011-300539.

Patel, R., (2005). Mechanistic Profiling of Novel Wafer Technology Developed for Rate-Modulated Oramucosal Drug Delivery. A dissertation submitted to the Faculty of Health Sciences. University of the Witwatersrand.

Patel, R., Pillay, V., Choonara, Y.E., (2007). A Novel Cellulose-Based Hydrophilic Wafer Matrix for Rapid Bioactive Delivery. *Journal of Bioactive and Compatible Polymers*, **22**, 119-142.

Patel, S., Alio, J. L., Perez-Santonja, J. J., (2004). Refractive index change in bovine and human corneal stroma before and after LASIK: a study of untreated and re-treated corneas implicating stromal hydration. *Investigative Ophthalmology & Visual Science,* **45**, 3523-3530.

Pato, E., Muñoz-Fernández, S., M. D, Francisco, F., Abad, M. A., Maese, J., Ortiz, A., and Carmona, L., (2011). Systematic Review on the Effectiveness of Immunosuppressants and Biological Therapies in the Treatment of Autoimmune Posterior Uveitis. *Seminars in Arthritis Rheumatism,* **40**, 314-323.

Perrie, Y., Badhan, R.K.S., Kirby, D.J., Lowry, D., Mohammed, A.R., Ouyang, D., (2012). The impact of ageing on the barriers to drug delivery, *Journal of Controlled Release*, **161**, 389–398.

Petrich, M.A., and Rosen, L.A., (1995). Irradiation-Induced Changes in Hydroxypropyl Cellulose MRS Spring Meeting. MRS Proceedings, 394 - 161, doi:10.1557/PROC.

Phillips, C.I., Bartholomew, R.S., Levy, A.M., Grove, J., and Vogel, R., (1985). Penetration of timolol eye drops into human aqueous humour: the first hour. *British Journal of Ophthalmology*. **69**, 217-218.

Pikal, M.J., (1990). Freeze-drying of proteins. Part I: process design. *BioPharm*, **3**,14-26.

Pikal, M.J., Dellerman K. and Roy M.L., (1992). Formulation and stability of freeze-dried proteins: effects of moisture and oxygen on the stability of freeze-dried formulations of human growth hormone. *Developments in Biological Standadization,* **74**, 21-37.

Pillay, V., and Fassihi, R., (1999). In vitro release modulation from crosslinked pellets for site-specific drug delivery to the gastrointestinal tract: I. Comparison of pH-responsive drug release and associated kinetics. *Journal of Controlled Release*, **59**, 229–242.

Plackett, R.L., and Burman, J.P., (1946). The design of multifactorial experiments. *Biometrika*, **33**, 305-25.

Presl, A., and Myatt, J., (2010). Ocular anatomy and physiology relevant to anaesthesia. *Anaesthesia and Intensive Care Journal*, **11**, 391-450.

Pujara, N.D., Gokani, R.K., Paun, J.S., (2012). Bilayer tablet-an emerging trend. *International journal of pharmaceutical development*, **4**, 102-111.

Qiu, Y., Chen, Y., Liu, L., and Zhang, G.G.Z., (2009). Developing Solid Oral Dosage Forms: Pharmaceutical Theory and Practice. Academic press 2009

Quigley, H. A., Pollack, I. P., Harbin, T. S., (1975). Pilocarpine Ocuserts. Long term clinical trials and selected pharmacodynamics. *Archives of Ophthamology*, **93**, 771-775.

Quigley, H.A., (1996). Number of people with glaucoma worldwide. *British Journal of Ophthalmology*, **80**, 389-393.

Rabea, E.L., Badawy, M.E.T., Stevens, C.V., Smagghe, G., Steurbaut, W., (2003). Chitosan as antimicrobial agent: applications and mode of action. *Biomacromolecules*, 4, 1457–1465.

Rajas, N.J., Kavitha, K., Gounder, T., Mani, T., (2011). In situ ophthalmic gels: a developing trend. *International Journal of Pharmaceutical Sciences Review and Research*, **7**, 8-14.

Rajendran, N.N., Natrajan R, Kumar, R.S., and Selvaraj, S., (2010). Acyclovir-loaded chitosan nanoparticles for ocular delivery, *Asian Journal of Pharmaceutics*, **4**, 220-226.

Rathore, K.S., Nema, R.K., (2009). An insight into Ophthalmic drug delivery. *International Journal of Pharmaceutical Sciences and Drug Research,* **1**, 1-5.

Reddy, I.K., Bodor, N.S., (1994). Novel approaches to design and deliver safe and effective antiglaucoma agents to the eye. *Advanced Drug Delivery Reviews*, **14**, 251-267.

Refai, H., and Tag, R., (2011). Development and characterization of sponge-like acyclovir ocular minitablets. *Drug Delivery,* **18**, 38-45.

Remon, J.P, Corveleyn, S., (2000). Freeze – Dried Disintegrating Tablets. US Patent 6,010,719.

Ricci, E.J., Lunardi, L.O., Nanclares, D.M.A., and Marchetti, J.M., (2005). Sustained release of lidocaine from Poloxamer 407 gels. *International Journal of Pharmaceutics,* **288**, 235-244.

Rinaki E., Valsami G., Macheras, P., (2003). The power law can describe the 'entire'
Robinson, J.C., (1993) Ocular anatomy and physiology relevant to ocular drug delivery. In: Mitra AK, eds. *Ophthalmic drug delivery systems.* New York: Marcel Dekker, 29-58.

Saettone, F.M., Chetoni, P., Cerbai, R., Mazzanti, G., Braghiroli, L., (1996). Evaluation of ocular permeation enhancers: in vitro effects on corneal transport of four fl-blockers, and in vitro/in vivo toxic activity. *International Journal of Pharmaceutics*, **142**, 103-113.

Saettone, M.F, Chetoni, P ., Bianch, L.M., Giannaccin, B., Conte, U. and Sangalli, M.E. (1995). Controlled release of timolol maleate from coated ophthalmic mini-tablets prepared by compression. *International Journal of Pharmaceutics,* **126**, 79-82.

Saettone, M.F., Chetoni, P., Bianch, L.M., Giannaccin, B., Conte, U., and Sangalli, M.E., (1995). Controlled release of timolol maleate from coated ophthalmic mini-tablets prepared by compression. *International Journal of Pharmaceutics*, **126,** 79-82.

Saettone, M.F., Salimen, L., (1995). Ocular inserts for topical delivery. *Advanced Drug Delivery Reviews*, **16**, 95–106.

Sastry, S,V., Nyshadham, J.R., and Fix JA., (2000). Recent technological advances in oral drug delivery. A review. *Pharmaceutical Science and Technology Today*, **3**, 138–145.

Sastry, S.V., Nyshadham, J.R., and Fix, J.A., (2000). Recent technological advances in oral drug delivery. A review. *Pharmaceutical Science and Technology Today*, **3**, 138–145.

Scheel, J., Kleber, M., Kreutz, J., Lehringer, E., Mehling, A., Reisinger, K., and Steiling, W., (2011). Eye irritation potential: Usefulness of the HET-CAM under the Globally Harmonized System of Classification and Labeling of Chemicals (GHS). Regulatory Toxicology and Pharmacology, **59**, 471-92. doi: 10.1016/j.yrtph.2011.02.003. Epub 2011 Feb 16.

Schrage, A., Gamer, A.O., van Ravenzwaay, B., and Landsiedel, R., (2010). Experience with the HET-CAM method in the routine testing of a broad variety of chemicals and formulations. *Alternatives to Laboratory Animals*, **38**, 39–52.

Schwartz, G. F., and Quigley, H. A., (2008). Adherence and Persistence with Glaucoma Therapy. *Survey of Opthamology,* **53**, 57-68.

Seager, H., (1998). Drug delivery products and the Zydis fast-dissolving dosage form. *Journal of Pharmacy and Pharmacology,* **50**, 375-382.

Shailesh, S., Shankar, H.S., and Gupta, G.D., (2009). Novel in-vitro disintegration evaluation for fast dissolving tablets. *Journal of Global Pharma Technology*, **1,** 113-120.

Shakhashiri, B.Z., (1989). In Chemical Demonstrations: A Handbook for Teachers of

Short, B.S., (2008). Safety Evaluation of Ocular Drug Delivery Formulations: Techniques and Practical Considerations. *Toxicological Pathology*, **36**, 49-62.

Sihvola. P., and PuustjÄRvi, T., (1980). Practical problems in the use of Ocusert®-pilocarpine delivery system. *Acta Ophthalmologica,* **58**, 933-7.

Simamora, P., Nadkarni, S. R., Lee, Y. C., Yalkowsky, S. H., (1998). Controlled delivery of pilocarpine.2. In vivo evaluation of Gelfoam device. *International Journal of Pharmaceutics,* **170**, 209-214.

Siminiceanu, I., Lazau, I., Ecsedi, Z., Lupa, L., Burciag, C., (2008). Textural Characterization of a New Iron-Based Ammonia Synthesis Catalyst. *Chemical Bulletin*, **53**, 1-2.

Simon, S.L., Bernazzani, P., and McKenna, G.B., (2003). Effects of freeze-drying on the glass temperature of cyclic polystyrenes. *Polymer*, **44**, 8025-8032.

Sinco, P., (1999). Inside a gamma sterilizer Isotopes & Radiation nuclear news, 92-96.

Sobral, P.J.A., Telis, V.R.N., Habitante, A.M.Q.B., and Sereno, A., (2001). Phase Diagram for freeze-dried persimmon. *Thermochimica Acta*, **376**, 83-89.

South African Glaucoma society (2006). Glaucoma Algorithm and guidelines for glaucoma.

Spielmann, H., (1991). Interlaboratory assessment of alternatives to the Draize eye irritation test in Germany. *Toxic in Vitro*, **5**, 539-542.

Statement for the Use of Animals in Ophthalmic and Visual Research. www.arvo.org/policies/ statement_for_the_use_of_animals_in_ophthalmic_and_visual_research/
[Accessed 10 January 2013]

Stoltenberg, I., and Breitkreutz, J., (2011). Orally disintegrating mini-tablets (ODMTs) – A novel solid oral dosage form for paediatric use. *European Journal of Pharmaceutics and Biopharmaceutics,* **78**, 462–469.

Super Absorbent Polymers Teacher's Guide. www.watercampws.uiuc.edu/waterclear/.../polymers_teacher_guide.p.
[Accessed 1 July 2012]

Suverkrup, R.J., Krasichkova, O.A., Diestelhorst, M., and Maier, S., (2004). Production of Ophthalmic Lyophilisate Carriers by Fast Precision Freeze Drying (FPFD). *Investigative Ophthalmology and Visual Sciences*, **45**, E-Abstract 5047.

Symonds, J., Vidosic, J.P., Hawkins, H.V., (1982). Strength of materials. *Qualitywww2.hcmuaf.edu.vn/data/.../Strength%20of%20Material.pdf.*
[Accessed 15 June 2012].

Sznitowska, M., Placzek, M., and Klunder, M., (2005). The physical characteristics of lyophilized tablets containing a model drug in different chemical forms and concentration. *Acta Poloniae Pharmaceutica ñ Drug Research,* **62**, 25-29.

Tai, M.C., Cosar, C.B,, Cohen, E.J,, Rapuano, C.J., and Laibson, P.R., (2002). The clinical efficacy of silicone punctal plug therapy. *Cornea*, **2**, 135-9.

Takayama, K., (2008). Computer-aided design and optimization for pharmaceutical formulations. Dosis, **24**, 114-118.

Tarabishy, A.B., and Jeng, B.H., (2008). Bacterial conjunctivitis: A review for internists. *Cleveland Clinical Journal of Medicine,* **75**, 137-144.

Tavˇcar, E., Turk, E., Kreft, S., (2012). Simple Modification of Karl-Fischer Titration Method for Determination of Water Content in Colored Samples. *Journal of Analytical Methods in Chemistry*, **2012**, 1- 6.

Thakur, R.R., and Kashiv, M., (2011). Modern Delivery Systems for Ocular Drug Formulations: A Comparative Overview W.R.T Conventional Dosage Form. *International Journal of Research in Pharmaceutical and Biomedical Sciences,* **1**, 8-18.

Thijs, H.M.L., Becer, C.M., Guerrero-Sanchez, C., Fournier, D., Hoogenboom, R., and Schubert, U.S., (2007). Water uptake of hydrophilic polymers determined by a thermal gravimetric analyzer with a controlled humidity chamber. *Journal of Materials Chemistry*, **17**, 4864-4871.

Thrimawithana, T.R., Young, S., Bunt, C.R., Green, C., and Alany, R.G., (2010). Drug delivery to the posterior segment of the eye. *Drug Discovery Today,* **16**, 270-277.

Tian, B., Luo, Q., Song, S., Lui, D., Pan, H., Zhang, W., He, L., and Ma, S., (2011). Pharmaceutics, Preformulation and Drug Delivery Novel Surface-Modified Nanostructured Lipid Carriers with Partially Deacetylated Water-Soluble Chitosan for Efficient Ocular Delivery. *International Journal of Pharmaceutics*, **403,**185-191.

Tissen, C., Woertz, K., Breitkreutz, J., and Kleinebudde, P., (2011). Development of mini-tablets with 1 mm and 2 mm diameter. *International Journal of Pharmaceutics*, **15**, 164-170.

Toda, I., Shinozaki, N., and Tsubota, K., (1996). Hydroxypropyl methylcellulose for the treatment of severe dry eye associated with Sjo¨ gren's syndrome. *Cornea*, **15**,120– 128.

Torchilin, V.P., (2005). Recent advances with liposomes as pharmaceutical carriers. *Nature Reviews and Drug Discovery,* **4**, 145–160.

Tsinontides, S.C., Rajniak, P., Pham, D., Hunke, W.A., Placek, J., and Reynolds, S.D., (2004). Freeze drying—principles and practice for successful scale-up to manufacturing. International Journal of Pharmaceutics, **280**,1–16.

Tsonis, P.A., (2008). Animal models in eye research, Pub Academic Press, San Diego, USA, 187-188.

UN, (2009). Globally Harmonized System of Classification and Labelling of Chemicals

Unterman, S.R., Rootman, D. S., Hill, J. S., Parelman, J. J., Thomsan, H. W., Kaufman, H. E., (1988). Collagen shield drug delivery: therapeutic concentrations of tobramycin in the rabbit eye and aqeous humour. *Journal of Cataract and Refractive Surgery,* **15**, 500-504.

Upasani, R.S., and Banga, A.K., (2004). Response surface methodology to investigate the iontophoretic delivery of tacrine hydrochloride. *Pharmaceutical Research*, **21**, 2293-9.

Urtti, A., (2006). Challenges and obstacles of ocular pharmacokinetics and drug delivery. *Advanced Drug Delivery,* **58**, 1131–1135.

Urtti, A., and Salminen, L., (1993). Minimizing systemic absorption of topically administered ophthalmologic drugs. *Survey of Ophthalmology*, **37**, 435–456.

Urtti, A., Pipkin, J. D., Rork, G. S., Sendo, T., Finne, U., and Repta, A.J., (1990). Controlled drug delivery devices for experimental ocular studies with timolol. Ocular and systemic absorption in rabbits. *International Journal of Pharmaceutics,* **61**, 241–249.

Vargas, A., Zeisser-Labouèbe, M., Lange, N., Gurny, R., and Delie, F., (2007). The chick embryo and its chorioallantoic membrane (CAM) for the in vivo evaluation of drug delivery systems. *Advanced Drug Delivery Reviews*, **59**, 1162–1176.

Velpandian, T., Bankoti, R., Humayun, S., Ravi, A.K., Kumari, S.S., and Biswas, N.R., (2006). Comparative evaluation of possible ocular photochemical toxicity of fluoroquinolones meant for ocular use in experimental models, *Indian Journal of Experimental Biology*, **5**, 387.

Virely, P., and Yarwood, R., (1990). Zydis – a novel, fast dissolving dosage form. *Manufacturing Chemist*, **61**, 36–37.

Wagh, V.D., Inamdar, B., Samanta, M.K., (2008). Polymers used in ocular dosage form and drug delivery systems. *Asian Journal of Pharmaceutics*, **2**, 12-7.

Wang, Y., Boolchand, P., and Micoulaut, M., (2000). Glass structure rigidity transitions and the intermediate phase in the Ge-As-Se ternary. *Europhysics Letters ,* **52**, 633-639.

Weiner, A., (2010). Drug delivery systems in ophthalmic applications. In: Yorio T, Clark A, Wax M eds. *Ocular Therapeutics: Eye on New Discoveries.* New York: Elsevier Press/Academic Press, 7–43.

Weiner, A.L., and Gilger, B.C., (2010). Advancements in ocular drug delivery. *Veterinary Ophthalmology,* **6**, 395–406.

Weyenberg, W., Bozdag, S., Foreman, P., Remon, J. P., and Ludwig, A., (2006). Characterization and in vivo evaluation of ocular minitablets prepared with different bioadhesive Carbopol–starch components. *European Journal of Pharmaceutics and Biopharmaceutics,* **62**, 202–209.

Weyenberg, W., Vermeire, A., Remon, J. P. and Ludwig, A. (2003). Characterization and in vivo minitablets compressed at different forces. *Journal of Controlled Release,* **89**, 329–340.

Weyenberg, W., Vermeire, A., Vandervoorta, J., Remon, J. P. and Ludwig, A. (2005). Effects of roller compaction settings on the preparation of bioadhesive granules and ocular minitablets. *European Journal of Pharmaceutics and Biopharmaceutics,* **59**, 527–536.

Wilson, C.G., (2004). Topical drug delivery in the eye. *Experimental Eye Research*, **78**, 737–743.

Wunderlich, B., Jin, Y., and Boller, A., (1994). Mathematical description of differential scanning calorimetry based on periodic temperature modulation. *Thermochimica Acta,* **238**, 277-293.

Xia, W., Liu, P., Zhang, J., and Chen, J., (2010). Biological activities of chitosan and chitooligosaccharides. *Food Hydrocolloids.* doi:10.1016/j.foodhyd.2010.03.003.

Xu, J., Li, X., and Sun, F., (2010). Cyclodextrin-containing hydrogels for contact lenses as a platform for drug incorporation and release. *Acta Biomaterialia,* **6**, 486–489.

Yan, H., and Zhengbiao, G.U., (2010). Morphology of modified starches prepared by different methods. *Food Research International*, **3**, 767-722.

Yunxia, B., Yorinobu, Y., and Hisakazu, S., (1999). Rapidly disintegrating tablets prepared by the wet compression method: mechanism and optimization. *Journal of Pharmaceutical Sciences*, **88**, 1004–10.

Zhang, J., Xia, W., Liu, P., Cheng, Q., Tahirou, T., Gu, W., and Li, B., (2010). 1,3 Chitosan Modification and Pharmaceutical/Biomedical Applications. *Marine Drugs,* **8,** 1962-1987.

Zhang, Y., Huo, M., Zhou, J., Zou, A., Li, W., Yao, C., and Xie, S., (2010). DDSolver: An Add-In Program for Modeling and Comparison of Drug Dissolution Profiles .*The AAPS Journal,* **12**,263-271.

Zhu, H., Ibrahim, J.G., and Cho, H., (2012). Perturbation and scaled cook's distance. *Annals of Statistics*, **40**, 785–811.

Zimmer, A., and Kreuter, J., (1995). Microspheres and nanoparticles used in ocular delivery systems. *Advanced Drug Delivery Reviews*, **16**, 61–73.

APPENDIX A1

Review

Topically Administered 'Matriserts' Developed for Drug Delivery to the Anterior Segment of the Eye

Viness Pillay[1*], Raeesa M. Moosa[1], Valence M. K. Ndesendo[2], Yahya E. Choonara[1], Lisa C. du Toit[1], Pradeep Kumar[1], Lomas K. Tomar[1], Charu Tyagi[1] and Trevor Carmichael[3]

[1]University of the Witwatersrand, Faculty of Health Sciences, Department of Pharmacy and Pharmacology, 7 York Road, Parktown 2193, Johannesburg, Gauteng, South Africa
[2]St. John's University of Tanzania, School of Pharmacy & Pharmaceutical Sciences, Dodoma, Tanzania
[3]University of the Witwatersrand, Faculty of Health Sciences, Department of Neurosciences Division of Ophthalmology, 7 York Road, Parktown 2193, Johannesburg, Gauteng, South Africa

*Corresponding Author:
Professor Viness Pillay
Tel: +27-11-717-2274
Fax: +27-11-642-4355
Fax2Email: +27-86-553-4733
Email: viness.pillay@wits.ac.za

Abstract

The human eye is a unique and intricate structure. However, due to anatomical and physiological aspects, drug delivery to this organ is an interesting challenge. Conventional systems such as eye drops are not always efficient for the treatment of anterior eye diseases. It is for this reason that advanced systems such as ocular mini-tablets have been developed to address the challenges. In this review a concerted effort has been made to provide a detailed overview of various topically administered ocular mini-tablets and other solid devices that have been developed for drug delivery to the anterior portion of the eye. Significant *in vitro* and *in vivo* results of these mini-tablets in comparison to liquid preparations are noticeable. Solid ophthalmic dosage forms have several advantages that can contribute to assisting with patient compliance and effective disease treatment. In addressing the difficulties associated with topical ocular drug delivery, improvements by means of solid dosage forms can be implemented. The requirement for advancements in the ocular field is still emphasized.

Key words drug delivery; anterior segment of the eye; mini-tablets; rapidly dissolving tablet

APPENDIX B1

Moosa Mahomed Raeesa

Viness Pillay, Yahya E. Choonara, Lisa C. du Toit, Pradeep Kumar, Valence M. K. Ndesendo and Trevor Carmicheal

School of therapeutic Sciences Department of Pharmacy and Pharmacology

Oral

Characterization of an Instantly Soluble Eye Drop Device (ISED) developed for drug delivery to the anterior segment of the eye

Ocular diseases of the anterior segment are on the increase and the development of improved drug delivery systems for improved treatment is therefore necessitated. The aim of this study was to fabric and evaluate instantly dissolvable biodegradable topical ocular solid eye drops. The porous nature of lyophilized ocular drops results in fluid ingression which ensures rapid hydration and dissolution of the system. This would reduce the foreign body sensation in the eye. The solid drops were prepared by lyophilization of polymeric solutions. The polymers employed were Hydroxypropylcellulose (HPC) and Pluronic F-68 (PF68). Di-glycine (DG) was used as a collapse inhibitor, Polyacrylic acid sodium (PAA-Na) was used to enhance solubility of the solid drops and Maltodextrin (MD) was added to improve the hardness of the formulation. Design of Experiments by selection of a Face Centred Central Composite methodology was employed for the determination of significant effects of variables on properties of the solid eye drops. Variables included PF68 and MD concentrations. Textural characteristics, disintegration profiling, water uptake, *in vitro* drug release and permeation studies were measured. Statistical optimization with Minitab was used for the determination of the ideal formulation combinations for attainment of an optimized formulation.

APPENDIX B2

DETERMINATION OF *EX VIVO* PERMEATION AND IRRITATION POTENTIAL OF RAPIDLY DISINTEGRATING TOPICALLY ADMINISTERED SOLID EYE DROPS

Raeesa M. Moosa[1], Yahya E. Choonara[1], Lisa C. du Toit[1], Pradeep Kumar[1], Valence M. K. Ndesendo[2], Trevor Carmicheal[3] and Viness Pillay[1*]

[1]University of the Witwatersrand, Faculty of Health Sciences, Department of Pharmacy and Pharmacology, 7 York Road, Parktown 2193, Johannesburg, Gauteng, South Africa
[2]St. John's University of Tanzania, School of Pharmacy & Pharmaceutical Sciences, Dodoma, Tanzania
[3]University of the Witwatersrand, Faculty of Health Sciences, Department of Neurosciences, Division of Ophthalmology, 7 York Road, Parktown 2193, Johannesburg, Gauteng, South Africa
*Corresponding Author: Professor Viness Pillay, Tel: +27-11-717-2274. Fax: +27-11-642-4355, Fax2Email: +27-86-553-4733, Email: viness.pillay@wits.ac.za

Introduction

Topical ocular drug delivery using a conventional system such as liquid eye drops is associated with several drawbacks. Reflex eye closure, poor bioavailability and difficulty in manipulating the eye drop bottle are some examples. This results in poor patient compliance and hinders the treatment process. Ocular diseases such as glaucoma are on the increase and development of novel drug delivery systems for improved treatment is therefore necessitated.

Objective

To fabricate and pragmatically evaluate instantly dissolvable biodegradable topical ocular solid eye drops.

Aims

1. Design of experiments (DOE) was implemented and prediction of an optimized formulation by constraint optimization.
2. Evaluation of design formulations by *ex vivo* permeation studies of model drug timolol maleate across rabbit corneas.
3. Conduction of ocular toxicity tests of optimized formulation.

Methods

Permeation testing was conducted using the Franz diffusion cell apparatus (Permagea, Arnie Systems, USA). The methodology for HET CAM (Hens Egg Choriolontic Membrane) test involved using fertilized hen's eggs and scoring of any injury due to samples on the CAM.

Purpose

To determine the permeation capability of the formulations compared to a pure drug dispersion. The occurrence of any injury due to a substance in the HET CAM test can be compared to that of the eye *in vivo.*

Results

Ex vivo permeation studies revealed that the solid eye drop formulations had improved flux (0.0041-0.0052mg.cm^{-2}.min^{-1}) compared to pure drug (0.00378 mg.cm^{-2}.min^{-1}). Ocular toxicity studies revealed that the formulation was practically non-irritant.

Conclusions

Results indicated that the optimized formulation was safe for topical ophthalmic application. *In vivo* studies are currently underway.

APPENDIX B3

Design, development and optimization of a novel instantly soluble topical ophthalmic device

Raeesa M. Moosa[1], Yahya E. Choonara[1], Lisa C. du Toit[1], Pradeep Kumar[1], Valence M. K. Ndesendo[2],Trevor Carmicheal[3] and Viness Pillay[1]

[1]University of the Witwatersrand, Faculty of Health Sciences, Department of Pharmacy and Pharmacology, 7 York Road, Parktown 2193, Johannesburg, Gauteng, South Africa
[2]St. John's University of Tanzania, School of Pharmacy & Pharmaceutical Sciences, Dodoma, Tanzania
[3]University of the Witwatersrand, Faculty of Health Sciences, Department of Neurosciences, Division of Ophthalmology, 7 York Road, Parktown 2193, Johannesburg, Gauteng, South Africa

Purpose:
The aim of this study was to fabricate and evaluate a solid rapidly soluble polymeric system for topical ocular delivery.

Methods:

Solid matrices were prepared by lyophilization of polymeric solutions. Excipients were added to improve the hardness of the formulation. Design of Experiments by selection of a Face Centred Central Composite methodology was employed for the determination of significant effects of variables. Textural analysis in terms of matrix resilience (%) was used to characterize the compressibility of the solid drop using a Texture Analyzer (TA.XT*Plus*, Stable Microsystems, UK). Disintegration profiling was conducted employing the Texture Analyzer by lowering of the matrix into a perspex test vessel containing 2mL Simulated Lachrymal Fluid (SLF, pH 7.4, 35°C). The Franz diffusion cell was used for drug release studies. Timolol maleate was employed as the model drug. The diffusion cell donor chamber contained 2mL SLF which and the receptor solution of 12mL Simulated Aqueous Humour (SAH, pH 7.4, 37 °C) was contained in the receptor chamber. Aliquots of 2mL were withdrawn from the receptor compartment at regular intervals and replaced an equal volume of dissolution medium. The samples were analyzed spectrophotometrically at 295 nm to determine the drug release. Mean dissolution time when 50% of drug was released ($MDT_{50\%}$) was calculated. Statistical comparisons were made using MINITAB® V14 (Minitab®, USA).

Results:

Textural analysis revealed that formulation 1 had the highest resilience (8.469%) conferring the highest overall matrix strength. Formulation 11 displayed the fastest disintegration time of 0.200s. Disintegration rate was taken as the first gradient of the descending region from the onset of disintegration. The highest disintegration rate was noted for formulation 11 (10mm/sec). All formulations showed initial burst release. The lowest MDT correlated with the fastest drug release (12.50 minutes).

Conclusions:

These findings provide a step forward in the formulation of versatile instantaneously disintegrating systems with enhanced physicochemical properties.

APPENDIX B4

IN VIVO EVALUATION OF TOPICALLY ADMINISTERED SOLID EYE DROPS IN THE RABBIT MODEL.

Moosa RM[1], Choonara YE[1], du Toit LC[1], Kumar P[1], Ndesendo VMK[2], Carmichael T[3] & Pillay V[1]

[1]University of the Witwatersrand, Faculty of Health Sciences, Department of Pharmacy and Pharmacology

[2]St. John's University of Tanzania, School of Pharmacy & Pharmaceutical Sciences

[3]University of the Witwatersrand, Faculty of Health Sciences, Department of Neurosciences, Division of Ophthalmology

OBJECTIVES: To determine the *in vivo* behaviour of novel instantly soluble solid eye drops administered in the cul-de-sac of the New Zealand Albino rabbit eye.

DESIGN & METHOD: A pilot study was conducted initially on 6 rabbits. Timolol maleate was used as a model drug. Drug-loaded devices were gently administered to the cul-de-sac. Drug-free devices were inserted in the opposing eye for comparison purposes. The following were noted: ease of administration at the defined site and presence of any untoward reactions in the rabbit eye following visual assessment and/or slit-lamp examination (for corneal thickening or conjunctival hyperemia) after insertion. Rabbits were assessed using an irritancy scale. Evaluation of irritation was conducted according to a 0 (absence) to 3 (highest) clinical evaluation scale of discharge, conjuctival chemosis and conjuctival redness.

RESULTS: Overall irritation was calculated by summing the total clinical evaluation scores. A score of 0 was obtained for all samples. No irritation or toxicity was noted after both drug-free and drug-loaded solid eye drop application.

CONCLUSION: The formulation was regarded as safe for topical ophthalmic application. Experimental drug release studies on aqueous humour samples and histological evaluation are underway.

APPENDIX C1

AESC3

STRICTLY CONFIDENTIAL

ANIMAL ETHICS SCREENING COMMITTEE (AESC)

CLEARANCE CERTIFICATE NO. 2012/12/05

APPLICANT: **Ms R Moosa**

DEPARTMENT: **Pharmacy and Pharmacology**

PROJECT TITLE: *In vivo* assessment of an instantly dissolvable solid eye drop device for topical drug delivery in the rabbit eye

Number and Species

66 New Zealand albino rabbits (both sexes)

Approval was given for to the use of animals for the project described above at an AESC meeting held on **24 April 2012**. This approval remains valid until **30 April 2014**.

The use of these animals is subject to AESC guidelines for the use and care of animals, is limited to the procedures described in the application form and to the following additional conditions:

Conditions:

- Rabbits should be housed singly. This will allow both sexes to be used in the study.
- Dr Kennedy Erlwanger should replace Dr. Leith Meyer in table 13 (Dr. Meyer will soon be leaving Wits).
- 15% (not 20%) loss in body mass should be used as the humane end point.
- This is not a conventional draize test and should not be referred to as such (Generally, Wits will not give permission for draize tests.
- A suitably qualified person must sign for the drugs (Dr. Meyer will soon be leaving Wits).
- Note that the route of administration for ketamine and xylazine is not I.V. (incorrect in the InfoEd version of the application.

Signed: _____ (Chairperson, AESC) Date: 4/5/12

I am satisfied that the persons listed in this application are competent to perform the procedures therein, in terms of Section 23 (1) (c) of the Veterinary and Para-Veterinary Professions Act (19 of 1982)

Signed: _____ (Registered Veterinarian) Date: 4/5/12

cc: Supervisor:
Director: CAS

APPENDIX D1

Synergy Sterilisation
SOUTH AFRICA (PTY) LTD
(Reg. No. 1998/024219/07)
5 Waterpas Street
Isando Extension 3
P.O. Box 3219
Kempton Park 1620
Tel: (011)974-8851
Fax: (011)974-8986

Gamma Radiation Processing

Certificate Of Gamma Irradiation

This is to certify that

SYNERGY STERILISATION SA (PTY) LTD

Has given an irradiation treatment in accordance with :

. The national and international quality assurance system standards: ISO 9001:2008

. The precision and accuracy of the dosimetry system used is traceable to International Standards

to the following goods (as described by the Manufacturer):

Customer	UNIV OF WITWATERSRAND DEPT OF PI	Customer Order No.	GRN date
Synergy Internal order number (Certificate No)	38788 \1	1	8/23/2012
Synergy Stock Code	000 025 TR01	Conforms to the Specified Irradiation Dose of :	
Product description	TRIAL SAMPLE 25KGY.DENS	Minimum :	25 kGy
Quantity of Containers	Mass Of Containers Kg	Maximum :	0 kGy
1	1.00	Routine Dose Reading :	27.7 kGy
		Ref. Dose Mapping :	

Irradiation Completion Date 27/08/2012 Product Released By Quality Department

ISO-9 REV 12

APPENDIX E1

Animal Welfare Score sheet used to assess welfare of rabbits during the study *(One sheet per animal to record parameters listed below)*
Researcher:……
Supervisor:…….
Animal Technician:……....
Date of treatment/operation:……..
Rabbit number:……..
Cage number:……

Note:

- Whenever obvious welfare problems are detected, the technician or veterinarian must be notified

Date											
Day											

BODY WEIGHT & B.A.R (bright, alert, responsive) SCORE (normal is 0, score 1,2,3 for ↑ in severity)

Original body weight											
Body weight yesterday											
Body wt today											
Body wt change											
B.A.R.											
Approach response (inquisitive behaviour, investigates your presence)											

GENERAL CLINICAL SIGNS (score normal animal as 0, score 1,2,3 for ↑ in severity)

Inactive											
Loss of appetite											
Dehydration											

LOCAL EFFECTS OF TIMOLOL MALEATE ON EYE (score normal animal as 0, score 1, 2, 3 for ↑ in severity)

Redness											
Lachrymation											
Discharge											

SYSTEMIC EFFECT OF TIMOLOL MALEATE (score normal animal as 0, score 1, 2, 3 for ↑ in severity)

Bradycardia											

SYSTEMIC EFFECTS OF ANEASTHETICS

Apnoea											
Bradycardia											

SIGNATURE											

Humane end points:

- **Loss of 15% of body weight from baseline weight when assigned to the protocol.**
- **Clinical or behavioral signs in rabbits unresponsive to appropriate intervention (See abnormalities)**
- **Abnormalities would include:**

1. **Inactivity**
2. **Labored breathing**
3. **Sunken eyes**
4. **Hunched posture**
5. **Piloerection/mattered fur**
6. **One or more unresolving skin ulcers**
7. **Abnormal vocalization when handled**

- **Specific ocular injuries identified by the experts that would not be expected to reverse within 21 days could be used as humane endpoints to end the study**